The Dissertation Committee for Yoen Ju Son Certifies that this is the approved version of the following dissertation:

Dry Powder Antibiotics for Inhaled Anti-Tuberculosis Therapy

Committee:

Jason T. McConville, Supervisor

James W. McGinity

Robert O. Williams, III

Krishnendu Roy

Nathan Wiederhold

Dry Powder Antibiotics for Inhaled Anti-Tuberculosis Therapy

by

Yoen Ju Son, B.Sc.; M.Sc.

Dissertation

Presented to the Faculty of the Graduate School of

The University of Texas at Austin

in Partial Fulfillment

of the Requirements

for the Degree of

Doctor of Philosophy

The University of Texas at Austin

December, 2010

Dedication

To my parents.

Acknowledgements

A dissertation is never the work of just one person. I would have never come so far without the advise, discussions, and support I received from many people. First, I would like to sincerely thank my supervisor, Dr. Jason T. McConville, for his enthusiastic guidance and endless encouragement throughout my Ph.D. studies. Being in your research group has been a great and valuable experience for me that I cannot appreciate enough. Special thanks are given to my dissertation committee members, Dr. James W. McGinity and Dr. Robert O. Williams, for their invaluable knowledge in the field of pharmaceutics and their support during my entire studies. I also appreciate the assistant from my committee members, Dr. Nathan Wiederhold and Dr. Krishnendu Roy, for their encouraging words and comments, which helped shape the scope this dissertation. I would also like to thank Dr. Robert Pearlman and Dr. Salomon A. Stavchanski for their encouraging words and comments.

I am especially grateful to my lab. mates, including Shin-Fan Jang for his lots of supports, to Thiago Carvalho, whose creativity in the lab and his positive attitude was always an encouragement, to Simone Carvalho for her enthusiastic discussions, in addition to her exceptional friendship, to Sumalee Thitinan for uplifting camaraderie that helped to make our discussions about research more fun, to Javier Morales for his support and friendship, and to Michelle Horng for her assistance with editing all my manuscripts.

I am very thankful to the staff of the College of Pharmacy for making my busy life easier, specifically, Yolanda Abasta, Mickie Sheppard, Stephanie Crouch, Claudia McClelland, Joyce McClendon, Janet Larsen, Jay Hamman, and Mr. Jim Baker.

I would also like to thank all of the past and present post doctoral fellows, graduate students for their friendship, assistance, and guidance. Specifically, I'm thankful to Keat Theng Chow, Dr. James DiNunzio, Dr. Troy Purvis, Dr. Caroline Dietzsch, Dr. Dorothea Sauer, Dr. Sandra Schilling, Dr. Shawn Kucera, Dr. Justin Tolman, Dr. Eric Wang, Dr. Ashishi Rastogi, Dr. Alan Watts, Dr. Piyanuch Wonganan, Jin Huk Choi, Yubin Wu, Bo Long, Helene Lirola, Kevin O'Donnell, Nicole Nelson, Stephanie Bosselmann, Loni Coots, and many others.

Finally, I thank my parents for instilling in me the greatest motivation to learn and their constant love and support, and to Doe Hyun, who has been so supportive throughout the years, enduring my moodiness through stressful days and always treating me with love and patient.

Dry Powder Antibiotics for Inhaled Anti-Tuberculosis Therapy

Publication No._____

Yoen Ju Son, Ph.D.

The University of Texas at Austin, 2010

Supervisor: Jason T. McConville

The aim of this research was to develop and fully investigate a novel method of antibiotic drug delivery to the lung that will address problems with current therapeutic regimens for treatment of airway infections. To demonstrate the performance of prepared formulations, the design of suitable characterization methods were also aimed. A novel dissolution method for evaluating the *in vitro* dissolution behavior of inhalation formulations was developed. The membrane holder was designed to enclose previously air-classified formulations so that they could be uniformly tested in the dissolution apparatus. Dissolution procedures, the apparatus, the dose collection, the medium, and test conditions were developed and the dissolution behaviors of test compounds were evaluated by experimental and mathematical analysis. It was proved that the aerodynamic separation of formulation prior to dissolution assessment have a significant influence on the dissolution profiles. The optimized test method using the membrane holder was applied to evaluate in vitro dissolution profiles of the manufactured formulations of

rifampicin (RF). The carrier/excipient-free RF dry powder formulation was investigated. The rifampicin dihydrate (RFDH) powders having MMAD of 2.2 μm were prepared using a simple recrystallization process. The RFDH powders have a thin flaky structure, and this unique morphology provides improved aerosolization properties at maximal API loading. The manufactured RFDH formulation showed 80 % drug release within 2 hours. To retard the release rate of RF, the prepared RFDH crystals were coated with hydrophobic polymer, PLA or PLGA, using spray-dryer equipped with multi-channel spray nozzles. The multi-channel spray nozzle used in this study has two separate nozzles for aqueous solution and one for gas fluid. The RFDH crystals and the coating solutions were sprayed through the two separate liquid nozzles at the same time. The coated RFDH formulations were prepared using multi-channel spray nozzles. The coated formulations contained at least 50 % w/w of RF with no change of their flaky morphology. The initial RF release was lowered by coating; the lowest initial RF release was observed from the coated powders with PLA polymer as 32 % among the coated formulations. Overall, the 80 % of RF was released within 8 hours. The RFDH and coated RFDH formulations delivered via the pulmonary route would be anticipated to provide higher local (lung) drug concentrations than that of orally delivered powders. Particularly, the coated RFDH powders deposited in the alveolar region may prolong the drug residence time in the site of infections. Additionally, it was proved that the RFDH and coated RFDH formulations provided much better stability than the amorphous RF.

Table of Contents

List of Tables

List of Figures

Chapter 1: Introduction[1]

1.1. DRY POWDER INHALERS

Drug delivery to the lung has changed dramatically in recent years. Commercialization of the pressurized metered dose inhaler (pMDI), containing a chlorofluorocarbon (CFC) propellant, began as a convenient system for asthma management in the 1950s. The pMDI has become the most popular device for out-patient inhalation therapy, with its worldwide production exceeding 300 million per year [1, 2]. However, concerns have often been highlighted over potential drawbacks of pMDIs: an altogether environmentally incompatible propellant, harmful effects of Freon to patients and perhaps of most concern is the extensive oropharyngeal deposition of the active pharmaceutical ingredients (APIs) included in the device [3-5]. Because the contribution to ozone depletion of CFC was initially hypothesized by Molena and Rowland (1974), pharmaceutical companies were forced to find alternative propellants [6, 7]. As a result, hydrofluoroalkane (HFA)-based and propellant-free pMDIs were developed as a way to replace CFCs [8-11]. However, this replacement strategy has not been altogether successful because of several setbacks, including potency, manufacturing cost increase, and reformulation difficulty amongst others [12, 13].

[1]Parts of this chapter were taken from :
1) Yoen-Ju Son, Jason T. McConville, "Advancements in dry powder delivery to the lung", Drug Development and Industrial Pharmacy, 2008, 34, P: 948–959.
2) Yoen-Ju Son, Jolyon P. Mitchell, and Jason T. McConville, "In vitro performance testing for pulmonary drug delivery", in "Controlled Release Science and Technology: Pulmonary Delivery", Controlled Release Society (CRC) Book Series (In Press).

Problems with the pMDI performance and operational restrictions have spurred the exploration of dry powder systems. As a consequence, many dry powder inhalers (DPIs) have emerged, and a number of them have been introduced onto the market. Since the first single-dose DPI product, the Spinhaler® (Sanofi-Aventis, Holmes Chapel, UK) (formerly Fisons, Loughborough, UK), appeared on the market, new DPIs have made remarkable progress in various aspects such as dose-metering, dose-dispensing, and aerosolization systems for dry powder particles [14-17]. Additionally, attempts have been made to deliver a variety of active pharmaceutical ingredients (APIs) via pulmonary route using novel inhalation devices such as Exubra® (Nektar therapeutics, San Carlos, CA, USA), Spiro® (Dura Pharmaceuticals, San Diego, CA, USA), and AIR™ (Alkermes Cambridge, MA, USA).

1.1.1. Advantages of dry powder inhalers

The pulmonary route of administration has many potential advantages for the delivery of APIs over other administration routes. Advantages include: a large surface area for drug absorption, high permeability through a thin alveolar membrane [18, 19], few proteases for degradation of APIs [18], no first-pass hepatic clearance/metabolism [18, 19], and the reported excellent bioavailability for some molecules [20, 21]. Specifically, DPIs have become widely known as a very attractive platform for drug delivery by virtue of its propellant-free nature, high patient compliance, improved formulation stability and patient protection from harmful Freon [14, 22, 23]. Moreover, it has been known that the DPIs offer better drug deposition in central and peripheral

regions of the lung, with minimal oropharyngeal deposition, than the pMDI [24]. This is due to the differences in the aerosol generation mechanism between delivery devices. DPIs are generally activated by the patient's inspiratory airflow, which require little or no coordination of actuation and inhalation. Whereas pMDIs are activated by pressurized propellant at high velocity, which can result in premature drug deposition in the oropharynx [25, 26]. Consequently, many patients have traditionally used DPIs to treat asthma and chronic obstructive pulmonary disease (COPD) [15, 27-29]. Recently, the development of new DPIs for delivering therapeutic proteins and antibiotics has also been accelerated by patient demands, and innovative research [30-32]. The current market for DPIs has over 20 devices presently in use and many devices under development for delivering a variety of therapeutic agents, for a variety of therapeutic needs.

1.1.2. Particle deagglomeration mechanism

Deaggregation and deagglomeration are the processes by which particle aggregates are dispersed into primary particles of suitable size for deep lung deposition by interaction with airflow. In pulmonary drug delivery, particles within the aerodynamic size range of 1-5 μm are effectively delivered to alveoli region by sedimentation [18]. However, due to their small particle size, powders used in DPIs are extremely adhesive and cohesive. To minimize the inter-particulate forces caused between those fine particles, most dry powder formulations contain coarse carrier materials, such as lactose [16]. However, these carriers can markedly affect the aerosolization properties of the powder [16, 33, 34], since the aerosolization performances of DPIs are predominantly

governed by the deagglomeration of fine particles from the surface of larger carrier particles; the incomplete detachment of fine API particles from the carrier particles leads to the poor aerosolization of APIs [35, 36]. To successfully overcome adhesive forces between the fine particles and the carriers, most DPI devices have been designed to incorporate their own particle separation mechanisms.

The DPI devices can be divided into two categories according to energy sources to deagglomerate the fine particles: (1) passive devices and (2) active devices, as shown in Figure 1.1. The energy source for most passive DPIs is a patient's inspiratory flow rate and volume, and in this case a patient's inspiratory air flow pulls particles though a specific deagglomeration zone in a given device, where fine drug particles are separated. At present, the principal mechanism leading to powder deagglomeration in passive inhalers are frictional forces, drag and lift forces provided by air turbulence, and internal forces [37-40]. However, it's often reported that the passive devices may not provide therapeutically effective amounts of drug aerosol particles to the patient with asthma, chronic obstructive pulmonary disease (COPD), or in elderly patients and young children since their inspiratory airflow is not sufficient to achieve optimal aerosol generation [41, 42]. Therefore, active devices, which have power-assisted powder dispersion systems, have been proposed to make up for potential variability displayed by passive devices as described above. Mechanical energy in the form of springs which can generate the compressed air or electrical energy, battery storage systems, and battery-driven impeller have all been used to generate the necessary separating forces for the particles in these systems [39]. A possible advantage of this type of device is that achieving uniformity of

dosage is less dependent on the patient's inspiration capability. Different types of powder dispersion mechanisms are displayed in Table 1.1.

1.2. DRY POWDER FORMULATIONS

1.2.1. Excipients to improve aerosolization properties

1.2.1.1. Carrier particle

The most common excipient in carrier-based DPI system is a lactose monohydrate due to its favorable toxicological profile, physicochemical stability, availability and compatibility with the majority of low molecular weight drugs [16]. Currently, a variety of lactose particle size grades are available from various suppliers. There are considerable number of studies have been explored to compare the capabilities for improving the aerosolization performances between different lactose grades since the physico-chemical characteristics of the lactose carrier, such as crystallinity, surface roughness, moisture sorption, shape factors, surface area and particle size, have a significant influence on the aerosolisation performance of the APIs [16, 43, 44].

However, lactose may not be a choice of carrier for some APIs, such as formoterol, or protein/peptide drugs, due to its reducing sugar function that may interact with the functional groups of these APIs [45]. It is therefore reasonable to look for alternative carriers that still possess the positive aspects but overcome the above mentioned drawbacks of lactose monohydrate. The potential alternatives to lactose that have been investigated include carbohydrates, such as fructose, sucrose, trehalose;

alditols (such as mannitol and xylitol), maltodextrin, dextrans, and cyclodectrins [16, 45].

1.2.1.2. Ternary components

The idea of adding ternary components to the binary drug-carrier mixture to modify strong inter-particulate forces that often lead to low level of fine particle detachment from the carrier has been widely accepted. Although the mechanism of action of ternary components has not been clearly defined, it is generally believed that the additional ternary particles adhere preferentially to the high energy sites of carrier particle surface, thus forcing drug particles to adhere to less active sites of carrier surface [46, 47]. During aerosolisation of the formulation, drug particles are therefore more easily liberated from the carrier, increasing the amount of drug available for inhalation. Materials that have been widely examined as ternary components are as follows: L-leucine, magnesium stearate, lactose fines, polyethylene glycol 6000, and lecithin [16].

1.2.2. Particle engineering technologies

1.2.2.1. Milling

The majority of currently marketed DPI products consist of micronized APIs in either agglomerated or blended form. The most well-developed and convenient technique for size reduction of highly crystalline APIs is milling. There are many different milling methods, but only a few are able to mill powder to the respirable particle size range of 1 to 5 μm. Vibration milling, ball milling and, in particular, jet-milling (fluid energy) are

well-established techniques used to manufacture dry powders for inhalation [40, 44]. Generally, the characteristic particle shape of milled crystalline API is either tabular or round showing high surface roughness, as shown in Figure 1.2 (A).

The milling processes can adversely alter the surface and solid-state properties of APIs due to the harsh processing conditions, and are always accompanied with a heat generation and triboelectric charge generation [44]. It is often reported that the milling process generates amorphous domains on the particle surface that may possibly be subject to chemical degradation or recrystallization leading to crystal growth on the milled particle surface. Moreover, the cohesive and adhesive nature of milled crystals is known to be the primary hurdle in aerosol generation from the dry powder aggregates.

Overall, the milling method, although it is a well-established technique, can only provide limited opportunity to manipulate and control the particle characteristics. It is generally not suitable for fragile molecules and more complex engineered structures, such as porous/hollow particles, non-spherical particles, composites, nano-aggregates as well as surface-modified, coated or encapsulated materials [44].

1.2.2.2. Spray drying

Spray drying technology has been widely applied to various pharmaceutical processes due to its simplicity, availability of large-scale equipment and ability to produce composite materials. However, the production of resipirable particles using a spray drying method is a relatively new area; there is no marketed product available, with several products under development stage. One major reason for this is the limitations in

the size reduction capability of this method; generally an intense process optimization and large amount of excipients are required to achieve the desired powder properties. Additionally, there is common concern regarding a thermal degradation of sprayed products and the physical instability of amorphous-structured products. Nevertheless, the spray drying method is rapidly expanding as the technology becomes more optimized. Several new formulation approaches utilizing the spray drying technique have been introduced [44, 48].

The concept of low density or hollow particles as a respirable dry powder formulation has been introduced [44, 48, 49]. Several studies have indicated that large porous particles (> 5 μm) which have low density are adventurous for pulmonary drug delivery since they improve dispersibility and delivery efficiency by lowering the aerodynamic diameter of the particles [44, 48, 49]. In terms of powder deagglomeration, these large particles do not require much energy input for generation an aerosol, because the large porous particles aggregate less and deaggregate more easily under less shear force than smaller and non-porous particles. The carrier particles that usually added to the micronized API formulations are not required for this type of formulation, indicating that the inhalation device having simpler and more compact features than other devices used for traditional carrier-based formulations can be applied for aerosol generation [39].

PulmoSpheres™ (Nektar Therapeutic, San Carlos, CA, USA) formulations have been engineered to show improved powder flow and dispersibility relative to traditional micronized dry powder formulations. These microparticles are manufactured by a spray drying of an emulsion, in which the dispersed phase typically has a submicron droplet

size and consists of a liquid that evaporates slower than the dispersed phase [50, 51]. Manufactured particles have a sponge-like appearance (Figure 1.2 (C)), unlike typical spray-dried particles that have a smooth and spherical morphology (Figure 1.2 (D)).

Highly corrugated particles as shown in Figure 1.2 (B) can be created by using shell forming agents or materials with a high Péclet (*Pe*) number, such as leucine, trileucine, dipalmitoylphosphatidylcholine (DPPC), and materials with high molecular weight as polymers [48]. These materials cause early separation of a soft surface layer during the spray drying process since the diffusion of molecules from the atomized droplet surface to the inner core is slow, thus, the surface becomes enriched with shell former or molecules associated with the high *Pe* number, which finally folds to form a wrinkled morphology [44, 48]. Particles having a more corrugated morphology have shown better dispersion under shear force, than smoother particles due to less surface contact area, which will results in reduced van der Waals force of attraction [49, 50, 52-55].

Encapsulated drug particles by dispersibility enhancers, such as leucine and trileucine, have been engineered by spray drying. This type of formulation can be manufactured by modifying the diffusion coefficient of components using co-solvent systems. For instance, the dispersibility enhancers dissolved with APIs in aqueous/organic solvent mixture are rapidly supersaturated on the atomized droplet surface in the drying process due to their low aqueous solubility, implying that the surface of dried particles mainly consists of the molecules of dispersibility enhancers [48].

1.2.2.3. Polymorphic transformation

Polymorphic transformation of drugs can be considered as a powerful particle engineering technique in the manufacture of respirable dry powders, although this method hasn't been widely applied for pulmonary drug delivery systems. Most drugs exhibit structural polymorphism and it is preferable to develop the most thermodynamically stable and physico-chemically favorable polymorph of the drug to achieve desired powder properties and the reproducible bioavailability of the product. At the molecular level, different particle shapes of crystalline materials may have different chemical functional groups on specific faces of the particles, leading to a variation in the surface energy, hygroscopicity, and electrostatic interactions. These differences will be manifested in the interparticulate forces at the particulate level. It has been proved that improved aerosolization properties can be achieved under such transformations, since the morphology of a particle can play the most important role in powder aerodynamic performance [54-58]. Several APIs have been successfully engineered as crystals with elongated (Figure 1.2 (E)) [56, 58], and flaky structures (Figure 1.2 (F)) [59]. These structural changes show significantly improved inhalation properties following polymorphic transformation [57-59]. Particularly, the elongated particles show very unique aerodynamic behaviors; the aerodynamic diameter of an elongated fiber is determined mainly by the width rather than by the length of the particle. Gonda and Khalik showed that the ratio of the aerodynamic diameter (D_a) to the physical diameter (width, D_f) of an elongated particle increases with the aspect ratio (length/width) of the

particle and levels off at a value of about 2-2.5 when the aspect ratio is bigger than 15-20 (Figure 1.3) [60].

1.2.3. Pulmonary sustained release formulations

Recently, there has been an increased interest in research in focusing on DPI formulations to prolong drug residence time in the lung [61-65] since the sustained release (SR) system has certain advantages, including reduced dosing frequency by extending the duration of drug action, improved management of therapy, improved patient compliance, and reduction in side effects [64, 66]. However, there are many limitations reported in manufacturing inhaled-SR formulations which produce a desired drug loading, release and aerosolization properties. The challenges are mostly related to the production of micron sized particles, since with a reduction in size there is a significant increase in surface area to mass ratio. Subsequently, with an increase in surface area, it becomes more difficult to produce a controlled release profile and incorporate effective release agents. Finding suitable non-toxic excipients is also known to be very challenging since excipients that have been used for pulmonary drug delivery, to date, is very limited.

1.2.3.1. Microencapsulation

Polymer-based matrix systems have been applied for modifying release systems of inhaled pharmaceuticals. Many synthetic and natural materials have been used to prepare controlled release microparticle systems. These microparticle systems include

biocompatible synthetic polymers such as poly lactic-co-glycolic acid (PLGA), polylactic acid (PLA), PEG, polyvinyl alcohol (PVA), and natural polymers or proteins such as chitosan or albumin [62, 64, 65, 67].

PLGA and PLA have been the most commonly reported polymers utilized for potential respiratory sustained release systems [65, 68, 69]. These polymer matrices are typically prepared by spray drying co-dissolved API and polymer in vehicle solvent, or by using a multi-emulsion method (or solvent-evaporation method). However, common multi-emulsion techniques produce microspheres that have very low encapsulation efficiencies (1-10%), which is not ideal for pulmonary delivery due to the limitation in using potentially toxic polymers [65, 70]. A non emulsion spray drying process provides more flexible drug loading to the final formulation compared to the multi-emulsion method, but drug molecules are randomly positioned in the polymer matrix, but are mainly deposited on the spray-dried particle surface due to the diffusion rate difference between small drug molecules and large polymer molecules. Thus, traditionally spray-dried microspheres show faster and more uncontrolled release rates than those prepared using a multi-emulsion method [62, 65, 71].

1.2.3.2. Aggregates of nanoparticles and micriparticle encapsulated nanoparticles

Microparticles whose outer layer consists of polymeric nanoparticles encapsulating APIs have been investigated [63]. The preparation of this type of polymeric nanoparticle is achieved by the spray drying nanoparticles suspended in a continuous phase (vehicle solvent) that contains a shell former. Generally, spray-dried

nanoparticle aggregates show improved aerodynamic properties due to their hollow or porous structure, however, the porous structure may accelerate the release rate of encapsulated APIs [72]. For instance, PLGA nanoparticle aggregates encapsulating rifampicin show almost 90% drug release from the polymer matrix within 15 minutes [63]. Additionally, a large amount of drug loading into the nanoparticles is hard to achieve, as was previously discussed with the multi-emulsion method due to the similarity in drug encapsulation mechanism into the microparticles or nanoparticles.

Lipid microspheres entrapping nanoparticles of hydrophilic drug can be prepared using a spray-drying approach [61]. Up to 33% of drug loading was achieved with retarded drug release profiles. However, the two phase systems required complicate manufacturing process.

1.2.3.3. Hydrophobic coating

Generally, hydrophobic coatings constitute approximately 10% to 50% of the final particle mass, which is substantially higher drug loading compared to the microencapsulated formulations. In US patent 6,984,404 [73], a physical vapor deposition (PVD) method using pulsed laser ablation (PLD), this is applied to achieve PLGA deposition onto the target particle surface, which offers nanometer thickness of coating layer with more than 90% drug loading. However, the use of a PLD method may possibly cause decomposition or degradation of APIs or polymers, due to severe processing conditions, which include exposure to UV radiation, high pressure, and heat. Moreover, the coating of each separate particle is difficult to achieve since there is no

suitable method to fluidize or agitate ultra-fine particles (1-5 μm) that exhibit strong cohesion properties during the coating process. A coating onto aggregated particles may lead to poor aerosolization performances, as the particle size of formulated particles will increase.

A spray dry method to obtain coated particles has also been widely evaluated [74, 75]. This technique is a relatively simple one-step process over other coating techniques. However, the application of this method is limited as micronized core forming particles have to be dispersed in the coating solution without dissolving the core-forming particle.

Consequently, although several conventional methods have been attempted to coat particles classified into a Geldart Group C group or smaller particles [76, 77], those techniques have not been successfully applied for inhalation formulations.

1.3. *IN VITRO* PERFORMANCE TESTING

1.3.1. Aerodynamic particle size analysis

Multi-stage cascade impactors (CIs) are defined in the US and European pharmacopeias (Table 1.2) for the measurement of inhaler aerosol aerodynamic particle size distribution (APSD). CIs are used both in the development and subsequent quality control (QC) of marketed inhaler products and the qualification of the clinical batches [78].

In its simplest form, a single stage impactor comprises a nozzle plate containing one or more circular or slot-shaped jets (nozzles) of diameter (W) located a fixed distance

(S) from a flat collection surface (Figure 1.4). Incoming particles are size classified on the basis of their differing inertia, which reflects the resistance to a change in direction of the flow. Liquid impingers are a variant in which the particles are captured in a liquid medium rather than on a solid substrate, an advantage is that particle bounce and re-entrainment is avoided. Additionally, the liquid in the impinger can be the eluent medium for recovery and assay of active pharmaceutical ingredient(s). The multistage CI is constructed by coupling several stages (typically 7 or more) together with progressively finer and/or reduced number of jets such that particle velocity and hence inertia is progressively increased. In this way the device fractionates the incoming aerosol into particles covering discrete and well-defined size ranges [79].

The ACI (Figure 1.5 (A)) is currently still the most widely used multistage impactor for inhaler aerosol testing, although the NGI (Figure 1.5 (B)) is becoming more widely used as familiarity with its capability grows. Both CIs can operate in the flow rate range of interest for pMDI and DPI testing (30 to 100 L/min), but the ACI requires the removal of the lowermost stages (6 and/or 7) and insertion of new stages at the upper end (stages 1 and 2) for use at flow rates of 60 and 100 L/min [80]. On the other hand, the NGI does not require stage replacement [81] and can operate over the entire range with excellent size resolution [82]. It can even be used without its pre-separator and a back-up filter substituted for the multi-orifice collector [83]. Other CIs in use are the Marple-Miller 5-stage design that uses collection cups, similar in concept to the NGI (Figure 1.5 (C))) and which is available in a low flow version (4.9 and 12 L/min) for testing inhalers intended for pediatric use [84], as well as in the standard versions that operate at 30 and

60 L/min for routine testing of pMDIs and DPIs [85]. The 4-stage multi-stage liquid impinger (MSLI, Figure 1.5 (D)) is the last widely used CI for inhaler aerosol evaluations, being a popular choice where collection of the active substance in the eluent for subsequent assay is possible [86].

Although the underlying principle for the CI method is simple to understand, its practical implementation is technically challenging because it is labor-intensive, requiring a high degree of manual skill. Thus, the following factors have to be taken into account in method development [87]:

1) Collection solvent (impingers) or recovery solvent (dry impactor systems);
2) Quantitation lower limit for the active pharmaceutical ingredient(s);
3) Recovery techniques for the active pharmaceutical ingredient(s);
4) Use of a pre-separator (important for many DPIs, in particular those based on the drug-carrier particle delivery principle);
5) Environmental factors (barometric pressure, temperature, relative humidity).

1.3.2. *In vitro* dissolution studies for evaluating inhalation products

Dissolution testing allows one to examine the drug release behavior of pharmaceutical dosage forms *in vitro* in order to differentiate formulation types, and perhaps give an estimate of a dissolution behavior *in vivo*. Several USP general chapters (i.e. <711>, <724>, <1088>, and <1092>) play a key role in these evaluations as the gold standard tests. Those tests are routinely successfully applied to estimate *in vitro* dissolution behaviors of solid, or semi-solid dosage forms [88]. However, there is no such

universally accepted method to estimate the dissolution behavior of inhaled active ingredients, although many dissolution methods for testing aerosols have been investigated [89]. Designing a standardized method applicable to the lung is not an easy task, as the lung has several unique features which are difficult to replicate *in vitro*, such as the extremely small amount of aqueous fluid, and the presence of endogenous lung surfactants [19, 89].

For inhalation products, one of the most important steps with *in vitro* performance testing is characterization of the delivery of a given API from a specified delivery device using a pharmaceutical impactor/impinger to estimate actual dose delivered to the target site of the lung. Only a fraction of the API emitted from standard delivery devices is usually delivered to the target site of the deep lung since most inhaler products are mixture of fine API particles and course carrier particles or propellants [18]. Thus, an ideal dissolution test procedure for inhalation formulations would involve particle classification followed by an evaluation of the dissolution behavior for the classified drug particles that may deposit at various sites in the respiratory tract. Additionally, a stagnant dissolution system, rather than well stirred system would be required to estimate lung dissolution as the volume of lung fluid is approximately 10-20 mL/100 m^2 [19].

Experimental difficulties exist in dose collection due to very fine powder and their electrostatic characteristics [89]. Therefore, to date most dissolution procedures on powders have been performed in the absence of aerodynamic classification, whereby formulations may have been directly dispersed into an apparatus 2 dissolution tester [90], or placed directly into a modified basket to prevent drug particles from escaping directly

into to the dissolution medium [62, 91]. However, these methods using existing configurations of dissolution apparatuses have following limitations:

1) Formulations intended for pulmonary delivery are hard to disperse homogeneously into the vessel/basket;
2) Dispersed particles stick on the vessel wall and/or paddle/basket during such dissolution tests;
3) Floating powders may be inadvertently collected during the sampling procedure.
4) Existing paddle/basket apparatus provide well-stirred environment;

In an attempt to make up for some of the shortfalls of this type of testing using commercially available dissolution systems, several diffusion systems, a custom built diffusion cell [61], a twin-stage impinger (TSI) [92], and a dissolution cell [93, 94], have been investigated. However, no single *in vitro* test system has yet emerged as the ideal choice for performing dissolution measurements for inhalation formulations.

1.3.3. Surface morphology

The morphology (roughness or corrugation) of particles play a very important role in aerosolization performance of pharmaceutical powders. It has been shown that the broad adhesion force distributions between particles are attributed to the morphology of surface, in particular, the surface roughness [53, 95, 96]. A considerable number of studies have been explored to correlate the surface structure of particles with powder flow and aerosolization performance, and the interest keeps growing as various engineered particles having unique structural features have been introduced to the market. Commonly, scanning electron microscopy (SEM) is widely being applied to analyze the

surface morphology of particles, however, this method is only limited to visualize the particle structure, and cannot provide numerical values for the degree of difference since it is a qualitative analysis method [95]. The quantification of surface morphology can be achieved by various techniques, such as the atomic force microscopy (AFM) and the light scattering methods [52, 53, 97, 98].

The AFM is the most common and most well-established method used to evaluate the surface roughness of a particle. The AFM consists of a cantilever with a fine tip at its end that is used to scan the specimen surface. When the tip is brought onto a sample's surface, the forces between the tip and the sample lead to a deflection of the cantilever, according to Hooke's law. In a study conducted by Islam et al., the surface roughness of various lactose carriers was quantified by AFM imaging, and the results showed significant roughness, even though the SEM images of those particles seemed to be smooth [96]. It has also been verified quantitatively by AFM imaging, that spray dried BSA particles having a high degree of surface corrugation have a better aerosolization efficiency than that of smooth particles [53].

1.4. PULMONARY TUBERCULOSIS

Tuberculosis (TB) is a chronic infectious disease, which is considered the foremost cause of death due to a single microorganism [99]. According to the World Health Organization (WHO), approximately 9,270,000 people were newly diagnosed with the disease in 2007, about 1,300,000 people died, and about one third of the overall

population in the world was infected with the tubercles bacillus [100]. The occurrence of TB is most often due to *Mycobacterium tuberculosis* (MTB) infection and the lung is the primary site of infection; 80% of TB cases are of pulmonary TB alone [31].

MTB is an intracellular parasitic bacterium that mainly infects the respiratory tract and hides in alveolar macrophages (AMs). AMs are one type of immunecompetent cell present in the lungs. When foreign substances such as a disease organism are inhaled and reach an alveolus, they are endocytosed by AMs and eventually transported to phagosomes. The endocytosed foreign substance is then degraded by the digestive enzymes in the phagosome. However, when MTB is endocytosed, it inhibits formation of phagolysosomes and avoids degradation in the AM, resulting in a latent infection [101].

1.4.1. Treatment

1.4.1.1. Antibiotics for treatment of pulmonary tuberculosis

The most common treatment for TB involves oral administration of high systemic doses of single or combined antibiotics [102-104]. The chemotherapy regimens consist of four first line anti-TB drugs namely, rifampicin , isoniazid, pyrazinamide and ethambutol, used in an initial intensive treatment phase of two months and a continuation phase usually lasting 4-6 months [103, 104]. The recommended daily doses of four anti-TB drugs are 5, 10, 25 and 15 mg/body weight (kg) for rifampicin, isoniazid, pyrazinamide and ethambutol, respectively [103]. However, it has been reported that inappropriate monotheraphy can cause the development of TB that resistance to the first-line drugs [102-104]. To avoid problems associated with monotherapy, such as, over-dose or under-

dosing, the first-line drugs have been recommended to be taken in combination [103, 104]. Several fixed-dose combination (FDC) products containing rifampicin, isoniazid, pyrazinamide, and ethambutol are in use today [102, 103, 105].

However, concern has been expressed on the poor bioavailability and the unstable chemical potency of rifampicin from FDC products containing isoniazid and/or pyrazinamide [106, 107]. The existence of rifampicin in different crystal forms and the change from one form to another during processing are repeatedly quoted as the reasons for the variable bioavailability of rifampicin from FDC products [108-111]. The rifampicin is an important component in anti-TB therapy, thus using FDC tablets with poor rifampicin bioavailability could lead directly to treatment failure and may encourage drug resistance. Furthermore, clinical and bacteriological investigations have revealed that the anti-bacterial activity of rifampicin is dose-dependent [112]. Therefore, a good quality FDC tablet with demonstrated bioavailability of rifampicin is an absolute requirement for successful TB treatment.

1.4.1.2. Anti-tubercular inhaled therapy

To date, no aerosol products containing anti-TB drugs have been developed yet. However, several current studies are under investigation for administration of anti-TB drugs to the primary infection site, the lung, with the idea of increasing the local therapeutic effect and reducing overall systemic exposure [63, 65, 68, 113-116]. Specifically, pulmonary delivery of rifampicin has been widely studied [63, 65, 68, 113, 115, 117] as it is the first choice drug in the treatment of TB [99, 118]. Furthermore,

pulmonary delivery bypasses drawbacks seen in current oral delivery systems, specifically, delivery of rifampicin to the neutral milieu of the lung avoids severe chemical decomposition of rifampicin in the acidic conditions of the stomach when taken orally [28, 102, 119]. Several respirable forms of rifampicin, such as nano/microparticles [63, 65, 68], liposome [115], and liquid [116], have been introduced to localize the rifampicin in the lung.

Recently, there has been an increased interest in research in focusing on DPI formulations to prolong drug residence time in the lung [61-65] since the SR system has several advantages [64, 66]. Specifically, in anti-TB inhaled therapy, it's well established that the SR formulation enhances the efficacy of anti-TB drugs, presumably by targeting AMs and building up high intracellular drug concentrations. Generally, the phagocytic uptake of inhaled particles by AMs has been known to be the primary hurdle in extending drug residence time in the lung [64, 66]. However, in pulmonary anti-TB therapy, the phagocytic activities play a useful role in terms of targeting anti-TB drugs at the main site of the MTB proliferation [120, 121]. Several SR formulations that encapsulate anti-TB drugs into the polymeric microspheres have been introduced to target the AMs [63, 65, 122, 123]. Respirable PLGA/PLA microspheres showing up to 3 days of *in vitro* drug release capability were manufactured by means of a solvent evaporation and a spray drying method [65, 120, 121]. A formulation consisting of PLGA nanoparticle aggregates was also introduced by sung et al. [63]. However, there are still numerous limitations in manufacturing the dry powder forms of SR formulations to have good aerosolization properties with controlled drug release capabilities due to their fine particle size.

Additionally, the low payload of APIs has been shown to be one of the problems in inhaled TB treatment, since the bactericidal activity is directly proportional to the concentration at the target site [112, 116] . Consequently, ideal SR formulations used to effectively treat airway infections like TB require both high drug payload and prolonged drug release from the delivery platform.

Another issue in delivering the dry powder form of anti-TB antibiotics to the lung is that there are no DPI devices specifically designed to carry a large amount of antibiotic formulation. Currently available devices are all designed for delivering small amounts (microgram dose) of bronchodilators or steroids [39]. Only single-dose capsule devices have a capability to hold the substantial amount of (milligram dose) formulations among the current devices. However, those devices are relatively old type and show poor aerosolization properties compared to novel active devices. Thus, the development of formulations that show a low device dependency and good aerosolization performances is required to deliver a maximum potency formulation of the antibiotic directly to the lung.

1.5. TABLES

Table 1.1 Particle dispersion mechanisms used in selected devices

	Device	Developer	Mechanism	Type
Passive	Clickhaler®	ML Laboratories	Impaction body	Multi dose (Reservoir)
	Easyhaler®	Orion Pharma	Narrow passage	Multi dose (Reservoir)
	Novolizer®	Viatris	Air classifier	Multi dose (Reservoir)
	Airmax™	Yamanouchi	Cyclone separator	Multi dose (Reservoir)
	Taifun®	Leiras OY	Vortex chamber	Multi dose (Reservoir)
	AIR®	Alkermes	Narrow passage	Single dose (Capsule)
Active	Exubera®	Nektar therapeutics	Air pump	Multi dose (Blister)
	Aspirair®	Vectura	Air chamber	Multi dose (Blister)
	Spiros®	Dura Pharmaceutical	Battery powder	Multi dose (Disk)
	Jethaler®	RatioPharm GmbH	Mechanical cutter	Multi dose (Ring tablet)

Table 1.2 Identification of apparatuses for APSD measurement in the US and European Pharmacopeias

Impactor	**US Pharmacopeia**	**European Pharmacopeia***
Glass Twin Impinger (TI)	Not Used	Apparatus A for pMDIs, DPIs and nebulizers
Andersen 8-stage without pre-separator (ACI)	Apparatus 1 for pMDIs	Apparatus D for pMDIs
Marple Miller Model 160 (MMI)	Apparatus 2 for DPIs	Not Used
Andersen 8-stage with pre-separator (ACI)	Apparatus 3 for DPIs	Apparatus D for DPIs
Multi-Stage Liquid Impinger (MSLI)	Apparatus 4 for DPIs	Apparatus C for pMDIs and DPIs
Next Generation Pharmaceutical Impactor (NGI)	Apparatus 5 for DPIs Apparatus 6 for pMDIs	Apparatus E for pMDIs and DPIs

* Apparatus B was the single-stage 'Metal Impinger' that was withdrawn from the European Pharmacopeia in 2005 (Supplement 5.1)

1.6. FIGURES

Figure 1.1 Schematic diagram of the particle deagglomeration mechanisms in passive and active DPI systems [40].

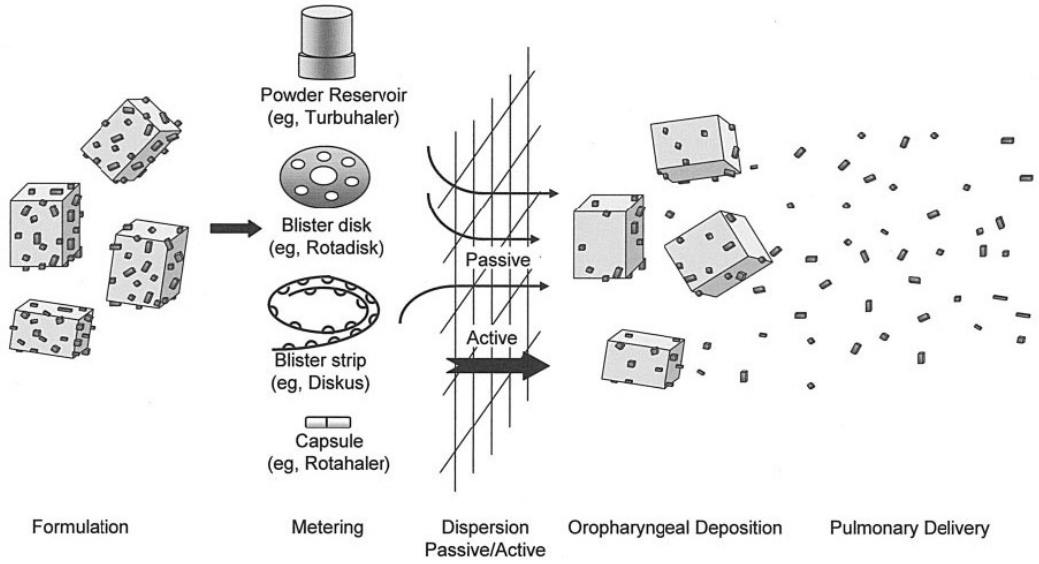

Figure 1.2 Morphologies of engineered particles by various micronization techniques; (A) milled API crystals, (B) highly corrugated particles, (C) low-density porous powders (D) smooth spherical particles, (D) elongated API crystals, and (E) flake-like API crystals [55, 59].

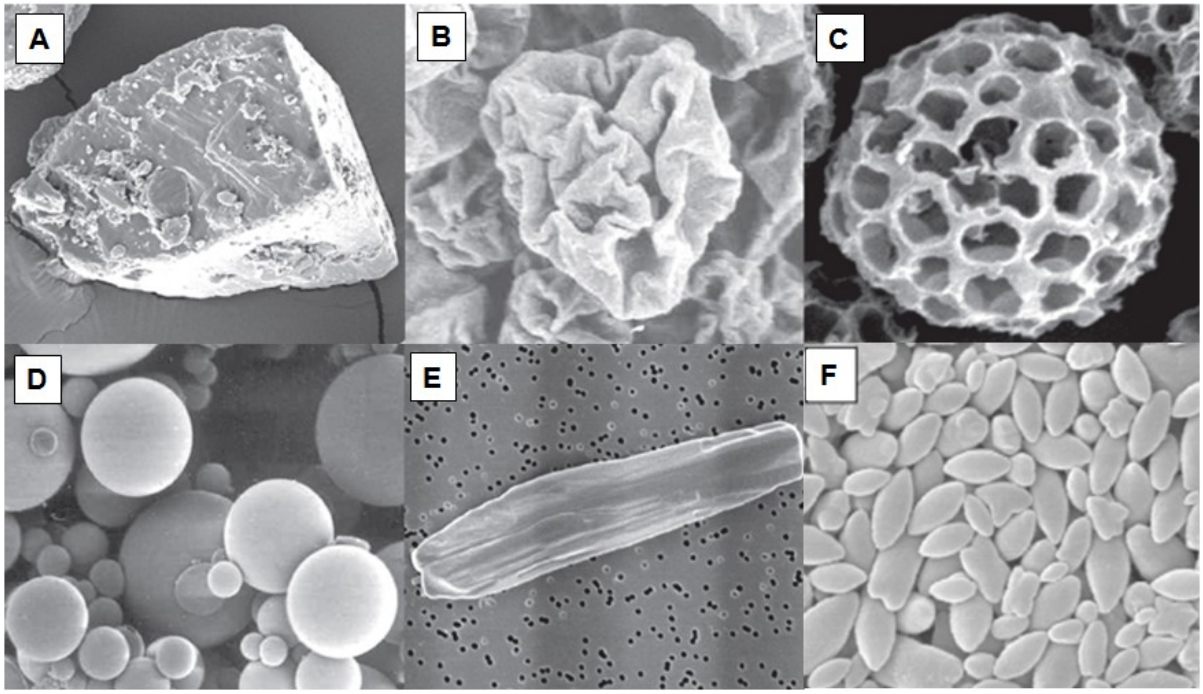

Figure 1.3 Influence of the aspect ratio of fibers on the aerodynamic diameter of the particles [60].

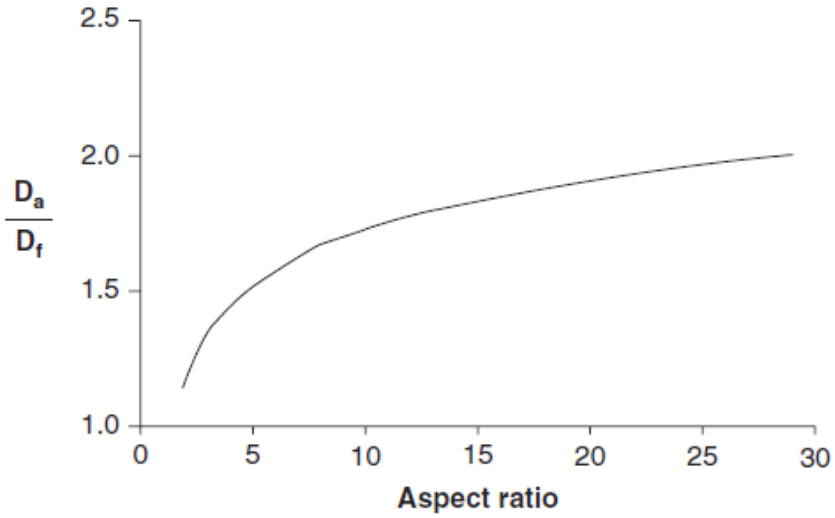

Figure 1.4 Schematic of a single stage inertial impactor

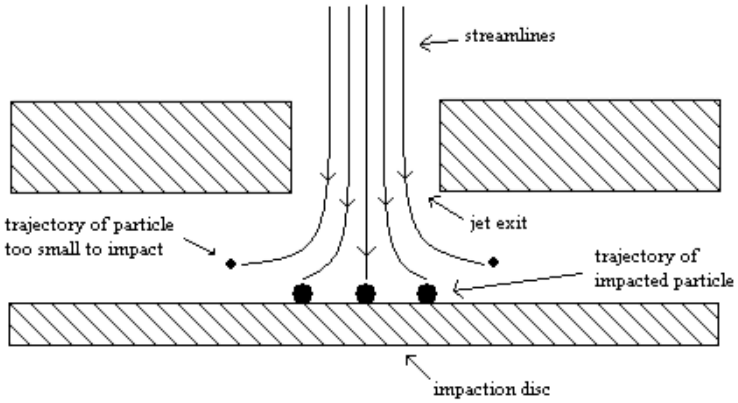

Figure 1.5 Compendial cascade impactors (A) ACI, (B) NGI, (C) MMI, and (D) MSLI

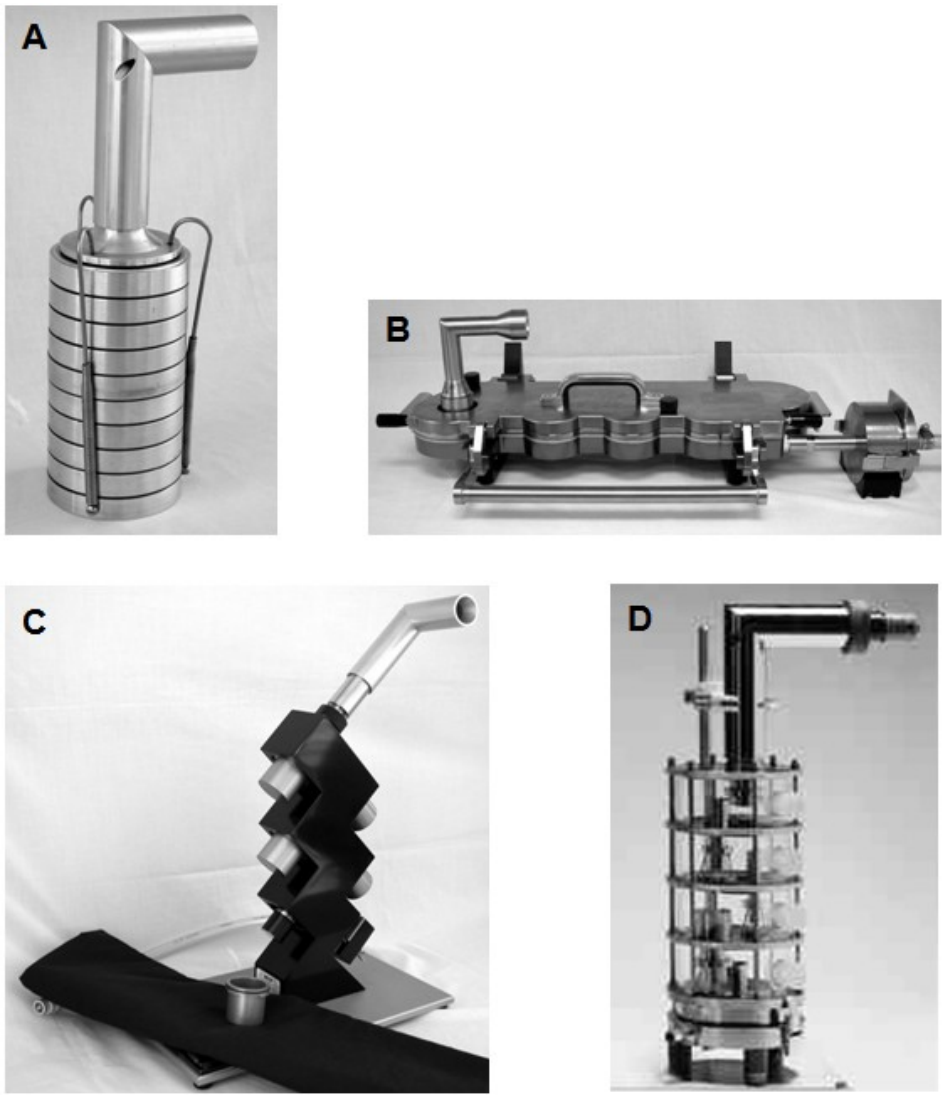

1.7. REFERENCES

[1] K.J. McDonald, G.P. Martin, Transition to CFC-free metered dose inhalers - into the new millennium. Int. J. Pharm. 201(1) (2000) 89-107.

[2] S.K. Vaswani, P.S. Creticos, Metered dose inhaler: past, present, and future. Ann. Allergy Asthma Immunol. 80(1) (1998) 11-19.

[3] L. Hendeles, G.L. Colice, R.J. Meyer, Current concepts - Withdrawal of albuterol inhalers containing chlorofluorocarbon propellants. N. Engl. J. Med. 356(13) (2007) 1344-1351.

[4] M.J. Molina, Rowland, F.S., Stratospheric risk for chlorofluoromethanes: chlorine atom-catalysed destruction of ozone. Nature 249 (1974) 810-812.

[5] R.J. Oenbrink, Unexpected adverse effects of Freon 11 and Freon 12 as medication propellants Journal of the American Osteopathic Association, Vol. 93, 1993, pp. 714-718.

[6] M. Dolovich, New propellant-free technologies under investigation. J. Aerosol Med.-Depos. Clear. Eff. Lung 12 (1999) S9-S17.

[7] D. Lewis, Metered-dose inhalers: actuators old and new. Expert Opin. Drug Deliv. 4(3) (2007) 235-245.

[8] D. Acerbi, G. Brambilla, I. Kottakis, Advances in asthma and COPD management: Delivering CFC-free inhaled therapy using Modulite (R) technology. Pulm. Pharmacol. Ther. 20(3) (2007) 290-303.

[9] R. Dalby, M. Spallek, T. Voshaar, A review of the development of Respimat((R)) Soft Mist (TM) Inhaler. Int. J. Pharm. 283(1-2) (2004) 1-9.

[10] C.L. Leach, P.J. Davidson, R.J. Boudreau, Improved airway targeting with the CFC-free HFA-beclomethasone metered-dose inhaler compared with CFC-beclomethasone. Eur. Resp. J. 12(6) (1998) 1346-1353.

[11] M. Zeidler, Corren, J., Hydrofluoroalkane formulations of inhaled corticosteroids for the treatment of asthma. Treatments in Respiratory Medicine 3 (2004) 35-44.

[12] G. Brambilla, D. Ganderton, R. Garzia, D. Lewis, B. Meakin, P. Ventura, Modulation of aerosol clouds produced by pressurised inhalation aerosols. Int. J. Pharm. 186(1) (1999) 53-61.

[13] J. Peart, Magyar, C., Byron, P.R. , Aerosol electrostatics—metered dose inhalers (MDIs): Reformulation and device design issues. Proceedings of Respiratory Drug Delivery VI, South Carolina (1998) 227-233.

[14] I. Ashurst, Malton Ann, Prime David, Sumby Barry, Latest advances in the development of dry powder inhalers Pharmaceutical Science & Technology Today 3 (2000) 246-256.

[15] I.J. Smith, M. Parry-Billings, The inhalers of the future? A review of dry powder devices on the market today. Pulm. Pharmacol. Ther. 16(2) (2003) 79-95.

[16] H.D.C. Smyth, Hickey, A.J., Carriers in Drug Powder Delivery: Implications for Inhalation System Design. American Journal of Drug Delivery 3 (2005) 117-132.

[17] N.R. Labiris, M.B. Dolovich, Pulmonary drug delivery. Part II: The role of inhalant delivery devices and drug formulations in therapeutic effectiveness of aerosolized medications. Br. J. Clin. Pharmacol. 56(6) (2003) 600-612.

[18] N.R. Labiris, M.B. Dolovich, Pulmonary drug delivery. Part I: Physiological factors affecting therapeutic effectiveness of aerosolized medications. Br. J. Clin. Pharmacol. 56(6) (2003) 588-599.

[19] J.S. Patton, Mechanisms of macromolecule absorption by the lungs. Advanced Drug Delivery Reviews 19(1) (1996) 3-36.

[20] J.S. Patton, Deep-lung delivery of therapeutic proteins. Chemtech 27(12) (1997) 34-38.

[21] J.S. Patton, J. Bukar, S. Nagarajan, Inhaled insulin. Adv. Drug Deliv. Rev. 35(2-3) (1999) 235-247.

[22] D. Prime, P.J. Atkins, A. Slater, B. Sumby, Review of dry powder inhalers. Advanced Drug Delivery Reviews 26(1) (1997) 51-58.

[23] M.P. Timsina, G.P. Martin, C. Marriott, D. Ganderton, M. Yianneskis, Drug-Delivery To The Respiratory-Tract Using Dry Powder Inhalers. International Journal of Pharmaceutics 101(1-2) (1994) 1-13.

[24] L. Borgstrom, E. Derom, E. Stahl, E. WahlinBoll, R. Pauwels, The inhalation device influences lung deposition and bronchodilating effect of terbutaline. American Journal of Respiratory and Critical Care Medicine 153(5) (1996) 1636-1640.

[25] D. Ganderton, General factors influencing drug delivery to the lung. Respiratory Medicine 91 (1997) 13-16.

[26] S.P. Newman, S.W. Clarke, BRONCHODILATOR DELIVERY FROM GENTLEHALER, A NEW LOW-VELOCITY PRESSURIZED AEROSOL INHALER. Chest 103(5) (1993) 1442-1446.

[27] M.G. Cochrane, M.V. Bala, K.E. Downs, J. Mauskopf, R.H. Ben-Joseph, Inhaled corticosteroids for asthma therapy - Patient compliance, devices, and inhalation technique. Chest 117(2) (2000) 542-550.

[28] R. Sankar, N. Sharda, S. Singh, Behavior of decomposition of rifampicin in the presence of isoniazid in the pH range 1-3. Drug Development and Industrial Pharmacy 29(7) (2003) 733-738.

[29] P.J. Barnes, Drugs for asthma. British Journal of Pharmacology 147 (2006) S297-S303.

[30] D. Traini, P.M. Young, Delivery of antibiotics to the respiratory tract: an update. Expert Opinion on Drug Delivery 6(9) (2009) 897-905.

[31] R. Pandey, G.K. Khuller, Antitubercular inhaled therapy: opportunities, progress and challenges. Journal of Antimicrobial Chemotherapy 55(4) (2005) 430-435.

[32] M.T. Newhouse, P.H. Hirst, S.P. Duddu, Y.H. Walter, T.E. Tarara, A.R. Clark, J.G. Weers, Inhalation of a dry powder tobramycin PulmoSphere formulation in healthy volunteers. Chest 124(1) (2003) 360-366.

[33] M. Tobyn, J.N. Staniforth, D. Morton, Q. Harmer, M.E. Newton, Active and intelligent inhaler device development. Int. J. Pharm. 277(1-2) (2004) 31-37.

[34] P.M. Young, R. Price, M.J. Tobyn, M. Buttrum, F. Dey, Investigation into the effect of humidity on drug-drug interactions using the atomic force microscope. Journal of Pharmaceutical Sciences 92(4) (2003) 815-822.

[35] G. Saint-Lorant, P. Leterme, A. Gayot, M.P. Flament, Influence of carrier on the performance of dry powder inhalers. Int. J. Pharm. 334(1-2) (2007) 85-91.

[36] H. Steckel, P. Markefka, H. teWierik, R. Kammelar, Functionality testing of inhalation grade lactose. Eur. J. Pharm. Biopharm. 57(3) (2004) 495-505.

[37] A.H. de Boer, P. Hagedoorn, D. Gjaltema, J. Goede, H.W. Frijlink, Air classifier technology (ACT) in dry powder inhalation - Part I. Introduction of a novel force distribution concept (FDC) explaining the performance of a basic air classifier on adhesive mixtures. Int. J. Pharm. 260(2) (2003) 187-200.

[38] A. Voss, W.H. Finlay, Deagglomeration of dry powder pharmaceutical aerosols. Int. J. Pharm. 248(1-2) (2002) 39-50.

[39] Y.J. Son, J.T. McConville, Advancements in dry powder delivery to the lung. Drug Development and Industrial Pharmacy 34(9) (2008) 948-959.

[40] M.J. Telko, A.J. Hickey, Dry Powder Inhaler Formulation. Respiratory Care 50 (2005) 1209-1227.

[41] P.S.A. Sarinas, T.E. Robinson, A.R. Clark, J. Canfield, R.K. Chitkara, R.B. Fick, Inspiratory flow rate and dynamic lung function in cystic fibrosis and chronic obstructive lung diseases. Chest 114(4) (1998) 988-992.

[42] D. Stanescu, C. Veriter, K.P. Van de Woestijne, Maximal inspiratory flow rates in patients with COPD. Chest 118(4) (2000) 976-980.

[43] E. Guenette, A. Barrett, D. Kraus, R. Brody, L. Harding, G. Magee, Understanding the effect of lactose particle size on the properties of DPI formulations using experimental design. International Journal of Pharmaceutics 380(1-2) (2009) 80-88.

[44] A.H.L. Chow, H.H.Y. Tong, P. Chattopadhyay, B.Y. Shekunov, Particle engineering for pulmonary drug delivery. Pharmaceutical Research 24(3) (2007) 411-437.

[45] H. Steckel, N. Bolzen, Alternative sugars as potential carriers for dry powder inhalations. International Journal of Pharmaceutics 270(1-2) (2004) 297-306.

[46] M.D. Jones, R. Price, The influence of fine excipient particles on the performance of carrier-based dry powder inhalation formulations. Pharmaceutical Research 23(8) (2006) 1665-1674.

[47] X.M. Zeng, G.P. Martin, S.K. Tee, A. Abu Ghoush, C. Marriott, Effects of particle size and adding sequence of fine lactose on the deposition of salbutamol sulphate from a dry powder formulation. International Journal of Pharmaceutics 182(2) (1999) 133-144.

[48] R. Vehring, Pharmaceutical particle engineering via spray drying. Pharmaceutical Research 25(5) (2008) 999-1022.

[49] D.A. Edwards, J. Hanes, G. Caponetti, J. Hrkach, A. BenJebria, M.L. Eskew, J. Mintzes, D. Deaver, N. Lotan, R. Langer, Large porous particles for pulmonary drug delivery. Science 276(5320) (1997) 1868-1871.

[50] L.A. Dellamary, T.E. Tarara, D.J. Smith, C.H. Woelk, A. Adractas, M.L. Costello, H. Gill, J.G. Weers, Hollow porous particles in metered dose inhalers. Pharm. Res. 17(2) (2000) 168-174.

[51] S.P. Duddu, S.A. Sisk, Y.H. Walter, T.E. Tarara, K.R. Trimble, A.R. Clark, M.A. Eldon, R.C. Elton, M. Pickford, P.H. Hirst, S.P. Newman, J.G. Weers, Improved lung delivery from a passive dry powder inhaler using an engineered PulmoSphere (R) powder. Pharm. Res. 19(5) (2002) 689-695.

[52] H. Adi, D. Traini, H.K. Chan, P.M. Young, The influence of drug morphology on the aerosolisation efficiency of dry powder inhaler formulations. Journal of Pharmaceutical Sciences 97(7) (2008) 2780-2788.

[53] S. Adi, H. Adi, P. Tang, D. Traini, H.K. Chan, P.M. Young, Micro-particle corrugation, adhesion and inhalation aerosol efficiency. European Journal of Pharmaceutical Sciences 35(1-2) (2008) 12-18.

[54] H.K. Chan, Dry powder aerosol drug delivery - Opportunities for colloid and surface scientists. Colloids and Surfaces a-Physicochemical and Engineering Aspects 284 (2006) 50-55.

[55] H.K. Chan, What is the role of particle morphology in pharmaceutical powder aerosols? Expert Opinion on Drug Delivery 5(8) (2008) 909-914.

[56] H.K. Chan, I. Gonda, Physicochemical characterization of a new respirable form of nedocromil. J. Pharm. Sci. 84(6) (1995) 692-696.

[57] H.K. Chan, I. Gonda, Respirable form of crystals of cromoglycic acid. J. Pharm. Sci. 78(2) (1989) 176-180.

[58] K. Ikegami, Y. Kawashima, H. Takeuchi, H. Yamamoto, N. Isshiki, D. Momose, K. Ouchi, Improved inhalation behavior of steroid KSR-592 in vitro with Jethaler (R) by polymorphic transformation to needle-like crystals (beta-form). Pharmaceutical Research 19(10) (2002) 1439-1445.

[59] T.T. Hu, H. Zhao, L.C. Jiang, Y. Le, J.F. Chen, J. Yun, Engineering Pharmaceutical Fine Particles of Budesonide for Dry Powder Inhalation (DPI). Industrial & Engineering Chemistry Research 47(23) (2008) 9623-9627.

[60] I. Gondaa, A.F.A.E. Khalikb, On the calculation of aerodynamic diameter of fibers. Aerosol Science and Technology 4(2) (1985) 233-238.

[61] R.O. Cook, R.K. Pannu, I.W. Kellaway, Novel sustained release microspheres for pulmonary drug delivery. Journal of Controlled Release 104(1) (2005) 79-90.

[62] T.P. Learoyd, J.L. Burrows, E. French, P.C. Seville, Chitosan-based spray-dried respirable powders for sustained delivery of terbutaline sulfate. European Journal of Pharmaceutics and Biopharmaceutics 68(2) (2008) 224-234.

[63] J.C. Sung, D.J. Padilla, L. Garcia-Contreras, J.L. VerBerkmoes, D. Durbin, C.A. Peloquin, K.J. Elbert, A.J. Hickey, D.A. Edwards, Formulation and Pharmacokinetics of Self-Assembled Rifampicin Nanoparticle Systems for Pulmonary Delivery. Pharmaceutical Research 26(8) (2009) 1847-1855.

[64] R.O. Salama, D. Traini, H.K. Chan, P.M. Young, Preparation and characterisation of controlled release co-spray dried drug-polymer microparticles for inhalation 2: Evaluation of in vitro release profiling methodologies for controlled release respiratory aerosols. European Journal of Pharmaceutics and Biopharmaceutics 70(1) (2008) 145-152.

[65] P. O'Hara, A.J. Hickey, Respirable PLGA microspheres containing rifampicin for the treatment of tuberculosis: Manufacture and characterization. Pharmaceutical Research 17(8) (2000) 955-961.

[66] J.G. Hardy, T.S. Chadwick, Sustained release drug delivery to the lungs - An option for the future. Clinical Pharmacokinetics 39(1) (2000) 1-4.

[67] R. Salama, D. Traini, H.-K. Chan, P.M. Young, Recent advances in controlled release pulmonary therapy. Current Drug Delivery 6 (2009) 404-414.

[68] S. Suarez, P. O'Hara, M. Kazantseva, C.E. Newcomer, R. Hopfer, D.N. McMurray, A.J. Hickey, Respirable PLGA microspheres containing rifampicin for the treatment of tuberculosis: Screening in an infectious disease model. Pharmaceutical Research 18(9) (2001) 1315-1319.

[69] P. Muttil, J. Kaur, K. Kumar, A.B. Yadav, R. Sharma, A. Misra, Inhalable microparticles containing large payload of anti-tuberculosis drugs. European Journal of Pharmaceutical Sciences 32 (2007) 140-150.

[70] M.J. Kwona, J.H. Baea, J.J. Kima, K. Nab, E.S. Lee, Long acting porous microparticle for pulmonary protein delivery. International Journal of Pharmaceutics 333(1-2) (2007) 5-9.

[71] R. Salama, S. Hoe, H.K. Chan, D. Traini, P.M. Young, Preparation and characterisation of controlled release co-spray dried drug-polymer microparticles for inhalation 1: Influence of polymer concentration on physical and in vitro characteristics. European Journal of Pharmaceutics and Biopharmaceutics 69(2) (2008) 486-495.

[72] Y. Yang, N. Bajaj, P. Xu, K. Ohn, M.D. Tsifansky, Y. Yeo, Development of highly porous large PLGA microparticles for pulmonary drug delivery. Biomaterials 30(10) (2009) 1947-1953.

[73] J.D. Talton, G. Hachhaus, R.K. Snigh, J.M. Fiz-Gerld, Method for preparing coated particle and phamraceutical formulations thereof. US. 6,984,404 (2006).

[74] M. Katsuma, H. Kawai, T. Mizumoto, Novel dry powder inhalation for lung-delivery and menufacturing method thereof. US 2004/0184995 (2004).

[75] M.K. Taylor, A.J. Hickey, M. VanOort, Manufacture, characterization, and pharmacodynamic evaluation of engineered ipratropium bromide particles. Pharm. Dev. Technol. 11(3) (2006) 321-336.

[76] Y.H. Chen, J. Yang, A. Mujumdar, R. Dave, Fluidized bed film coating of cohesive Geldart group C powders. Powder Technology 189(3) (2009) 466-480.

[77] S. Watano, H. Nakamura, K. Hamada, Y. Wakamatsu, Y. Tanabe, R.N. Dave, R. Pfeffer, Fine particle coating by a novel rotating fluidized bed coater. Powder Technology 141(3) (2004) 172-176.

[78] J.P. Mitchell, R.N. Dalby, Characterization of Aerosol Performance. Chapter 5 in Pulmonary Drug Delivery – Basics, Applications and Opportunities for Small Molecules and Bio-Pharmaceuticals, Editio Cantor Verlag, Aulendorf, Germany, , 2006.

[79] V.A. Marple, B.Y.H. Liu, Characteristics of laminar jet impactors. Environmental Science & Technology 8(7) (1974) 648-654.

[80] S.C. Nichols, D.R. Brown, M. Smurthwaite, New concept for the variable flow rate Andersen cascade impactor and calibration data. Journal of Aerosol Medicine-Deposition Clearance and Effects in the Lung 11 (1998) S133-S138.

[81] V.A. Marple, D.L. Roberts, F.J. Romay, N.C. Miller, K.G. Truman, M.J. Holroyd, J.P. Mitchell, D. Hochrainer, Next generation pharmaceutical impactor (A new impactor for pharmaceutical inhaler testing). Part I: Design. Journal of Aerosol Medicine-Deposition Clearance and Effects in the Lung 16(3) (2003) 283-299.

[82] V.A. Marple, B.A. Olson, K. Santhanakrishnan, J.P. Mitchell, S.C. Murray, B.L. Hudson-Curtis, Next generation pharmaceutical impactor (A new impactor for pharmaceutical inhaler testing). Part II: Archival calibration. Journal of Aerosol Medicine-Deposition Clearance and Effects in the Lung 16(3) (2003) 301-324.

[83] M. Tsukada, R. Irie, Y. Yonemochi, R. Noda, H. Kamiya, W. Watanabe, E.I. Kauppinen, Adhesion force measurement of a DPI size pharmaceutical particle by colloid probe atomic force microscopy. Powder Technology 141(3) (2004) 262-269.

[84] B.A. Olson, V.A. Marple, J.P. Mitchell, M.W. Nagel, Development and calibration of a low-flow version of the Marple-Miller impactor (MMI (TM)). Aerosol Science and Technology 29(4) (1998) 307-314.

[85] V.A. Marple, B.A. Olson, N.C. Miller, A low-loss cascade impactor with stage collection cups- calibration and pharmaceutical inhaler applications. Aerosol Science and Technology 22(1) (1995) 124-134.

[86] L. Asking, B. Olsson, Calibration at different flow rates of a multistage liquid impinger. Aerosol Science and Technology 27(1) (1997) 39-49.

[87] D. Christopher, P. Curry, B. Doub, K. Furnkranz, M. Lavery, K. Lin, S. Lyapustina, J. Mitchell, B. Rogers, H. Strickland, T. Tougas, Y. Tsong, B. Wyka, Considerations for the development and practice of cascade impaction testing, including a mass balance failure investigation tree. Journal of Aerosol Medicine-Deposition Clearance and Effects in the Lung 16(3) (2003) 235-247.

[88] R. USP 32- NF27, MD, US Pharmacopeial Convention, Inc. (2009).

[89] V.A. Grey, A.J. Hickey, P. Balmer, N.M. Davies, C. Dunbar, T.S. Foster, B.L. Olsson, M. Sakagami, V.P. Shah, M.J. Smurthwaite, J.M. Veranth, K. Zaidi, The Inhalation Ad Hoc Advisory Panel for the USP Performance Tests of Inhalation Dosage Forms. Pharmacopeial Forum 34(4) (2008) 1068-1074.

[90] M. Asada, H. Takahashi, H. Okamoto, H. Tanino, K. Danjo, Theophylline particle design using chitosan by the spray drying. International Journal of Pharmaceutics 270(1-2) (2004) 167-174.

[91] S. Jaspart, P. Bertholet, G. Piel, J.M. Dogne, L. Delattre, B. Evrard, Solid lipid microparticles as a sustained release system for pulmonary drug delivery. European Journal of Pharmaceutics and Biopharmaceutics 65(1) (2007) 47-56.

[92] J.T. McConville, N. Patel, N. Ditchburn, M.J. Tobyn, J.N. Staniforth, P. Woodcock, Use of a novel modified TSI for the evaluation of controlled-release aerosol formulations. I. Drug Development and Industrial Pharmacy 26(11) (2000) 1191-1198.

[93] E. Ansoborlo, R.A. Guilmette, M.D. Hoover, V. Chazel, P. Houpert, M.H. Henge-Napoli, Application of in vitro dissolution tests to different uranium compounds and comparison with in vivo data. Radiation Protection Dosimetry 79(1-4) (1998) 33-37.

[94] S. Sdraulig, R. Franich, R.A. Tinker, S. Solomon, R. O'Brien, P.N. Johnston, In vitro dissolution studies of uranium bearing material in simulated lung fluid. Journal of Environmental Radioactivity 99(3) (2008) 527-538.

[95] N.Y.K. Chew, H.K. Chan, Use of solid corrugated particles to enhance powder aerosol performance. Pharmaceutical Research 18(11) (2001) 1570-1577.

[96] N. Islam, P. Stewart, I. Larson, P. Hartley, Surface roughness contribution to the adhesion force distribution of salmeterol xinafoate on lactose carriers by atomic force microscopy. Journal of Pharmaceutical Sciences 94(7) (2005) 1500-1511.

[97] A.J. Hickey, H.M. Mansour, M.J. Telko, Z. Xu, H.D.C. Smyth, T. Mulder, R. McLean, J. Langridge, D. Papadopoulos, Physical characterization of component particles included in dry powder inhalers. I. Strategy review and static characteristics. Journal of Pharmaceutical Sciences 96(5) (2007) 1282-1301.

[98] N.Y.K. Chew, P. Tang, H.K. Chan, J.A. Raper, How much particle surface corrugation is sufficient to improve aerosol performance of powders? Pharmaceutical Research 22(1) (2005) 148-152.

[99] Rifampin. Tuberculosis 88(2) (2008) 151-154.

[100] Global Tuberculosis Control, 2007. WHO REPORT (2009).

[101] K. Pethe, D.L. Swenson, S. Alonso, J. Anderson, C. Wang, D.G. Russell, Isolation of Mycobacterium tuberculosis mutants defective in the arrest of phagosome maturation. Proceedings of the National Academy of Sciences of the United States of America 101(37) (2004) 13642-13647.

[102] S. Singh, T.T. Mariappan, R. Sankar, N. Sarda, B. Singh, A critical review of the probable reasons for the poor/variable bioavailability of rifampicin from anti-tubercular fixed-dose combination (FDC) products, and the likely solutions to the problem. International Journal of Pharmaceutics 228(1-2) (2001) 5-17.

[103] Treatment of tuberculosis; guidelines. World Health Organization Fourth edition (2010).

[104] R. Panchagnula, S. Agrawal, Y. Ashokraj, M. Varma, K. Sateesh, V. Bhardwaj, S. Bedi, L. Gulati, J. Parmar, C.L. Kaul, B. Blomberg, B. Fourie, G. Roscigno, R. Wire, R. Laing, P. Evans, T. Moore, Fixed dose combinations for tuberculosis: Lessons learned from clinical, formulation and regulatory perspective. Methods and Findings in Experimental and Clinical Pharmacology 26(9) (2004) 703-721.

[105] H. Bhutani, T.T. Mariappan, S. Singh, The physical and chemical stability of anti-tuberculosis fixed-dose combination products under accelerated climatic conditions. International Journal of Tuberculosis and Lung Disease 8(9) (2004) 1073-1080.

[106] G. Pillai, P.B. Fourie, N. Padayatchi, P.C. Onyebujoh, H. McIlleron, P.J. Smith, G. Gabriels, Recent bioequivalence studies on fixed-dose combination anti-tuberculosis drug formulations available on the global market. Int. J. Tuberc. Lung Dis. 3(11) (1999) S309-S316.

[107] C.J. Shishoo, S.A. Shah, I.S. Rathod, S.S. Savale, M.J. Vora, Impaired bioavailability of rifampicin in presence of isoniazid from fixed dose combination (FDC) formulation. International Journal of Pharmaceutics 228(1-2) (2001) 53-67.

[108] S.Q. Henwood, M.M. de Villiers, W. Liebenberg, A.P. Lotter, Solubility and dissolution properties of generic rifampicin raw materials. Drug Development and Industrial Pharmacy 26(4) (2000) 403-408.

[109] S.Q. Henwood, W. Liebenberg, L.R. Tiedt, A.P. Lotter, M.M. de Villiers, Characterization of the solubility and dissolution properties of several new rifampicin polymorphs, solvates, and hydrates. Drug Development and Industrial Pharmacy 27(10) (2001) 1017-1030.

[110] G. Pelizza, M. Nebuloni, P. Ferrari, G.G. Gallo, Polymorphism of rifampicin. Farmaco-Edizione Scientifica 32(7) (1977) 471-481.

[111] S. Agrawal, Y. Ashokraj, P.V. Bharatam, O. Pillai, R. Panchagnula, Solid-state characterization of rifampicin samples and its biopharmaceutic relevance. European Journal of Pharmaceutical Sciences 22(2-3) (2004) 127-144.

[112] T. Gumbo, A. Louie, M.R. Deziel, W.G. Liu, L.M. Parsons, M. Salfinger, G.L. Drusano, Concentration-dependent Mycobacterium tuberculosis killing and prevention of resistance by rifampin. Antimicrobial Agents and Chemotherapy 51(11) (2007) 3781-3788.

[113] S. Suarez, P. O'Hara, M. Kazantseva, C.E. Newcomer, R. Hopfer, D.N. McMurray, A.J. Hickey, Airways delivery of rifampicin microparticles for the treatment of tuberculosis. Journal of Antimicrobial Chemotherapy 48(3) (2001) 431-434.

[114] R. Sharma, D. Saxena, A.K. Dwivedi, A. Misra, Inhalable microparticles containing drug combinations to target alveolar macrophages for treatment of pulmonary tuberculosis. Pharmaceutical Research 18(10) (2001) 1405-1410.

[115] S.P. Vyas, M.E. Kannan, S. Jain, V. Mishra, P. Singh, Design of liposomal aerosols for improved delivery of rifampicin to alveolar macrophages. International Journal of Pharmaceutics 269(1) (2004) 37-49.

[116] F. Tewes, J. Brillault, W. Couet, J.C. Olivier, Formulation of rifampicin-cyclodextrin complexes for lung nebulization. Journal of Controlled Release 129(2) (2008) 93-99.

[117] F. Ito, K. Makino, Preparation and properties of monodispersed rifampicin-loaded poly(lactide-co-glycolide) microspheres. Colloids and Surfaces B-Biointerfaces 39(1-2) (2004) 17-21.

[118] C. Becker, J.B. Dressman, H.E. Junginger, S. Kopp, K.K. Midha, V.P. Shah, S. Stavchansky, D.M. Barends, Biowaiver Monographs for Immediate Release Solid Oral Dosage Forms: Rifampicin. J. Pharm. Sci. 98(7) (2009) 2252-2267.

[119] C.J. Shishoo, S.A. Shah, I.S. Rathod, S.S. Savale, J.S. Kotecha, P.B. Shah, Stability of rifampicin in dissolution medium in presence of isoniazid. International Journal of Pharmaceutics 190(1) (1999) 109-123.

[120] K. Hirota, T. Hasegawa, H. Hinata, F. Ito, H. Inagawa, C. Kochi, G.I. Soma, K. Makino, H. Terada, Optimum conditions for efficient phagocytosis of rifampicin-loaded PLGA microspheres by alveolar macrophages. Journal of Controlled Release 119(1) (2007) 69-76.

[121] T. Onoshita, Y. Shimizu, N. Yamaya, M. Miyazaki, M. Yokoyama, N. Fujiwara, T. Nakajima, K. Makino, H. Terada, M. Haga, The behavior of PLGA microspheres containing rifampicin in alveolar macrophages. Colloids and Surfaces B-Biointerfaces 76(1) 151-157.

[122] T. Mizoe, T. Ozeki, H. Okada, Application of a Four-fluid Nozzle Spray Drier to Prepare Inhalable Rifampicin-containing Mannitol Microparticles. Aaps Pharmscitech 9(3) (2008) 755-761.

[123] P. Muttil, J. Kaur, K. Kumar, A.B. Yadav, R. Sharma, A. Misra, Inhalable microparticles containing large payload of anti-tuberculosis drugs. European Journal of Pharmaceutical Sciences 32(2) (2007) 140-150.

Chapter 2: Research Outline

2.1. Overall Objectives

The goal of this research was to develop and fully investigate a novel method of antibiotic drug delivery to the lung that will address problems with current therapeutic regimens for treatment of airway infections, specifically, pulmonary tuberculosis (TB). The development of respirable form of dry powder formulations that encapsulate maximum potency of anti-TB drugs and show controlled drug release manner was aimed to increase both the therapeutic effect of delivered drug at the site of infections and the patient compliance. To demonstrate the performance of prepared formulations, suitable characterization methods were also investigated, more specifically, *in vitro* dissolution test method, since there is no optimized *in vitro* model to predict the rate and extent of drug dissolution in the lung following inhalation.

2.2. Specific Objectives

2.2.1. Development of novel *in vitro* dissolution method for inhaled pharmaceutical formulations

There are several *in vitro* methods that exist for the prediction of respirable fraction and site of deposition in the lung following pulmonary administration (e.g. Andersen Cascade Impactor, Next Generation Impactor, Twin Stage Impinger). However, there is no optimized *in vitro* model to predict the rate and extent of drug

dissolution in the lung following inhalation. Currently available methods for evaluating the dissolution behavior of inhalation products rarely consider the impact of particle classification on the dissolution behavior. With pulmonary drug delivery systems, unlike other pharmaceutical dosage forms, only a fraction of the API emitted from standard delivery devices is delivered to the target site of the lung, and the deposited particles in the lung are in a deagglomerated state. Thus, an ideal dissolution test procedure for inhalation formulations would involve a particle classification step followed by an evaluation of the dissolution behavior of those discreet drug particles that could be deposited at various sites in the respiratory tract. The objective of this study was to develop a potential test method to characterize the dissolution properties of aerodynamically classified inhalation formulations. This study was focused the impact of the aerodynamic classification of aggregated powders on dissolution behaviors.

2.2.2. Study factors affecting the dissolution behaviors of aerosol products using experimental and mathematical analysis

A prototype membrane holder that was designed to be used to evaluate the dissolution behaviors of aerodynamically separated particles. Practically this membrane holder method demonstrated that the aerodynamic separation prior to dissolution assessment, has significant influence on the dissolution profile. However, in the dissolution setup using prototype membrane holder, the modification of NGI was required to collect aerodynamically classified drug particles on the membrane, and the whole dose collected on the membrane could not be used for dissolution testing due to a

substantial limitation imparted by the prototype holder frame size. The objective of this study was to develop a new membrane holder which can be directly incorporated with a pharmaceutical impactor, specifically, a Next Generation Impactor (NGI), and to investigate a standardized dissolution method using the newly manufactured NGI membrane holder. Several factors affecting the dissolution behaviors of aerodynamically separate aerosol particles in the NGI membrane holder were determined by both experimental and mathematical analysis.

2.2.3. A new respirable form of rifampicin

Several current studies have been proposed for the administration of anti-tubercular drugs to the primary infection site, the lung, with the idea of increasing the local therapeutic effect and reduce the overall systemic exposure. Specifically, pulmonary delivery of rifampicin (RF) has been widely studied since it is the first choice drug in the treatment of TB. However, the aerosolization properties of developed formulations haven't been adequately addressed to date, and represent the most important factors in determining the drug dose to the target site. The objective of this study was to develop a novel carrier/excipient-free dry powder inhalation (DPI) formulation of RF that has improved aerodynamic properties as well as a good stability profile. This study focused how the dihydrated form of RF (RFDH) was prepared from the pure RF form I, and how the crystalline structure and the physicochemical properties of RFDH were characterized by various analyses. The aerodynamic behavior of prepared RFDH was described with two DPIs; the Aerolizer® and Handihaler®.

2.2.4. Preparation of sustained release rifampicin microparticles for inhalation

Recently, there has been an increased interest in research focusing on DPI formulations to prolong drug residence time in the lung. A sustained release (SR) system has several advantages, including: reduced dosing frequency, improved patient compliance, and reduction in side effects. Specifically, in anti-TB inhaled therapy, it is well established that a SR formulation can enhance the efficacy of anti-TB drugs, presumably by targeting AMs and building up high intracellular drug concentrations [1-3] . However, there are still numerous limitations in manufacturing SR formulations that have good aerosolization properties, high drug payload with controlled drug release capabilities due to their fine particle size. The objective of this study was to develop a novel carrier-free DPI formulation of RF that has a high drug payload, improved aerodynamic properties, and a sustained release capability. A spray-drying method was used to impart a hydrophobic coating of the dihydrate form of RF. The impacts of spray nozzles used for coating process on the coating properties were studied. The aerodynamic behaviors of prepared formulations were studied with a DPI device, the Aerolizer®. The dissolution behaviors of coated and uncoated formulations were evaluated using a newly developed membrane holder method.

2.3. REFERENCES

[1] S. Suarez, P. O'Hara, M. Kazantseva, C.E. Newcomer, R. Hopfer, D.N. McMurray, A.J. Hickey, Respirable PLGA microspheres containing rifampicin for the treatment of tuberculosis: Screening in an infectious disease model. Pharmaceutical Research 18(9) (2001) 1315-1319.

[2] S. Suarez, P. O'Hara, M. Kazantseva, C.E. Newcomer, R. Hopfer, D.N. McMurray, A.J. Hickey, Airways delivery of rifampicin microparticles for the treatment of tuberculosis. Journal of Antimicrobial Chemotherapy 48(3) (2001) 431-434.

[3] J.C. Sung, D.J. Padilla, L. Garcia-Contreras, J.L. VerBerkmoes, D. Durbin, C.A. Peloquin, K.J. Elbert, A.J. Hickey, D.A. Edwards, Formulation and Pharmacokinetics of Self-Assembled Rifampicin Nanoparticle Systems for Pulmonary Delivery. Pharmaceutical Research 26(8) (2009) 1847-1855.

Chapter 3: Development of a Novel Dissolution Test Method for Inhaled Pharmaceutical formulations[3]

Abstract

The aim of this research was to investigate a potential standardized test method to characterize the dissolution properties of formulations intended for pulmonary delivery. A USP type 2 dissolution tester was adapted to be used as a testing apparatus by incorporation of a membrane containing holder. The membrane holder was designed to enclose previously size-classified formulations, so that they could be uniformly tested in the dissolution apparatus. The influence of particle size, amount of drug loading, and the composition of a simulated lung fluid (SLF) dissolution media on the dissolution rate were studied. Dissolution rate was significantly affected by the uniformity of drug loading, and particle size. Diffusion coefficients, estimated using the Higuchi model, showed an increase from 2.28×10^{-7} cm^2/hr to 9.60×10^{-7} cm^2/hr as the particle size decreased. Addition of DPPC (0.02% w/v) to the SLF dissolution media also resulted in an increase in the diffusion coefficient value. This study demonstrated that developed method was reproducible and may be used to evaluate the dissolution properties of pharmaceutical inhalation products following their aerodynamic particle classification.

[3]Significant portions of this chapter were taken from : Yoen-Ju Son and Jason T. McConville, "Development of a standardized dissolution test method for inhaled pharmaceutical formulations", International Journal of Pharmaceutics, 2009, 382, P:15–22.

3.1. INTRODUCTION

Dissolution testing is an extremely well established and standardized test in all the Pharmacopoeias for evaluating solid and semi-solid dosage forms. Dissolution testing allows one to examine the dissolution behavior of pharmaceutical dosage forms *in vitro* in order to differentiate formulation types and perhaps give an estimate of a dissolution behavior *in vivo*. Dissolution testing is routinely used in quality control (QC) studies such as batch to batch consistency, stability, and detection of manufacturing deviations. While there are many standardized dissolution test methods for solid dosage forms such as tablets and capsules, there is no applicable method to estimate the dissolution behavior of inhaled active ingredients, although many dissolution methods for testing aerosols have been attempted [1]. Designing a standardized method applicable to the lung is not an easy task, as the lung has very unique features which are difficult to replicate *in vitro*, such as the extremely small amount of aqueous fluid and lung surfactant [1, 2]. Additionally, it would require that the collection of the specific API size fraction from the entire formulation before dissolution testing, as many inhalation products contain large carrier materials. Additionally, several experimental difficulties exist on dose collecting due to very fine and electrostatic powder characteristics [1].

Commercial dissolution systems have been widely used to study the dissolution of aerosols. Dry powders have been directly dispersed into an apparatus 2 dissolution tester [3], or placed directly into a modified basket to prevent drug particles from escaping directly into to the dissolution media [4, 5]. However, dry powders intended for

pulmonary delivery are hard to disperse homogeneously into the vessel/basket, and dispersed particles stick on the vessel wall and/or paddle/basket during such dissolution tests. In addition, floating powders may be inadvertently collected during the sampling procedure. In an attempt to make up for some of the shortfalls of this type of testing using standardized pharmacoepial dissolution systems, several custom built dissolution apparatuses have been investigated. Davies and Feddah modified a flow-through cell by direct incorporation of HPLC pump [6]. In this method the aerosol particles, obtained using impaction, were collected onto a glass pre-filter for dissolution studies. In another study using a horizontal diffusion cell, manufactured powders were dispersed onto the hydrated membrane and the dissolution rate was estimated by observing their diffusion rate [7]. In addition to these methods, twin-stage impinger (TSI) [8], dissolution cell [9, 10], transwell [11] and shaking incubator [12, 13] apparatuses were also modified to conduct *in vitro* dissolution studies of dry powders. Although, these approaches do in some way make up for the drawbacks indicated above for standardized dissolution apparatuses, problems are still evident such as the impact of the amount of drug loading, adequate particle dispersion, and the uniformity of particle size distribution. Therefore, no single *in vitro* test system has yet emerged as the ideal choice for performing dissolution measurements for inhalation formulations.

The aim of this paper is to describe a potential standardized test method to characterize the dissolution properties of the multitude of formulation types available for pulmonary delivery. Micronized hydrocortisone (HC) was selected as a model drug to

conduct *in vitro* dissolution on dry powders that were aerodynamically classified using the Next Generation Impactor (NGI).

3.2. MATERIALS AND METHODS

3.2.1. Materials

Micronized hydrocortisone (HC) (USP grade) and size 3 empty gelatin capsules were purchased from the Spectrum Chemical Co. (Gardena, CA). Dipalmitoyl phosphatidylcholine (DPPC) was purchased from Avanti Polar Lipid, Inc. (Alabaster, AL). InhaLac®70 was donated by Meggle (Wasserburg, Germany). Polycarbonate (PC) membranes of 0.05 μm and 1 μm were purchased from Whatman (Florham Park, NJ). Cellulose acetate (CA) dialysis membranes with molecular weight cut-off (MWCO) sizes of 3500 and 12000 were purchased from Spectrum®Laboratories INC. (Rancho Dominguez, CA). An Aerolizer® was donated by Schering-Plough (Kenilworth, NJ). Histology cassettes were purchased from VWR International, LLC (Suwanee, GA). Methanol (HPLC grade) and all other reagents were purchased from the Sigma Chemical Co. (St. Louis, MO).

3.2.2. Solubility studies

The solubility of HC was determined in simulated lung fluid (SLF), and modified simulated lung fluid (mSLF). The mSLF contained 0.02% w/v DPPC in addition to the standard ingredients contained in the SLF. Samples of HC (100 mg) were added to 20 mL

SLF, or 20 mL mSLF and shaken for 24 hours at 37°C. Samples (1 mL) were taken from each vial at 1, 2, 4, 8, 12, and 24 hour intervals and filtered using 0.45μm syringe filters. All the samples were analyzed using a Agilent 8453 UV/VIS spectrophotometer (Santa Clara, CA) at 248 nm, the resultant equilibrium sample concentration was used to calculate the saturated solubility concentration.

3.2.3. Dissolution apparatus

A standard type 2 dissolution tester, Hanson SR8-plus dissolution test station (Hanson Co., Chatsworth, CA), was employed to conduct the dissolution study of micronized HC particles. A schematic diagram of modifications to the dissolution apparatus is shown in Figure 3.1. The two main components of the dissolution setup include: Component (A) the dissolution test station and component (B) a membrane holder. (A) the dissolution station consisted of i) mini-paddles (for 150 mL vessel), ii) dissolution vessels (150 mL glass vessel round-bottom), iii) a water bath, and iv) a sampling probe with 10 μm filter tip. The membrane holder (B) was customized and consisted of a histology cassette frame, with two pieces of selected membrane sandwiched inside the frame (acting a powder holding device).

3.2.4. Dose collection

3.2.4.1. Aerodynamic particle separation

Particle separation of both bulk HC, or HC mixed with carrier lactose was conducted using a modified Next Generation Impactor (NGI) (MSP Co. Shoreview, MN).

Figure 3.3 (A) shows assembled NGI collecting plates. The NGI was fitted with a PC membrane at the base of each dose-collection plate. This membrane was placed beneath wax paper (which had been pre-trimmed to match the plate shape). A rectangular uniformly sized hole was pre-cut (2×2.5 cm) in the center of the trimmed wax paper that exposed the PC membrane situated beneath it. Micronized HC (2 g) was mixed with 30 g InhaLac® 70, and 150 mg of the powder mixture was filled into #3 empty gelatin capsules. Bulk HC (50 mg), without carrier, was also filled into #3 empty gelatin capsules. Capsules were placed into the Aerolizer® (Schering-Plough, Kenilworth, NJ) and the device was primed according to the manufacturer's guidelines. Each of the HC containing capsules were dispersed into the NGI through the USP induction port at the flow rate 60 L/min, for 15 seconds per each actuation. The flow rate was measured by a Model DMF 2000 flow meter (MSP Co. Shoreview, MN).

3.2.4.2. Scanning electron microscopy (SEM)

Micronized bulk HC, and HC following particle separation by impingement were observed using a LEO 1530 SEM (Zeiss/LEO, Oberkochen, Germany). In this procedure each PC membrane containing separated HC particles was removed from the appropriate dose-collection plate of NGI and cut into a small segment (suitable for mounting on a pin plate SEM stub). The cut membrane segments from each dose-collection plate were mounted separately onto the stubs using double-sided copper tape, before sputter coating with Ag for 40 seconds under vacuum at 30 mTorr. Additionally, bulk HC powder was

mounted and coated as described above. The SEM was operated at high vacuum with accelerating voltage 5kV and specimen working distance of 4 mm.

3.2.5. Dissolution testing

3.2.5.1. Dissolution media

Simulated lung fluid (SLF), and modified SLF (mSLF) containing 0.02% (w/v) of dipalmitoylphosphatidylcholine (DPPC) were used for dissolution study. The SLF was first developed by Moss [14], and was described as being close to that of actual lung fluid in ionic composition and pH. The mSLF differs from the SLF by adding 200 μg/mL DPPC to 100 mL of SLF solution. Both SLF and mSLF have been used in previous published *in vitro* dissolution studies due to their similarity in composition to actual lung fluid [6, 9, 10].

To prepare the mSLF, DPPC (200 mg) was weighed into a 500 mL round bottom flask and dissolved into a 40 mL chloroform/methanol (1:1) mixture. The solvent was evaporated by rotary evaporation (Buchi Corporation, New Castle, DE). The dry thin film was rehydrated with 200 mL distilled water at 55°C and rotated for 2 hrs. The warm suspension was placed into a Branson 5500 sonic bath (Branson ultrasonics, Denbury, CT) and sonicated at 55°C for 1 hour. The concentrated DPPC solution (0.2% w/v) was stored at 4°C. The stock DPPC solution (0.2% w/v) was diluted 10 fold with SLF before use.

3.2.5.2. Dissolution testing of bulk HC particles

Using the apparatus setup described above the dissolution medium was equilibrated at 37°C and the paddle speed was set to 50 rpm. Both bulk micronized HC and dispersed HC onto a membrane was tested. Firstly, bulk micronized HC (3 mg) was carefully weighed, and dispersed into each of 3 dissolution vessels containing 100 mL of SLF. Secondly, 3 mg HC was weighed separately onto a membrane (either PC or CA dialysis membranes). A second pre-soaked membrane with SLF of the same type was placed on top of the first membrane containing the powder; this was then sandwiched together and fitted into the membrane holder. Each holder was placed into a small volume dissolution vessel containing 100 mL of SLF (sink conditions were given all the test samples). Samples were manually withdrawn from the dissolution vessel at 0.5, 1, 1.5, 2, 3, 4, and 6 hours to be analyzed by HPLC. The cumulative amount of dissolved HC was determined from the sum total of HC released.

3.2.5.3. Dissolution testing of aerodynamically separated HC particles

To aerodynamically classify carrier-free HC and carrier-mediated HC, capsules containing each formulation were fired separately into the NGI at the flow rate 60 L/min as previously described. The NGI dose-collection plates were assembled as above (with PC membranes and wax paper impaction templates). Following actuation for a given formulation the wax paper impaction template was removed from each dose-collection plate, and a PC membrane (pre-soaked with the appropriate dissolution media) was placed onto the top of each plate membrane (that now contained impinged HC particles).

The sandwiched membrane enclosed into the membrane holder as above, was then placed into a dissolution vessel (100 mL, 37°C, and 50 rpm, sink conditions were maintained for all of the test samples). The release rate of HC in either SLF and mSLF media were evaluated. Samples were withdrawn manually at the following time points: 10, 20, 40, 60, 90, 120 minutes (SLF), and 5, 15, 30, 60, 90 minutes (mSLF). All samples were analyzed by HPLC. The residual amount of HC on the membranes was determined after the test by washing with 5 mL mobile phase prior to analysing using a validated HPLC method. The total amount of HC initially loaded between two membranes was back calculated using the sum of cumulated amount of HC, plus the remaining quantity of HC on each of the membrane holder.

3.2.6. Analysis of HC dissolution with SLF or mSLF

Collected samples from the dissolution studies that used SLF or mSLF were analysed by using a HPLC system (Waters Co., Milford, MA) with UV detection. The system consisted of a 717 plus autosampler, 2487 dual wavelength detector, 1525 binary pump, and 1500 column heater. Dissolution samples of HC in SLF or mSLF were filtered using 0.45 μm PTFE syringe filter before injection. Chromatography was performed using a Capcell Pak C18 5 μm 4.6×250 mm column (The Shiseido Fine Chemicals, Tokyo, Japan) and a SecurityGuard™ guard column (Phenomenex®, Torrance, CA). The mobile phase which consisted of methanol, water, and phosphate buffer solution pH 7.4 in a ratio of 10:10:0.4 respectively, was eluted at a flow rate of 1.0 mL/min and the UV

detector was set to a wavelength 220 nm [15]. The column temperature was maintained at 40°C and the volume of each sample injected was 20 μL [15].

3.2.7. Mathematical modeling

A diffusion coefficient for each dissolution study was determined using computer fitted data. The least square method was performed using MatLab (The Mathworks Inc., Natick, MA). The multidimensional unconstrained nonlinear minimization (Nelder-Mead) method was used as an algorithm.

3.2.8. Statistical analysis

Data were expressed as the mean plus/minus standard deviation (SD). The statistical differences of release rates were studied by analysis of variance (ANOVA) using Jump 7.0 software (SAS Institute Inc., Cary, NC). Dissolution rate differences between, each NGI dose-collection plate containing different median particle sizes, were compared at several time points using a 1-way ANOVA. To identify the statistically significant differences between groups, Tukey-Kramer test was used. α value of 0.05 was applied to denote statistical significance. SD values were compared to assess consistency of release. *P* values of less than 0.05 were considered as statistically significant.

3.3. RESULTS

3.3.1. Solubility

The saturated solubilities of HC in mSLF and SLF were 461 μg/mL and 345 μg/mL, respectively. As indicated in the results, the addition of DPPC to SLF increased the solubility of HC. These results are in good agreement with the solubilising effect of lung surfactant, previously reported in the literature by several groups [16, 17].

3.3.2. Membrane holder optimization

A membrane holder was newly designed for conducting the dissolution studies of dispersed particles (Figure 3.1). To select a suitable membrane as the diffusion layer of dissolved drug, dissolution studies of model drug, HC, with three different membranes were conducted. In a comparison study between PC and CA dialysis membranes, the PC membrane demonstrated faster release of HC than that of other membranes as shown in Figure 3.2. An additional advantage was that the sandwiched PC membranes did not facilitate the formation of entrapped air between membranes, and visually demonstrated a tight seal due to their thin and rigid structure within the membrane holder. In contrast, entrapped air was readily seen between sandwiched CA dialysis membranes during dissolution.

3.3.3. Aerodynamic particle separation of HC particles

HC aerosol particles were collected using the NGI (impaction plates before and after device actuation impingements are shown in Figure 3.3). In the figure, the wax paper impaction template can be clearly seen. Separated particles accumulated on the wax paper templates and exposed area of the PC membranes (under the template) on each dose-collection plate. The dispersion state of particles collected on each dose-collection plate was observed by SEM and is shown Figure 3.4. The SEM images show that bulk HC particles consist of irregularly shaped crystals ranging <1 to 5 μm. On the other hand, aerodynamically separated particles on each dose-collection plate displayed a very homogenous dispersion. The sizes of collected particles on dose-collection plates 3, 5, and 6 could be separated into ranges of approximately 3, 1, <1 μm, respectively. Dose-collection plate cut-off particle sizes calibrated from the NGI are reported to be 4.46, 2.82, 1.66, 0.94, 0.55, 0.34 μm at an inlet flow rate 60 L/min for dose-collection plates 2-7, respectively [18, 19].

3.3.4. Dissolution

3.3.4.1. Dissolution testing of bulk HC particles

The dissolution behavior of micronized bulk HC was compared using two different dissolution methods, dissolution setup with a membrane holder and without a membrane holder. In this study, the impact of powder loading into the dissolution vessels on the test reproducibility and the dissolution of HC powders were investigated. As shown in Figure 3.5, the dissolution profiles of dispersed HC powders without membrane

holder into the dissolution vessel was much more variable than that of the same powder enclosed inside the membrane holder. However, there were no significant differences in the total dissolved amount of HC between the two methods. This result suggests that the membrane holder used in this study had no significant influence on the diffusion of dissolved drug, or diffusion of dissolution media into the holder.

3.3.4.2. Dissolution testing of aerodynamically separated HC particles

Influence of membrane pore size

The influence of membrane pore size on the drug release profile was studied. PC membranes having different pore sizes (0.05 μm and 1μm) were tested. Figure 3.6 shows the release profiles of HC enclosed in two different membrane holders. It appears that the release profiles of HC particles accumulated in dose-collection plate 2 are not significantly different between the membranes. The PC membrane having pore size of 1 μm hindered initial drug release of HC particles accumulated in dose-collection plate 6 which have a median particle size of 0.55 μm. There is greater than a 20% difference in drug release rate in the first 40 minutes.

Influence of particle size and drug loading

The influence of powder presentation inside the membrane holder on the dissolution was studied. The total amount of loaded HC, by mass, following aerodynamic separation for dissolution studies is summarized in Table 3.1. Figure 3.7 shows release

profiles of HC for each NGI dose-collection plate. When the formulation contains a lactose carrier, the accumulated amount of HC on each dose-collection plate appeared to increase, as the NGI dose-collection plate number decreases (demonstrating the apparent efficiency of the carrier at preventing particle aggregation prior to deposition). The results demonstrate that the release rate of HC increases with decreasing particle size and amount of loading in accordance with the Noyes-Whitney equation for dissolution (as the exposed surface area is increased per unit mass of drug deposited). The degree of significance of these two factors on the release rate was further confirmed by the following studies. Multiple actuations were conducted to obtain different drug loadings, followed by dissolution testing. For each actuation, an average dose of 300 μg was collected on dose-collection plate 2, and 70 μg of HC powders were accumulated on the dose-collection plate 6. As shown in Figure 3.8, the dissolution rates of smaller particles are less affected by amount of loading drug compared to that of bigger particles.

As expected for the carrier-free HC, amount of loading is much more variable between actuations of the Aerolizer® compared to the carrier-mediated HC powders as shown in Table 3.1. The release profiles shown in Figure 3.9 reflect this non-uniform drug loading very well. A large degree of variability due to the irregular powder deposition is observed.

Influence of dissolution media

Figure 3.10 shows the release profiles of HC for dose-collection plates 2 and 6 in SLF or mSLF. The release rates of HC increased with the addition of 0.02% DPPC,

which was expected given the results from the solubility study that demonstrated increased saturation solubility in the media containing DPPC. The media containing DPPC may increase the wettability of hydrophobic drugs, and prevent aggregation to allow an enhanced dissolution rate [16, 17].

3.3.5. Diffusivity from the membrane holder

To verify the agreement between experimentally obtained results and a present mathematical diffusion model, the release profiles of HC particles were fitted to the Higuchi model (Equation 1), using the least square method, as shown in Figure 3.11. According to the Higuchi model [20], the cumulative amount of drug released from the holder per unit area, Q ($\mu g/cm^2$), under sink condition is as follows:

$$Q = hC_o\left[1 - \frac{8}{\pi^2}\sum_{m=0}^{\infty}\frac{1}{(2m+1)^2} \times \exp\left(-\frac{D(2m-1)^2\pi^2 t}{4h^2}\right)\right] \qquad \text{(Equation 1)}$$

Where, h = thickness of PC membrane, C_0 = initial loading concentration of drug, D = diffusion coefficient of drug, t = time after application and m = integer (from 0 to ∞).

Using this fit from Equation 1, C_0 and D could be calculated from the data (Table 3.2). An important parameter, the volume of media (V) inside the holder could be calculated from obtained the C_0 and from the experimental data. As shown in Table 3.2, overall volume of media between two membranes was constant, approximately 6 μL, suggesting that the test condition inside the holder are very reproducible. C_0 increased

with increasing HC mass (M) in the membrane holder. The diffusion constant (D) also increased with decreasing particle size, decreasing C_0, or the addition of 0.02% DPPC. The D values, therefore, suggest that DPPC helps the migration of HC molecule from inside the holder into the dissolution vessel.

3.3.6. Statistical analysis

The HC mixed with carrier lactose shows more consistent release rates compared to that of carrier-free HC. Overall the relative standard deviation (% RSD) values were <10 in the case of carrier-mediated HC and > 30 for carrier-free HC. The release rate differences between the NGI dose-collection plates were much clearer with the carrier-mediated HC particles ($p < 0.05$) than that of carrier-free HC particles ($p > 0.05$). For the carrier-mediated HC, the dissolution rate of the particles accumulated on dose-collection plate 6 was significantly different from that of all other groups for initial 40 minutes by Tukey-Kramer test. The differences between groups became less defined as dissolution reached 100% release. The influence of DPPC (0.02% w/v) on the release rate was not statistically significant, although DPPC helps with the solubilization of the drug as evidenced by the solubility data.

3.4. DISCUSSION

3.4.1. Dissolution apparatus

A novel dissolution method for inhaled pharmaceutical formulations was developed, which comprised a commercial dissolution system, and a membrane holder as a formulation holding device. The mechanism of this dissolution method can be explained by dissolution-diffusion controlled drug release from the membrane holder. During the dissolution process using the membrane holder, the dispersed drug sandwiched between two membranes undergoes dissolution as dissolution media migrates through the pores on the membrane surface and the dissolved drug then releases out to the reservoir by diffusion.

A PC membrane was selected as a diffusion layer of the holder. As shown in Figure 3.2, the PC membrane demonstrated almost a two-fold increase in drug release rate than CA dialysis membranes over the test period. This difference can be explained by the differences in physical structure of the two membranes. PC membranes are thin (approximately 6 μm) but still relatively robust for their handling requirements. Additionally, they do not swell and have a well-defined uniform pore size [21, 22], consisting homogeneous 0.05 μm cylindrical pores on the surface, to allow free diffusion of dissolved drug and dissolution media. These uniform characteristics are important for the purposes of this dissolution study because they can affect diffusion properties of dissolved drug. In contrast to PC membranes, although CA membranes have been successfully applied in various dialysis studies [23], many drawbacks have been reported

such as reduction of permeability induced by protein adsorption on the membrane surface, thick membrane structure, and swelling [24, 25].

The PC membrane surface of the holder constitutes a perfect sink for the released drug. Dissolution media is able to rapidly diffuse into the holder and reach the drug inside through the numerous pores, subsequently allowing dissolved (released) drug to be immediately removed from the exposed membrane face under suitable hydrodynamic conditions. In comparison study between two different dissolution setups (with or without a membrane holder), no significant difference was found in the total dissolved amount of HC between the two methods, but the reproducibility was greatly affected (Figure 3.5). The differences in test reproducibility may suggest that dissolution properties of the dispersed particles varies considerably depending on their degree of aggregation, and may have a more profound meaning when one considers the electrostatic properties of inhalable formulations. As previously mentioned, fine dry powders are hard to disperse homogeneously, they may stick on the dissolution vessel wall or paddle, and they may also agglomerate. Conversely, powders enclosed within the membrane holder demonstrated a very consistent dissolution rates. This is due mainly to the uniform diffusion area of membrane holder (10 cm^2), presented to the dissolution media, and the uniformity of the membrane barrier preventing premature particle escape (and a subsequent change in the surface area of drug presented to the media).

3.4.2. Dissolution studies

It was confirmed that the PC membrane having a pore size of 0.05 μm provided a perfect sink condition to the aerodynamically separated HC particles inside the holder. As shown in Figure 3.6, the obtained release profiles from two membrane holders are almost same for the big particles (dose-collection plate 2 of the NGI). However, PC membranes with larger pores often act as a diffusion barrier for small particles with similar particle size distribution to the membrane pore size. The enclosed particles are homogeneously separated thus, are easily released into the reservoir in the undissolved form and may clog the membrane pores in the process of escaping.

The dissolution profiles of inhalation formulations were influenced by powder presentation inside the holder. As shown in Figure 3.3 (B), the dispersed powders form a powder bed on each dose-collection plate and the thickness of the powder bed is dependent on the amount drug loaded on each membrane. A larger amount of drug loaded on each dose-collection plate corresponds to a thicker powder bed deposited on the membrane (which would possibly lead to particle bounce with older types of vertical cascade impaction designs). Given that a thicker powder layer is deposited on the PC membrane then it follows that there will be more dissolution/diffusion activity required to release all of the drug from the inner space of the membrane holder. The size distributions of drug particles which constitute a powder bed also have effect on the dissolution rate. Bigger particles loaded inside the holder require more energy input to be completely dissolved and released out because the portion of the drug that remains undissolved inside the membrane holder acts as reservoir, allowing drug to dissolve in

accordance with the Noyes-Whitney equation [26]. Thus, the release rate of drug could be attributed to both particle size and amount of loading. The extent of significance of these two factors on the release rate can be explained from the data presented in Figure 3.8. The results demonstrated that the release rates of the powder bed consisting of smaller particles were less influenced by the amount of loaded drug on the membrane due to their ability to wet and dissolve quickly (as the exposed surface area is increased per unit mass of drug). It indicates that the amount of loading may determine the extent of powders wetting, and particle size could determine dissolution rate of the wetted particles inside the holder.

This dissolution test setup may be directly applicable to the quality control studies for inhalation products, where the performance of carrier based delivery and the effect of electrostatic interaction of powders is critical for lung deposition and disease management. As shown in Figure 3.9, the dissolution profiles of aerodynamically dispersed particles reflect a powder dispersion status. For the carrier-free HC powder, a large degree of variability in test reproducibility was found due to the non-uniform drug loading, which can be directly attributed to the propensity of powder wetting within the membrane holder. Additionally, this method can be used to examine the dissolution behaviors of inhalation dosage forms with similar particle distribution by selecting drug particles accumulated in same dose-collection plate. It can be expected that dissolution of particles having similar size distribution may provide more discriminative capability to the result in formulation variables.

The dissolution media containing DPPC (mSLF) can be used to predict the solubility and solubilization process of inhalation formulations which have very low aqueous solubility. DPPC increases the wettability of hydrophobic drugs, and prevents aggregation to allow for an enhanced dissolution rate [16, 17] as shown in Figure 3.10. These results are in good agreement with the solubilising effect of lung surfactant, previously reported in the literature by several groups [16, 17].

3.4.3. Mathematical modeling

Higuchi model was applied to calculate several unknown factors, such as D, C_o and V. The Higuchi model is known to be a very simplified mathematical model to evaluate the release behaviours of matrix systems [26]. In particular, the Higuchi equation well describes the release kinetics of models based on a moving dissolution front that proceeds inwards with time separating a region of coexisting solid and dissolved drug from a region of completely dissolved drug. From the Higuchi equation (Eq. 1), D values for all the experimental release data were calculated (Table 3.2). The calculated D values are in good agreement with experimentally obtained release data. D values increased with decreasing particle size, decreasing C_0, or the addition of 0.02% DPPC. The D values, therefore, suggest that DPPC helps the migration of dissolved HC molecules from inside the membrane holder into the dissolution vessel. Additionally, it indicates that non-uniform drug loading, and non-uniform size distributions (which are directly related to the device or aerosol performance) could contribute to diffusion rate of drug from the membrane holder. Generally, beyond saturated solubility, the amount of

initially loaded drug inside holder doesn't affect its release, if drug particles are evenly dispersed in the whole holder [27]. However, in the holder, sandwiched powders between two membranes form a layer so that the dissolution of drug gradually progresses inward layer by layer, until all solid drug particles have been wetted and dissolved. Consequently, the diffusion rate of molecules is governed by the thickness of the drug layer, and the solubilization rate of that drug layer.

3.5. CONCLUSION

A new dissolution testing prototype apparatus for evaluating the *in vitro* dissolution behavior of inhalation formulations was designed. The dissolution rate of drug can be successfully estimated by analyzing the amount of drug released from the prototype membrane holder. This dissolution method may be used to quality control study for various dry powder inhalers (DPIs); in particular, the *in vitro* dissolution profiles of drug may provide an estimate of its dispersion characteristics which directly related to the device or aerosol performances.

3.6. TABLES

Table 3.1 Loaded amount of HC into the membrane holder for each stage. HC powders were loaded by aerodynamic separation of carrier-free HC and carrier-mediated HC.

NGI Collection-Plate	Carrier-Free HC (mg)			Carrier-Mediated HC (mg)		
	Run 1	Run 2	Run 3	Run 1	Run 2	Run 3
Stage 2	2.97	0	3.02	0.76	0.60	0.80
Stage 3	4.33	5.14	6.12	0.37	0.46	0.59
Stage 5	2.31	6.10	1.57	0.32	0.36	0.29
Stage 6	0.53	2.70	0.76	0.05	0.07	0.05

Table 3.2 Estimated parameters calculated by data from release experiments. Standard deviation was calculated on three different tests.

Test Sample	M (mg ± SD)	C_0 (μg/mL)	V (μL)	D (cm^2/hr)
Stage 2-SLF	0.72 ± 0.11	10.9×10^4	6.62	2.28×10^{-7}
Stage 3-SLF	0.47 ± 0.11	7.90×10^4	5.96	2.70×10^{-7}
Stage 5-SLF	0.32 ± 0.04	5.22×10^4	6.15	3.15×10^{-7}
Stage 6-SLF	0.06 ± 0.01	0.86×10^4	6.41	9.60×10^{-7}
Stage 2-mSLF	0.62 ± 0.05	9.54×10^4	6.55	4.86×10^{-7}
Stage 6-mSLF	0.06 ± 0.02	1.46×10^4	6.20	18.9×10^{-7}

3.7. FIGURES

Figure 3.1 Schematic diagram of the dissolution apparatus. Component A: dissolution station i) mini-paddles (for 150 mL vessel), ii) dissolution vessels (150 mL glass vessel round-bottom), iii) water bath, and iv) sampling probe with 10 µm filter tip. Component B: membrane holder.

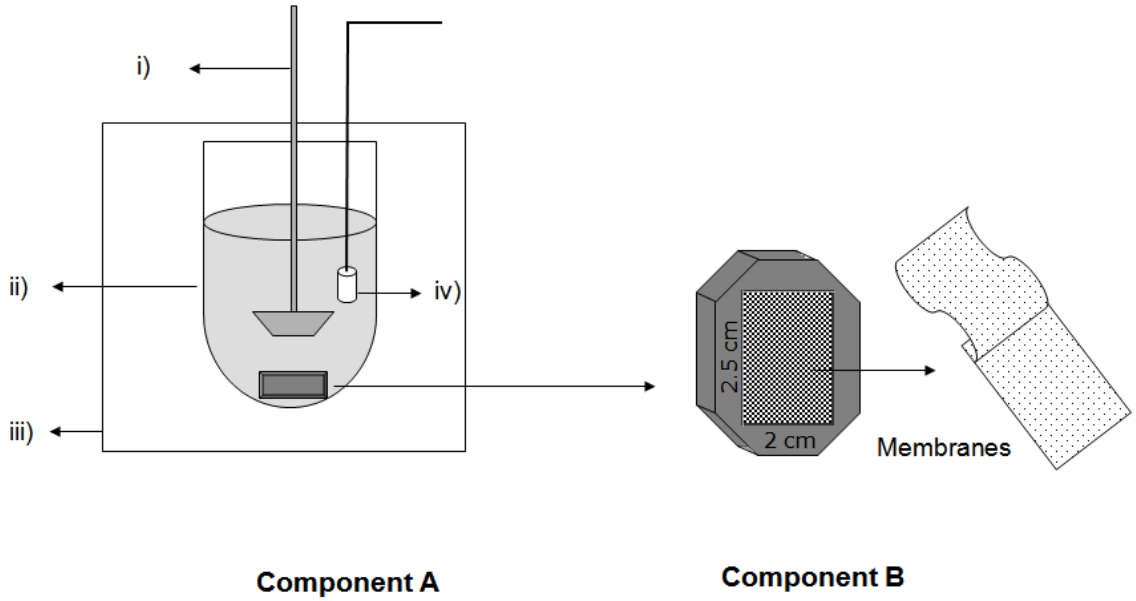

Figure 3.2 Release profiles of HC powders placed into the three different types of membrane holders (CA membrane: MWCO 3,500 and 12,000, PC membrane: 0.05 μm pore size). The error bars indicate the standard deviation of three tests.

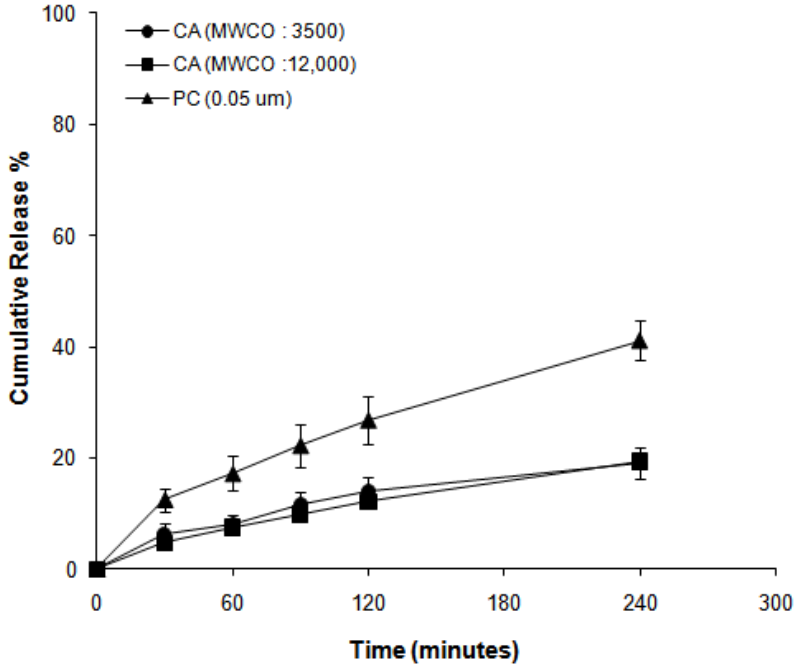

Figure 3.3 Modified next generation impactor (NGI). (A) NGI setup before impingement, and (B) resulting impingement.

A) Before impingement **B) After impingement**

Figure 3.4 Scanning electron microscope (SEM) images of non-separated bulk HC powders (A), of aerodynamically separated HC into the dose-collection plate 3 (B), 5 (C), and 6 (D).

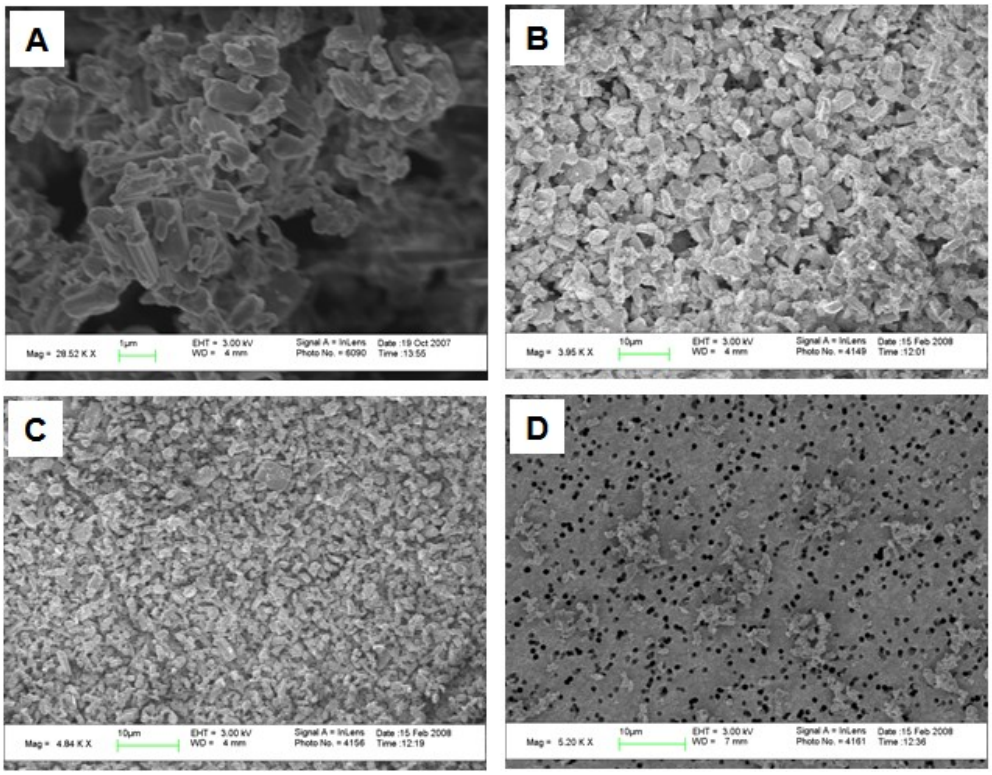

Figure 3.5 Dissolved amount of HC dispersed into the dissolution vessel and placed into the membrane holder in SLF. The error bars indicate the standard deviation of three tests.

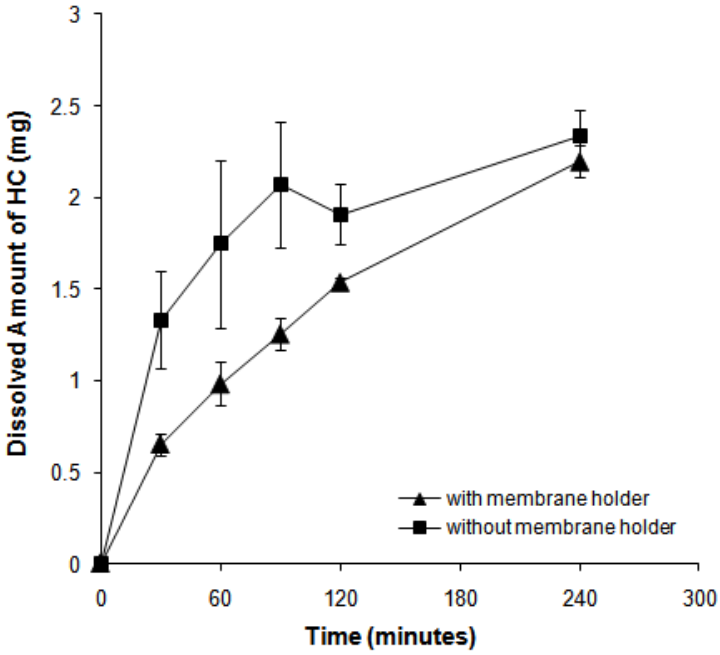

Figure 3.6 Release profiles of HC from two membrane holders having different pore size on the surface in mSLF for dose-collection plate 2, and 6. HC separated from the lactose carrier. The error bars indicate the standard deviation of three tests.

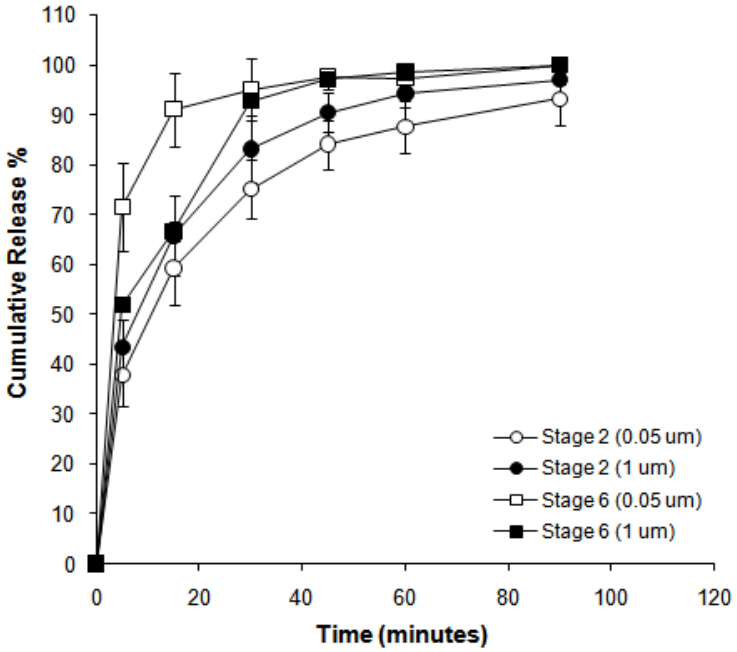

Figure 3.7 Release profiles of HC separated from the lactose carrier in SLF for dose-collection plate 2, 3, 5, and 6. The error bars indicate the standard deviation of three tests.

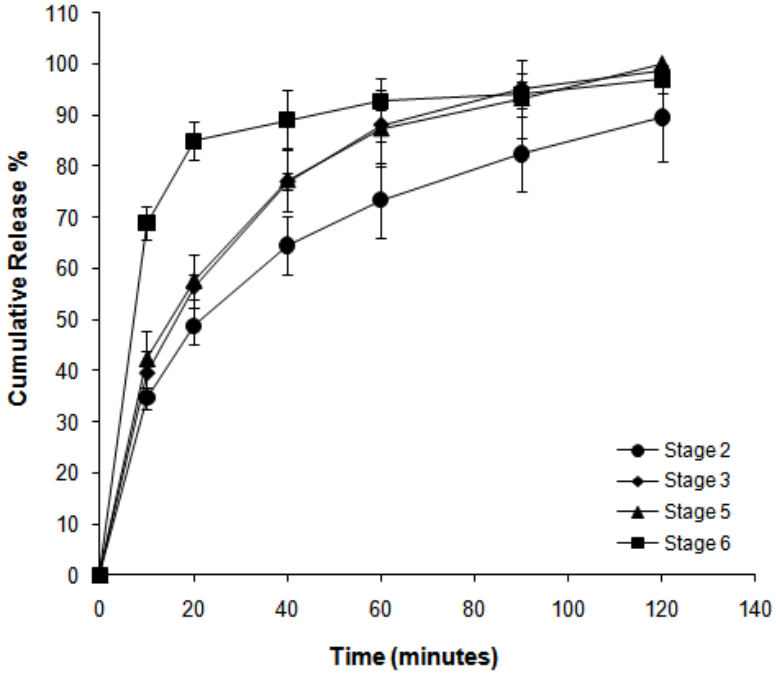

Figure 3.8 Release profiles of HC from the membrane holder having different drug-loading in SLF for dose-collection plate 2 (A) and 6 (B). HC separated from the lactose carrier. The error bars indicate the standard deviation of three tests.

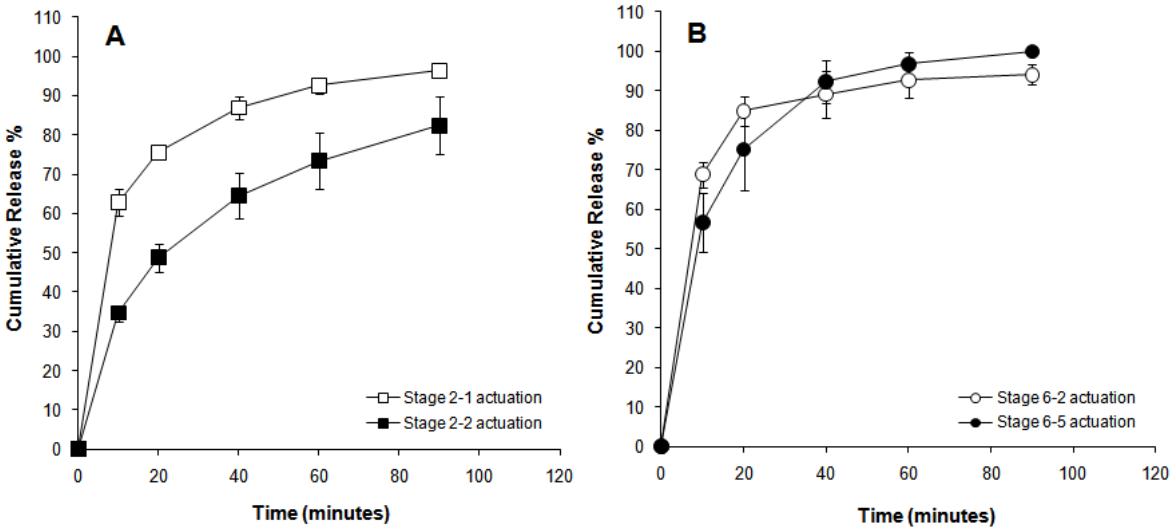

Figure 3.9 Release profiles of HC separated from the carrier-free HC in SLF for dose-collection plate stage 2, 3, 5, and 6. The error bars indicate the standard deviation of three tests.

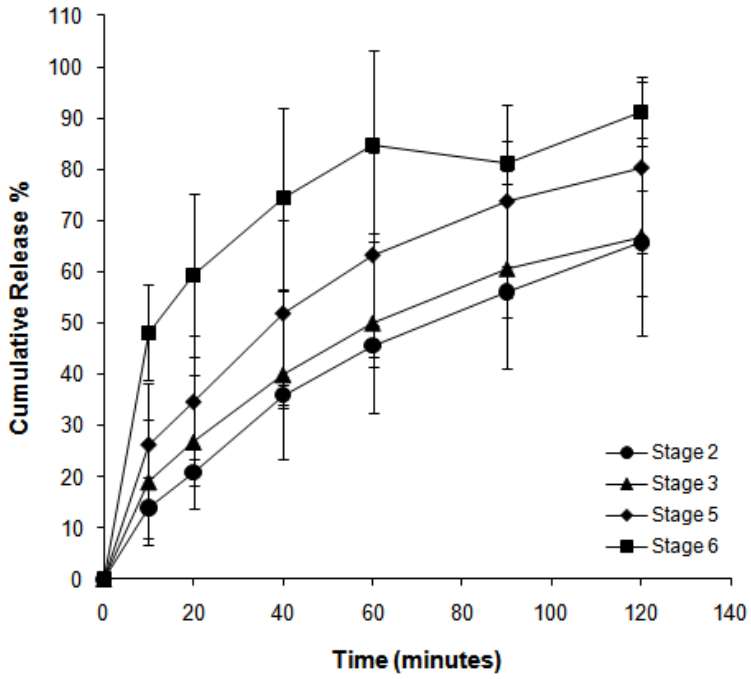

Figure 3.10 Release profiles of HC separated from the lactose carrier in SLF and mSLF for dose-collection plate 2 and 6. The error bars indicate the standard deviation of three tests.

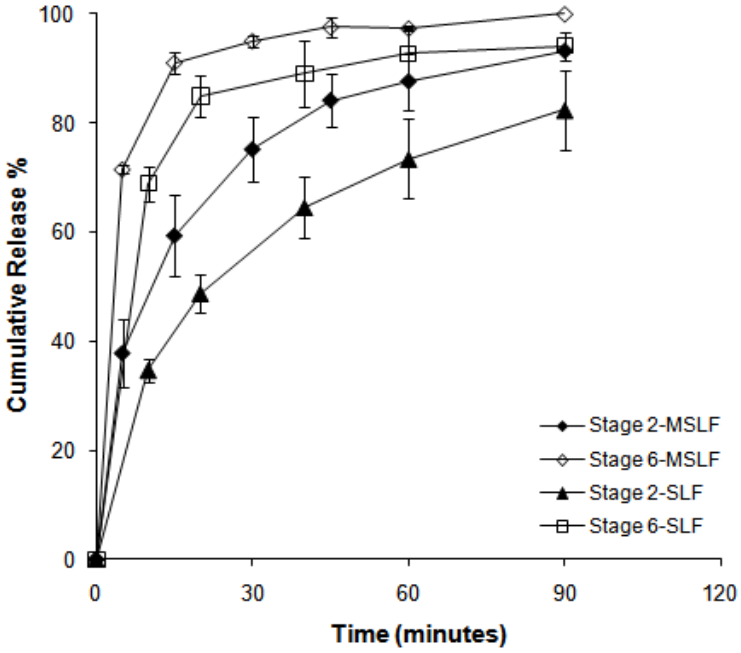

Figure 3.11 Release profiles of HC (open circle) from the membrane holder. Line shows a theoretical curve fit by Higuchi eq.

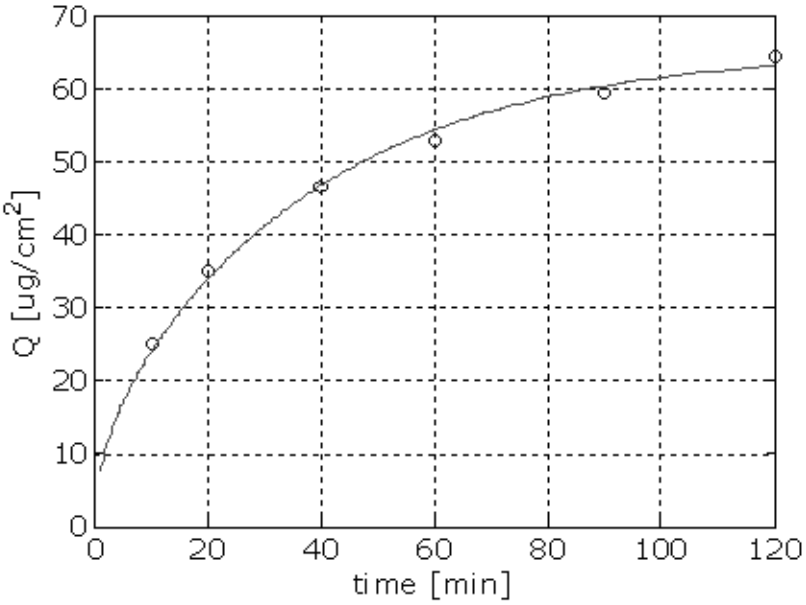

3.8. REFERENCES

[1] V.A. Grey, A.J. Hickey, P. Balmer, N.M. Davies, C. Dunbar, T.S. Foster, B.L. Olsson, M. Sakagami, V.P. Shah, M.J. Smurthwaite, J.M. Veranth, K. Zaidi, The Inhalation Ad Hoc Advisory Panel for the USP Performance Tests of Inhalation Dosage Forms. Pharmacopeial Forum 34(4) (2008) 1068-1074.

[2] J.S. Patton, Mechanisms of macromolecule absorption by the lungs. Advanced Drug Delivery Reviews 19(1) (1996) 3-36.

[3] M. Asada, H. Takahashi, H. Okamoto, H. Tanino, K. Danjo, Theophylline particle design using chitosan by the spray drying. International Journal of Pharmaceutics 270(1-2) (2004) 167-174.

[4] S. Jaspart, P. Bertholet, G. Piel, J.M. Dogne, L. Delattre, B. Evrard, Solid lipid microparticles as a sustained release system for pulmonary drug delivery. European Journal of Pharmaceutics and Biopharmaceutics 65(1) (2007) 47-56.

[5] T.P. Learoyd, J.L. Burrows, E. French, P.C. Seville, Chitosan-based spray-dried respirable powders for sustained delivery of terbutaline sulfate. European Journal of Pharmaceutics and Biopharmaceutics 68(2) (2008) 224-234.

[6] N.M. Davies, M.I.R. Feddah, A novel method for assessing dissolution of aerosol inhaler products. International Journal of Pharmaceutics 255(1-2) (2003) 175-187.

[7] R.O. Cook, R.K. Pannu, I.W. Kellaway, Novel sustained release microspheres for pulmonary drug delivery. Journal of Controlled Release 104(1) (2005) 79-90.

[8] J.T. McConville, N. Patel, N. Ditchburn, M.J. Tobyn, J.N. Staniforth, P. Woodcock, Use of a novel modified TSI for the evaluation of controlled-release aerosol formulations. I. Drug Development and Industrial Pharmacy 26(11) (2000) 1191-1198.

[9] E. Ansoborlo, R.A. Guilmette, M.D. Hoover, V. Chazel, P. Houpert, M.H. Henge-Napoli, Application of in vitro dissolution tests to different uranium compounds and comparison with in vivo data. Radiation Protection Dosimetry 79(1-4) (1998) 33-37.

[10] S. Sdraulig, R. Franich, R.A. Tinker, S. Solomon, R. O'Brien, P.N. Johnston, In vitro dissolution studies of uranium bearing material in simulated lung fluid. Journal of Environmental Radioactivity 99(3) (2008) 527-538.

[11] D. Arora, K.A. Shah, M.S. Halquist, M. Sakagami, In Vitro Aqueous Fluid-Capacity-Limited Dissolution Testing of Respirable Aerosol Drug Particles Generated from Inhaler Products. Pharmaceutical Research 27(5) (2010) 786-795.

[12] M.J. Kwon, J.H. Bae, J.J. Kim, K. Na, E.S. Lee, Long acting porous microparticle for pulmonary protein delivery. International Journal of Pharmaceutics 333(1-2) (2007) 5-9.

[13] F. Ungaro, G. De Rosa, A. Miro, F. Quaglia, M.I. La Rotonda, Cyclodextrins in the production of large porous particles: Development of dry powders for the sustained release of insulin to the lungs. European Journal of Pharmaceutical Sciences 28(5) (2006) 423-432.

[14] O.R. Moss, Simulants of lung interstitial fluid. Health Phys. 36 (1979) 447-448.

[15] J.M. Barichello, H. Handa, M. Kisyuku, T. Shibata, T. Ishida, H. Kiwada, Inducing effect of liposomalization on the transdermal delivery of hydrocortisone: Creation of a drug supersaturated state. Journal of Controlled Release 115(1) (2006) 94-102.

[16] T.S. Wiedmann, R. Bhatia, L.W. Wattenberg, Drug solubilization in lung surfactant. Journal of Controlled Release 65(1-2) (2000) 43-47.

[17] S. Pham, T.S. Wiedmann, Dissolution of aerosol particles of budesonide in Survanta (TM), a model lung surfactant. Journal of Pharmaceutical Sciences 90(1) (2001) 98-104.

[18] V.A. Marple, D.L. Roberts, F.J. Romay, N.C. Miller, K.G. Truman, M.J. Holroyd, J.P. Mitchell, D. Hochrainer, Next generation pharmaceutical impactor (A new impactor for pharmaceutical inhaler testing). Part I: Design. Journal of Aerosol Medicine-Deposition Clearance and Effects in the Lung 16(3) (2003) 283-299.

[19] V.A. Marple, B.A. Olson, K. Santhanakrishnan, J.P. Mitchell, S.C. Murray, B.L. Hudson-Curtis, Next generation pharmaceutical impactor (A new impactor for pharmaceutical inhaler testing). Part II: Archival calibration. Journal of Aerosol Medicine-Deposition Clearance and Effects in the Lung 16(3) (2003) 301-324.

[20] W.I. Higuchi, Analysis of data on the medicament release from ointments. J. Pharm. Sci. 51 (1962) 802-804.

[21] S. Rzepka, B. Neidhart, Transport processes through track-etch membrane filters in a reagent delivery cell. Fresenius Journal of Analytical Chemistry 366(4) (2000) 336-340.

[22] S. Marre, J. Palmeri, Theoretical study of aerosol filtration by nucleopore filters: The intermediate crossover regime of Brownian diffusion and direct interception. Journal of Colloid and Interface Science 237(2) (2001) 230-238.

[23] R.E. Kesting, Synthetic polymeric membranes - A structural perspective. Wiley-Interscience, New York (1985).

[24] G. Arthanareeswaran, P. Thanikaivelan, K. Srinivasn, D. Mohan, M. Rajendran, Synthesis, characterization and thermal studies on cellulose acetate membranes with additive. European Polymer Journal 40(9) (2004) 2153-2159.

[25] M. Cohen-Atiya, P. Vadgama, D. Mandler, Preparation, characterization and applications of ultrathin cellulose acetate Langmuir-Blodgett films. Soft Matter 3(8) (2007) 1053-1063.

[26] M.I. Cabrera, J.A. Luna, R.J.A. Grau, Modeling of dissolution-diffusion controlled drug release from planar polymeric systems with finite dissolution rate and arbitrary drug loading. Journal of Membrane Science 280(1-2) (2006) 693-704.

[27] T. Hayashi, T. Yamazaki, Y. Yamaguchi, K. Sugibayashi, Y. Morimoto, Release kinetics of indomethacin from pressure sensitive adhesive matrices. Journal of Controlled Release 43(2-3) (1997) 213-221.

Chapter 4: Study Factors Affecting the Dissolution Behaviors of Aerosol Products Using Experimental and Mathematical Analysis[4]

Abstract

The aim of this study was to investigate an optimized test method to characterize the dissolution properties of numerous formulation types available for pulmonary delivery. A USP type 2 dissolution apparatus was adapted for this purpose by the incorporation of a specially designed NGI membrane holder. The NGI membrane holder was designed to be directly incorporated with a Next Generation Impactor (NGI) to seamlessly transfer and enclose air-classified formulations. Dissolution procedures, the apparatus, the dose collection, the medium, and test conditions were developed with reference to the USP General Chapter <1092>. Aerodynamically classified drug particles were collected on the NGI membrane holder followed by dissolution study. Two commercially available products, Ventolin® HFA (albuterol sulfate) and PulmicortFlexhaler™ (budesonide) were tested. The dissolution profiles of budesonide (BD) and albuterol sulfate (AS) were successfully estimated by analyzing the amount of drug released from the NGI membrane holder. Additionally, several factors that influence dissolution behavior were also evaluated applying a mathematical model. This dissolution method has the potential to be widely used as an important quality control test procedure for inhalation products.

[4]Significat portions of this chapter were taken from : Yoen-Ju Son, Michelle Horng, Mark Copley, and Jason T. McConville, "Optimization of an in vitro dissolution test method for inhalation formulations", Dissolution Technologies, 2010, 17, P: 6-13.

4.1. INTRODUCTION

For inhalation products, the most important step with *in vitro* performance testing is the delivery of a given API from a specified delivery device, and evaluation of its deposition using a pharmaceutical impactor/impinger. The impaction method is used to estimate actual dose delivered to the target site of the lung. In pulmonary drug delivery, it is well accepted that particles within the size range of 1 to 5 μm can be successfully delivered to the targeted deep lung. However, only a fraction of the API emitted from standard delivery devices is usually delivered to this target site, due to the fine particle size distribution for most inhaler products [1]. Thus, an ideal dissolution test procedure for inhalation formulations would involve particle classification followed by an evaluation of the dissolution behavior of those sorted drug particles that may deposit at various sites in the respiratory tract.

Experimental difficulties exist in dose collection due to very fine and electrostatic powder characteristics [2]. Therefore, most existing dissolution procedures on powders have been performed with no aerodynamic classification [3-8], although the particle separation has been shown to have a significant influence on dissolution profiles [9]. In an attempt to make up for the problems associated with aerodynamic particle separation, several custom built dissolution apparatuses have been investigated. Davies and Feddah reported a modified flow-through cell system [10]. In this method, the aerosol particles were separated and collected on the membrane placed at the base of a standard USP induction port of the Anderson Cascade Impactor (ACI), followed by flow through

dissolution testing. Another study using a Transwell® permeable support system has been introduced by Arora et al.[11]. This permeability study also adopted the use of an ACI to separated aerosol particles on a membrane. Although, these approaches do, in some way, consider the particle separation prior to dissolution assessment, problems are still evident such as the amount drug loading, adequate dose collection on the impactor and hydrodynamic conditions employed. Moreover, there has been no reported study in focusing on mathematical modeling of the kinetics of dissolution, and permeation in the aforementioned dissolution apparatus.

Numerous mathematical approaches have been proposed to estimate the dissolution behaviors of pharmaceutical dosage forms, such as Higuchi model [12], and the Noyes-Whitney equation [13]. However, most of efforts have been devoted to describe the release/diffusion kinetics of dissolved drug from drug delivery platforms that are predominantly matrix systems, intended for oral or transdermal drug delivery [13-15]. The main reason for this may be because of the diversity of formulation design; there are a wide variety of products showing different dissolution/release mechanisms targeted to the oral/transdermal route of administration. Conversely, formulation diversity for inhaled products is very limited, and is generally limited to physical mixtures of carrier particles with micronized APIs. Recently, there has been an increased interest in research focusing on novel inhalation formulations having different characteristic features, such as porous structures and prolonged release profiles [3, 4, 16-20]. Thus the usefulness of developing a new dissolution apparatus/method along with an appropriate mathematical interpretation of the results is set to increase.

This article describes the features of a newly developed membrane holder which was designed specifically to be incorporated into the NGI for better dose collection performance, than the prototype membrane holder device reported in Chapter 3. Additionally, several factors affecting the dissolution behaviors of aerodynamically separated aerosol particles in the NGI membrane holder were determined by both experimental and mathematical analysis. In the previous Chapter, a prototype membrane holder was used to assess the dissolution profiles of aerodynamically separated drug particles [9]. It was clearly shown that there was significant difference in dissolution performance between the bulk hydrocortisone (HC) formulation and an aerodynamically classified HC particles in the dissolution profile; the air-classified HC particles demonstrated at least three-folded increase in dissolution rate than that of non-separate bulk HC particles over the test period [9]. However, in the previous dissolution setup, modification of NGI dose-collection plates with polycarbonate (PC) membranes and wax paper impaction templates was required to collect dispersed particles on the membrane, and the whole dose collected on the membrane couldn't be used for dissolution testing due to a substantial limitation imparted by the prototype holder frame size. The aim of this paper was to investigate a standardized dissolution procedure using the newly manufactured NGI membrane holder, and to develop an adequate mathematical model to estimate the dissolution mechanism of drug in the developed membrane holder.

4.2. MATERIALS AND METHODS

4.2.1. Materials

Ventolin® HFA was purchased from GSK (Research Triangle Park, NC) and a PulmicortFlexhaler™ was purchased from AstraZeneca LP (Wilmington, De). Budesonide (99%) was purchased from the Sigma Chemical Co. (St. Louis, MO). Albuterol sulfate, USP was purchased from the Spectrum Chemical Co. (Gardena, CA). Dipalmitoyl phosphatidylcholine (DPPC) was purchased from Avanti Polar Lipid, Inc. (Alabaster, AL). Polycarbonate (PC) membranes of 0.05 μm (76 mm) were purchased from Whatman (Florham Park, NJ). Methanol (HPLC grade) and all other reagents were purchased from the Sigma Chemical Co. (St. Louis, MO).

4.2.2. Experimental analysis

4.2.2.1. Dissolution apparatus

A United States Pharmacopeia (USP) apparatus 2, Hanson SR8-plus dissolution test station (Hanson Co., Chatsworth, CA) was used to conduct the dissolution study. A NGI membrane holder (Copley Scientific Limited, Nottingham, UK) in position in the vessel of a standard USP apparatus 2 is shown in Figure 4.1 (A). The NGI membrane holder assembly (Figure 4.1 (B)) was customized and consists of a NGI dissolution cup (a), a removable impaction inset (b), a sealing ring (c), two sealing 0-rings, and a polycarbonate (PC) membrane to function as a highly porous diffusional powder retaining layer.

4.2.2.2. Dose collection

To select a suitable particle size cut-off ranges for the subsequent dissolution study, aerodynamic particle separation was achieved using the NGI. Either the Ventolin® HFA device or the PulmicortFlexhaler™ device was actuated 5 times to obtain a quantifiable amount of drug. The NGI was operated at a flow rate of 30 L/min or 60 L/min, for the Ventolin® HFA or the PulmicortFlexhaler™, respectively. Air classified particles from each dose-collection plate of the NGI, which were not used in the dissolution studies, were reconstituted with mobile phase and analyzed using a validated HPLC method [21, 22].

For the dissolution studies, the dissolution cup assembled with the impaction insert was placed in the NGI as shown in Figure 4.2 (A). Either the Ventolin® HFA or the PulmicortFlexhaler™ device was fired into the NGI at the same flow fate as above. Following actuation, the impaction insert was removed from the NGI dissolution cup for dissolution test.

4.2.2.3. Scanning electron microscopy (SEM)

BD particles following particle separation by impingement were observed using a LEO 1530 SEM (Zeiss/LEO, Oberkochen, Germany). In this procedure each PC membrane containing separated BD particles were removed from the dose-collection plate of NGI and cut into a small segment (suitable for mounting on a pin plate SEM stub). The cut membrane segments from each dose-collection plate were mounted

separately onto the stubs using double-sided copper tape, before sputter coating with Ag for 40 seconds under vacuum at 30 mTorr.

4.2.2.4. Dissolution media

Simulated lung fluid (SLF), and 0.2M phosphate buffer (pH 7.4), phosphate buffered saline (PBS), modified PBS (mPBS) containing dipalmitoylphosphatidylcholine (DPPC), and PBS containing polysorbate 80 (tPBS) were used in the dissolution studies. To prepare the mPBS, DPPC (500 mg) was weighed into a 500 mL round bottom flask and dissolved in a 100 mL of chloroform/methanol (1:1) mixture. The solvent was evaporated by rotary evaporation (Buchi Corporation, New Castle, DE). The dry thin film was rehydrated with 250 mL of PBS at 55°C and rotated for 2 hrs. The warm suspension was placed into a Branson 5500 sonic bath (Branson ultrasonics, Danbury, CT) and sonicated at 55°C for 1 hour. The concentrated DPPC solution (0.2%) was stored at 4°C. The prepared stock DPPC solution (0.2%) was diluted 10 fold with PBS before use.

4.2.2.5. Solubility study

The solubility of BD was determined in SLF solution. Samples of BD (10 mg) were added to 100 mL of SLF solution and shaken for 24 hours at 37°C. Samples (1 mL) were taken from each vial at 0.5, 1, 2, 4, 6, and 8 hour intervals and filtered with 0.45µm syringe filter. All the samples were analyzed using a validated HPLC method [21] .

4.2.2.6. Dissolution study

To aerodynamically classify budesonide (BD) and albuterol sulphate (AS) from the PulmicortFlexhaler™ device, or the Ventolin® HFA device, each formulation was fired into the NGI as previously described. The NGI dose-collection plates were assembled as above (with the dissolution cup assembled with the impaction insert). Following actuation for a given formulation, the impaction insert was removed from the dissolution cup, and a PC membrane (pre-soaked with dissolution medium) was placed onto the top and sealed in place with the sealing ring of the NGI membrane holder. The sealed NGI membrane holder was then placed into each dissolution vessel containing 300 mL of dissolution media (Figure 4.1 (A)). Dissolution testing was conducted at 50, 75, or 100 rpm, to evaluate the effect of hydrodynamic conditions. Dissolution media (3 mL) was withdrawn manually using a glass syringe at timed intervals of 5, 15, 30, 60, 90, and 120 minutes for the BD samples and at 5, 15, 30, 45, and 60 minutes for the AS samples. Collected dissolution samples of BD (2 mL) were diluted by adding 1 mL of mobile phase and filtered using 0.45 μm PTFE syringe filters before analyzing. Alternatively, collected dissolution samples of AS were filtered using 0.45 μm PTFE syringe filters. Fresh dissolution media (3 mL) was replaced into each vessel after sampling. All the samples were analyzed using a validated HPLC method [21, 22]. Adsorption of the drugs onto the syringe and filter was evaluated prior to the dissolution studies.

The residual amount of BD and AS on the NGI membrane holder was determined after dissolution test by washing a membrane and the impaction insert with mobile phase (5 mL) prior to analyzing. The total amount of BD and AS initially loaded on the NGI

membrane holder was back calculated using the sum of cumulated release amount of each API, plus the remaining quantity of each API on the membrane holder. The percent drug release of AS and BD were calculated by dividing the amount of APIs released by the drug initially impacted and collected on to the membrane holder.

4.2.2.7. Validated HPLC Analysis of BD and AS in the dissolution media

Samples were analyzed by using a Waters HPLC system (Waters Co., Milford, MA) with UV detection. The system consisted of a 717 plus autosampler, 2487 dual wavelength detector, 1525 binary pump, and 1500 column heater. Chromatography was performed using a Capcell Pak C18 5μm 4.6×250 mm column (Shiseido Fine Chemicals, Tokyo, Japan) for BD and a Alltima™ C18 5μm 4.6×150 mm column (Grace, Deerfield, IL) for AS. The mobile phase for BD which consisted of methanol, acetonitrile, water, and acetic acid in a ratio of 50:10:28.3:1.7 respectively, which was eluted at a flow rate of 1.7 mL/min and the UV detector was set to a wavelength of 242 nm [21]. The mobile phase for AS which consisted of methanol and 0.1% ammonium acetate acetonitrile (pH 4.5) in a ratio of 45:55 respectively, this was eluted at a flow rate of 0.8 mL/min and the UV detector was set to a wavelength 276 nm [22]. The column temperature for both APIs was maintained at 25°C and the volume of each sample injected was 100 μL for BD samples and 20 μL for AS samples.

4.2.2.8. Statistical analysis

Data were expressed as the mean plus/minus standard deviation (SD). The statistical differences of release rates were studied by calculating a similarity factor (f_2) [23]. For curves to be considered similar, f_2 values should be close to 100. Generally, f_2 values greater than 50 (50-100) ensure sameness or equivalence of the two curves [23].

4.2.3. Mathematical analysis

4.2.3.1. Theory

The mathematical model has been derived for controlled release systems that show the sustained release of pharmaceutical compounds from a planer matrix system with simultaneous dissolution of crystal [13, 14]. This mathematical model was modified to evaluate the dissolution mechanism in the NGI membrane holder. As shown in Figure 4.3 (A), a matrix containing solid drug particles assembled on the cross-sectional area of the matrix at $x=x_1$, which is assumed to be achieved by one time actuation of aerosol generation device. In this system, as the solid drug dissolves and diffuses out, the size of the particles reduces with a dynamic that is governed by a finite dissolution rate. After the solid drug particles are fully dissolved in the media, the release process is governed by diffusion only. This primary model is extended to describe matrix systems containing solid drug particles assembled on N cross-sectional areas arbitrarily located at $x_1, x_2,\ldots x_n$ (Figure 4.3 (B)) since the loaded drug particles into the membrane holder by aerodynamic separation do not always create a single layer. After a certain time, the exhaustion of the

particles begins and progresses inwards the matrix until all the solid drug particles are dissolved into the dissolution media.

4.2.3.2. Model assumptions

The underlying assumptions of the model to be mathematically formulated are: i) the mass transport of drug is one-dimensional; it takes place in the x-direction only (x_0= no mass flux), (ii) the drug diffusion process is described according to Fick's second law, (iii) the drug dissolution kinetics are explained by Noyes-Whitney equation, (iv) particles distributed in the membrane holder are the same size, v) every device actuation creates a single particle layer, vi) solid drug particles dissolve keeping constant the original shape, which is assumed to be spherical, vii) the diffusion of dissolved drug through the membrane is not hindered, and viii) the membrane on the surface of holder is non-erodible and non-swellable. Accordingly, the release process for the particles arbitrarily loaded in the membrane holder is described by following equations (the details of derivation procedures are described in appendix A):

$$\frac{\partial}{\partial x} C(x_0, t) = 0, at\ x = 0, t > 0 \ \text{(no flux)} \quad (1)$$

$$\emptyset_D\,(x_n, t) = \frac{dm}{dt} = K_{\mathrm{D}} S_{\mathrm{n}} a_{\mathrm{n}}(t)[C_{\mathrm{s}} - C(x_{\mathrm{n}}, t)] \quad (2)$$

($\emptyset_D$: a surface mass source arising from drug dissolution process at $x = x_{\mathrm{n}}$, n = 1, 2,…, N)

$$D\frac{\partial}{\partial x} C(x, t) = -P[C(x, t) - C_{\mathrm{B}}(t)], at\ x = L, t > 0 \quad (3)$$

(Permeation of dissolved drug molecule through the PC membrane)

The equation (1), (2), and (3) can be described by a single equation as follows:

$$\frac{\partial}{\partial t}C(x,t) - D\frac{\partial^2}{\partial x^2}C(x,t) = \sum_{1}^{N}\delta(x-x_1)K_{\mathrm{D}}S_{\mathrm{n}}a_{\mathrm{n}}(t)\,[C_{\mathrm{s}} - C(x_{\mathrm{n}},t)] \qquad (4)$$

(in $0 < x < L$, $t > 0$, n =1, 2,.., N, and $N \to \infty$)

to solve the time-dependent surface area (a_{n}) function at $x_1, x_2, \ldots x_{\mathrm{n}}$, following equation can be used:

$$\frac{d}{dt}a_{\mathrm{n}}(t) = -\frac{2K_D\sqrt{(a_{\mathrm{n}}^0)^3}}{3m_{\mathrm{n}}^0}\cdot\sqrt{a(x_{\mathrm{n}},t)}\cdot[C_{\mathrm{s}} - C(x_{\mathrm{n}},t)] \qquad (5)$$

For n = 1, 2,…, N, $t > 0$ with $a_1^0, a_2^0, \ldots\ldots a_{\mathrm{n}}^0$ as initial conditions

Variables and parameters used in this modeling are displayed in Table 4.1.

4.2.3.3. Numerical solution

To simulate the changes in concentration gradient and surface area of loaded drug particles in the progress of drug dissolution within the membrane holder, equation (1) and (2) were combined in the form of partial differential equation (PDE) as follows:

$$\frac{\partial}{\partial t}\begin{bmatrix}C(x,t)\\a(x,t)\end{bmatrix} = \frac{\partial}{\partial x}\begin{bmatrix}D\dfrac{\partial}{\partial x}C(x,t)\\0\end{bmatrix} + \begin{bmatrix}K_{\mathrm{D}}\cdot S(x)\cdot a(x,t)\cdot[C_{\mathrm{S}} - C(x,t)]\\-\dfrac{2K_D\sqrt{(a_{\mathrm{n}}^0)^3}}{3m_{\mathrm{n}}^o}\cdot\sqrt{a(x,t)}\cdot[C_{\mathrm{S}} - C(x,t)]\end{bmatrix} \qquad (6)$$

Which are subjected to the following boundary conditions;

$$\frac{\partial}{\partial x}C(x,t) = O, at\ x = 0$$

$$D\frac{\partial}{\partial x}C(x,t) = -P[C(x,t) - C_{\mathrm{B}}(t)], at\ x = L$$

To calculate the drug concentration (C (x,t)) and the surface area of loaded drug (a) at any position in the membrane holder, equation (3) was solved by the PDEPE solver function in MATLAB® (The Mathworks Inc., Natick, MA).

4.3. Results and Discussion

4.3.1. Dissolution apparatus

NGI membrane holders were placed at the bottom of dissolution vessels, with their release surface side up, and with the distance between the bottom edge of the paddle and the surface of the membrane holder maintained at 20 ± 2 mm (Figure 4.1 (A)). The distance between the paddle and the surface of the NGI membrane holder can be adjusted within the range that allows for the paddle to effectively remove released drug from the exposed membrane surface and provide continuous circulation to the media in the vessel.

The mechanism of this dissolution method can be explained by dissolution-diffusion controlled drug release from the NGI membrane holder. During the dissolution process the dispersed drug within the membrane holder undergoes dissolution as dissolution media migrates through the pores on the membrane surface and the dissolved drug then releases out to the reservoir by diffusion [9]. Therefore, membrane properties, such as: pore size, pore tortuosity, and membrane thickness will have a profound effect on the release behavior of each drug. A PC membrane was selected as the diffusion barrier [9]. In the previous study reported by this group, the PC membrane demonstrated almost a twofold increase in drug release rate when compared to cellulose acetate (CA)

dialysis membranes [9]. This difference is attributed to the differences in the physical structure of the two membranes. PC membranes are thin (approximately 6 μm) but still relatively robust for their handling requirements. Additionally, they do not swell, do not create air bubbles, have a well-defined uniform pore size [24, 25], and consist of homogeneous 0.05 μm non-tortuous cylindrical pores on the surface that allow free diffusion of dissolved drug and dissolution media.

4.3.2. The dissolution procedure

4.3.2.1. Dose collection

Aerodynamic particle classification was achieved with the NGI for both Ventolin® HFA and PulmicortFlexhaler™ to select a suitable particle size cut-off and the amount of drug loading for the following dissolution study. Unlike usual dissolution methods, drug loading into the NGI membrane holder is achieved by the particle impingement activity, thus, the particle deposition profile on each dose-collection plate is essential in determining the amount of initial drug loading and the particle size cut-off. Dose-collection plate 4 for PulmicortFlexhaler™ and plate 5 for Ventolin® HFA were selected for dissolution method validation study as these consistently displayed the maximum deposition for each product, as shown in Figure 4.4. Additionally, the median aerodynamic particle size values (D_{50}) for dose-plate 4 and plate 5 of the NGI fall into the respirable particle size range (1-5 μm) as 1.66 and 1.36 μm at a flow rates of 60 L/min and 30 L/min, respectively [26].

To enable the dissolution studies, the impaction insert of the NGI membrane holder was inserted into the pre-selected NGI dissolution cup of the NGI (impaction plates before, and after device actuation impingements are shown in Figure 4.2). The amount of BD or AS that was collected on the impaction insert of the NGI membrane holder is presented in Table 4.2. The NGI membrane holder assembly used in this study was designed to facilitate maximum particle collection over a uniform collection area (18 cm^2). Particles having different particle size distributions can be easily collected by replacing a standard dose-collection plate with a dissolution cup, equipped with the impaction insert of the NGI membrane holder. Additionally, this method can be used to examine the dissolution behaviors of inhalation dosage forms with similar aerodynamic particle distributions by selecting drug particles accumulated in same dose-collection plate. It would be anticipated that dissolution of particles having a similar aerodynamic size distribution would provide more inter formulation discrimination.

Dissolution profiles of BD particles having different particle size cut-off were conducted to evaluate particle size dependency in dissolution process. For the dissolution study, an average 25 μg of BD powder were collected on the impaction insert placed in dose-collection plates 2-5. Figure 4.5 shows that the release profiles of BD particles accumulated on NGI dose-collection plates 2, 3, and 4 reached 80% after 15 minutes, with a significant difference in initial release rates. The similarity factors (f_2) are 52.5 for dose-collection plate 2 and 59.7 for dose-collection plate 3 when individually compared to the dissolution profile of reference test, dose-collection plate 4 (Table 4.3). With particles accumulated on dose-collection plate 5, the overall dissolution profile is not

equivalent to the reference test (dose-collection plate 4), as f_2 is 40.6. This may be attributed to the fact that smaller particles have better wettability and dissolve more quickly due to their larger surface area, as explained in the previous study [9]. Dose-collection plate cut-off particle sizes calibrated from the NGI are reported to be 4.46, 2.82, 1.66, 0.94, 0.55, 0.34 μm at an inlet flow rate 60 L/min for dose-collection plates 2 through 7, respectively [26].

4.3.2.2. Hydrodynamic conditions

Dissolution tests of BD were conducted at 50, 75, and 100 rpm paddle speeds. Dissolution profiles obtained at a rate of 75 rpm were shown to be the most consistent, as shown Figure 4.6. For the paddle apparatus, 50 rpm is most commonly used, however, a higher paddle speed was required due to the "dead" volume between the NGI membrane holder and the bottom of the vessel. The dissolution media circulates through the gap between the holder and the vessel wall around the holder. However, due to the narrow gap, the circulation of media is somewhat hindered and a higher agitating speed is required to provide better circulation to the media under the holder. The release profile of BD at an agitating speed of 100 rpm was not plotted as an eddy was observed at that agitating speed (this was a consequence of using a relatively low volume of dissolution media was used in these studies).

4.3.2.3. Dissolution media

The dissolution profiles of BD (PulmicortFlexhaler™) in simulated lung fluid (SLF), 0.2 M phosphate buffer, and phosphate buffered saline (PBS) were investigated. The dissolution profiles from three media were similar as shown in Figure 4.7 (A). Table 4.3 shows the similarity factors (f_2) between PBS and phosphate buffer as 63.4 and 51.6 when compared to the SLF, respectively. Therefore, either phosphate buffer, or PBS could be used as an alternative dissolution media. The SLF used was first developed by Moss [27], and was described as being close to that of actual lung fluid in ionic composition and pH. SLF has been used in previous published *in vitro* dissolution studies due to their similarity in composition to actual lung fluid [5, 10, 27]. However, SLF media may not be preferable for the routine quality control (QC) study for inhalation products due to its low buffering effect. In particular, the use of SLF media would not be recommended for evaluating inhalation dosage forms that show pH-dependency or sustained-release manner in their dissolution profile. As shown in Figure 4.7 (B), the pH of SLF increases from 7.4 to 8.8 over 24 hours without continuous CO_2 bubbling. It has been reported that the pH of SLF media is significantly increased without CO_2 bubbling [27].

A volume of 300 mL media was used for the dissolution studies. This was determined to be a minimum volume needed to occupy the 20 ± 2 mm distance between the membrane holder surface and the bottom edge of paddle, as shown in Figure 4.1 (A). The volume of media may be raised up to 900 mL, and is dependent on the concentration and sink condition of the drugs to be evaluated. The dissolution of drug from the NGI

membrane holder occurs by diffusion of dissolution media through the pores on the membrane surface. The amount of dissolution media diffused through the pore was mainly determined by the paddle speed and pore size on the membrane surface, and not the amount of media in the vessels. Normally, for the paddle and basket apparatus, the volume of media is 500 mL to 1L, where 900 mL is most common volume. However, the dissolution system may optimally be less than sink conditions in order for test compounds to approximate dissolution behaviors of formulations in the lung, since the volume of lung fluid is extremely small, approximately 10-20 mL/100 m^2 of surface [1, 2]. The NGI membrane holder, used in this study, was designed to maintain a very thin liquid layer between the membrane and test powders. Dissolution media is continuously exchanged from the vessel reservoir to the drug particles enclosed inside the holder by agitation, and a very thin liquid layer is maintained to dissolve drug particles [9]. In other words, a dynamic equilibrium is rapidly established for solute exchange, following the commencement of a given dissolution test with the membrane holder.

4.3.2.4. Amount of drug loading

The amount of drug loading on the NGI membrane holder showed significant influence on the drug release rate, especially for the PulmicortFlexhaler™ which contains the hydrophobic steroid BD. The amount of drug loaded on the membrane holder is summarized in Table 4.2. It can be shown in Figure 4.8 (A) that 80% dissolution was achieved in 30 minutes when 29.4 μg of drug is loaded by 1 time device actuation (1T). As the loading amount increased from 29.4 μg (1T) to 224 μg (10T), the dissolution rate

significantly slowed. Conversely, the dissolution rates of Ventolin® HFA, that contains the hydrophilic AS, did not display the same degree of dose dependency as 90% dissolution was achieved in 5 minutes for all the test samples, as shown in Figure 4.9. This indicates that the loading amount may determine powder wetting inside the holder, and the significance of this was shown to be dependent on the hydrophobicity of the API used. When the device is actuated, dispersed powders form a powder bed on each dose-collection plate and the thickness of the powder bed is dependent on the amount of drug loaded on each dose-collection plate. A larger amount of drug loaded on the plate corresponds to a thicker powder bed, as shown in Figure 4.10. Given a thicker load of powder bed on the NGI membrane holder, there will be more dissolution/diffusion activity required to release all of the drug from the inner space of the NGI membrane holder as the dissolution of loaded drug gradually progresses inward layer by layer until all solid drug particles have been wetted and dissolved. Consequently, the release rate of molecules is governed by the thickness of the drug layer and by the solubilization rate of that drug layer. Ideally, the device needs to be actuated one time to obtain well dispersed particles in an approximately single layer. However, the thickness of the powder bed can also be varied according to the drug dose. For instance, a 1 time actuation of a high dose formulation can create a thicker powder bed than a 1 time actuation of a low dose formulation. Additionally, in some cases, multiple actuations may be necessary to obtain quantifiable drug concentration in the media since at least 300 mL of dissolution media is required to conduct dissolution study. Care must be taken when the loading dose is high or is obtained by multiple device actuations, especially for poorly water soluble drugs.

For very poorly soluble compounds, dissolution media may contain a percentage of surfactant to enhance drug solubility for testing very poorly soluble compounds [28]. To improve the wettability of BD particles and to help their solubilization, two different surfactants, polysorbate 80 and dipalmitoyl phosphatidylcholine (DPPC) were added to PBS media. Polysorbate 80 provided a better solubilization effect to the BD powder than that of DPPC, as shown in Figure 4.8 (B). DPPC may help powder wetting, however, the effect was not significant. Initial drug release rate of BD in the mPBS during first 45 minutes were similar to that of SLF media.

DPPC is a main component of lung surfactant and the effect of lowering surface tension at the air/water interface is essentially performed by a DPPC monolayer [29]. Due to their similarity in composition to actual lung fluid, the dissolution media containing 0.02% of DPPC has been used to predict the solubility and solubilization process of inhalation formulations that have very low aqueous solubility [10, 30]. However, in this study using the NGI membrane holder, DPPC in the media may not be able to freely diffuse and reach the drug particles inside the membrane holder as DPPC forms liposomal aggregates in aqueous media [31]. These liposomal aggregates have a bigger particle size distribution (50 -150 nm) than the membrane pore size on the surface. Thus, although wettablity of BD powders was somewhat increased by adding DPPC, significant wetting, or solubilizing of BD was not found over the test period. As shown in 4.8 (B) and Table 4.3. PBS containing 0.2% w/v polysorbate 80 was found to be an ideal dissolution media to evaluate 5 times actuated BD, as f_2 was 64.7 when it is compared with the dissolution curve of 1 time actuated BD which is assumed to be an ideal dose for

dissolution. The concentration of surfactant needs to be justified by showing profiles at several different concentrations for variety of different dose loadings, and dissolution profiles need to be compared with that of standard sample to determine a suitable concentration of surfactant.

4.3.3. Mathematical analysis

4.3.3.1. Mathematical model

There has been several mathematical models to analyze drug release from systems containing both diffusion of dissolved compound and dissolution of dispersed compound in the matrix system [13, 14]. These mathematical models consist of a dissolution reaction term described as the Noyes-Whitney equation with a diffusion term described as Fick's law. In these models, unlike general diffusion models that show only the mass flux of dissolved drug in pharmaceutical matrix systems, the effects of the relative rate of drug dissolution to drug diffusion and of non-uniform drug loadings on the drug release pattern for planar matrix systems were taken into account. Due to the similarities in the dissolution/release mechanism of loaded drug particles from, which can be explained by the dissolution-diffusion controlled drug release from the planar matrix systems, the developed mathematical model was applied to analyze the factors affecting the dissolution of loaded drugs in the membrane holder. In the mathematical analysis, the sealed NGI membrane holder with a PC membrane is considered as a planar matrix system consisting of a thin liquid layer and loaded drug particles in the form of either a single or multi-layer. The existing mathematical model was simplified with parameters

and variables having unit instead of dimensionless parameters used in the existing models. For numeric calculation, Eq.(4) in the form of Dirac delta function may be converted to the continuous function of x as Eq.(6). The numerical calculations were performed by the PDEPE solver function in MATLAB® (The Mathworks Inc., Natick, MA). Full description of the derivation procedures is given in Appendix A.

4.3.3.2. Single layer system

The dissolution kinetics of drug particles loaded in the NGI membrane holder was analyzed by mathematical simulations. Specifically, the mathematical analysis focused on the impacts of the amount of hydrophobic drug (BD) in the membrane holder, which was shown to be the most critical factor in dissolution study, on the dissolution profiles. The results of mathematical calculation for the 1 time actuated sample (1T), which was assumed to be the ideal condition for dissolution study, is shown in Figure 4.11. There was no concentration gradient observed at any positions within the membrane holder (from x=0 to x=L, x=0 represents the very bottom layer of the powder bed, and x=L represents the very front layer of the powder bed facing the PC membrane); the levels of BD concentration were equal throughout the membrane holder. This data implies that the diffusion of dissolved drug toward the PC membrane layer is not retarded by dissolution media or undissolved particles in the holder, unlike usual matrix systems having release retarding layer, such as polymers and gels. It has been known that the concentration gradient in the matrix system is usually created by the slowed diffusion of drug molecule in the release retarding layer of matrix, leading to sustained drug dissolution/release [13,

14, 32]. As shown in Figure 4.11, the concentration of BD in the NGI membrane holder increased as time passed, whereas the surface area of drug particles gradually decreased as a function of time, indicating that the dissolution media in the NGI membrane holder is immediately replaced with the dissolution media containing dissolved BD in the reservoir (dissolution vessel), with continuous dissolving of BD particles loaded in the holder.

4.3.3.3. Multi-layer system

For the 10 times actuated sample (10T), contrary to the result of 1T sample, the difference in BD concentrations at different positions of the membrane holder was observed; overall, BD concentrations at x=0 were slightly higher than the concentrations at x=L over the period of dissolution time, as shown in Figure 4.12 (B). The difference in the concentration gradient between 1T and 10T samples can be explained by the relative rate of BD dissolution to the diffusion of dissolution BD molecule through the powder bed having different thickness (L). In the mathematical calculation, it was assumed that the BD particles loaded x=x_n position dissolve at the same dissolution rate (K_D) and the diffusivities (D) of dissolved BD molecules in the NGI membrane holder are same for 1T and 10T samples. From the calculation results applying the conditions above, it was found that the dissolution of BD particles within the powder bed was relatively faster than the diffusion of dissolved molecule through the powder bed. This indicates that the dissolved BD molecules close to x=0 position require more time to reach x=L layer than the molecules close to x=L position to be released out to the reservoir. Consequently, more dissolved BD molecule is accumulated in the powder bed as the thickness of

powder bed (L) increases. From the series of results, it may be estimated that the concentration gradient within the NGI membrane holder (consisting of a powder bed) become more significant if the diffusion of dissolved molecule is slowed by the powder bed consisting of undissolved drug particles.

To simulate the impact of diffusivity (D) of drug molecule in the powder matrix (powder bed) on the BD concentration at $x=x_n$ positions, different D values in the range of 6.3×10^{-6} to 6.3×10^{-8} cm^2/s were applied to the mathematical calculation. The value of 6.3×10^{-6} was the free diffusion coefficient of BD in the dissolution media calculated by applying the Stoke-Einstein equation [33] and other values were assumed. The decrease in the diffusion coefficient as drug particle size and the amount of powder loading increased was confirmed by our previous study [9]. The simulation results were shown in Figure 4.13. The images show the BD concentration at $x=x_n$ positions as a function of time for the D values of 6.3×10^{-6}, 6.3×10^{-7}, and 6.3×10^{-8} cm^2/s. The degree of concentration gradient created within the NGI membrane holder (consisting of a powder bed) increased as D values decreased, indicating that a powder bed consisting of more packed and denser particle aggregates may act as a release retarding layer, resulting in a sustained drug release from the powder matrix (powder bed). It was clearly seen from Figure 4.13 (B) that the lowest D values, 6.3×10^{-8}, demonstrated a marked difference in the BD concentrations within the NGI membrane holder (from x = 0 to L) compared to higher D values. Moreover, the BD concentrations in the NGI membrane holder were much more concentrated than that of reservoir until the BD concentrations between the holder and the reservoir reached a hydrodynamic equilibrium state at 120 minutes. This

result is opposite of what was obtained with higher D values (3×10^{-6} and 6.3×10^{-7} cm^2/s), indicating the dissolved BD molecule is trapped within the packed powder bed. The plateaus at the BD release profiles obtained from 5T and 10T samples shown in Figure 4.8 (A) can be explained by the series of data above; the dissolution of BD particle in the powder bed may be slowed by limited amount of dissolution media, and the diffusion of dissolved BD molecules may be hindered and finally stopped by saturated BD concentration in the powder bed. It can be more clearly seen from Figure 4.14 that the difference in BD concentration at $x=0$ and $x=L$ increased as D values decreased from 6.4×10^{-6} to 6.4×10^{-8} cm^2/s as a function of time, implying that more BD molecules stacked up in the powder bed instead of releasing out to the reservoir due to the slow diffusion of BD molecule in the powder bed. It was clearly shown that the thickness and density of powder bed (amount of drug particles) had significant influence on the release profiles of drug molecules. As mentioned above, a monolayer created by 1 time device actuation is ideal condition to conduct this type of dissolution study, however, this condition cannot be applied for all dissolution studies of inhalation products since high dose formulations can create a thicker powder bed by 1 time actuation than low dose formulations. Besides, the thick powder bed does not always retard drug release. Even though, the powder bed is thick, the release rate may not be delayed by the thick powder bed if the drug particles rapidly create void spaces in the powder bed by dissolving as the case of AS. Therefore, the amount of drug loading may be varied with the physicochemical properties of drug molecule subject to dissolution study.

4.4. CONCLUSION

A new easy to use NGI membrane holder for evaluating the *in vitro* dissolution behavior of inhalation formulations was designed. The dissolution rates of commercially available drug formulations were successfully estimated by analyzing the amount of drug released from this attachment for the NGI. Factors having impact on the dissolution profiles were evaluated by mathematical model. This dissolution method may be used for a quality control studies for various dry powder inhalers, in particular, the *in vitro* dissolution profiles of drug may provide an estimate of its dispersion character.

4.5. TABLES

Table 4.1 Parameters and variables used for modeling*

Factors	Abbreviation	Unit	Value
Diffusion coefficient (when particles are aligned in monolayer, Figure 4.1(A))	D	cm^2/s	$6.3e^{-6}$
Thickness of membrane	h_M	cm	$6e^{-4}$
Partition coefficient (matrix/membrane)	K	-	1
Permeability coefficient	P	cm/s	$1.01e^{-2}$
Saturation solubility of drug in the matrix	C_s	g/cm^3	16.2
Drug concentration in the reservoir	C_B	g/cm^3	Experiment data
Surface area of single drug particle at $x = x_n$ (as an initial condition)	a_n^0	cm^2/s	Varies with the particle size deposited on each NGI dose-collection plate
Number of particles associated to the drug dissolution source at $x = x_n$	S_n	-	Varies with the amount of drug loaded on the NGI membrane holder
Dissolution rate constant	K_D	cm/s	$6e^{-4}$
Thickness of matrix	L	cm	Varies with both the number of device actuation and the particle size

* Derivation procedures are listed in appendix A

Table 4.2 Amount of drug loaded on the dose-collection plate 4 (BD) and plate 5 (AS) for dissolution studies. (The amount of loading was calculated by adding a remaining quantity of APIs on the NGI membrane holder to the total quantity of APIs released from the holder, the error bars indicate the standard deviation of six tests).

PulmicortFlexhaler™ (BD)		Ventolin® HFA (AS)	
Number of Actuation (T)	Amount of Loading (μg)	Number of Actuation (T)	Amount of Loading (μg)
1	29.4 ± 5.1	15	259.5 ± 42.4
2	55.2 ± 3.8	20	320.7 ± 17.7
5	151 ± 12.7		
10	224 ± 5.3		

Table 4.3 Similarity factors (f_2) between two dissolution curves of BD collected from PulmicortFlexhaler™ device (Rt: reference performance, Tt: test performance, T: number of actuation)

Rt	Tt	f_2	Rt	Tt	f_2	Rt	Tt	f_2
SLF - 1T	PBS- 1T	63.4	SLF-1T	mPBS-5T (0.02%)	25.1	Stage 4 (SLF-1T)	Stage 2 (SLF-1T)	52.5
	Phosphate Buffer-1T	51.6		tPBS-5T (0.02%)	40.7		Stage 3 (SLF-1T)	59.7
				tPBS-5T (0.2%)	64.7		Stage 5 (SLF-1T)	40.6

4.6. FIGURES

Figure 4.1 Schematic diagram of the dissolution apparatus. NGI membrane holder in position in the vessel of a standard USP 2 test apparatus (A), and NGI membrane holder assembly (B): a) a NGI dissolution cup, b) an impaction insert and c) a sealing ring.

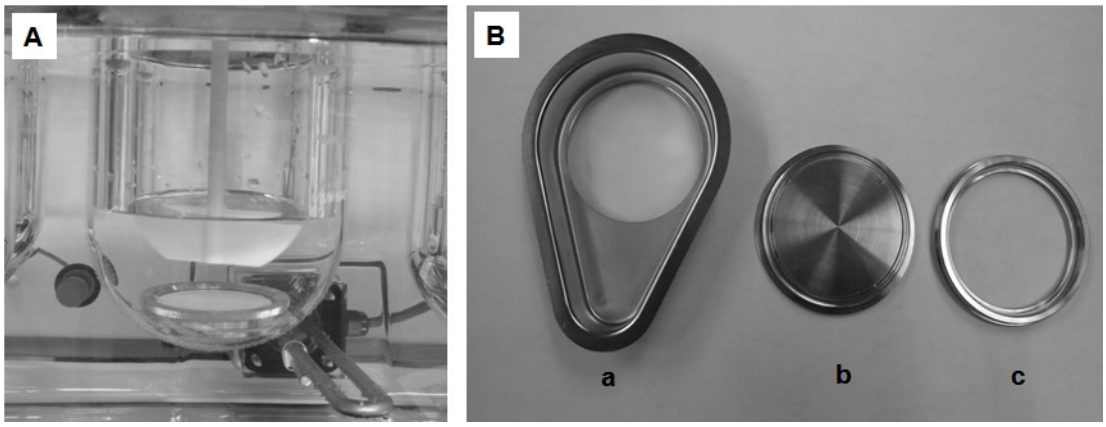

Figure 4.2 Modified next generation impactor (NGI). (A) NGI setup before impingement, and (B) resulting impingement.

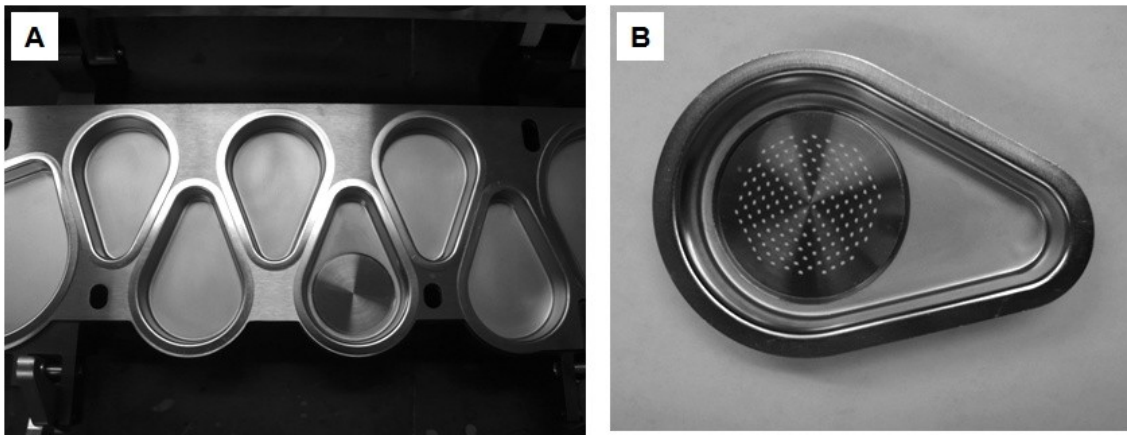

Figure 4.3 Schematic illustration of different architectures of membrane holder containing aerodynamically classified drug particles to be mathematically described within a framework: (A) monolayer and (B) multilayer system.

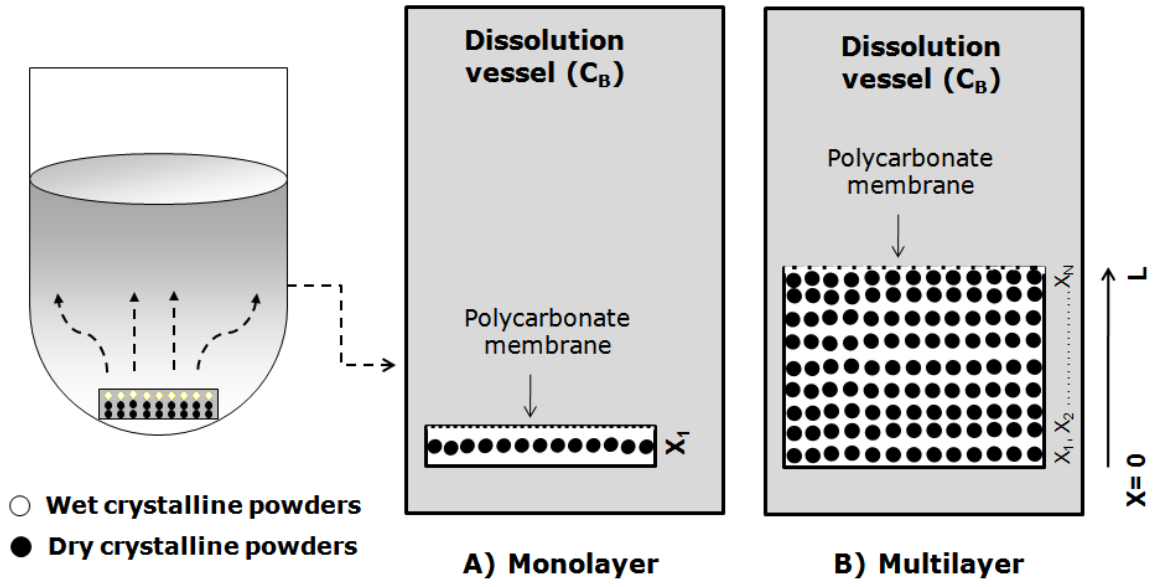

Figure 4.4 Particle deposition at each dose-collection plate of NGI for Ventolin® HFA, and PulmicortFlexhaler™ (Ventolin® HFA, and PulmicortFlexhaler™ were actuated 5 times at 30 L/min and 60 L/min, respectively. The error bars indicate the standard deviation of three tests).

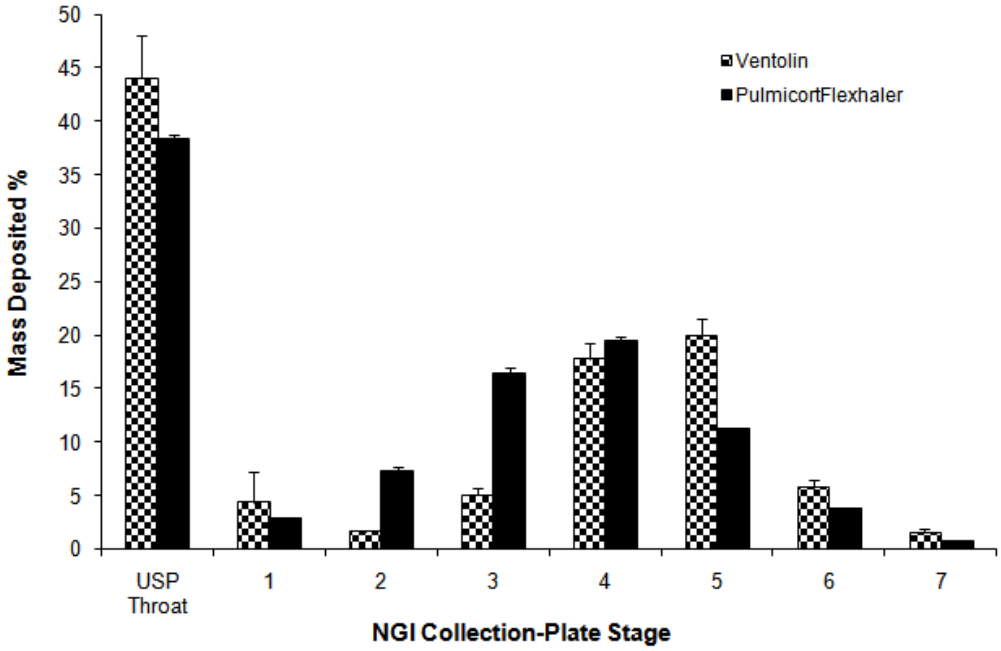

Figure 4.5 Release profiles of BD for dose-collection plate 2-5 (T: Number of actuation, the error bars indicate the standard deviation of three tests).

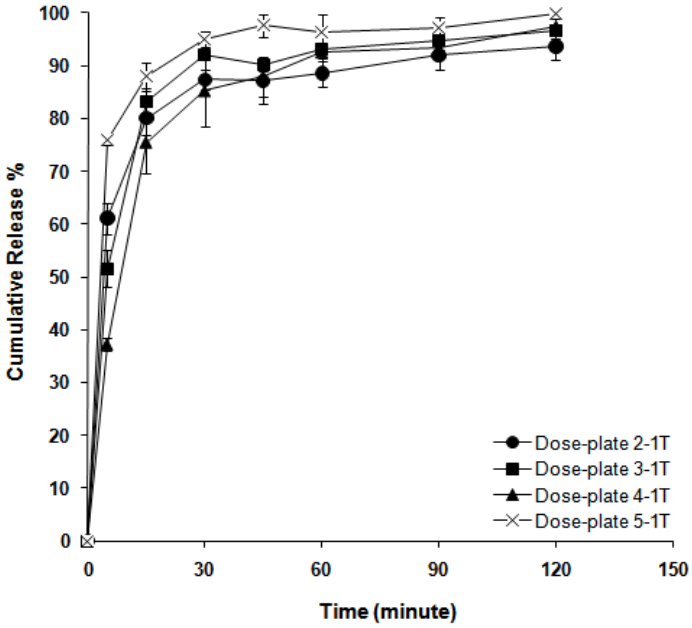

Figure 4.6 Release profiles of BD at rotating speed of 50 rpm, and of 75 rpm.(T: Number of actuation, the error bars indicate the standard deviation of three tests).

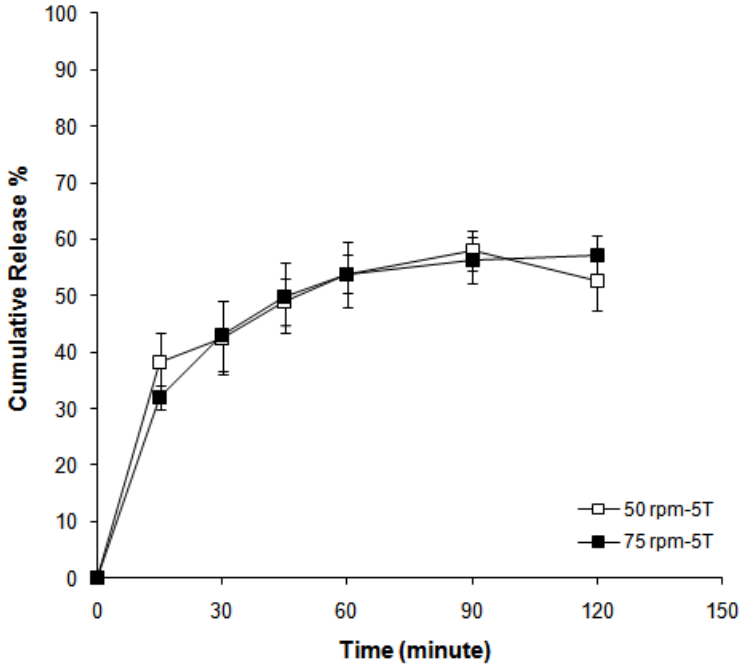

Figure 4.7 Release profiles of BD in three different dissolution media, PBS, 0.2 M phosphate buffer and SLF (A), and pH of PBS, 0.2 M phosphate buffer and SLF media measured for 24 hours without continuous CO_2 bubbling (B) (T: Number of actuation, the error bars indicate the standard deviation of three tests).

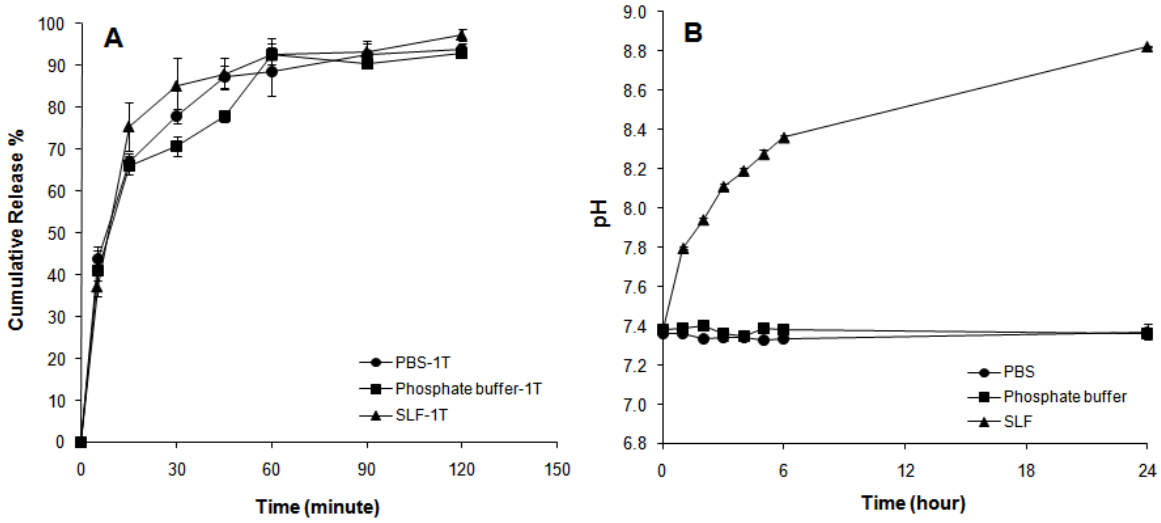

Figure 4.8 Release profiles of BD from the NGI membrane holder having different drug-loadings in SLF media for dose-collection plate 4 (A) and release profiles of BD in PBS media containing 0.02% DPPC, 0.02% polysorbate 80, and 0.2% polysorbate 80 (B). (T: Number of actuation, the error bars indicate the standard deviation of six tests).

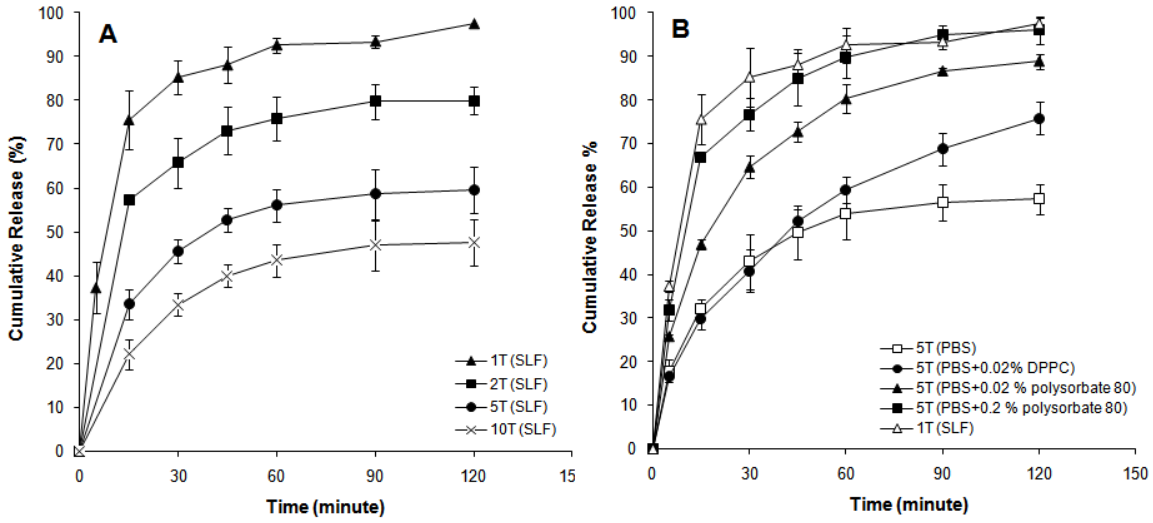

Figure 4.9 Release profiles of AS in SLF medium (T: Number of actuation, the error bars indicate the standard deviation of six tests).

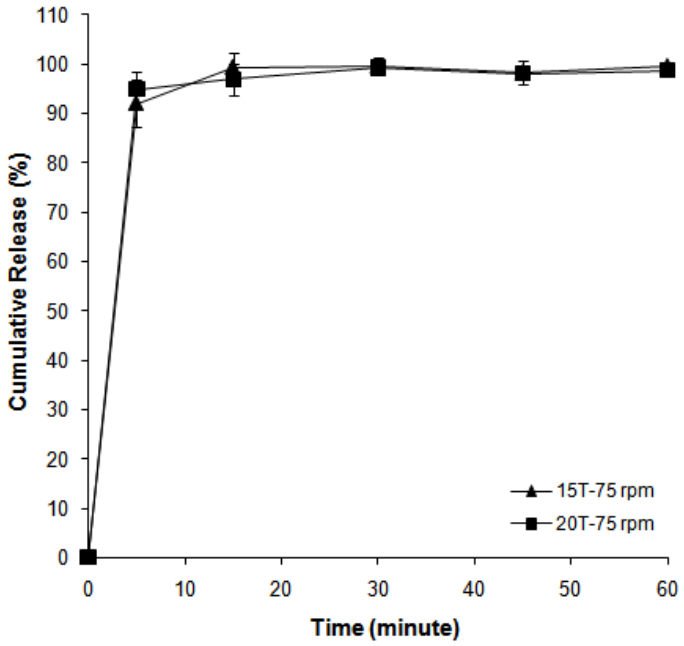

Figure 4.10 Scanning electron microscope (SEM) images of aerodynamically separated BD particles on the NGI dose-collection plate stage 4: (A) 1 time device actuation (1T), (B) 2T, (C) 5 T, and (D) 10 T.

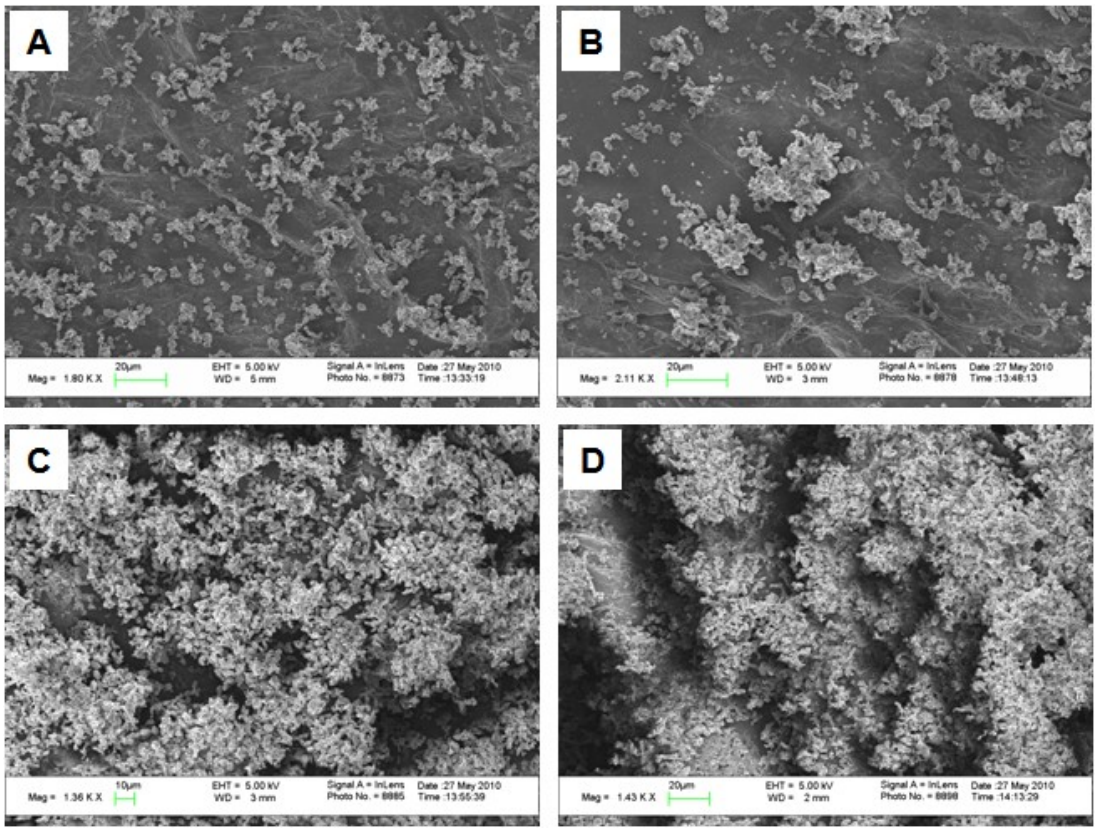

Figure 4.11 Profiles of (A) surface area of single BD particle and (B) BD concentration as function of axial coordination, at every 24 minutes intervals, for BD particles collected on the NGI dose-collection plate 4 by 1T device actuation. The calculation performed using parameters listed in Table 4.1. Solid line in blue, red and black represent mathematically calculated values at 0, 24,48 minutes, respectively, and broken line in blue red and black represent mathematically calculated values at 72, 96, and 120 minutes, respectively.

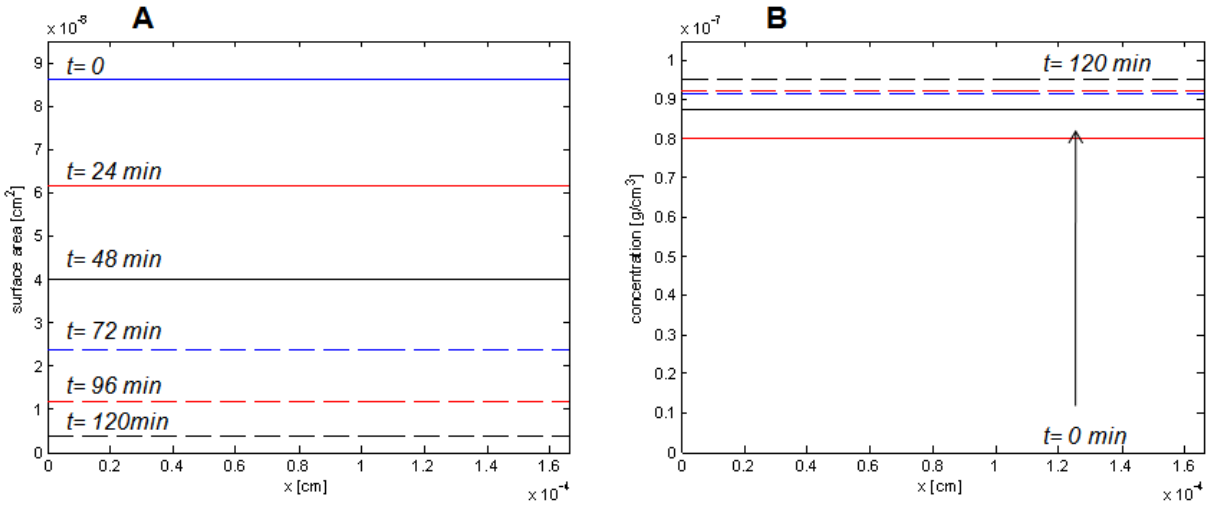

Figure 4.12 Profiles of (A) surface area of single BD particle and (B) BD concentration as function of axial coordination, at every 24 minutes intervals, for BD particles collected on the NGI dose-plate 4 by 10T device actuations. The calculation performed using parameters listed in Table 4.1. Solid line in blue, red and black represent mathematically calculated values at 0, 24,48 minutes, respectively, and broken line in blue red and black represent mathematically calculated values at 72, 96, and 120 minutes, respectively.

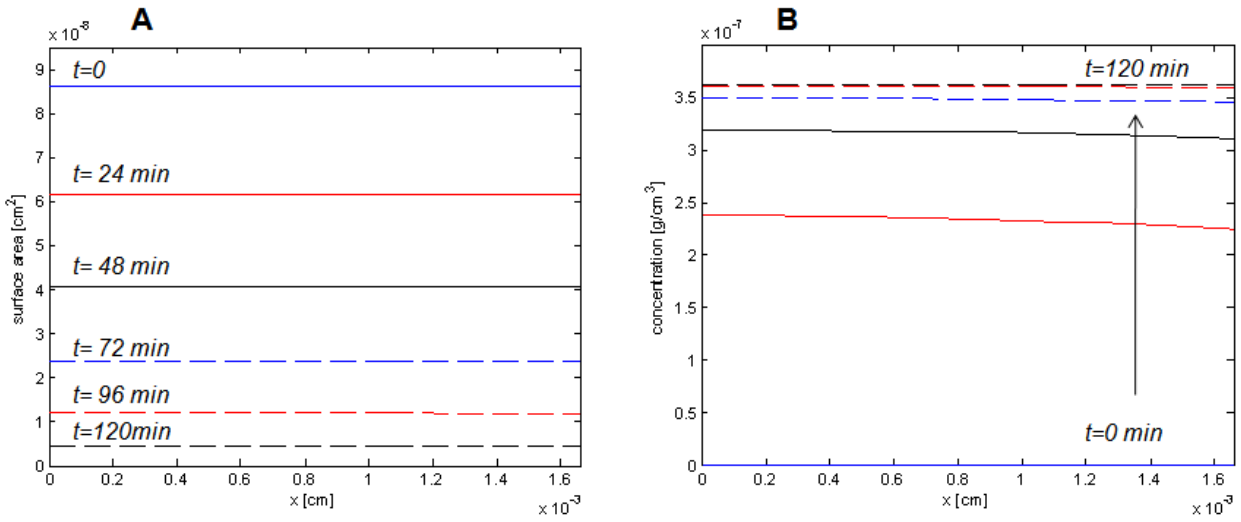

Figure 4.13 Profiles of BD concentration in the NGI membrane holder as a function of time for BD particles collected on the NGI dose-collection plate 4 by 10T device actuations: (A) calculation results in 3D image and (B) in 2D image for *D* values of (a) $6.3e^{-6}$, (b) $6.3e^{-7}$, and (c) $6.3e^{-8}$. Other parameters are listed in Table 4.1 Solid line in blue, red and black represent mathematically calculated values at 0, 24,48 minutes, respectively, and broken line in blue red and black represent mathematically calculated values at 72, 96, and 120 minutes, respectively.

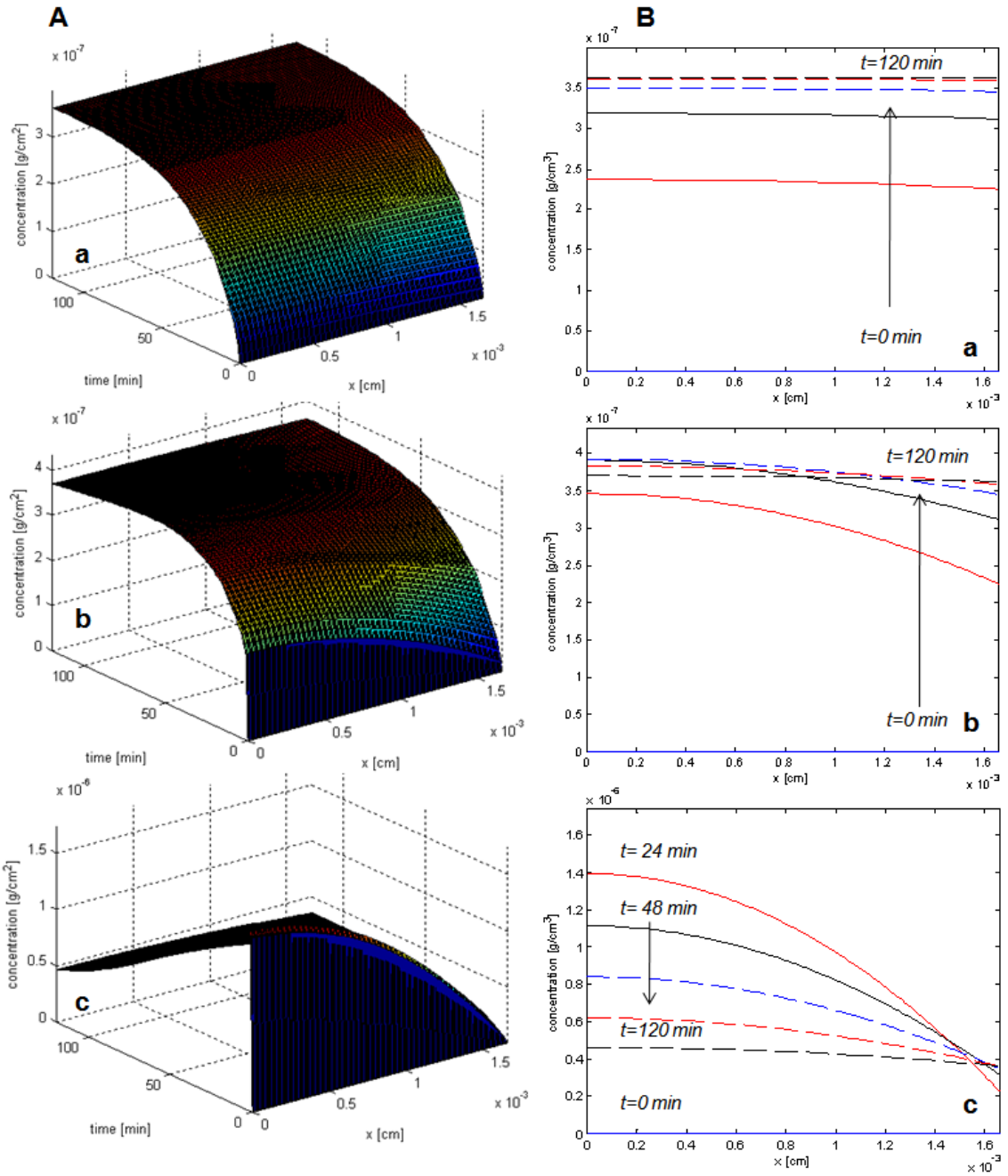

Figure 4.14 Profiles of BD concentration at x=0 and x=1 planar as a function of time for BD particles collected on the NGI dose-collection plate 4 by 10T device actuations: D values used for calculation are (A) $6.3e^{-6}$, (B) $6.3e^{-7}$, and (C) $6.3e^{-8}$. Other parameters are listed in Table 4.1. Solid line in blue and red represent mathematically calculated concentrations of BD at x=0 and x=L.

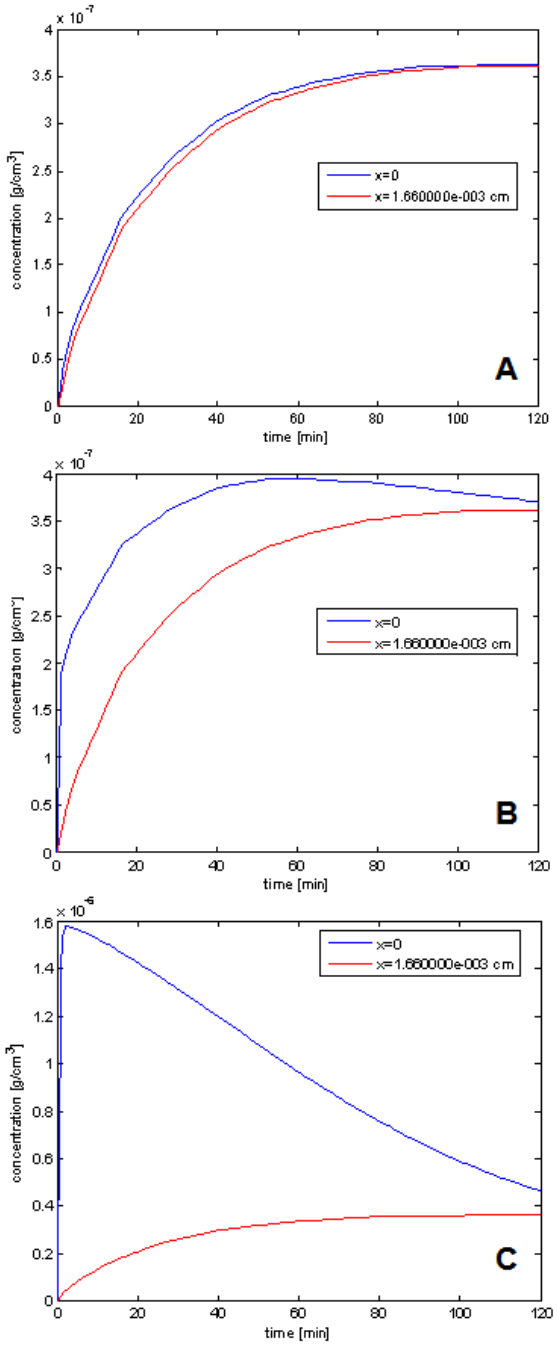

4.7. REFERENCES

[1] J.S. Patton, Mechanisms of macromolecule absorption by the lungs. Advanced Drug Delivery Reviews 19(1) (1996) 3-36.

[2] V.A. Grey, A.J. Hickey, P. Balmer, N.M. Davies, C. Dunbar, T.S. Foster, B.L. Olsson, M. Sakagami, V.P. Shah, M.J. Smurthwaite, J.M. Veranth, K. Zaidi, The Inhalation Ad Hoc Advisory Panel for the USP Performance Tests of Inhalation Dosage Forms. Pharmacopeial Forum 34(4) (2008) 1068-1074.

[3] R.O. Cook, R.K. Pannu, I.W. Kellaway, Novel sustained release microspheres for pulmonary drug delivery. Journal of Controlled Release 104(1) (2005) 79-90.

[4] T.P. Learoyd, J.L. Burrows, E. French, P.C. Seville, Chitosan-based spray-dried respirable powders for sustained delivery of terbutaline sulfate. European Journal of Pharmaceutics and Biopharmaceutics 68(2) (2008) 224-234.

[5] E. Ansoborlo, R.A. Guilmette, M.D. Hoover, V. Chazel, P. Houpert, M.H. Henge-Napoli, Application of in vitro dissolution tests to different uranium compounds and comparison with in vivo data. Radiation Protection Dosimetry 79(1-4) (1998) 33-37.

[6] M. Asada, H. Takahashi, H. Okamoto, H. Tanino, K. Danjo, Theophylline particle design using chitosan by the spray drying. International Journal of Pharmaceutics 270(1-2) (2004) 167-174.

[7] S. Jaspart, P. Bertholet, G. Piel, J.M. Dogne, L. Delattre, B. Evrard, Solid lipid microparticles as a sustained release system for pulmonary drug delivery. European Journal of Pharmaceutics and Biopharmaceutics 65(1) (2007) 47-56.

[8] S. Sdraulig, R. Franich, R.A. Tinker, S. Solomon, R. O'Brien, P.N. Johnston, In vitro dissolution studies of uranium bearing material in simulated lung fluid. Journal of Environmental Radioactivity 99(3) (2008) 527-538.

[9] Y.-J. Son, J.T. McConville, Development of a standardized dissolution test method for inhaled pharmaceutical formulations. International Journal of Pharmaceutics 382(1-2) (2009) 15-22.

[10] N.M. Davies, M.I.R. Feddah, A novel method for assessing dissolution of aerosol inhaler products. International Journal of Pharmaceutics 255(1-2) (2003) 175-187.

[11] D. Arora, K.A. Shah, M.S. Halquist, M. Sakagami, In Vitro Aqueous Fluid-Capacity-Limited Dissolution Testing of Respirable Aerosol Drug Particles Generated from Inhaler Products. Pharmaceutical Research 27(5) (2010) 786-795.

[12] W.I. Higuchi, Analysis of data on the medicament release from ointments. J. Pharm. Sci. 51 (1962) 802-804.

[13] M.I. Cabrera, J.A. Luna, R.J.A. Grau, Modeling of dissolution-diffusion controlled drug release from planar polymeric systems with finite dissolution rate and arbitrary drug loading. Journal of Membrane Science 280(1-2) (2006) 693-704.

[14] R.T. Kurnik, R.O. Potts, Modeling of diffusion and crystal dissolution in controlled release systems. Journal of Controlled Release 45(3) (1997) 257-264.

[15] T. Hayashi, T. Yamazaki, Y. Yamaguchi, K. Sugibayashi, Y. Morimoto, Release kinetics of indomethacin from pressure sensitive adhesive matrices. Journal of Controlled Release 43(2-3) (1997) 213-221.

[16] J.C. Sung, D.J. Padilla, L. Garcia-Contreras, J.L. VerBerkmoes, D. Durbin, C.A. Peloquin, K.J. Elbert, A.J. Hickey, D.A. Edwards, Formulation and Pharmacokinetics of Self-Assembled Rifampicin Nanoparticle Systems for Pulmonary Delivery. Pharmaceutical Research 26(8) (2009) 1847-1855.

[17] R.O. Salama, D. Traini, H.K. Chan, P.M. Young, Preparation and characterisation of controlled release co-spray dried drug-polymer microparticles for inhalation 2: Evaluation of in vitro release profiling methodologies for controlled release respiratory aerosols. European Journal of Pharmaceutics and Biopharmaceutics 70(1) (2008) 145-152.

[18] P. O'Hara, A.J. Hickey, Respirable PLGA microspheres containing rifampicin for the treatment of tuberculosis: Manufacture and characterization. Pharmaceutical Research 17(8) (2000) 955-961.

[19] D.A. Edwards, J. Hanes, G. Caponetti, J. Hrkach, A. BenJebria, M.L. Eskew, J. Mintzes, D. Deaver, N. Lotan, R. Langer, Large porous particles for pulmonary drug delivery. Science 276(5320) (1997) 1868-1871.

[20] D.B. Muchmore, B. Silverman, A. de la Pena, J. Tobian, The AIR (R) Inhaled Insulin System: System components and pharmacokinetic/glucodynamic data. Diabetes Technol. Ther. 9 (2007) S41-S47.

[21] M.R. Feddah, K.F. Brown, E.M. Gipps, N.M. Davies, In-vitro characterisation of metered dose inhaler versus dry powder inhaler glucocorticoid products: Influence of inspiratory flow rates. Journal of Pharmacy and Pharmaceutical Sciences 3(3) (2000) 317-324.

[22] J.A. Harris, S.W. Stein, P.B. Myrdal, Evaluation of the TSI aerosol impactor 3306/3321 system using a redesigned impactor stage with solution and suspension metered-dose inhalers. Aaps Pharmscitech 7(1) (2006) E1-E8.

[23] Guidance for Industry: Dissolution Testing of Immediate Release Solid Oral Dosage Forms. U.S. Department of Health and Human Services, Food and Drug Administration (FDA) (1997).

[24] S. Marre, J. Palmeri, Theoretical study of aerosol filtration by nucleopore filters: The intermediate crossover regime of Brownian diffusion and direct interception. Journal of Colloid and Interface Science 237(2) (2001) 230-238.

[25] S. Rzepka, B. Neidhart, Transport processes through track-etch membrane filters in a reagent delivery cell. Fresenius Journal of Analytical Chemistry 366(4) (2000) 336-340.

[26] V.A. Marple, D.L. Roberts, F.J. Romay, N.C. Miller, K.G. Truman, M.J. Holroyd, J.P. Mitchell, D. Hochrainer, Next generation pharmaceutical impactor (A new impactor for pharmaceutical inhaler testing). Part I: Design. Journal of Aerosol Medicine-Deposition Clearance and Effects in the Lung 16(3) (2003) 283-299.

[27] O.R. Moss, Simulants of lung interstitial fluid. Health Phys. 36 (1979) 447-448.

[28] General chapter <1092>: The Dissolution Procedure Development and Validation,USP32-NF27, Rockville, MD, 2009.

[29] R. Veldhuizen, K. Nag, S. Orgeig, F. Possmayer, The role of lipids in pulmonary surfactant. Biochimica Et Biophysica Acta-Molecular Basis of Disease 1408(2-3) (1998) 90-108.

[30] Nancy A. Dennis, H. Mark Blauser, J.E. Kent, Dissolution fractions and half-times of single sorce yellowcake in simulated lung fluids. Health Phys. 42(4) (1982) 469-477.

[31] D.D. Lasic, Liposomes in gene delivery,CRC Press Boca Raton, FL, 1997.

[32] N. Hada, T. Hasegawa, H. Takahashi, T. Ishibashi, K. Sugibayashi, Cultured skin loaded with tetracycline HCl and chloramphenicol as dermal delivery system:

Mathematical evaluation of the cultured skin containing antibiotics. Journal of Controlled Release 108(2-3) (2005) 341-350.

[33] Y.G. Ma, C.Y. Zhu, P.S. Ma, K.T. Yu, Studies on the diffusion coefficients of amino acids in aqueous solutions. Journal of Chemical and Engineering Data 50(4) (2005) 1192-1196.

Chapter 5: A New Respirable Form of Rifampicin[5]

Abstract

The aim of this research was to investigate a novel dry powder formulation of Rifampicin (RF) that presents an improved lung deposition profile by means of a polymorphic transformation into a flake-like crystal hydrate. Rifampicin dihydrate (RFDH) was prepared by recrystallization of RF in anhydrous ethanol and amorphous RF (SP-RF) was prepared by spray-drying. The physicochemical properties of the RFDH and the SP-RF were characterized. Aerosol performances of RFDH and SP-RF were studied using a Next Generation Impactor (NGI). The RFDH powder, successfully prepared using a simple recrystallization process, had a MMAD of 2.2 μm. The RFDH powders were characterized as having a very thin flaky structure; this morphology provided improved aerosolization properties. The maximum fine particle fraction (FPF_{TD}) of 68% for the RFDH was achieved with the Aerolizer® device. Significant chemical degradation was not observed from the RFDH, while the SP-RF showed significant chemical degradation over a 9 month period. The flaky morphology of RFDH resulted in a reduced agglomeration tendency, relative to spherical SP-RF particles. The excipient free formulation of the RFDH would offer the benefit of delivering a maximum potency formulation of the antibiotic directly to the site of infection, the lung.

[5]Significat portions of this chapter were taken from : Yoen-Ju Son, and Jason T. McConville, "A new respirable form of rifampicin", European Journal of Pharmaceutics and Biopharmaceutics (In press).

5.1. INTRODUCTION

Tuberculosis (TB) is a chronic infectious disease, which is considered the foremost cause of death due to a single microorganism [1]. The occurrence of TB is most often due to *Mycobacterium tuberculosis* (MTB) infection and the lung is the primary site of infection. The most common treatment for TB involves oral administration of high systemic doses of single or combined antibiotics, which causes unwanted side-effects by high systemic exposure of said antibiotics [2]. Several current studies have been proposed for the administration of anti-tubercular (TB) drugs to the primary infection site, the lung, with the idea of increasing the local therapeutic effect and reduce the overall systemic exposure [3-9]. Pulmonary delivery of rifampicin (RF) has been widely studied [3-6, 8, 10] since it is the first choice drug in the treatment of TB [1, 11]. Several respirable forms of RF, such as nano/microparticle [3-5], liposome [8], and liquid [9], have been introduced to localize the RF in the lung. However, the aerosolization properties of these types of formulation have not been adequately addressed to date, and represent the most important factors in determining the drug dose to the target site. The aerosolization properties are especially important in dry powder inhalation (DPI) formulations, as the dispersion and subsequent deposition profiles of powders are predominantly governed by the physicochemical properties of the drug and the excipient used for manufacturing [12-15].

The polymorphic transformation of drugs may be considered to be a powerful particle engineering technique in the manufacture of respirable dry powders. Improved

aerosolization properties may be achieved under such transformations, since the morphology of a particle can play the most important role in powder aerodynamic performance. It has been shown that adhesion force distributions between particles can be attributed to their morphology, for instance, the surface roughness [16-18], and the crystal shape [19-21]. Several active pharmaceutical ingredients (APIs) have been successfully engineered as crystals with elongated [19, 21], and flaky structures [20]. These structural changes may show significantly improved inhalation properties following polymorphic transformation [19, 20, 22]. Current research strategies for respirable dry powder RF formulations are predominantly focused on the amorphous form, having a spherical shape [3, 4, 6]. This is due to the fact that they are prepared by a microencapsulation followed by either a spray-drying or solvent evaporation process [3, 4, 6]. These spherical particles may be either blended with carrier materials [6, 23], or manufactured as a carrier-free low density powders containing relatively large amounts of excipient [4], in an effort to minimize adhesion forces between particles. However, low density particles have limitations in the drug payload due to this significant quantity of incorporated excipient. And in the case of RF a substantial amount (milligram dose) needs to be delivered to the lung to be efficacious [4, 5]. Additionally, the amorphous form of several investigated RF formulations may not provide long term stability, since amorphous materials often undergo chemical degradation or a recrystallization processes.

The aim of this study is to develop a novel carrier-free dry powder inhalation (DPI) formulation of RF that has improved aerodynamic properties as well as a good stability profile. It is the goal of this research to demonstrate that the use of a

polymorphic transformation directly from RF crystals can offset some of the aforementioned limitations with other investigated formulation types. This study describes how the dihydrated form of RF (RFDH) was prepared from the pure RF form I, and how the crystalline structure and the physicochemical properties of RFDH were characterized by various analyses. The aerodynamic behaviors of prepared RFDH are also described with two dry powder inhalers (DPIs), the Aerolizer® and Handihaler®.

5.2. MATERIALS AND METHODS

5.2.1. Materials

Rifampicin (RF) was purchased from the Sigma Chemical Co. (St. Louis, MO). Size 3 hydroxypropylmethyl cellulose (HPMC) capsules were donated from Capsugel (Peapack, NJ). Polycarbonate membranes of 0.05 μm, were purchased from Whatman (Florham Park, NJ). An Aerolizer® dry powder inhaler device was donated by Schering-Plough (Kenilworth, NJ). A Handihaler® device was donated from Boehringer Ingelheim GmbH (Rhein, Germany). A NGI membrane holder was provided by Copley Scientific (Nottingham, UK). All other reagents were purchased from the Sigma Chemical Co. (St. Louis, MO).

5.2.2. Preparation of rifampicin hydrate and amorphous rifampicin

Rifampicin dihydrate (RFDH) was prepared by heating the anhydrous ethanol suspension of the form I rifampicin (RF) to 60°C. RF powder (900 mg) was added to the

hot anhydrous ethanol solution (30 mL) and stirred until a saturated solution was obtained, after the solution had been allowed to cool to room temperature. The suspension was homogenized with a Ultra-Turrax® high-shear homogenizer (IKA® Works Inc., Wilmington, NC) at 10,000 rpm for 2 minutes to homogeneously disperse the particles. The resultant suspension was then spray dried with constant stirring using a Büchi Minispray dryer B-290 (Büchi Laboratory-Techniques, Flawil, Switzerland). The following conditions were used during spray drying: drying airflow, 40 m^3/h; spraying airflow, 500 L/h; suspension feed rate, 5 mL/min; nozzle size, 0.5 mm; the inlet temperature was established at 70ºC and the outlet temperature was between 40 and 50ºC. To measure the dissolved amount of RF in the suspension, the suspension containing recrystallized particles was prepared as above and centrifuged at 10,000 rpm for 5 minutes and the RF content in the filtered solution was analyzed using a validated HPLC method [3].

Amorphous RF (SP-RF) was prepared as a control formulation by spray drying. 1g of RF was dissolved in 50 mL of dichloromethane and spray-dried under the same spray conditions as above. The resultant powders, RFDH and SP-RF were stored at ambient condition (25°C/50% RH).

The content uniformities of the RF, RFDH, and SP-RF powders were determined using HPLC. A stock solution of each sample was prepared; each powder (25 mg) was weighed separately and dissolved with 25 mL of methanol. 1 mL of each stock solution was diluted with 9 mL of mobile phase. For identification of RFDH and SP-RF, a concentration of 100 μg/mL RF, SP-RF, and RFDH solution were each prepared from

their respective stock solutions. The prepared RF solution (10 mL) was then spiked with the RFDH and the SP-RF solutions (10 mL) and analyzed using HPLC [3].

5.2.3. Characterization

5.2.3.1. Fourier transform infrared spectroscopy (FTIR)

Potassium bromide (KBr) pellets were prepared by compressing 1-2 mg of sample mixed with 300-400 mg of dried KBr. Spectra were recorded using a Nicolet 360 FTIR spectrophotometer (Thermo Fisher Scientific Inc, Waltham, MA), and the data was analyzed using Omnic ESP software (Thermo Fisher Scientific Inc, Waltham, MA).

5.2.3.2. X-ray diffraction of powders

The crystalline structures of prepared samples were examined using wide angle X-ray diffraction (XRD). A Philips 1710 X-ray diffractometer (Philips Electronic Instruments Inc., Mahwah, NJ) with a copper target (CuKα1,λ = 1.54056 Å), and a nickel filter, at a voltage of 40 kV and a current at 40 mA, was used to obtain the XRD patterns. . Samples were analyzed in the 2-theta (2θ) range from 5 to 50° using a step size of 0.02 2θ degree with a dwell time of 2 sec.

5.2.3.3. Thermal analysis

Thermograms were measured using a differential scanning calorimetry (DSC), Model 2920 (TA Instruments, New Castle, DE). Dry nitrogen gas was used as the purge gas through the DSC cell at a flow rate of 40 mL/min. Samples (5 mg) were weighed into

aluminum crimped pans. The mass of the empty sample pan was matched with that of the empty reference pan within ± 0.2 mg. Samples were heated at a ramp rate of 10°C/min from 30 to 350°C. Thermogravimetric anaysis (TGA) was conducted using a Perkin Elmer TGA 1 system (Perkin Elmer Inc., Waltham, MA). Mass loss from 5 mg samples at a heating rate of 10°C /min from 30 to 350°C under a nitrogen purge (40 mL/min) was recorded.

5.2.3.4. Moisture sorption analysis

Dynamic vapor sorption (DVS) was used to investigate the moisture sorption of RFDH RF, and SP-RF powders. Samples (10 mg) were pre-weighed and added to quartz sample pans which were placed in the sample chamber of a DVS-1 apparatus (Surface Measurement Systems Ltd., London, UK). During this measurement, all samples, RF, SP-RF, or RFDH, were separately exposed to a continuous flow of N_2. Each sample was dried at 0% RH for two hours before being exposed to 10% RH increments for two 0-90% RH cycles at 25°C. To prevent desolvation, another condition was applied for RFDH. The humidity increments started from 50% RH to 90% RH. Equilibrium moisture content at each increment was determined by a dm/dt of 0.002%/min.

5.2.3.5. Particle size distribution, density and aerodynamic diameter

Particle size distributions, based on volume fractions of prepared powders were measured using a Spraytec® particle size analyzer equipped with an inhalation cell specifically modified to measure the particle size diameter (PSD) generated from aerosols

(Malvern Instruments, Ltd., Worcestershire, UK). It consisted of a Spraytec® unit with a USP inhalation induction port held in place by the inhalation cell, and a connection for the selected aerosol generating device. The entire assembly operated in a closed system, and allowed for a controlled airflow rate (60 L/min) through the measurement zone. Size 3 HPMC capsules were filled with 15 mg of powder, and loaded in to the Aerolizer® device. The Aerolizer® device was then fired into the Spraytec® particle size analyzer at flow rate of 60 L/min to allow the particle size distribution of DPIs to be measured under simulated actuation conditions.

The bulk densities of the SP-RF and RFDH powders were determined by pouring a known mass of powder (approximately 0.1 g) under gravity into a calibrated measuring cylinder, then recording the volume occupied by the powder. The tapped density was measured by following a USP method [24]. Theoretical estimates of aerodynamic diameter (d_{ae}) were derived from the particle sizing ($d_{0.5}$) and tapped density data (p), according to Eq. 1 [25].

$$d_{ae} = d \times \sqrt{\frac{\rho}{\rho_1}} \quad \text{, Where} \quad \rho_1 = 1 \text{ g cm}^{-3} \tag{1}$$

5.2.3.6. Scanning electron microscopy (SEM)

The morphology of prepared samples, RF, SP-RF and RFDH, was observed using a LEO 1530 SEM (Zeiss/LEO, Oberkochen, Germany). Each sample was mounted separately onto SEM stubs using double-sided copper tape before sputter coating with Ag

for 30 seconds under vacuum at 30 mTorr. The SEM was operated at high vacuum with accelerating voltage 5 kV and specimen working distance 4 mm.

5.2.3.7. Hot stage microscopy

Thermal events of each of the prepared samples: RFDH, SP-RF, and RF, were observed on a hot stage (Mettler FP 82 HT, Mettler Instrument Corp., Highstwon, NJ) under optical microscope equipped with polarizer (Olympus BX 60, Olympus America Inc., Center Valley, PA). The samples were mounted on a glass slide, without a cover slip, and heated from 25ºC to 200ºC at a rate of 10ºC/min. Images were transferred via a Spot Insight QE Color 4.2 (Diagnostic Instruments, Sterling Heights, MI) and analyzed using SPOT™ imaging software (version 3.5.5).

5.2.3.8. Saturation solubility

The solubility of each sample, RFDH, SP-RF, and RF, was determined in pH 7.4 phosphate buffered saline (PBS) containing 0.02% (w/v) ascorbic acid as an antioxidant, to prevent the oxidative degradation of the dissolved samples [3]. Samples (50 mg) were added to 20 mL of the prepared PBS and shaken for 24 hours at 37°C. Samples (1 mL) were taken from each vial at 1, 2, 4, 6, 8 and 24 hour intervals and filtered with a 0.45 μm polytetrafluoroethylene (PTFE) syringe filter. Ethanol (100 μL) was added to the 900 μL of collected samples and analyzed using a validated HPLC method [3]. The resultant equilibrium sample concentration was used to calculate the saturated solubility concentration.

5.2.3.9. High performance liquid chromatography (HPLC)

Drug content, solubility and dissolution samples were analysed using a HPLC system (Waters Co., Milford, MA) with UV detection. The system consisted of a 717 plus autosampler, 2487 dual wavelength detector, 1525 binary pump, and 1500 column heater. Chromatography was performed using a Bondapak C_{18} 10 μm 3.9×300 mm column (Waters, Milford, MA) and a SecurityGuard™ guard column (Phenomenex®, Torrance, CA). The mobile phase, consisting of methanol, acetonitrile and phosphate buffer solution pH 5.2 in a ratio of 50:17:33 respectively, was eluted at a flow rate of 1.2 mL/min and the UV detector was set to a wavelength 337 nm. The column temperature was maintained at 25°C and the volume of each sample injected was 50 μL [3].

5.2.4. Aerosol classification

The aerosolization performaces of RFDH and SP-RF were studied using a Next Generation Impactor (NGI) (MSP Co., Shoreview, MN). The prepared RFDH powders (7, 15, or 30 mg) and 15 mg of SP-RF powders were filled into the size 3 HPMC capsules and placed into either an Aerolizer® or Handihaler® dry powder inhaler (DPI). Each capsule was pierced and actuated into an NGI though a stainless steel USP throat adapter (aerosol induction port) at a flow rate 30 L/min or 60 L/min for 8 and 4 seconds, respectively. The powder deposited in the throat, in each dose collection-plate of the NGI, and in the remaining capsule, were each reconstituted with 10 mL of acetone. The powders remaining in the device were washed with 10 mL of ethanol. Collected samples

were analyzed by an 8453 UV/VIS spectrophotometer (Agilent, Santa Clara, CA) at 474 nm [26].

The emitted dose (ED), defined as the percent of total loaded powder mass exiting the capsule, was determined by subtracting the amount remaining in the capsule from the initial mass loaded into the capsule. The fine particle fraction (FPF_{TD}), defined as the total dose of particles with aerodynamic diameters smaller than 5 μm, was calculated via interpolation from the cumulative mass against the cutoff diameter of the respective stages of the NGI. The FPF_{TD} is expressed as a percentage of the total drug dose, and not of the emitted dose. Each measurement was repeated three times. The MMAD was determined by the % cumulative undersize on probability scale versus logarithmic aerodynamic diameter data.

5.2.5. Dissolution studies

Dissolution behaviors of air classified RFDH and SP-RF were studied using a membrane holder method previously developed by this group [27, 28]. To briefly summarize, the prepared powders (7 mg) were filled into size 3 HPMC capsules, placed into the Aerolizer® device, and actuated into the NGI equipped with a dissolution cup (MSP Co. Shoreview, MN) equipped with a dissolution impaction insert (Copley Scientific, Nottingham,UK) at a flow rate of 60 L/min for 4 seconds. The impaction insert containing air classified particles was removed from the dissolution cup, and a pre-soaked polycarbonate membrane was placed onto the top and sealed in place with a push fitted sealing ring. The sealed NGI membrane holders were placed into each dissolution

vessel containing 300 mL of PBS containing 0.02% ascorbic acid. Dissolution testing was conducted at 75 rpm. The dissolution media (2 mL) was withdrawn manually using a glass syringe and filtered using a 0.45 μm PTFE syringe filter at timed intervals of 15, 30, 60, 120, 180, 240, 360, and 480 minutes. Fresh dissolution media (3 mL) was replaced into each vessel after sampling to maintain a constant volume. Ethanol (100 μL) was added to the 900 μL of collected samples and analyzed using the validated HPLC method, described above [3].

5.2.6. Stability

The prepared samples, SP-RF and RFDH, were stored at ambient conditions in amber vials (25°C/50% RH). Drug contents and thermal behavior using differential scanning calorimetry (DSC), of stored samples were monitored every two months using the method described above.

The desolvation behavior of RFDH was studied. The prepared powder stored in the uncapped amber vial was vacuum dried (25°C/5% RH) in the desiccators for 1 week. The dried samples were analyzed using DSC to confirm the desolvation and the crystalline structure were examined using the XRD procedure described above.

5.2.7. Statistical analysis

Data were expressed as the mean plus/minus standard deviation (SD). Statistical differences were studied by analysis of variance (one-way ANOVA) using Jump 7.0

software (SAS Institute Inc., Cary, NC). *P* values of less than 0.05 were considered as statistically significant.

5.3. RESULTS

5.3.1. Physicochemical characteristics

Bulky RFDH powders were prepared as shown in Figure 5.1. Flake-like RFDH crystals were the result of a polymorphic transformation of RF, as shown in SEM images (Figure 5.1). The original crystals of RF and SP-RF powders indicate a rod shape and a corrugated spherical shape, respectively (Figure 5.1). The spray-dried RFDH crystals contain approximately 3.5% (w/w) of the amorphous RF form, as the dissolved RF in the suspension was also sprayed with the solid crystal.

The chemical identification for the RFDH and the SP-RF samples were conducted via the spiking test. The retention time (Rt) for both spiked samples with RF was found at 5.9 minutes, and one completely overlapped peak was observed from the HPLC chromatogram. The RF contents of samples, RF, RFDH and SP-RF, were 99.4, 95.8 and 102, respectively as shown in Table 5.1.

The saturation solubilities of RF, SP-RF, and RFDH in PBS buffer (pH 7.4) containing 0.02% (w/v) ascorbic acid, were determined to be 0.59, 1.32 and 1.28, respectively (Table 5.1). The solubility study was continued for 24 hours and the saturated concentration was achieved at 8 hours for all samples as shown in Figure 5.2.

It was found that the RFDH is a dihydrate, as indicated by thermal analysis, with the main thermal events summarized in Table 5.1. The DSC thermogram of RFDH shows two endothermic processes associated with weight loss as seen in Figure 5.3 (A). The first one corresponds to the evaporation of physically absorbed water and the second one at 90-150ºC is consistent with the release the water of crystallization. The dehydrated RFDH melts at 180ºC, followed by the decomposition of the product at 257ºC. The thermal events of RFDH crystal can also be clearly seen from Figure 5.4; the bright orange color of RFDH crystals mounted on the hot stage was gradually darken as temperature increased, and finally melt at 180ºC. From the TGA analysis (Figure 5.3 (B)), the total weight loss of 5.2% (w/w) upon drying was determined, and the weight loss corresponding to the dehydration of the water of crystallization measured over a temperature range (65-110ºC), was 4.2% (w/w). The series of thermal events for RFDH was further confirmed by a hot stage microscope (HSM) study. The transparency and brightness of crystals gradually decreased until they were melted at 180ºC while maintaining their original shape (Figure 5.5), indicating that desolvation causes the crystalline lattice to collapse.

The thermograms of SP-RF and RF were also studied (Figure 5.3). In DSC and TGA analysis, no thermal event or weight loss was observed for pure RF until it decomposed at 260ºC. For the SP-RF, the glass transition temperature (Tg) was observed at 165ºC, followed by thermal decomposition at 257ºC.

The crystalline structure of prepared samples was analyzed using XRD. As shown in Figure 5.6, the characteristic peaks of the RF form I appeared at 13.65 and 14.3 2θ°,

respectively. The SP-RF was judged to be an amorphous structure since no characteristic peaks for RF were observed, and a halo at the baseline appeared on the x-ray diffractogram. The RFDH crystal shows characteristic peaks, although the intensity of those peaks, and the subsequent degree of crystallinity, appears to be lower than that of the pure RF form. It was also found that the RFDH is a different polymorphic form than that of pure RF, as the XRD diffraction patterns were not identical. After desolvation of water from the RFDH crystal, the XRD pattern shifted, with a small halo at the baseline indicating that the crystal lattice collapses upon desolvation as confirmed by HSM study.

Representative moisture sorption isotherms for the SP-RF, the RFDH spray dried and pure RF form I are shown in Figure 5.7 (A), (B) and (C), respectively. In general, the two samples, SP-RF and RFDH, had very different gravimetric responses to moisture sorption. The SP-RF shows 14% moisture uptake between 0-90% RH and a remarkable hysteresis is seen on Figure 5.7 (A) indicating extensive surface moisture binding capacity. Contrary to SR-RF, the RFDH showed an approximately 2.3% moisture uptake between 50-90% RH. No remarkable hysteresis was shown from the isotherm graph (Figure 5.7 (B)). The moisture sorption study for the RFDH was conducted under two separate conditions, 0-90% RF cycle and 50-90% RH cycle, however, the 50-90% RH condition was chosen, as the RFDH showed very fast desolvation at 0% RH. The RF showed a 1% moisture uptake between 0-90% RH without hysteresis (Figure 5.7 (C)).

Difference in H-bonding of prepared samples were characterized by FTIR spectroscopy and interpreted based on the article by Pelizza et al. [29]. The SP-RF exhibited double peaks at 1714 cm^{-1} and 1733 cm^{-1}, the main peaks of interest to define

the existence of an H-bond between acetyl C=O and C_{23}-OH [29-32]. Contrary to the SP-RF, a single peak was observed at 1727 cm^{-1} from the RFDH and the RF samples. The absorption band due to the ansa OH in the RF manifested as a sharp peak at 3490 cm^{-1}, but was seen as a broad band 3250-3600 cm^{-1} in the SP-RF and the RFDH samples. The main observed absorption bands are listed in Table 5.2.

The median particle sizes ($d_{0.5}$) of SP, SP-RF, and RFDH were 116, 26.4, and 8.8 μm, respectively as listed in Table 5.3. The SP-RF and the RF powder samples showed much higher variability in particle size than that of the RFDH. It was clearly seen from Figure 5.8 that the SP-RF powder sample showed a bimodal distribution, indicating that particles were not completely deagglomerated at the airflow (60 mL/min), whereas RFDH powder samples demonstrated a unimodal distribution. The calculated d_{ae} value for the RFDH was 2.3 μm and the d_{ae} value for SP-RF could not be obtained since the tapped density could not be measured properly due to the cohesive properties of powders.

5.3.2. Aerodynamic properties

The aerosolization properties of RFDH and SP-RF were compared using two DPI devices, the Aerolizer® and the Handihaler®. The ED, FPF_{TD}, and MMAD of SP-RF and RFDH powders are displayed in Table 5.4. The aerodynamic performances of the RFDH powders were improved by changing the crystalline structure to a flake-like dihydrate form, with at least 60% FPF_{TD} for each DPI device. Although, the SP-RF was manufactured as a highly corrugated powder to improve the dispersibility, the FPF_{TD} values obtained from Handihaler® and Aerolizer® were lower than those of RFDH, at

50.9% and 36.6% respectively. The mass of RFDH powders deposited on each dose collection-plate was not dependent on the capsule fill mass, as shown in Figure 5.9. The FPF_{TD} values of RFDH obtained from different capsule fill masses (7, 15, and 30 mg) were 59.1, 63.8, and 60%, respectively, with more than 90% of the capsule contents being emitted during aerosolisation testing at an air flow of 60 L/min. The flow rate has an influence on the dispersion of RFDH powder as the FPF_{TD} lowered to 47.8% at 30 L/min. The significant difference in the mass deposition between two different devices was also found for the SP-RF and the RFDH powders, as shown in Figure 5.10. For RFDH, the Aerolizer® shows better particle separation than that of the Handihaler®. Conversely, for the SP-RF, the Handihaler® shows better separation than the Aerolizer® as the FPF_{TD} values for RFDH and SP-RF were 63.8% and 50.9% with the Handihaler® device, and 68.5% and 36.6% with the Aerolizer® respectively. In particular, the ED of SP-RF showed a significant difference between the two devices.

The MMAD of RFDH calculated from the Handihaler® device was in the range of 3.1 to 3.7 μm at an air flow of 60 L/min compared to 2.2 μm in the Aerolizer® at the same airflow. The theoretical estimate of d_{ae} for RFDH powders was more similar to the MMAD value obtained from the Aerolizer® device, indicating that the Aerolizer® device is more efficient in particle deagglomeration than Handihaler®. For the SP-RF, MMAD values were 3.4 and 2.8 for Aerolizer® and Handihaler®, respectively.

5.3.3. Stability

The physicochemical stabilities of the SP-RF and RFDH were studied. The RF contents of stored formulations for 9 months are summarized in Table 5.5. No significant change in RF content was found from the RFDH samples over the 9 month study period. The DSC thermograms of RFDH samples at 4 and 6 months were identical to that of the initial sample, as shown in Figure 5.11. Contrary to the RFDH, the SP-RF showed a significant difference in drug content, which was lowered to 75.5% at 9 months. The DSC thermograms of 4 and 6 months samples show that the peaks corresponding to the Tg at 165°C are gradually shifted to 180°C, implying a change in the order of molecular arrangement (Figure 5.11). It also demonstrated by the DSC thermograms shown in Figure 5.11 that the peak corresponding to drug decomposition is broadened, and the onset of degradation is earlier than that of initial sample. Additionally, a color change was also observed for SP-RF powder (Figure 5.12 (A)). The recrystallization of SP-RF (4 month sample) was further confirmed by the hot stage microscope study (Figure 5.12 (B)). A bright interference color was observed with the 4 month samples of SP-RF powder over the temperature range of 30°C to 200°C.

Desolvation of the water of crystallization was confirmed by the DSC study. Following the drying procedure prior to analysis, the peak at 110-150°C had disappeared and the endothermic peak, corresponding to the physically absorbed water was increased, which was consistent with most of the particles losing their crystalline structure. Under vacuum, the desolvation was completed in 1 week. It was also found that this process was

accelerated by the N_2 gas used in the DVS study (The properties of desolvated RFDH are described in Appendix B).

5.3.4. Dissolution studies

Dissolution studies were performed with the SP-RF and RFDH formulations. For dose collection, the particles were air-classified using NGI as explained above, the particles deposited on the collection-plate stage 3 were used for the dissolution study as the particle size on this plate showed similar MMAD values for both formulations. The MMAD values for the RFDH and the SP-RF were 2.2 and 2.8 μm with Aerolizer® respectively and the particle size cut-off for dose collection-plate stage 3 was 2.82 μm [33]. The amount of powder deposited on stage 3 for both formulations was 1 mg. Figure 5.13 shows that 74% and 82% of the RF were released for the RFDH and the SP-RF samples from stage 3 within 1 hour.

5.4. DISCUSSION

5.4.1. Polymorphic transformation to the flake-like crystal of RF

The flake-like RF dihydrate crystal was prepared by recrystallization in anhydrous ethanol followed by spray drying of the prepared suspension, as shown in Figure 5.1. Generally, the drying of recrystallized particles involves heat and low pressure conditions to remove solvents used in the recrystallization process. However, those conditions may not be suitable if the prepared crystal is in the hydrate or solvate form since desolvation

may occur during the drying process [34, 35]. Desolvation of the hydrate form of crystal usually results in the rearrangement of the crystal lattice, generally leading to loss of crystallinity or significant structural change [34, 35]. Figure 5.6 shows that the desolvation of RF causes the crystalline lattice to collapse whether it is dried via vacuum conditions or N_2 gas purge. The properties of desolvated RFDH are described in Appendix B. The spray-drying process allows the RFDH crystals to dry without desolvation since it allows for very rapid drying. Thus, the crystals are not heated while they are drying [36]. Additionally, aggregation or caking of the RFDH particles was prevented as particles were further deaggregated by atomization involving the break-up of liquid feed into very fine droplets. The physicochemical properties of RFDH dried via filtering method were given in Appendix B.

The dihydrate form of RF was confirmed by thermal analysis. The DSC thermogram of RFDH (Figure 5.3 (A)) showed an endothermic peak corresponding to the release of the water of crystallization at 90-150ºC, and the TGA weight loss for the desolvation was 4.2% which was equivalent to 2 moles of water per mole of RF (Figure 5.3 (B)). Generally, a hydrate is formed from the aqueous media or the mixture of aqueous/organic solvent by the association of water molecules in the crystal lattice. However, in RF the formation of several hydrates, mono, di, and heptahydrate, from several organic solvents has been reported, which can be attributed to the traces of water in the solvents. Specifically, it was reported that the mono and heptahydrate forms of RF are a results of recrystallization from anhydrous ethanol (containing less than 1% water). These polymorphs are believed to be the product of the imbibitions of water [29,

31]. The extreme complexity in the chemical structure due to the various hydrogen bonding sites and ionization states that exist, may also contribute to the formation of various hydrate forms [29-31, 34, 35].

The hydrate of RF is presumed to be a stoichiometic hydrate due to the fading of the bright interference color after dehydration on the HSM study (Figure 5.5), and to the peak shift with the halo at the baseline on the XRD diffractogram (Figure 5.6), indicating that the majority of crystalline lattice changed to an amorphous state. This was further confirmed by DSC analysis. As indicated in Figure 5.3 (A), the melting of dehydrated RFDH at 180ºC is not accompanied with an endothermic process since no heat is required for amorphous material to pass to the liquid phase [29]. It is known that the water molecule in the stoichiometic hydrate is an essential component in the maintenance of the molecular network. Thus, desolvation results in a disordered crystalline state [29, 34, 35].

The XRD results of RFDH and RF confirm the polymorphic transformation of the RF form I to the different crystal form. Figure 5.6 shows that two main characteristic peaks of the RF form I, at 13.65 and 14.3 2θ°, disappear following recrystallization, and several different characteristic peaks appear on the XRD diffractogram of RFDH although the peak intensities are relatively low. The RFDH shows less crystallinity than the RF form I, which may be attributed to the disturbed crystalline packing of the water molecule inside the crystal lattice [29, 31]. The saturation solubility of RFDH was similar to that of amorphous structured SP-RF, at 1.28 mg/mL and 1.32 mg/mL, respectively (Table 5.1). This is because, although the RFDH has a crystalline structure, the packing

density is low and the surface area of those two powders, SP-RF and RFDH, are very large due to the small particle size.

The RFDH and the SP-RF are chemically identical to the RF form I. However, the arrangement of several hydrogen bonding sites, and the ionization state between samples are different. This results in different crystalline structures since the intra-molecular hydrogen bonding plays a critical role in RF crystalline packing. The main characteristic peak determining the packing density is the peak at 1727 cm^{-1}, implying a non hydrogen bonded acetyl C=O which allows for maximum conformational stability [29-32]. The IR spectra of RF form I and RFDH show a single peak at 1727 cm^{-1}, whereas the SP-RF spectrum shows double peaks at 1718 cm^{-1} and 1733 cm^{-1}, indicating that the ordered crystalline packing of the SP-RF is prevented by the two different conformations of the acetyl group [29-32]. The IR results are in agreement with the XRD data (Figure 5.6).

5.4.2. Dry powder formulation and the aerodynamic properties

As seen in Figure 5.1, the RFDH shows a very thin, flake-like crystal. As listed in Table 5.3, the median particle size ($d_{0.5}$) of the RFDH is about 8 μm, whereas the estimated aerodynamic diameter (d_{ae}) of 2.3 μm falls into the respirable particle size range (1-5 μm), due to the low powder density. The low density RFDH crystals were manufactured by a very simple recrystallization process without adding any excipients, unlike other low density dry powder formulations that generally involve complicated manufacturing processes and large amounts of excipients. The excipient-free RFDH

formulation allows a high RF dose and may also prevent chemical degradation caused by drug-excipient interaction.

As shown in Figure 5.10, the FPF_{TD} values of RFDH powders were higher than the SP-RF for both the Handihaler® and Aerolizer® devices. This is attributed to the flaky morphology and the large particle size ($d_{0.5}$: 8 μm) of the RFDH crystals that prevents the formation of strong aggregates with weak cohesion forces [20]. The morphology and geometric size distribution of particles has significant influence on the aerosol performance since the different particle size and shapes lead to a variation in surface energy and interparticulate forces [12, 14, 37, 38]. In general, more corrugated, larger, and lower density particles exhibit better aerosol dispersion than denser, smaller particles, due to weaker van der Waals forces, leading to easier deaggregation of particle aggregates within the air steam [12, 14, 16, 25, 39, 40]. It has been also reported that powders with elongated structures provide improved aerosolization performances since the contact state between fibrous particles is extremely unstable, leading to excellent fluidization and deaggregation [19, 21, 22]. The unique flaky shape of RFDH powders may also contribute to the formation of unstable aggregates by reducing the particle contact area as elongated particles. The powder dispersion behavior of prepared formulations at a given air flow (60 L/min) was further confirmed by the particle size distribution data generated using the Spraytec® light diffraction apparatus (Figure 5.8 and Table 5.3). As expected, it appears that the SP-RF powders require more energy to be deaggregated than the RFDH, due to the strong interparticulate forces which parallels the NGI results shown in Figure 5.10. It can be clearly seen from Figure 5.8 that the particle

size distribution of the SP-RF is very broad, with a median particle size ($d_{0.5}$) of 24.6, unlike the particle size shown in the SEM image (Figure 5.1) which indicates a range of about 2-3 μm. This finding suggests that the SP-RF powders form much stronger and more stable powder aggregates than the RFDH powders due to their smaller particle size and spherical shape. The significantly low yield of the SP-RF powders can also be explained by the data discussed above (Table 5.1). Contrary to the RFDH powder, the sprayed SP-RF powders were very adhesive/cohesive. Thus, the majority of powders were lost during the spray dryer recovery process.

Significant differences in the powder dispersion behaviors were observed between two different devices for both the RFDH and SP-RF formulations. The differences in FPF_{TD} and ED between the two devices were more obvious for the SP-RF powders than the RFDH crystals. In particular, the emitted dose of SP-RF powders obtained from the Handihaler® demonstrated almost a two-fold increase when compared to the Aerolizer® device. The different particle dispersion results between two devices can be explained by the difference in the device resistance. The Aerolizer® is classified as a low resistance device with a specific resistance of 0.056 cm $H_2O^{1/2}$/L/min [41], whereas the Handihaler® is classified as a high resistance device with a resistance of 0.18 cm $H_2O^{1/2}$/L/min [37, 42], implying the Handihaler® requires more inspiratory effort to operate the device. However, at a given flow rate, 60 L/min, a greater pressure drop across the device is achieved by the high resistance device, the Handihaler®, than the low resistance device, the Aerolizer®, resulting in higher shear force for powder entrainment

and aerosolization. Accordingly, the higher FPF_{TD} and ED for SP-RF powders are attributed to the high turbulence generated by Handihaler®, which is in general agreement with previous studies using DPI devices with different resistances; the higher the device resistance, the greater the powder deagglomeration is likely to be obtained [37, 38, 42].

Unexpectedly, the Aerolizer® provided maximum particle separation for the RFDH powders as the FPF_{TD} values for the Aerolizer® and Handihaler® were 68.5% and 63.8%, with more than 95% of capsule contents being emitted from both devices. The differences in the particle deposition on each NGI dose-plate between two different devices were also found. As shown in Figure 5.10, 5.8% and 30% of the RFDH powders were deposited at the earlier stages (stage 1 and 2) of NGI with maximum deposition at stage 4 and 3 for the Aerolizer® and Handihaler® devices, respectively. These results suggest that parts of the RFDH powders are emitted without being deagglomerated to fine particles by the dispersion force of the airstream in the Handihaler®. This may be due to the differences in the powder emptying mechanism through the capsule apertures between two devices. The size of the apertures on the capsule end pierced by the Handihaler® is bigger than those of the Aerolizer®, resulting in faster powder emptying from the device. A large aperture on the capsule allows agglomerates to readily empty from the capsule, but at the same time causes impaction at the earlier impactor stages and thus, reduces the FPF [43]. Therefore, the lower FPF_{TD} for the Handihaler® is attributed to the shorter powder emptying time, which is not enough time for all particle aggregates

to be deagglomerated into separated single particles. The similar MMAD (2.2 μm) and d_{ae} (2.3 μm) of the RFDH further confirmed that the Aerolizer® device was more efficient in particle deagglomeration for this sample than the Handihaler® device. The emitted SP-RF powders from two different devices showed similar powder distribution behavior to that of the RFDH powders. As shown in Figure 5.10, emitted SP-RF powders show maximum deposition at stage 1 (22%) and stage 4 (14.8%) for the Handihaler® and for the Aerolizer®, although the ED and FPF_{TD} values were higher for the Handihaler® than for the Aerolizer®. This data indicates that larger apertures may be better for withdrawal of highly aggregated SP-RF from the capsule. However, the emitted particle aggregates may not be completely deaggreagated due to the short powder emptying time. Overall, the differences in ED, powder distribution, and FPF_{TD} between devices for the RFDH are less significant than for the SP-RF powder, since the RFDH powders do not require much energy to be aerosolized, implying that the device-dependent aerosol performances can be minimized by using an engineered RFDH formulation.

The aerosol performances of RFDH were not dependent on the capsule fill mass since the powders were very bulky, thus the particles were not closely packed even at higher fill mass, as shown in Figure 5.9. The FPF_{TD} of RFDH obtained at different capsule fill masses (7, 15, and 30 mg) was at least 59% with more than 90% of ED at an air flow of 60 L/min. The particle deposition profiles on each dose-plate of NGI for three different samples (powder fill mass) were shown to be very similar each other. The flow rate influenced the dispersion of RFDH powder as the FPF_{TD} (particles on stage 3-5) was

lowered to 47.8% at 30 L/min (Table 5.4), although the amount of powder deposited on each dose-plate was shown to be similar to the data obtained at the higher air flow rate (60 L/min). Dose-plate cut-off particle sizes for NGI calibrated at 30 L/min were applied to calculate the FPF_{TD}.

5.4.3. Dissolution

As shown in Figure 5.13, the release rate for the RFDH and the SP-RF at 1 hour were 74 and 82%, respectively. Overall, release patterns between the two samples in the PBS media (pH 7.4) were similar, although differences in crystalline structure exist due to the small particle size of powders loaded on the membrane holder. The dissolution profile of RFDH was relatively slower for the first 4 hours than that of the SP-RF, and became similar to that of the SP-RF at 8 hours. This result is in good agreement with the saturated solubility data in Figure 5.2; the saturation solubility between two formulations was similar, but the RFDH showed much slower powder wetting than the SP-RF. In general, amorphous structured material is believed to provide higher solubility and faster dissolution rates than crystalline materials. However, in RF, the amorphous form shows the slowest dissolution rate, although the intrinsic dissolution rate (IDR) and the saturation solubility are not significantly different from that of the crystalline RF [30, 32, 44]. This behavior is attributed to the electrostatic properties of the very fine particles in the high energy amorphous powders, leading to poor powder wetting [30, 32, 44]. It has been reported that when the test compounds are added to the dissolution media, the amorphous RF aggregates to form a hydrophobic layer on the dissolution media surface

[32]. Therefore, to obtain accurate dissolution results, particle separation should be considered prior to dissolution assessment. Specifically, the test compound is very small and cohesive like the SP-RF and RFDH powders. In our previous study, we proved that the aerodynamic classification of aggregated powders in the powder introduction step into the dissolution apparatus, has a significant influence on the dissolution profiles [27, 28]. Thus, a new membrane holder method, designed specifically to be incorporated into the Next Generation Impactor (NGI) for easy particle separation, was applied to properly compare the dissolution profiles of the manufactured formulations. From the dissolution study, similar dissolution profiles between two different RF polymorphs were obtained. These results parallel the saturation solubility results and may be attributed to the good separation of powders.

RF has a pH-dependent dissolution profile [3, 30, 31]. The RF dissolves and degrades immediately in low pH media (pH 1.2), but dissolves and degrades slowly in neutral conditions, the dissolved RF decomposes rapidly by hydrolysis/oxidization [30, 31]. This pH dependent dissolution may indicate that the release rate of inhaled RF is potentially retarded in the lung compared to when it is delivered to the GI tract. A comparison study by Jang et al. clearly shows that RF formulations delivered to the lung showed higher plasma concentrations and a longer plasma duration than that of orally delivered RF following an *in vivo* pharmacokinetic study, although the *in vitro* dissolution profiles of prepared formulations were similar at neutral conditions (pH 7.2) [4]. This could be attributed to the pH-dependent dissolution behavior of RF as it is a Biopharmaceutic Classification System (BCS) class II drug of the, where rate and extent

of dissolution is critical for optimum bioavailability [30]. Additionally, it is widely known that the high variability in RF bioavailability is caused by the different solubility profiles between commercial RF forms [30, 44].

5.4.4. Stability studies

While Table 5.5 shows that the chemical potency of RFDH decreases by only 3% after 9 months at ambient storage conditions, the SP-RF shows significant decrease in drug content (26%). These results can be explained through the moisture uptake behavior of two formulations studied using DVS analysis. As shown in Figure 5.7 (A), the SP-RF powders take up 14% moisture between 0-90% RH and 10.3% moisture between 50-90% RH. A large hysteresis on the isotherm graph between sorption and desorption was also shown, indicating that water absorbed from the atmosphere was strongly bound to the SP-RF, and the chemical degradation or the crystalline structural rearrangement could be accelerated by this. It has been reported that the primary degradation product of RF in solid state is an 3-formylrifamycin, and the degradation is accelerated in the presence of moisture and/or light [45]. Contrary to the SP-RF, the RFDH showed a 2.3% moisture uptake between 50-90% RH and the hysteresis was not significant since the crystalline materials were less hygroscopic than the amorphous structure. Additionally, increased stability of RFDH is attributed to hydrogen bonding sites that may be stabilized by the water of recrystallization from hydrated structures. In contrast, the amorphous structure of SP-RF and subsequent lack of strong hydrogen bonding, may result in more rapid chemical degradation. The stabilities of the SP-RF and RFDH were further confirmed by

the DSC and the HSM study (Figure 5.11 and 5.12). The bright interference color was observed for amorphous SP-RF powder at 4 months and the bright color did not completely disappear upon heating to its Tg, indicating the presence of the crystalline forms of RF or an RF degradation product.

Desolvation of the water of crystallization was studied, as the presence of the water of crystallization in the crystal lattice significantly influences the stability of the RF crystalline structure [34, 35]. As shown in the Figure 5.3 (A), the desolvation of the RFDH occurred at temperature ranges of 90-150°C or at very low humidity (0% RH) (as confirmed by DVS study in Appendix B) [34, 35]. However, the RFDH is to date, very stable under ambient storage conditions.

5.5. CONCLUSION

The rifampicin dihydrate (RFDH) powders having MMAD of 2.2 μm were successfully prepared using a simple recrystallization process. The RFDH powders have a thin flaky structure, and this morphology provides improved aerosolization properties at maximal API loading. The maximum FPF_{TD} of the RFDH achieved with Aerolizer® device, was 68%. These powders are predicted to deposit predominately in the central and peripheral regions of the lung following inhalation, with minimal oropharyngeal deposition. RFDH powders delivered via the pulmonary route would be anticipated to provide higher local (lung) drug concentrations than that of orally delivered powders.

Additionally, RFDH powders can be estimated to have much better stability than the amorphous SP-RF.

5.6. TABLES

Table 5.1 Physical characterizations of prepared samples, RF, RFDH and SP-RF (values are means ± SD, n = 3).

	RF	RFDH	SP-RF
RF contents (%)	99.4 ± 0.47	95.8 ± 0.02	102 ± 1.06
Yield (%)*	-	91 ± 2.3	36 ± 6.3
Water contents (%)**	0.02	5.2	0.94
Desolvation (ºC)	-	90-150	-
Melting (ºC)	-	180	165 (Tg)
Decomposition (ºC)	260	257	257
Solubility at 37ºC (mg/mL)	0.59 ± 0.05	1.28 ± 0.01	1.32 ± 0.02

* Yield was calculated for 3 different batches

** Water contents were measured by weight loss on TGA analysis.

Table 5.2 Main characteristic infrared vibrations.

Samples	Wavelength (cm^{-1})				
	Ansa OH	Furanone C=O	Acetyl C=O	Amide C=O	N-CH_3
RF	3490	1648	1727	1569	2806
RFDH	3250-3565	1652	1727	1569	absent
SP-RF	3250-3565	1652	1718,1733	1569	2807

Table 5.3 Particle size distribution measured by Spraytec® at a flow rate of 60 L/min for RF form I, RFDH and SP-RF (values are means ± SD, n = 3).

Samples	$d_{0.1}$ (μm)	$d_{0.5}$ (μm)	$d_{0.9}$ (μm)	d_{ae} (μm)
RF	42.6 ± 4	116 ± 6.9	368 ± 57	-
RFDH	2.4 ± 0.02	8.8 ± 0.07	22.6 ± 0.71	2.3 ± 0.05
SP-RF	2.7 ± 2.1	24.6 ± 7.8	143 ± 19.8	-

Table 5.4 Aerodynamic characteristics of the formulations (values are means ± SD, n = 3).

	RFDH					SP-RF	
DPIs	Handihaler				Aerolizer	Handihaler	Aerolizer
Fill mass (mg) (flow rate L/min)	7 (60)	15 (60)	30 (60)	15(30)	15 (60)	15 (60)	15 (60)
ED (%)	91.4±1.5	97.6±0.3	95.2±1.9	96±0.6	98.3±0.2	94.1±1.7	56.1±0.2
PFP_{TD} (%)	59.1±1.2	63.8±1.5	60.2±3.7	47.8±1	68.5±2.4	50.9±2.2	36.6±0.4
MMAD (μm)	3.1±0.15	3.7±0.12	3.2±0.14	4.4±0.04	2.2±0.12	3.4±0.29	2.8±0.08

Table 5.5 RF contents analysis for RFDH and SP-RF formulations stored under ambient condition (25ºC/50% RH) over 9 months (values are means ± SD, n = 3).

Samples	Initial	2 Months	4 Months	6 Months	9 months
RFDH *	95.81 ± 0.57	95.81 ± 0.02 (100%)**	95.84 ± 0.30 (100%)	93.76 ± 0.25 (97.9%)	92.96 ± 0.56 (97%)
SP-RF	102 ± 1.06	91.2 ± 0.71 (89.4%)	84.23 ± 1.06 (82.6%)	80.77 ± 0.46 (79.2%)	75.46 ± 0.81 (74%)

* The drug contents of RFDH indicates RF contents

** Values in parentheses refer to % decrease in RF contents

5.7. FIGURES

Figure 5.1 Scanning electron microscopy images of (A) RF form I, (B) SP-RF, and (C) RFDH.

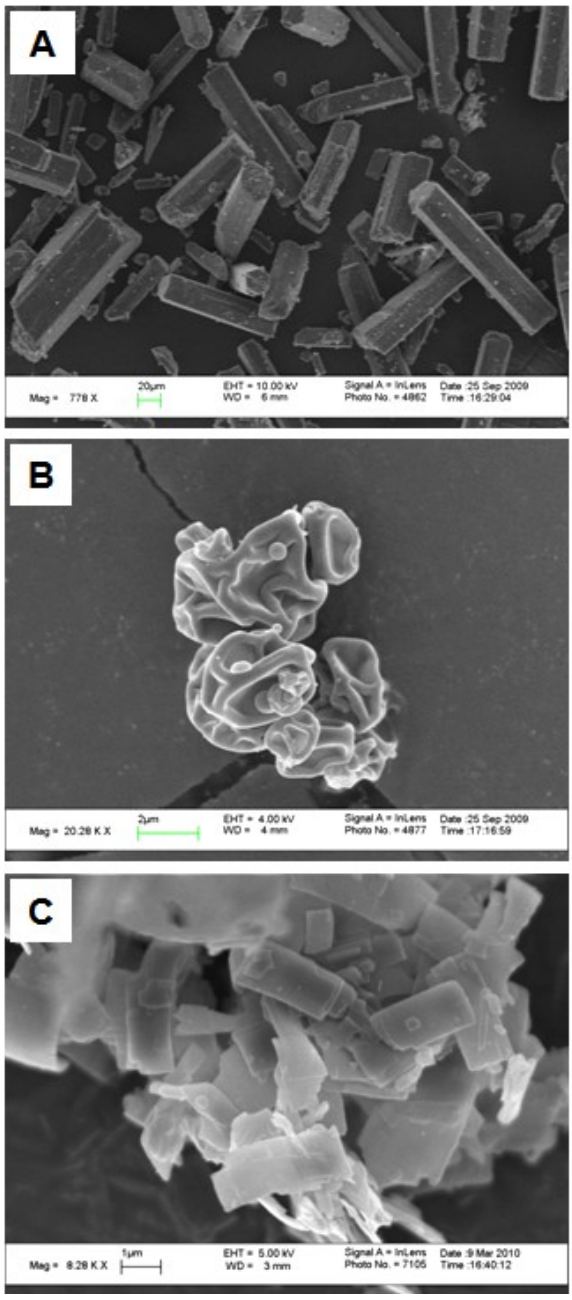

Figure 5.2 Saturation solubility of RF form I, RFDH, and SP-RF in SLF medium at 37 °C for 24 hours.

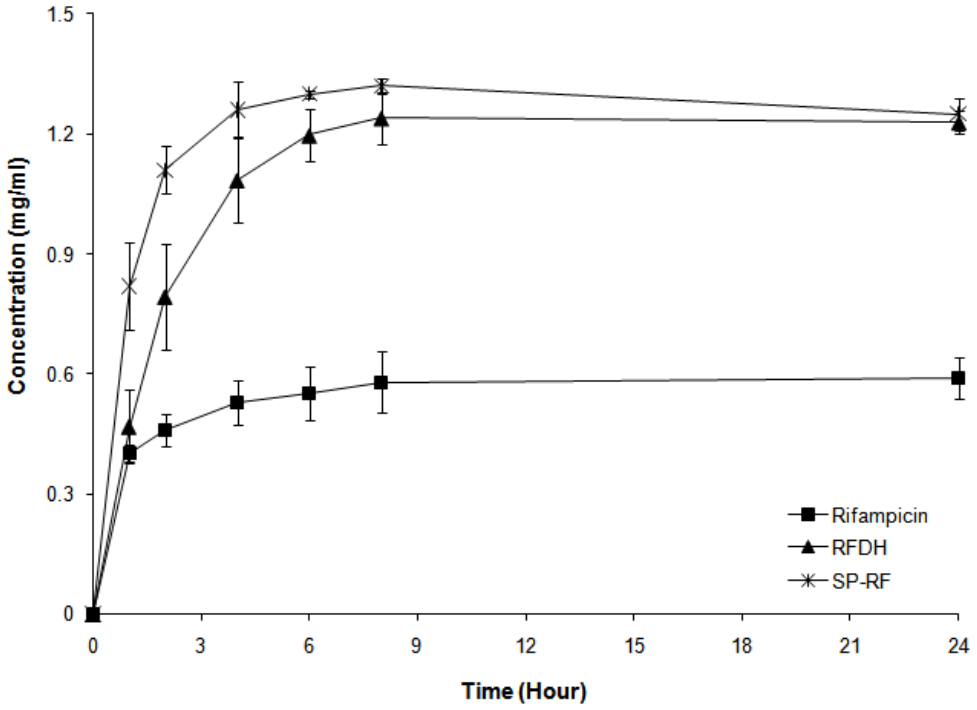

Figure 5.3 DSC thermogrmas (A) of (a) desolvated RFDH, (b) RFDH, (c) SP-RF and (d) RF form I, and TGA results (B) for (a) RF form I, (b) SP-RF and (c) RFDH.

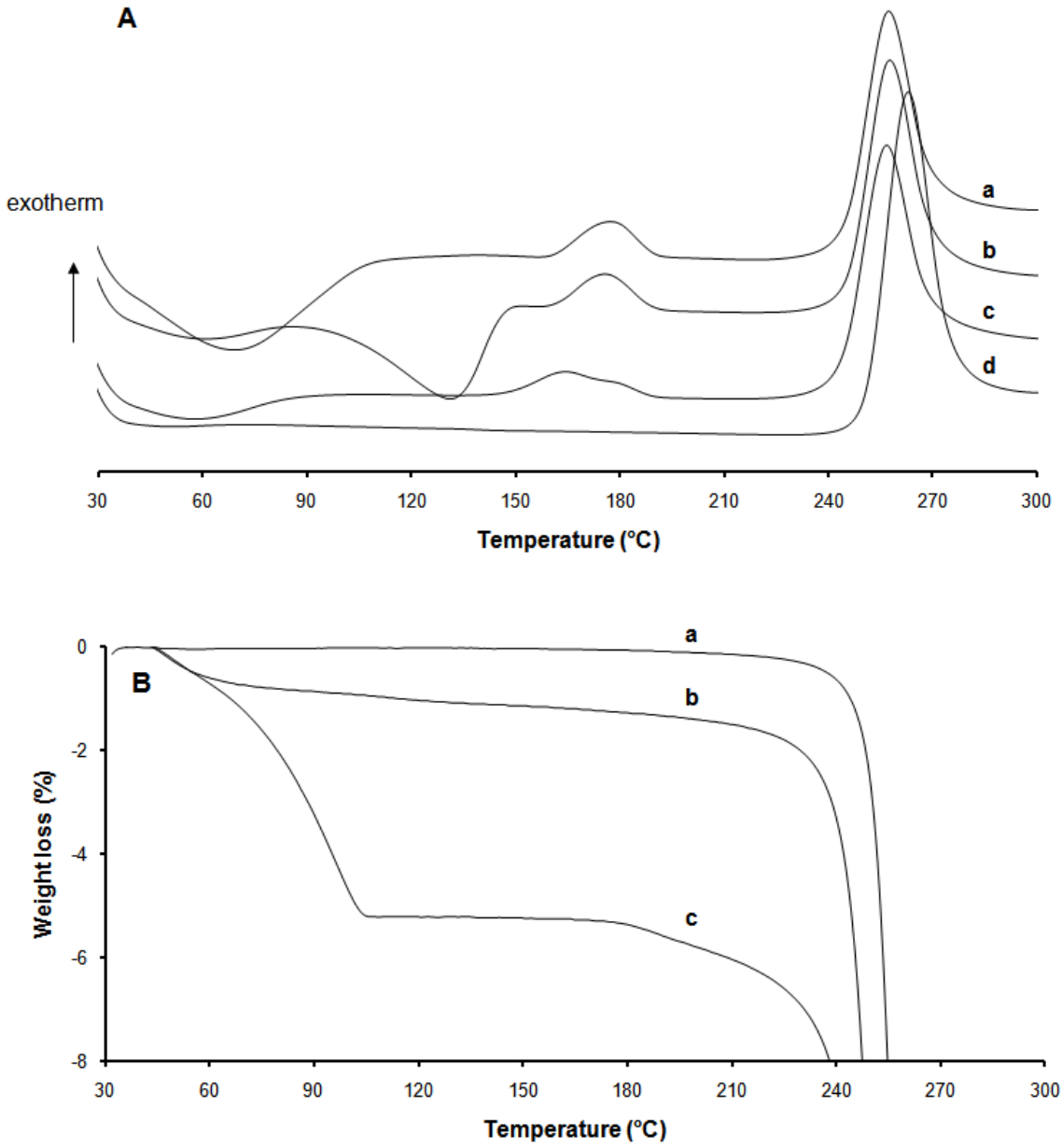

Figure 5.4 Photographic image of RFDH crystals on the hot stage at (A) 60°C, (B) 120 °C, (C) 160°C, and (D) 180°C.

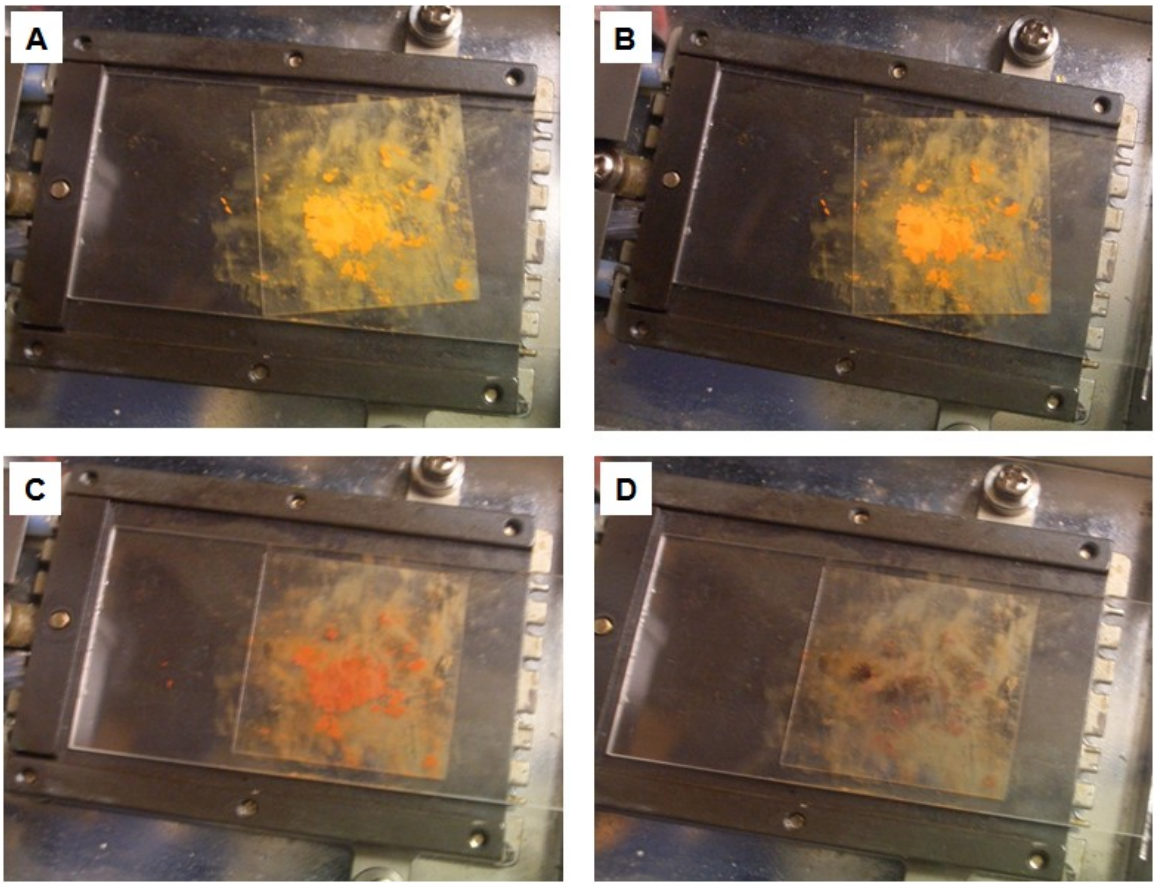

Figure 5.5 Hot stage microscopy images (HSM) of RFDH at (A) 30°C, (B) 120°C, (D) 140°C and 180°C.

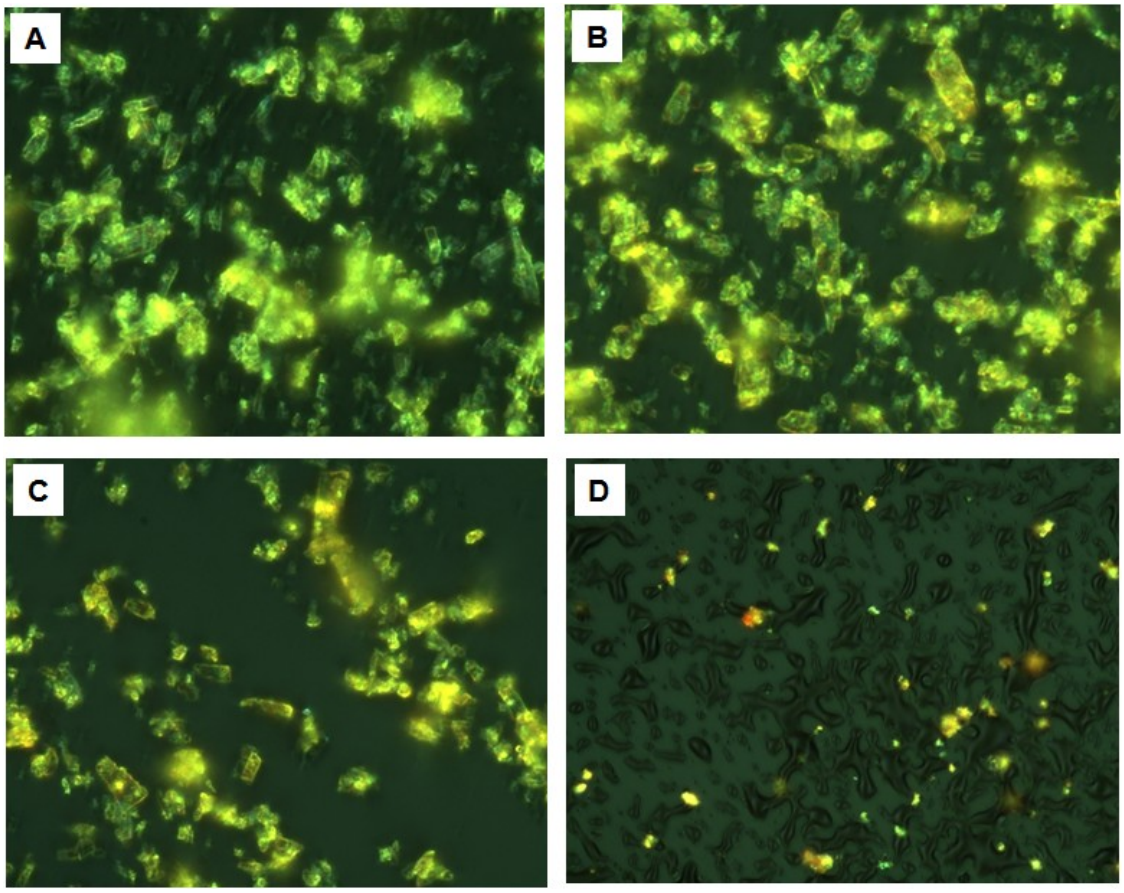

Figure 5.6 Powder X-ray diffractograms of (a) RF form I (characterization peaks of form I: 13.65 and 14.35), (b) RFDH, (c) desolvated RFDH and (d) SP-RF.

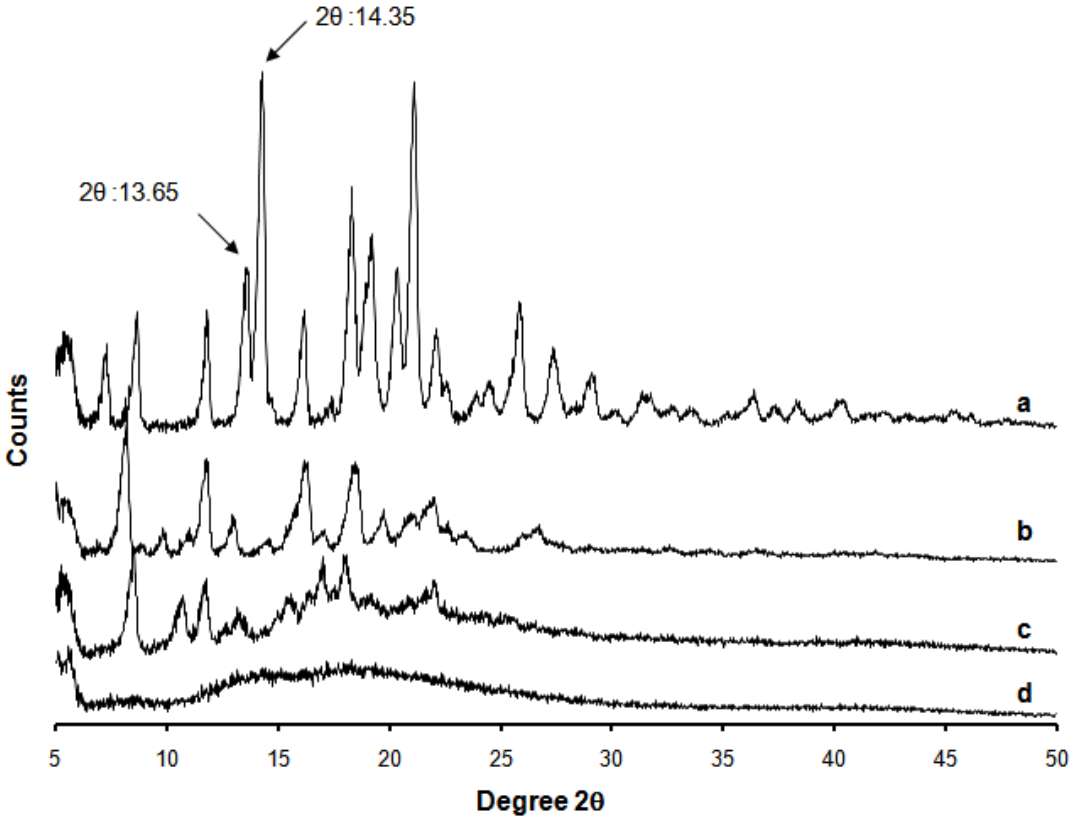

Figure 5.7 Dynamic vapor sorption (DVS) isotherm of (A) SP-RF, (B) RFDH, and (C) RF from I. The absorptions are shown as solid lines and desorptions as dashed lines.

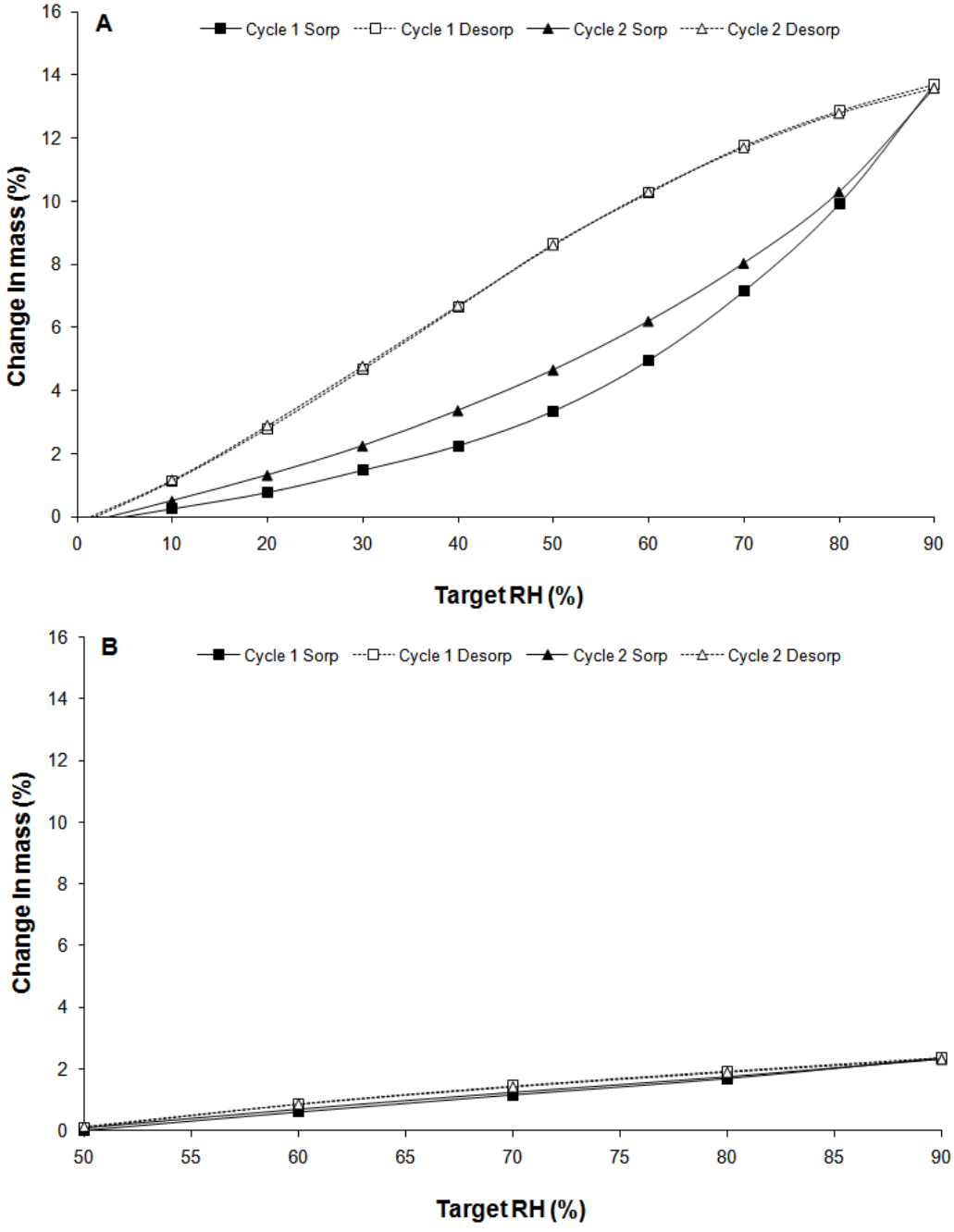

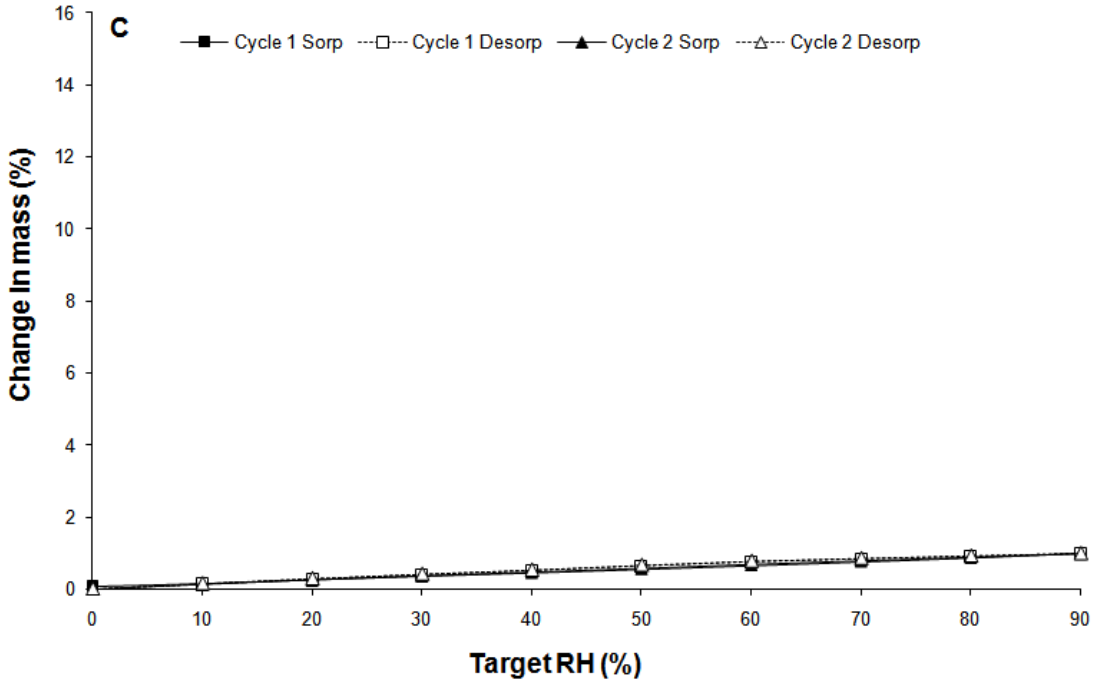
C
Cycle 1 Sorp
Cycle 1 Desorp
Cycle 2 Sorp
Cycle 2 Desorp
Change In mass (%)
16
14
12
10
8
6
4
2
0
0
10
20
30
40
50
60
70
80
90
Target RH (%)

Figure 5.8 Average particle size distribution measured by Spraytec® at a flow rate of 60L/min for (A) RF form I, (B) RFDH and (C) SP-RF.

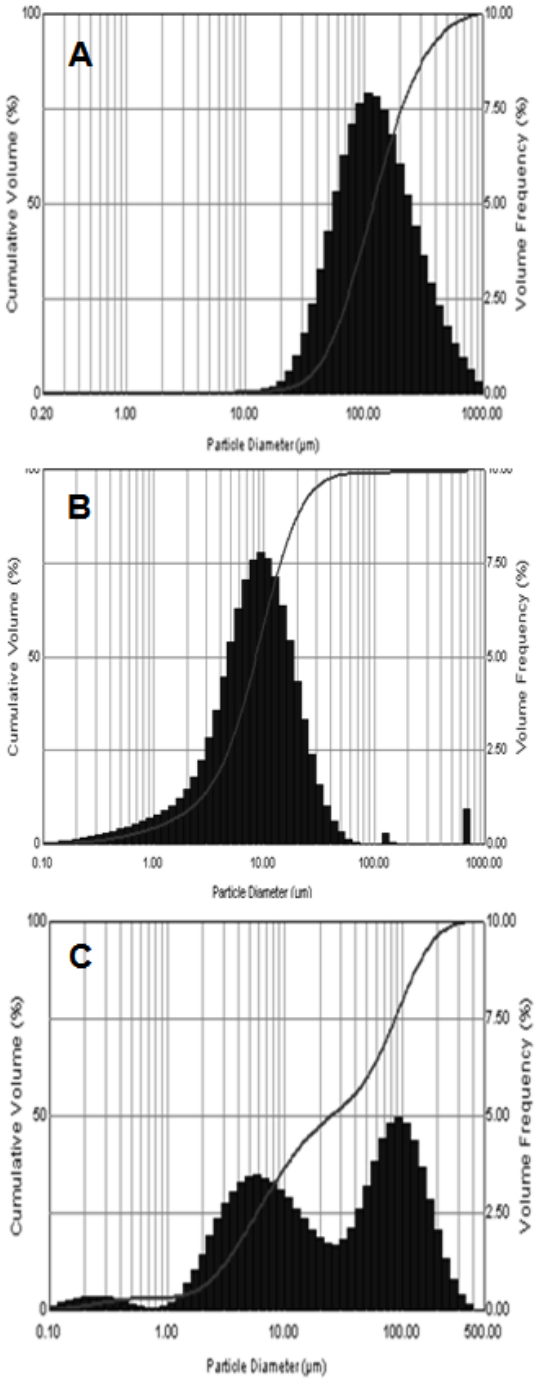

Figure 5.9 Powder deposition profiles for RFDH having different powder fill mass at a flow rate of 30 L/min or 60 L/min with Handihaler®, expressed as the percentage of total loaded dose (Values are means ± SD, n = 3)..

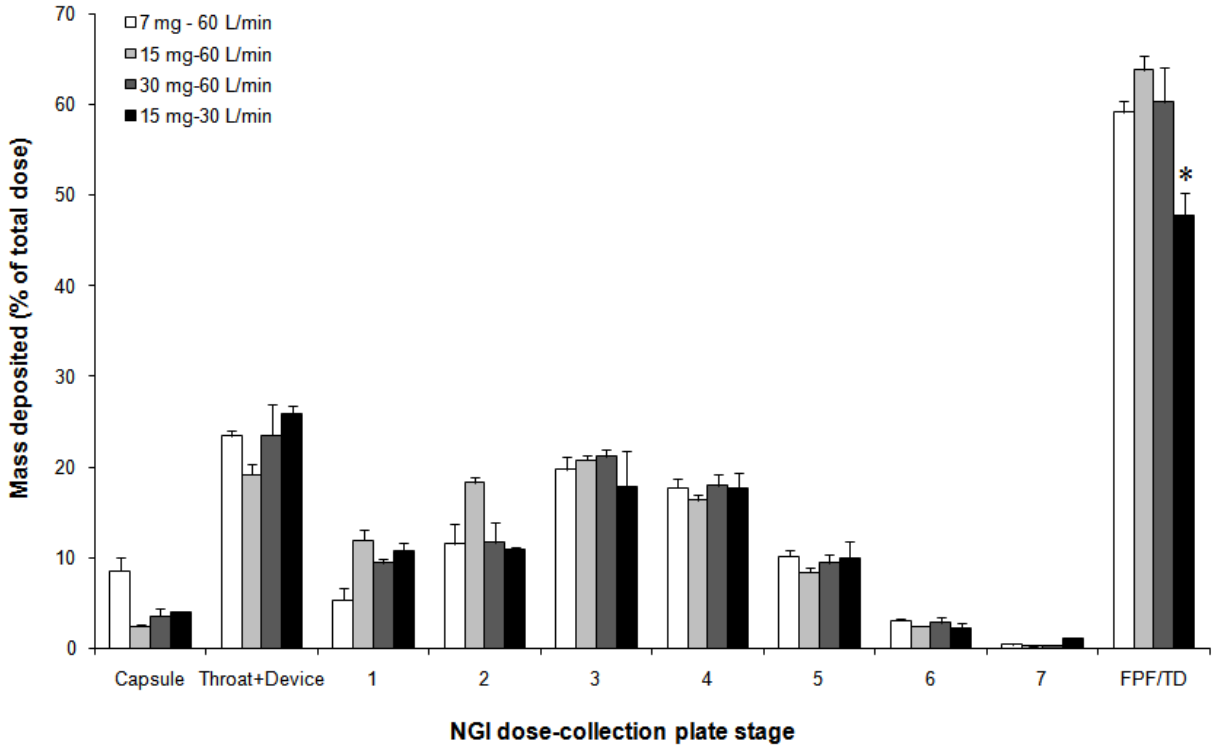

∗ The statistical difference between the PFP_{TD} at 30 L/min and 60 L/min for 15 mg capsule

Figure 5.10 Powder deposition profiles for the RFDH and the SP-RF actuated from two devices, Aerolizer® and Handihaler® at a flow rate of 60 L/min, expressed as the percentage of total loaded dose (Values are means ± SD, n = 3).

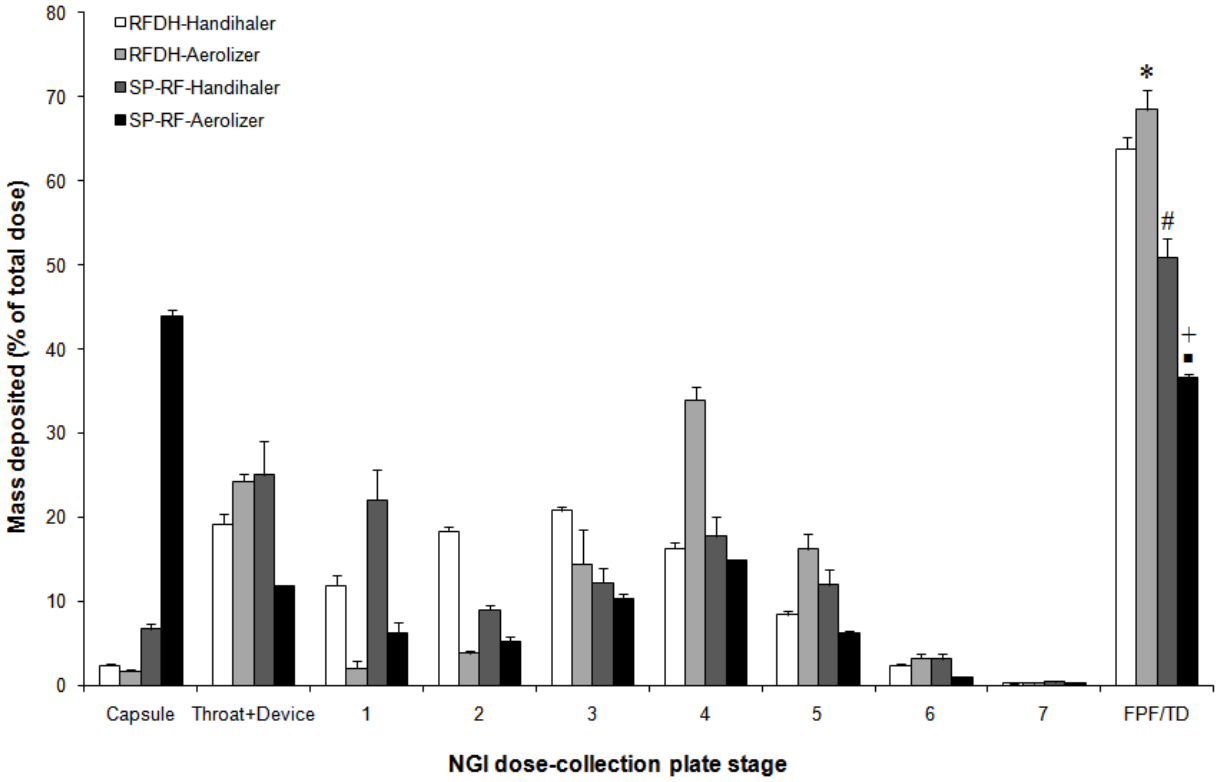

∗ The statistical difference between devices for the RFDH powders
+ The statistical difference between devices for the SP-RF powders
# The statistical difference between formulations for the Handihaler®
▪ The statistical difference between formulations for the Aerolizer®

Figure 5.11 DSC thermograms of (a) RFDH and (b) SP-RF over 6 months.

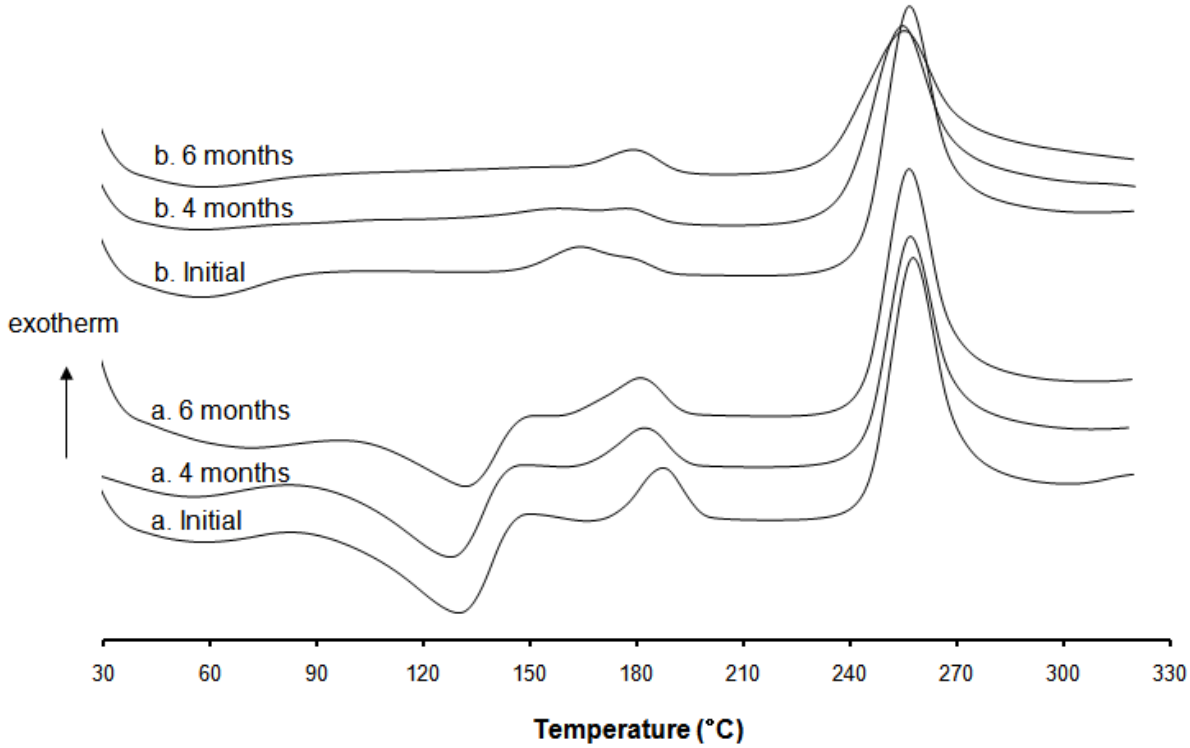

Figure 5.12 Photographic image of SP-RF powder (A) at a) initial, b) 4 months and c) 6 months, and Hot stage microscopy images (B) of the 4 months stability sample of SP-RF at a) 60°C, b) 180°C and 200°C.

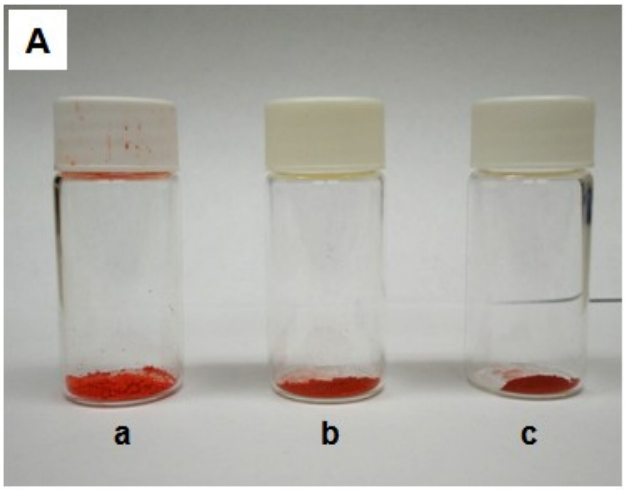

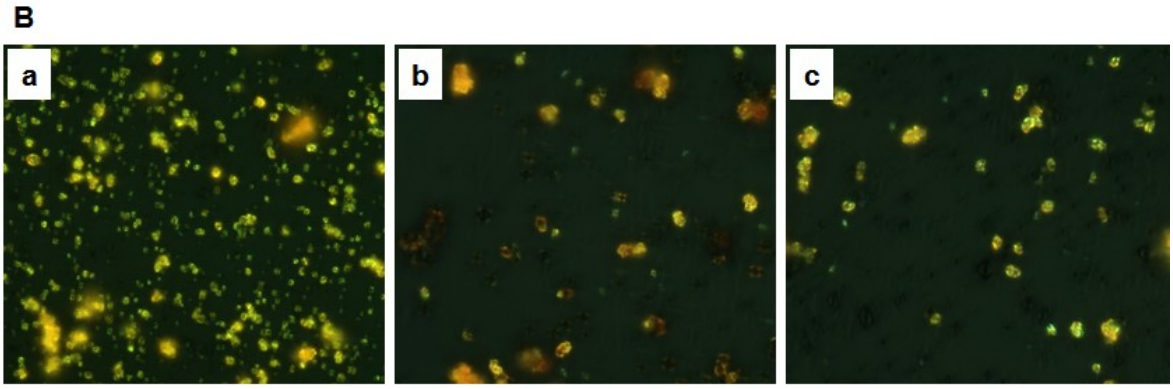

Figure 5.13 Release profiles of RFDH and SP-RF in PBS containing 0.02% ascorbic acid (pH 7.4). Powders accumulated on the dose-collection plate 3 were selected for dissolution assessment. The error bars indicate the standard deviation of three tests.

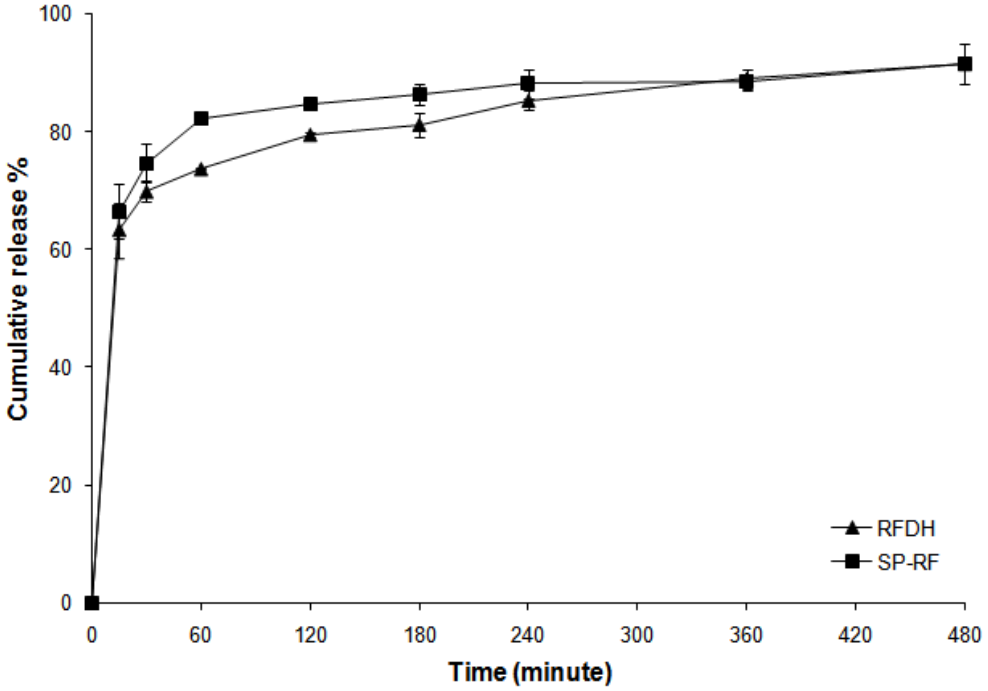

5.8. REFERENCES

[1] Rifampin. Tuberculosis 88(2) (2008) 151-154.

[2] J. Schreiber, G. Zissel, U. Greinert, M. Schlaak, J. Muller-Quernheim, Lymphocyte transformation test for the evaluation of adverse effects of antituberculous drugs. Eur J Med Res 4(2) (1999) 67-71.

[3] P. O'Hara, A.J. Hickey, Respirable PLGA microspheres containing rifampicin for the treatment of tuberculosis: Manufacture and characterization. Pharmaceutical Research 17(8) (2000) 955-961.

[4] J.C. Sung, D.J. Padilla, L. Garcia-Contreras, J.L. VerBerkmoes, D. Durbin, C.A. Peloquin, K.J. Elbert, A.J. Hickey, D.A. Edwards, Formulation and Pharmacokinetics of Self-Assembled Rifampicin Nanoparticle Systems for Pulmonary Delivery. Pharmaceutical Research 26(8) (2009) 1847-1855.

[5] S. Suarez, P. O'Hara, M. Kazantseva, C.E. Newcomer, R. Hopfer, D.N. McMurray, A.J. Hickey, Respirable PLGA microspheres containing rifampicin for the treatment of tuberculosis: Screening in an infectious disease model. Pharmaceutical Research 18(9) (2001) 1315-1319.

[6] S. Suarez, P. O'Hara, M. Kazantseva, C.E. Newcomer, R. Hopfer, D.N. McMurray, A.J. Hickey, Airways delivery of rifampicin microparticles for the treatment of tuberculosis. Journal of Antimicrobial Chemotherapy 48(3) (2001) 431-434.

[7] R. Sharma, D. Saxena, A.K. Dwivedi, A. Misra, Inhalable microparticles containing drug combinations to target alveolar macrophages for treatment of pulmonary tuberculosis. Pharmaceutical Research 18(10) (2001) 1405-1410.

[8] S.P. Vyas, M.E. Kannan, S. Jain, V. Mishra, P. Singh, Design of liposomal aerosols for improved delivery of rifampicin to alveolar macrophages. International Journal of Pharmaceutics 269(1) (2004) 37-49.

[9] F. Tewes, J. Brillault, W. Couet, J.C. Olivier, Formulation of rifampicin-cyclodextrin complexes for lung nebulization. Journal of Controlled Release 129(2) (2008) 93-99.

[10] F. Ito, K. Makino, Preparation and properties of monodispersed rifampicin-loaded poly(lactide-co-glycolide) microspheres. Colloids and Surfaces B-Biointerfaces 39(1-2) (2004) 17-21.

[11] C. Becker, J.B. Dressman, H.E. Junginger, S. Kopp, K.K. Midha, V.P. Shah, S. Stavchansky, D.M. Barends, Biowaiver Monographs for Immediate Release Solid Oral Dosage Forms: Rifampicin. J. Pharm. Sci. 98(7) (2009) 2252-2267.

[12] H.K. Chan, What is the role of particle morphology in pharmaceutical powder aerosols? Expert Opinion on Drug Delivery 5(8) (2008) 909-914.

[13] D. Traini, P.M. Young, F. Thielmann, M. Acharya, The influence of lactose pseudopolymorphic form on salbutamol sulfate-lactose interactions in DPI formulations. Drug Development and Industrial Pharmacy 34(9) (2008) 992-1001.

[14] H.K. Chan, Dry powder aerosol drug delivery - Opportunities for colloid and surface scientists. Colloids and Surfaces a-Physicochemical and Engineering Aspects 284 (2006) 50-55.

[15] X.M. Zeng, G.P. Martin, C. Marriott, J. Pritchard, The effects of carrier size and morphology on the dispersion of salbutamol sulphate after aerosolization at different flow rates. Journal of Pharmacy and Pharmacology 52(10) (2000) 1211-1221.

[16] S. Adi, H. Adi, P. Tang, D. Traini, H.K. Chan, P.M. Young, Micro-particle corrugation, adhesion and inhalation aerosol efficiency. European Journal of Pharmaceutical Sciences 35(1-2) (2008) 12-18.

[17] N.Y.K. Chew, H.K. Chan, Use of solid corrugated particles to enhance powder aerosol performance. Pharmaceutical Research 18(11) (2001) 1570-1577.

[18] N. Islam, P. Stewart, I. Larson, P. Hartley, Surface roughness contribution to the adhesion force distribution of salmeterol xinafoate on lactose carriers by atomic force microscopy. Journal of Pharmaceutical Sciences 94(7) (2005) 1500-1511.

[19] K. Ikegami, Y. Kawashima, H. Takeuchi, H. Yamamoto, N. Isshiki, D. Momose, K. Ouchi, Improved inhalation behavior of steroid KSR-592 in vitro with Jethaler (R) by polymorphic transformation to needle-like crystals (beta-form). Pharmaceutical Research 19(10) (2002) 1439-1445.

[20] T.T. Hu, H. Zhao, L.C. Jiang, Y. Le, J.F. Chen, J. Yun, Engineering Pharmaceutical Fine Particles of Budesonide for Dry Powder Inhalation (DPI). Industrial & Engineering Chemistry Research 47(23) (2008) 9623-9627.

[21] H.K. Chan, I. Gonda, Physicochemical characterization of a new respirable form of nedocromil. J. Pharm. Sci. 84(6) (1995) 692-696.

[22] H.K. Chan, I. Gonda, RESPIRABLE FORM OF CRYSTALS OF CROMOGLYCIC ACID. J. Pharm. Sci. 78(2) (1989) 176-180.

[23] M.A. Darbandi, N.A. Rouholamini, K. Gilani, H. Tajerzadeh, The effect of vehicles on spray drying of rifampicin inhalable microparticles: In vitro and in vivo evaluation. Daru-Journal of Faculty of Pharmacy 16(3) (2008) 128-135.

[24] General chapter <616>: Bulk density and tapped density,USP32-NF27, Rockville, MD, 2009.

[25] D.A. Edwards, J. Hanes, G. Caponetti, J. Hrkach, A. BenJebria, M.L. Eskew, J. Mintzes, D. Deaver, N. Lotan, R. Langer, Large porous particles for pulmonary drug delivery. Science 276(5320) (1997) 1868-1871.

[26] K. Tomoda, K. Makino, Effects of lung surfactants on rifampicin release rate from monodisperse rifampicin-loaded PLGA microspheres. Colloids and Surfaces B-Biointerfaces 55(1) (2007) 115-124.

[27] Y.-J. Son, M. Horng, M. Copley, J.T. McConville, Optimization of an in vitro dissolution test method for inhalation formulations. Dissolution Technologies 17(2) (2010) 6-13.

[28] Y.-J. Son, J.T. McConville, Development of a standardized dissolution test method for inhaled pharmaceutical formulations. International Journal of Pharmaceutics 382(1-2) (2009) 15-22.

[29] G. Pelizza, M. Nebuloni, P. Ferrari, G.G. Gallo, Polymorphism of rifampicin. Farmaco-Edizione Scientifica 32(7) (1977) 471-481.

[30] S. Agrawal, Y. Ashokraj, P.V. Bharatam, O. Pillai, R. Panchagnula, Solid-state characterization of rifampicin samples and its biopharmaceutic relevance. European Journal of Pharmaceutical Sciences 22(2-3) (2004) 127-144.

[31] S.Q. Henwood, W. Liebenberg, L.R. Tiedt, A.P. Lotter, M.M. de Villiers, Characterization of the solubility and dissolution properties of several new rifampicin polymorphs, solvates, and hydrates. Drug Development and Industrial Pharmacy 27(10) (2001) 1017-1030.

[32] R. Panchagnula, V. Bhardwaj, Effect of amorphous content on dissolution characteristics of rifampicin. Drug Development and Industrial Pharmacy 34(6) (2008) 642-649.

[33] V.A. Marple, D.L. Roberts, F.J. Romay, N.C. Miller, K.G. Truman, M.J. Holroyd, J.P. Mitchell, D. Hochrainer, Next generation pharmaceutical impactor (A new impactor for pharmaceutical inhaler testing). Part I: Design. Journal of Aerosol Medicine-Deposition Clearance and Effects in the Lung 16(3) (2003) 283-299.

[34] H.G. Brittain, Polymorphism in pharmaceutical solids,Informa healthcare 2 nd., New York, 2009.

[35] R. Hilfiker, Polymorphism in the pharmaceutical industry,Wiley-VCH Weinheim, 2006.

[36] K. Masters, Spray drying handbook,Longman Scientific & Technical 5th ed., 1991.

[37] M.D. Louey, M. Van Oort, A.J. Hickey, Aerosol dispersion of respirable particles in narrow size distributions produced by jet-milling and spray-drying techniques. Pharmaceutical Research 21(7) (2004) 1200-1206.

[38] M.D. Louey, M. Van Oort, A.J. Hickey, Aerosol dispersion of respirable particles in narrow size distributions using drug-alone and lactose-blend formulations. Pharmaceutical Research 21(7) (2004) 1207-1213.

[39] H. Adi, D. Traini, H.K. Chan, P.M. Young, The influence of drug morphology on the aerosolisation efficiency of dry powder inhaler formulations. Journal of Pharmaceutical Sciences 97(7) (2008) 2780-2788.

[40] L.A. Dellamary, T.E. Tarara, D.J. Smith, C.H. Woelk, A. Adractas, M.L. Costello, H. Gill, J.G. Weers, Hollow porous particles in metered dose inhalers. Pharm. Res. 17(2) (2000) 168-174.

[41] C.P. Criee, T. Meyer, W. Petro, K. Sommerer, P. Zeising, In vitro comparison of two delivery devices for administering formoterol: Foradil (R) P and formoterol ratiopharm single-dose capsule inhaler. Journal of Aerosol Medicine-Deposition Clearance and Effects in the Lung 19(4) (2006) 466-472.

[42] T. Srichana, G.P. Martin, C. Marriott, Dry powder inhalers: The influence of device resistance and powder formulation on drug and lactose deposition in vitro. European Journal of Pharmaceutical Sciences 7(1) (1998) 73-80.

[43] N.Y.K. Chew, H.K. Chan, D.F. Bagster, J. Mukhraiya, Characterization of pharmaceutical powder inhalers: estimation of energy input for powder dispersion and effect of capsule device configuration. Journal of Aerosol Science 33(7) (2002) 999-1008.

[44] S.Q. Henwood, M.M. de Villiers, W. Liebenberg, A.P. Lotter, Solubility and dissolution properties of generic rifampicin raw materials. Drug Development and Industrial Pharmacy 26(4) (2000) 403-408.

[45] H. Bhutani, T.T. Mariappan, S. Singh, The physical and chemical stability of anti-tuberculosis fixed-dose combination products under accelerated climatic conditions. International Journal of Tuberculosis and Lung Disease 8(9) (2004) 1073-1080.

Chapter 6: Preparation of Sustained Release Rifampicin Microparticles for Inhalation

Abstract

The aim of this research was to investigate whether a novel carrier-free dry powder formulation of rifampicin (RF) for inhalation, could present a controlled release profile. The RF dihydrate (RFDH) crystals were coated with hydrophobic polymers, PLGA and PLA, using a spray-dryer equipped with two different types of three-fluid (3F) spray nozzles; modified 3F nozzle (3F-M) and standard 3F (3F-S). Suspensions of RFDH crystals (the core forming particles), and polymer solutions were prepared separately. Each of the prepared liquid solutions was then sprayed through the separate channels of the 3F nozzles. Matrix polymeric microspheres encapsulating RF (MRF microsphere) were prepared as control groups by the co-spray drying of a dissolved RF and polymer in dichloromethane (DCM) using a standard two-fluid (2F) nozzle. The coated RFDH powder, encapsulating at least 50% of RF, was successfully prepared by simple *in-situ* coating methods using two different types of 3F nozzles. The coated RFDH powders had MMAD values of 3.5 to 4.6 μm. The thin flaky morphology of RFDH powders that provides improved aerosolization properties (Chapter 5) was maintained after coating. The coated RFDH formulations showed relatively low initial RF release, compared to the uncoated RFDH crystals followed by slow RF release (about 70%) over 8 hours in PBS media (pH 7.4). The coated RFDH powders also showed slower RF release in acidic dissolution media (pH 5.2) than it was in pH 7.4. Significant chemical degradations were

not observed from the crystalline-structured RFDH formulations, while the amorphous-structured MRF powders showed chemical degradation in 6 months. These polymer coated RFDH formulations may be a valuable alternative in the treatment of tuberculosis since the carrier-free formulation offers the benefit of delivering a maximum potency formulation of the antibiotic directly to the site of infection, with longer drug residence time in the lung imparted by the controlled release of the drug.

6.1. INTRODUCTION

Tuberculosis (TB) is a chronic infectious disease, which is considered the foremost cause of death due to a single microorganism [1]. The occurrence of TB is most often due to *Mycobacterium tuberculosis* (MTB) infection by inhalation and the lung is the primary site of infection. Once in the lung, MTB is phagocytosed by alveolar macrophages (AMs), where it remains alive. The most common treatment for TB involves oral administration of high systemic doses of single or combined antibiotics, which causes unwanted side-effects by high systemic exposure [2]. Several current studies have been proposed for the administration of anti-tubercular drugs to the primary infection site, the lung, with the idea of increasing the local therapeutic effect and reduce the overall systemic exposure [3-9]. Specifically, pulmonary delivery of rifampicin (RF) has been widely studied [3-6, 8, 10] since it is the first choice drug in the treatment of TB [1, 11] and several drawbacks in current oral delivery systems, mainly attributed with the severe chemical decomposition of RF in the acidic conditions of the stomach [12-14], can be avoided by delivering RF to the lung that has a neutral milieu. Several respirable forms of RF, such as nano/microparticles [3-5], liposome [8], and liquid [9], have been introduced to localize the RF in the lung.

Recently, there has been an increased interest in research in focusing on dry powder inhalation (DPI) formulations to prolong drug residence time in the lung [3, 4, 15-17] since the sustained release (SR) system has certain advantages, including reduced dosing frequency, improved patient compliance, and reduction in overall systemic side

effects [17, 18]. Specifically, in anti-tubercular (TB) inhaled therapy, it's well established that the SR formulation enhances the efficacy of anti-TB drugs, presumably by targeting AMs and building up high intracellular drug concentrations. Generally, the phagocytic uptake of inhaled particles by AMs has been known to be the primary hurdle in extending drug residence time in the lung [17, 18]. However, in pulmonary anti-TB therapy, the phagocytic activities play a useful role in terms of targeting anti-TB drugs at the main site of the MTB proliferation [19, 20]. Several SR formulations encapsulating anti-TB drugs into the polymeric microspheres have been introduced to target the AMs [3, 4, 21, 22]. Respirable PLGA/PLA microspheres that show up to 3 days of *in vitro* drug release capability were manufactured by means of a solvent evaporation and a spray drying method [3, 19, 23]. A formulation consisting of PLGA nanoparticle aggregates was also introduced by Sung et al. [4]. However, there are still numerous limitations in manufacturing SR formulations that have good aerosolization properties, with controlled drug release capabilities due to their fine particle size. Additionally, the low payload of APIs, typically in the range of 1 to 20%, offered by conventional microencapsulation methods, is one of the problems in inhaled TB treatment since the bactericidal activity is directly proportional to the concentration at the target site [9, 24] .

Hydrophobic coating methods have been applied under the modified release concept. Generally, these coatings constitutes approximately 10 to 50% of the final particle mass, which is substantially higher drug loading compared to the microencapsulated formulations. In US patent 6,984,404 [25], a physical vapor deposition (PVD) method using pulsed laser ablation (PLD) is applied to achieve the

PLGA deposition onto the target particle surface, which offers nanometer thickness of coating layer with more than 90% drug loading. However, the use of a PLD method may possibly cause decomposition or degradation of APIs or polymers during the process due to severe processing conditions, such as UV radiation, high pressure and heat. Moreover, the coating of each separate particle is difficult to achieve since there is no suitable method to fluidize or agitate ultra-fine particles (1-5 μm) that exhibit strong cohesion properties during the coating process. A spray dry method to obtain coated particles has also been widely evaluated [26, 27]. This technique is a relatively simple one-step process over other coating techniques. However, the application of this method is limited as micronized core forming particles have to be dispersed in the coating solution without dissolving the core-forming particle.

The aim of this study is to develop a novel carrier-free dry powder inhaler (DPI) formulation of RF that has a high drug payload, improved aerodynamic properties, and a sustained release capability. It is the goal of this research to demonstrate that the use of multi-channel spray nozzles can offset some of the aforementioned limitations with other investigated formulation types. In the previous study, the flake-like rifampicin dihydrate (RFDH) crystal having improved aerosolization properties was successfully prepared by a simple recrystallization process [28] (see Chapter 5). However, the RFDH formulation shows high initial drug release. Thus, we aimed to minimize the amount of initial RF release by means of surface coating. This study describes how the coating of RFDH crystal was achieved by spray drying with multi-channel spray nozzles, and how the physicochemical properties of coated RFDH were characterized. The aerodynamic

behaviors of prepared formulations were described using an Aerolizer® DPI device. And the dissolution behaviors of prepared formulations were evaluated using a newly developed membrane holder method [29, 30] (see Chapter 4).

6.2. MATERIALS AND METHODS

6.2.1. Materials

Rifampicin (RF), poly (DL-lactide) (PLA, Mw= 75,000-12,000), poly (DL-lactide-*co*-glycolide) (PLGA, lactic acid:glycolic acid ratio=75:25; molecular weight= 66,000-107,000) and cholesterol were purchased from the Sigma Chemical Co. (St. Louis, MO). Size 3 hydroxypropylmethyl cellulose (HPMC) capsules were donated from Capsugel (Peapack, NJ). Polycarbonate (PC) membranes of 0.05 μm, were purchased from Whatman (Florham Park, NJ). An Aerolizer® dry powder inhaler device was donated by Schering-Plough (Kenilworth, NJ). A dissolution membrane holder was provided by Copley Scientific (Nottingham, UK). All other reagents were purchased from the Sigma Chemical Co. (St. Louis, MO).

6.2.2. Formulation design

6.2.2.1. Preparation of rifampicin dihydrate (RFDH) and matrix microparticles (MRF) using a spray dryer equipped with two-fluid (2F) spray nozzle

Rifampicin dihydrate (RFDH) microcrystals were prepared by a polymorphic transformation of RF form I [28]. To briefly summarize, RF powder (900 mg) was added to 30 mL of hot anhydrous ethanol solution (60°C) and stirred until a saturated solution

was obtained. The suspension was placed into a Branson 5500 sonic bath (Branson ultrasonics, Danbury, CT) and sonicated at 25°C for 2 minutes to homogeneously disperse the particles. The resultant suspension was then spray dried with constant stirring using a Büchi Minispray dryer B-290 (Büchi Laboratory-Techniques, Flawil, Switzerland). The following conditions were used during spray drying: drying airflow, 40 m^3/h; spraying airflow, 500 L/h; suspension feed rate, 5 mL/min; nozzle size, 0.5 mm; the inlet temperature was established at 70°C and the outlet temperature was between 40 and 50°C.

Amorphous MRF microspheres were prepared by spray drying. 0.5 g of RF dissolved together with 0.5 g of either PLGA or PLA in 100 mL dichloromethane and spray dried under the same spraying conditions as above [5].

6.2.2.2. Preparation of coated RFDH using a spray dryer equipped with two different types of three-fluid (3F) spray nozzles

Polymer coated RFDH formulations were prepared by *in-situ* spray drying of the RFDH suspension and a coating solution. The RFDH suspension, consisting of 4% w/v of RF, was prepared by recrystallization of RF in anhydrous ethanol solution as above. The coating solutions of polymers, PLGA and PLA, (0.3% and 0.5% w/v), were prepared by dissolving polymers in acetone. Two prepared spraying solutions were sprayed separately through two different liquid channels of the 3F spray nozzle (Büchi Laboratory-Techniques, Flawil, Switzerland) as shown in Figure 6.1. The RFDH suspension was introduced through the inner nozzle with constant stirring at the feed

speed of 1 mL/min (40 mg/min). The coating solutions (0.3 and 0.5% w/v) were supplied to the outer spray nozzle disposed concentrically about a core nozzle at the feed speed of 8 mL/min, provided 62.5% and 50% RF loading, respectively. The 3F nozzles used in this study consisted of three separate nozzles: two for aqueous solution and one for a suitable gas fluid. The sizes of inner and outer aqueous nozzle are 0.7 and 2.0 mm, respectively. The distance between the bottom edge of the inner nozzle and the end of the outer nozzle is adjustable as 0 mm (standard 3F nozzle (3F-S)), and 1 mm (modified 3F nozzle (3F-M)), as shown in Figure 6.1. The spray drying was performed using a Büchi Minispray dryer B-290 (Büchi Laboratory-Techniques, Flawil, Switzerland) under following conditions for both nozzles: drying airflow, 40 m^3/h; spraying airflow, 600 L/h; the inlet temperature was established at 70°C and the outlet temperature was adjusted between 40 and 50°C.

6.2.3. Characterization

6.2.3.1. Assay

The RF contents of prepared formulations were determined using HPLC. A stock solution of each sample was prepared; each powder (25 mg) was weighed separately and dissolved with 25 mL of acetone. 1 mL of each stock solution was diluted with 9 mL of mobile phase and analyzed using validated HPLC method [3].

6.2.3.2. X-Ray diffraction of powders

The crystalline structure of prepared samples was examined using wide angle X-ray diffraction (XRD). A Philips 1710 X-ray diffractometer (Philips Electronic Instruments Inc., Mahwah, NJ) with a copper target (CuKα1,λ = 1.54056 Å), and a nickel filter, at a voltage of 40 kV and a current at 40 mA, was used to obtain the XRD patterns. . Samples were analyzed in the 2-theta range from 5 to 50° using a step size of 0.02 2θ degree with a dwell time of 2 sec.

6.2.3.3. Thermal analysis

Thermograms were measured using a differenctial scanning calorimetry (DSC), Model 2920 (TA Instruments, New Castle, DE). Dry nitrogen gas was used as the purge gas through the DSC cell at a flow rate of 40 mL/min. Samples (5 mg) were weighed into aluminum crimped pans. The mass of the empty sample pan was matched with that of the empty reference pan within ± 0.2 mg. Samples were heated at a ramp rate of 10°C/min from 30 to 350°C.

6.2.3.4. Moisture sorption analysis

Dynamic vapor sorption (DVS) was used to investigate the moisture sorption of prepared formulations. Samples (10 mg) were pre-weighed and added to quartz sample pans which were placed in the sample chamber of a DVS-1 apparatus (Surface Measurement Systems Ltd., London, UK). During this measurement, all samples were separately exposed to a continuous flow of N_2. Each sample was dried at 0% RH for two

hours before being exposed to 10% RH increments for two 0-90% RH cycles at 25°C. To prevent desolvation, another condition was applied for the coated RFDH samples. The humidity increments started from 50% RH to 90% RH. Equilibrium moisture content at each increment was determined by a dm/dt of 0.002%/min.

6.2.3.5. Particle size distribution, density and aerodynamic diameter

Particle size distributions, based on volume fractions of prepared powders was measured using a Spraytec® particle size analyzer equipped with an inhalation cell (Malvern Instruments, Ltd., Worcestershire, UK). It consists of a Spraytec® unit with a throat held in place by the inhalation cell, and a connection for an aerosol generating device. The entire assembly operated in a closed system that allowed for a controlled airflow rate (60 L/min) through the measurement zone. Size 3 HPMC capsules were filled with 15 mg of powder, and loaded in to the Aerolizer® device. The Aerolizer® device was then fired into the Spraytec® particle size analyzer at a flow rate of 60 L/min to allow the particle size distribution of DPIs to be measured under simulated actuation conditions.

The bulk densities of the prepared formulations were determined by pouring a known mass of powder (approximately 0.5 g) under gravity into a calibrated measuring cylinder, then recording the volume occupied by the powder. The tapped density was measured by following a USP method [31]. Theoretical estimates of aerodynamic diameter (d_{ae}) were derived from the particle sizing ($d_{0.5}$) and tapped density data (p), according to Eq. 1 [32].

$$d_{ae} = d \times \sqrt{\frac{\rho}{\rho_1}} \quad \text{, Where} \quad \rho_1 = 1 \text{ g cm}^{-3} \qquad 1)$$

6.2.3.6. Scanning electron microscopy

The morphology of prepared samples was observed using a LEO 1530 SEM (Zeiss/LEO, Oberkochen, Germany). Each sample was mounted separately onto SEM stubs using double-sided copper tape before sputter coating with Ag for 30 seconds under vacuum at 30 mTorr. The SEM was operated at high vacuum with accelerating voltage 5 kV and specimen working distance 4 mm.

6.2.3.7. Confocal microscopy

A laser scanning confocal microscope **(**Leica SP2 AOBS, Bannockburn, IL), equipped with an argon ion laser, was used to investigate the structure of the RFDH and the coated RFDH microparticles. For the imaging of coated particles, 40 mg of Fluorescein Isothiocyanate (FITC) was added to the prepared 0.5% w/v of PLA coating solution (80 mL) and sprayed with the 4% of RFDH suspension (10 mL) through the two separate liquid channels of the 3F-S nozzle as above. For RFDH imaging, no fluorescence dye was added since RFDH is an auto-fluorescing material. The prepared dry powders were dispersed onto the receiving glass slide without oil immersion (to prevent drug dissolution in oil). All samples were imaged with two excitation wavelengths of 488 nm and 594 nm for FITC and RFDH, respectively.

6.2.3.8. High performance liquid chromatography (HPLC)

Drug content and dissolution samples were analysed using a HPLC system (Waters Co., Milford, MA) with UV detection. The system consisted of a 717 plus autosampler, 2487 dual wavelength detector, 1525 binary pump, and 1500 column heater. Chromatography was performed using a Bondapak C_{18} 10 μm 3.9×300 mm column (Waters, Milford, MA) and a SecurityGuard™ guard column (Phenomenex®, Torrance, CA). The mobile phase, consisting of methanol, acetonitrile and phosphate buffer solution pH 5.2 in a ratio of 50:17:33 respectively, was eluted at a flow rate of 1.2 mL/min and the UV detector was set to a wavelength 337 nm. The column temperature was maintained at 25°C and the volume of each sample injected was 50 μL [3].

6.2.4. Aerosol classification

The aerosolization performances of prepared samples were studied using a Next Generation Impactor (NGI) (MSP Co., Shoreview, MN). 15 mg of each powder formulation were filled into size 3 HPMC capsules and placed into an Aerolizer® dry powder inhaler (DPI). Each capsule was pierced and actuated into an NGI though a stainless steel USP throat adapter at a flow rate of 60 L/min for 4 seconds, respectively. The powder deposited in the throat, in each dose collection-plate of the NGI, and in the remaining capsule were each reconstituted with 10 mL of acetone. The powders remaining in the device were washed with 10 mL of ethanol. Collected samples were analyzed by an 8453 UV/VIS spectrophotometer (Agilent, Santa Clara, CA) at 474 nm [33].

The emitted dose (ED), defined as the percent of total powder mass exiting the capsule, was determined by subtracting the amount remaining in the capsule from the initial mass loaded into the capsule. The fine particle fraction (FPF), defined as the total dose of particles with aerodynamic diameters smaller than 5 μm, was calculated via interpolation from the cumulative mass against the cutoff diameter of the respective stages of the NGI. The FPF is expressed as a percentage of the total drug dose (FPF_{TD}), and not of the emitted dose. Each measurement was repeated three times. The MMAD was determined by the % cumulative undersize on probability scale versus logarithmic aerodynamic diameter data.

6.2.5. *In vitro* dissolution testing using novel dissolution method

Dissolution behaviors of air classified powders were studied by a membrane holder method previously developed by this group [29, 30] (see Chapter 4). To briefly summarize, powder formulations containing approximately 1 mg of RF were loaded onto the membrane holder inserted in the NGI dose-collection plate at stage 3, by aerodynamic separation using the NGI. Appendix C describes how the amount of RFDH loading is determined. To achieve equal powder loading into the holder, the amount of powder added into the size 3 HPMC capsule was varied from 7 mg to 20 mg with the powder deposition profiles in each dose-collection plate of the NGI. The capsule fill mass was calculated by dividing the target RF loading amount by the powder deposition ratio in the dose-collection plate stage 3 obtained from the aerosol classification study. The capsule filled with powders was placed into the Aerolizer® device, and actuated into the NGI

equipped with a gravimetric sampling cup (MSP Co. Shoreview, MN) equipped with a dissolution impaction plate (Copley Scientific, Nottingham, UK) at a flow rate of 60 mL/min for 4 seconds. The dissolution impaction plate containing air classified particles was removed from the gravimetric sampling cup placed in the dose-collection plate of stage 3, and a pre-soaked PC membrane was placed onto the top and sealed in place with a push fitted sealing ring. The membrane covered dissolution impaction plate was placed into each dissolution vessel containing either 300 mL of PBS (pH 7.4) or 0.2 M citrate buffer (pH 5.2) containing 0.02% of ascorbic acid. Dissolution testing was conducted at 75 rpm. The dissolution media (2 mL) was withdrawn manually using a glass syringe and filtered using a 0.45 μm PTFE syringe filter at timed intervals of 15, 30, 60, 120, 180, 240, 360, and 480 minutes.

The residual amount of RF on the membrane holder was determined after dissolution test by washing a membrane and the impaction insert with acetone (10 mL) prior to analyzing. The total amount of RF loaded on the membrane holder was back calculated using the sum of cumulated release amount of API, plus the remaining quantity of API on the membrane holder and compared with the theoretical amount of powder loading calculated from the aerosol classification study. Fresh dissolution media (3 mL) was replaced into each vessel after sampling to maintain a constant volume. Ethanol (100 μL) was added to the 900 μL of collected samples and analyzed using the validated HPLC method, described above [3], to prevent decomposition of dissolved RF in the dissolution media.

6.2.6. Stability

The prepared formulations were stored at ambient conditions in amber vials (25°C/50% RH). Drug contents and thermal behavior, using differential scanning calorimetry (DSC), of stored samples were monitored every three months using the method described above.

6.2.7. Statistical analysis

Data were expressed as the mean plus/minus standard deviation (SD). Statistical differences were studied by analysis of variance (one-way ANOVA) using Jump 7.0 software (SAS Institute Inc., Cary, NC). *P* values of less than 0.05 were considered as statistically significant. To identify the statistically significant differences between groups, Tukey–Kramer test was used. α value of 0.05 was applied to denote statistical significance.

6.3. RESULTS AND DISCUSSION

6.3.1. Characteristics of sprayed formulations

The SEM images of the prepared formulations are shown in Figure 6.2. The RFDH particles show a very thin flake-like structure (less than 200 nm in thickness) with a smooth surface, which was the result of a polymorphic transformation of RF (Figure 6.2 (A)) [28]. The coated particles prepared by two different types of 3F nozzles also showed a flake-like structure with more corrugated surface structure than the core particle,

RFDH, due to the polymer layer on the surface (Figure 6.2 (C) and (D)). Generally, spray-dried large molecules as polymers have a very corrugated surface structures since the diffusion of molecule from the atomized droplet surface to the inner core is slow, thus, the surface becomes enriched with molecules associated with a high Peclet (*Pe*) number as polymers, resulting in a crumpled surface structure [34, 35]. It can also be shown from the Figure 6.2 (B) that MRF microspheres have a very corrugated spherical shape. The distribution of polymer on the coated particle surface was further confirmed by confocal laser scanning microscopy (Figure 6.3). The intensity profiles obtained from the cross-sectional confocal laser scanning images (CLSI) of coated and uncoated RFDH particles showed that the fluorescent intensity of FITC (λ_{ex}= 488) increased after coating with FITC embedded PLA, whereas the RFDH intensity (λ_{ex}= 594) decreased after coating.

The RF loaded formulations prepared by the spray drying process using three different types of spray nozzles, 2F, 3F-S, and 3F-M, are listed in Table 6.1 with the characterization results. The core-forming particles, RFDH, showed 95.8% of RF contents since it hosts 2 moles of water per one mole of RF molecule [28]. All other formulations contain about 50 or 60% w/w of RF and the loading efficiencies were in the range between 93 to 103% (w/w). Overall, the encapsulation efficiency of the formulations was close to the estimated values of drug loading. However, significant difference in product yield was found between the coated RFDH and MRF formulations. The significantly low yield of the MRF microspheres prepared by the 2F nozzle explains the cohesive nature of polymeric microspheres (Table 6.1). It was seen that the majority

of dried microspheres stuck on the wall of the cyclone separator gradually melted on the wall due to the low Tg of PLA/PLGA polymer. In contrast, the yield of coated formulations was not as low as those of MRF microsphere formulations, although the surface of the manufactured particles was modified with polymer. There was a higher yield for the coated particle because the bulky flake-like structure of microparticles was quickly removed from the cyclone separator due to low density and low inter-particulate forces, as evidenced in our previous study with the RFDH crystals [28] (see Chapter 5).

Representative x-ray diffractograms of the manufactured formulations, RFDH, coated RFDH, and MRF microsphere are shown in Figure 6.4. X-ray powder diffraction (XRD) patterns show that the coating process using a 3F nozzle did not affect the crystalline structure of RFDH, whereas the MRF microsphere shows no characteristic crystalline peaks with a halo at the baseline appearing on the x-ray diffractogram, indicating that the RFDH crystals sprayed through the inner nozzle were successfully coated without dissolving of the crystals in the stream of coating solution sprayed through the outer nozzle. The characteristic crystalline peaks representing the polymer-coated samples correspond to those for the RFDH, although peak intensity decreased due to an amorphous PLGA or PLA content in the formulations. The core-forming crystal, RFDH, is freely soluble in most organic solvents except ethanol, thus conventional coating methods that require a dispersion of core particles in organic coating solution, like a spray coating process using a 2F nozzle, can't be applied. This is unfortunate as spray coating using a spray dryer with 2F nozzle is a common method used to over other coating process to obtain coated particles since it is a relatively simple one-step process

and has the capability to coat very small particles [26, 27, 36]. The issues associated with solvents to dissolve or disperse RFDH and PLA/PLGA can be solved by spraying two prepared liquid solutions separately through the two liquid passages of 3F nozzle.

Laser diffraction data are presented in Table 6.1, with a representative size distribution displayed in Figure 6.5. The median (d_{50}) particle size of each of the coated and uncoated RFDH powders was in the range of 8 to 12 μm with a unimodal size distribution profile. In contrast, the MRF microspheres showed broad particle size distribution with d_{50} values of 22-25 μm, unlike the particle size shown in the SEM image (Figure 6.2 (B)), which indicates a range of 2-5 μm, suggesting that the MRF microspheres were not deagglomerated completely at the airflow (60 mL/min). The formation of strong aggregates is very undesirable for pulmonary administration, since it leads to a decrease in the fine particle dose (FPD) to the target site, the lung. The d_{ae} value for MRF formulations could not be obtained since the tapped density of those formulations wasn't measured properly due to the adhesive powder property. The calculated d_{ae} values for the RFDH and the coated RFDH formulations fell into the respirable particle size range (1-5 μm), although the d_{50} values were larger than 8 μm, due to the low density. The d_{ae} values of the coated RFDH, prepared using the 3F-M nozzle were larger than that of the particles coated by the standard 3F nozzle (3F-S), whereas the geometric particle size (d_{50}) were very similar to each other at about 10 μm (Table 6.1). This indicates the 3F-M nozzle produces a thicker coating layer on the RFDH surface than the 3F-S nozzle, resulting in an increase the settling velocity of airborne particles. From the study, we can estimate that the optimal aerodynamic properties of formulations

will be in the following rank order: RFDH > coated particles by 3F-S > coated particles by 3F-M.

6.3.2. Aerodynamic properties

In vitro aerosolization properties of manufactured formulations were compared using NGI with Aerolizer® device. The ED, FPF_{TD}, and MMAD of each formulation are displayed in Table 6.2. The aerodynamic performances of the RFDH powders were considerably improved by changing the crystalline structure to a flake-like dihydrate form, with 68% of FPF_{TD}. It has been known that the flaky or elongated morphology of microparticles significantly improves particle deaggragation and dispersion properties since the different particle shapes lead to a variation in surface energy and inter-particulate forces [37-40]. The FPF_{TD} and the MMAD values of coated RFDH formulations are in good agreement with the estimated aerodynamic properties of formulations from the d_{ae} values. The coated RFDH formulation by the 3F-S nozzle showed smaller MMAD and higher FPF_{TD} values of about 3.5 μm and 54% than those of powders coated using the 3F-M (bigger than 4 μm and about 40% FPF_{TD}), implying that the settling velocity of the coated particles by the 3F-M nozzle is faster than the particles coated by the 3F-S nozzle in the airborne state due to the larger amount of polymer deposited on the particle surface. It was also shown in Figure 6.6 that the maximum particle depositions of the RFDH, the coated RFDH by 3F-S and 3F-M nozzle were achieved at the NGI dose-collection plate stage of 4, 3 and 2 among the 7 dose-collection

plates, respectively, with more than 95% of the capsule contents being emitted during aerosolization testing at an air flow of 60 L/min.

The difference in coating thickness can be explained by the mechanisms of two coating methods using different 3F nozzles, 3F-S and 3F-M. As depicted in Figure 6.1, in the process using a 3F-S nozzle, two liquid phases are supplied to two separate spray channels and they are atomized by mixing of high-speed compressed air supplied through the separate gas channel at the end of nozzle tip (mixing zone), leading to a collision of atomized polymer mist with atomized solid RFDH crystals (core-forming particles) with a certain probability. As a result, the collided polymer mist is rapidly deposited on the core particle surface and forms a thin layer.

Contrary to the 3F-S process, in the process using the 3F-M nozzle, the ethanol suspension containing core-forming particles is combined with the coating solution in the outer nozzle followed by continuous atomization (Figure 6.1). The mixing of the ethanol suspension and the acetone coating solution may occur immediately due to the rapid diffusion of ethanol into the acetone without anti-solvent precipitation of PLGA/PLA polymer [41, 42]. The continuous polymer solution surrounding the core-forming particles forms a thin layer upon atomization. In the 3F-M process, the RFDH crystals do not dissolve upon contact with the acetone/ethanol solvent mixture as evidenced by the XRD data. This solvent stability of the RFDH crystals is likely due to the fact that the atomization of solvent mixture is achieved at almost the same time as the solvent mixing. Consequently, the polymer mist generated by the 3F-S nozzle forms a thinner coating

layer than the continuous liquid phase surrounding the core-forming particle in the 3F-M nozzle.

The ED values of the MRF microsphere formulations were significantly lower (about 70%) and more variable compared to the coated RFDH formulation, although the MRF formulations were manufactured as a highly corrugated powder to improve the dispersibility. This low ED is attributed to their small and spherical shape leading to a strong particle aggregation.

6.3.3. *In vitro* dissolution studies

Although several *in vitro* methods exist for the prediction of respirable fraction and site of deposition in the lung following pulmonary administration (e.g. Andersen Cascade Impactor, Next Generation Impactor, Twin Stage Impinger), there is no optimized *in vitro* model to predict the rate and extent of drug dissolution in the lung following inhalation. Currently available methods of evaluating the dissolution behavior of inhalation products rarely consider the impact of particle classification on the dissolution behavior [15, 16, 43, 44]. Unlike other pharmaceutical dosage forms, in pulmonary drug delivery systems, only a fraction of the API emitted from standard delivery devices is delivered to the target site, the lung, and the deposited particles in the lung are in a deagglomerated state. Thus, an ideal dissolution test method for inhalation formulations would involve a particle classification step prior to dissolution assessment. We have indicated that the aerodynamic classification of aggregated powders prior to the powder introduction step into the dissolution apparatus has a significant influence on the

dissolution profiles [29]. In this study, a new membrane holder method which was designed specifically to be incorporated into the Next Generation Impactor (NGI) for easy dose collection performance was applied to properly compare the dissolution profiles of the manufacture formulations [29, 30].

As expected, the uncoated RFDH powder underwent the most rapid dissolution among the formulations, with 63% of initial RF release in 15 minutes followed by a sustained RF release for 8 hours (Figure 6.7). The release rate at the first time points were mainly attributed to the pre-dissolved RFDH crystals in the membrane holder since the pre-soaked membrane replicating the thin lung lining fluid in the membrane holder setup may activate the drug dissolution by improving powder wetting before the sealed membrane holder is added to the dissolution media. Consequently, the actual drug dissolution rate between 0 and 15 minutes, although data are plotted as a straight line, may be slower than what is shown in the graph. Nevertheless, these studies do give comparative information about the rate of drug release from different formulations.

The coated RFDH formulations exhibited delayed release characteristics with a lowered initial burst, implying that the polymer layer surrounding the RFDH particle prevents the RFDH from dissolving at the early phase by minimizing the chance for the core-forming particles to contact the dissolution medium, which is in general agreement with the results of coated formulations with hydrophobic polymers [25, 45]. The formulations prepared by the 3F-M nozzle were associated with a lower initial RF release than the formulations prepared by the 3F-S nozzle. In particular, the PLA coated formulation, C50L-M, showed the lowest initial RF release as 32% with a moderated

biphasic release profile in the coated formulations. However, overall, RF release from the formulations coated by the 3F-M nozzle after the initial burst (15 min) was not significantly retarded when it is compared with the formulations prepared by the 3F-S nozzle. This explains the thickness of the coating layer obtained from two different spray nozzles is not considerably different to modify the diffusion rate of dissolution media through the membrane barrier, but the completeness of coating layer may be influenced by the type of spray nozzle. The higher initial RF release from the formulations prepared by the 3F-S may be due to the larger amount of incompletely coated RFDH portion in the formulation compared to that of powders coated by the 3F-M nozzle. The RF release profile from the formulation encapsulating a 60% of RF (C60L-M) was shown to be faster than that of the formulation loaded 50% of RF (C50L-M) due to the lower amount of polymer deposited on the RFDH particle surface. From the release studies with coated formulations, we can conclude that the 3F-M nozzle is more effective in controlling the initial RF release with higher drug loading than the 3F-S nozzle. In inhaled anti-TB antibiotic treatment, the formulations exhibiting a large initial release with high loading efficiency (high doses of encapsulated drug) has been known to be more effective for effective treatment of pulmonary TB than the formulation with no initial drug release [5, 6]. Accordingly, the well-controlled initial drug release from the coated formulations may be beneficial in achieving the therapeutic concentration immediately after dosing, followed by sustained release to maintain the achieved therapeutic dose in the lung until next the dose. Generally, sustained release formulations having no burst effect to maintain certain systemic drug concentration have been known to be ideal. However, that

is not always ideal to treat diseases, in particular, the use of initial burst as a first does may be more effective for the treatment of local respiratory infections as many bacterial species inoculated in the lung show slow proliferation by immediately reaching their minimum inhibitory concentration (MIC) [5, 46]. For instance, a study conducted by Suarez et al. shows that the formulation exhibiting a large initial RF release followed by sustained release is more effective to inhibit a MTB bacterial growth in the lung [5] since the antibiotic effect of RF against MTB bacteria is dose-time dependent [9, 24].

As shown in Figure 6.7, the largest burst effect was observed for the PLGA MRF microsphere formulations, M50LG, in the manufactured sustained release formulations, while the PLA MRF formulation, M50L, showed the lowest initial RF release (25%) with a plateau at 45%. The large initial RF release from the PLGA MRF formulation is attributed to the RF release from the superficial area of microparticles. It has been known that the most challenging part in microencapsulation is to effectively control drug loading to achieve both sufficient therapeutic doses and desired changes in the dissolution profile, since in most cases of sustained release systems, drug release rate is inversely proportionate to the amount of encapsulated drug. Polymers having higher molecular weight or having more hydrophobic moiety have been used to obtain formulations with more extended release profile, however, those polymers often lead to incomplete drug release from the microparticles due to the extremely slow erosion or diffusion characteristics of polymers [3] as the release profile of the PLA MRF microsphere shown in Figure 6.7.

The pH of the dissolution medium significantly affected RF release as well as the decomposition of dissolved RF. Dissolution data collected at 15 minutes and 8 hours were plotted (Figure 6.8). Dissolved RF in an acidic dissolution media (pH 5.2) decomposes rapidly by oxidization and hydrolysis [47, 48], thus dissolved RF contents in the dissolution media after 15 minutes couldn't be analyzed (Data collected at 8 hours was plotted against the RF amount subtracted from the initial loading from the remaining RF amount in the membrane holder). At pH 5.2, the initial drug release was decreased for both RFDH and the coated RFDH formulation compared to the values at neutral pH (pH 7.4) due to the pH-dependency of RF in dissolution [3, 47, 48]; the RF shows the fastest dissolution at pH 1.2, the slowest dissolution at slightly acidic conditions (pH 4-5) and a moderate dissolution in neutral conditions. However, difference in the cumulative amount of released RF for 8 hours in two different pHs is more significant for the coated RFDH formulations than uncoated one; for uncoated RFDH crystals, almost the same amount of RF was dissolved in pH 5.2 media as it was in pH 7.4 media for 8 hours, whereas the coated RFDH formulations released a 32% lower amount of RF at pH 5.2 compared to that at pH 7.4. This result suggests that the pH-dependent dissolution of RF, coupled with the minimum exposure of core-forming particles to dissolution medium by the polymer barrier on the surface, results in a much slower RF release in low pH dissolution media. This pH-dependent dissolution may be beneficial to target AMs, which is a safe site for their prolonged survival, since polymeric microparticles in the size range between 1 to 10 μm are very actively phagocytosed by AMs in 1 hour [19, 20]. From the *in vitro* dissolution study, it can be estimated that the deposited coated RFDH particles dissolves

quickly in the first hour to achieve therapeutic concentrations in the alveolar region (pH 7.4) followed by slow RF release from the coated particles either phagocytosed by AMs in the phago-lysosome interior (pH 4-5) or from those that could remain in the alveoli.

6.3.4. Correlation between stability and moisture uptake

In our previous study, the significant decrease in drug content for the spray-dried amorphous RF was found, which was 26% degradation in 9 months at ambient storage condition, whereas the RFDH crystal did not show a significant difference [28] (see Chapter 5). Thus, the impacts of moisture sorption-desorption properties of the manufactured formulations on the physicochemical stabilities were studied by means of DVS method. As shown in Table 6.3, the decrease in chemical potency for the crystalline-structured formulations was less significant than that of the amorphous-structured formulations. More hydrophobic polymer, PLA, was shown to be better excipient to protect RFDH from the chemical decomposition than PLGA. These results can be explained through the moisture uptake behavior of formulations studied using DVS analysis. It can be seen from Table 6.3 that the degree of chemical degradation is closely related to the hysteresis between the moisture sorption and desorption cycle; formulations showing larger hysteresis on the isotherm graph was associated with more chemical decomposition. As shown in Figure 6.9 (A), the MRF microspheres, M50LG, take up 3.5% moisture between 0-90% RH and 2.3% moisture between 50-90% RH. A large hysteresis between sorption and desorption isotherm profiles was also shown from amorphous formulations (Table 6.3), indicating that water absorbed from the atmosphere

is strongly bound to the amorphous RF when the powders are stored at ambient condition, and the chemical degradation or the crystalline structural rearrangement could be accelerated by this. Conversely, the coated RFDH formulations showed a range of 1.4 to 1.5% moisture uptake between 50-90% RH and the hysteresis was not significant due to the hydrophobic polymer layer on the surface. From the DVS study, we can deduce that the chemical stability of coated RFDH formulations by the 3F-M would not be significantly different from the formulations manufactured by the 3F-S, although the 6 month stability data have not yet been analyzed, since the moisture sorption-desorption profiles were quite similar each other. As shown above, the DVS study is a very useful tool to estimate the hygroscopicity of manufactured formulations. Additional DVS studies on further formulation compositions are given in Appendix D.

The stabilities of the prepared formulations over 6 months were further confirmed by the DSC (Figure 6.10). No change in thermograms was found for the coated and uncoated RFDH formulations, whereas the onset of RF decomposition at 6 months is earlier than that of initial sample. This is good agreement with our previous data that the spray-dried RF with amorphous structure showed significant change in DSC thermograms [28].

6.4. CONCLUSION

A novel surface coating method utilizing multi-channel spray nozzles has been introduced. A multi-channel nozzle spray drying method is often applied when spraying of two continuous liquid phases to manufacture composite materials of water insoluble and soluble drugs. In this study, we found the spraying of continuous liquid phase and the suspension can generate coated formulation. The coating performance of two different types of three-fluid (3F) nozzles, standard 3F nozzle (3F-S) and modified nozzle (3F-M), were compared. Coated rifampicin dihydrate (RFDH) powders with hydrophobic polymers, PLGA and PLA, were prepared using the two different types of 3F nozzles. The coated formulations contained at least 50% w/w of RF. The thin flaky morphology and crystalline structure of RFDH powders was maintained after coating, and this special flake-like morphology provides high spray drying yield with the RFDH formulation. Overall, the aerodynamic performance of coated RFDH particles were reduced compared to the RFDH due to an increased aerodynamic diameter by polymer coating; the MMAD values of coated formulations were in the range of 3.5 to 4.6 μm, whereas the RFDH has a 2.2 μm of MMAD. However, the coated formulations still provide more than 40% of FPF_{TD} without a carrier. The maximum FPF_{TD} was obtained from the powders coated by the 3F-S as 54%, which was higher than that of the powder coated by 3F-M, due to the thinner coating layer.

The coated formulations showed lowered initial RF release followed by slow RF release after initial release compared to the uncoated RFDH crystals. The lowest initial

RF release was observed from the coated powders with PLA polymer using the 3F-M nozzle as 32% among other coated formulations. Overall, the formulations coated by the 3F-M nozzle showed lower initial RF release with higher drug loading than 3F-S nozzle. The RF release from the coated RFDH formulation showed pH-dependency; the RF release slowed in slightly acidic dissolution medium (pH 5.2). The significance of pH-dependent RF dissolution was larger for the coated formulation than for the uncoated RFDH powders due to the polymer barrier surrounding the core particle. It could be anticipated that the delivered coated RFDH powders via the pulmonary route would provide higher local (lung) drug concentrations with a longer drug residence time in the lung than that of uncoated formulation. From the series of studies, we can infer that coated RFDH powders deposited in the alveolar region would first deliver an initial therapeutic dose of RF, followed by sustained release (maintenance dose) from the coated particles. Additionally, coated particles may phagocytosed by alveoli macrophages (AMs), which is the main site of the *Mycobacterium tuberculosis* (MTB) proliferation, thus the targeting AMs and building up high intracellular drug concentrations could be possible. The coated RFDH powders are predicted to provide much better stability than the amorphous RF or uncoated RFDH crystals due to their reduced hygroscopicity.

6.5. TABLES

Table 6.1 Physical characterizations of prepared formulations.
(Values are means ± SD, n = 3)

Sample*	SD yield (%)	Drug loading** (%)	Loading efficiency (%)	Particle size ($d_{50,}$ μm)	Tapped density (g/cm^{-3})	d_{ae} (μm)
RFDH (Core particle)	91	95.8 ± 0.02	100	8.8 ± 0.1	0.068	2.3
M50LG	37.5	52.0 ± 0.6	104	24.5± 2.3	-	-
M50L	43.8	49.0 ± 0.9	98	22.7 ± 1.6	-	-
C50LG-M	72.5	49.9 ± 0.4	99.8	10.9 ± 0.2	0.128	3.9
C50L-M	78	49.7 ± 0.1	99.4	12.0 ± 0.8	0.119	4.1
C60L-M	70	58.3 ± 0.6	93.3	10.2 ± 0.4	0.108	3.3
C50LG-S	75	51.5 ± 0.6	103	10.4 ± 0.4	0.110	3.4
C50L-S	75	50.5 ± 0.6	101	10.1 ± 0.2	0.125	3.6

*The sample name is coded as follows:

i) M and S represent a matrix form and coated form, respectively
ii) The digits, 50 and 60, represent the amount of encapsulated RF
iii) LG and L represent a PLGA and PLA, respectively
iv) S and M represent standard 3F nozzle and modified 3F nozzle, respectively

**The loading indicates the amount of RF loaded in the formulations

Table 6.2 Aerodynamic characteristics of the formulations at a flow rate of 60 L/min with Aerolizer® (values are means ± SD, n = 3).

Formulation	ED (%)	PFP_{TD} (%)	MMAD (μm)
RFDH	98.3 ± 0.2	68.5 ± 2.4	2.2 ± 0.1
M50LG	71.0 ± 6.9[‡]	32.6 ± 2.9*	4.3 ± 0.5
M50L	72.9 ± 4.5[‡]	35.5 ± 2.0*	2.8 ± 0.1
C50LG-M	98.0 ± 0.3	40.4 ± 2.1*	4.2 ± 0.4
C50L-M	97.6 ± 0.6	37.6 ± 1.7*	4.6 ± 0.3
C60L-M	98.0 ± 0.2	40.8 ± 1.0*	3.6 ± 0.3
C50LG-S	98.2 ± 0.2	53.7 ± 1.6*[†]	3.6 ± 0.1
C50L-S	98.1 ± 0.26	54.4 ± 1.8*[†]	3.5 ± 0.1

[‡] Statistical difference among the groups
*Statistical difference from RFDH
[†] Statistical difference between two groups coated by two different types of 3F nozzles (Tukey–Kramer test, $\alpha < 0.05$)

Table 6.3 RF contents analysis for the prepared formulations stored under ambient condition (25 ºC/50 RH) over 6 months (values are means ± SD, n = 3), and the moisture sorption analysis for the prepared samples.

Formulations	Structure	Initial* (%)	Degradation in 6 months*(%)	Change in mass at 90% RH (%)	Hysteresis at 50% RH (%)
RFDH	Crystalline	95.8 ± 0.6	2.1	2.4	0.1
M50LG	Amorphous	52.0 ± 0.6	7.1	3.5	1.0
M50L	Amorphous	49.0 ± 0.9	4.5	3.1	0.6
C50LG-S	Crystalline	51.5 ± 0.6	1	1.5	0.05
C50L-S	Crystalline	50.5 ± 0.6	0.2	1.5	0.02
C50LG-M	Crystalline	49.9 ± 0.4	N.A.	1.5	0.08
C50L-M	Crystalline	49.7 ± 0.1	N.A	1.4	0.05

*The drug contents of RFDH indicates RF contents
N.A. : study is ongoing

6.6. FIGURES

Figure 6.1 Schematic diagram of two types of three-fluid (3F) spray nozzle for *in-situ* spray coating process; (A) modified 3F nozzle (3F-M), and (B) standard 3F nozzle (3F-S).

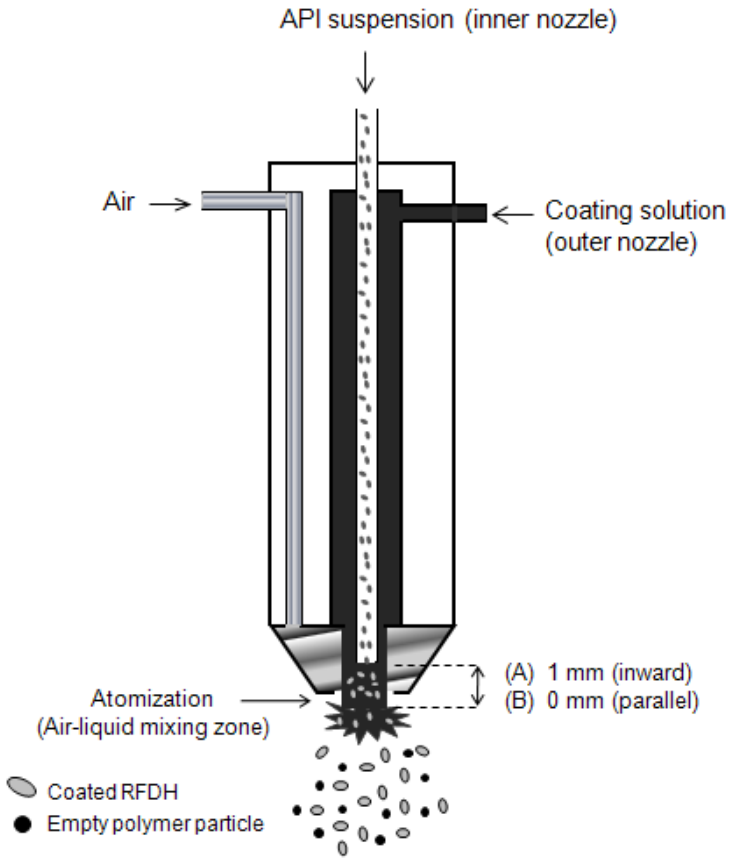

Figure 6.2 Scanning electron microscopy images of (A) RFDH, (B) MRF microsphere (M50LG), (C) coated RFDH with standard 3F nozzle (C50L-S), and (D) coated RFDH with modified 3F nozzle (C50LG-M).

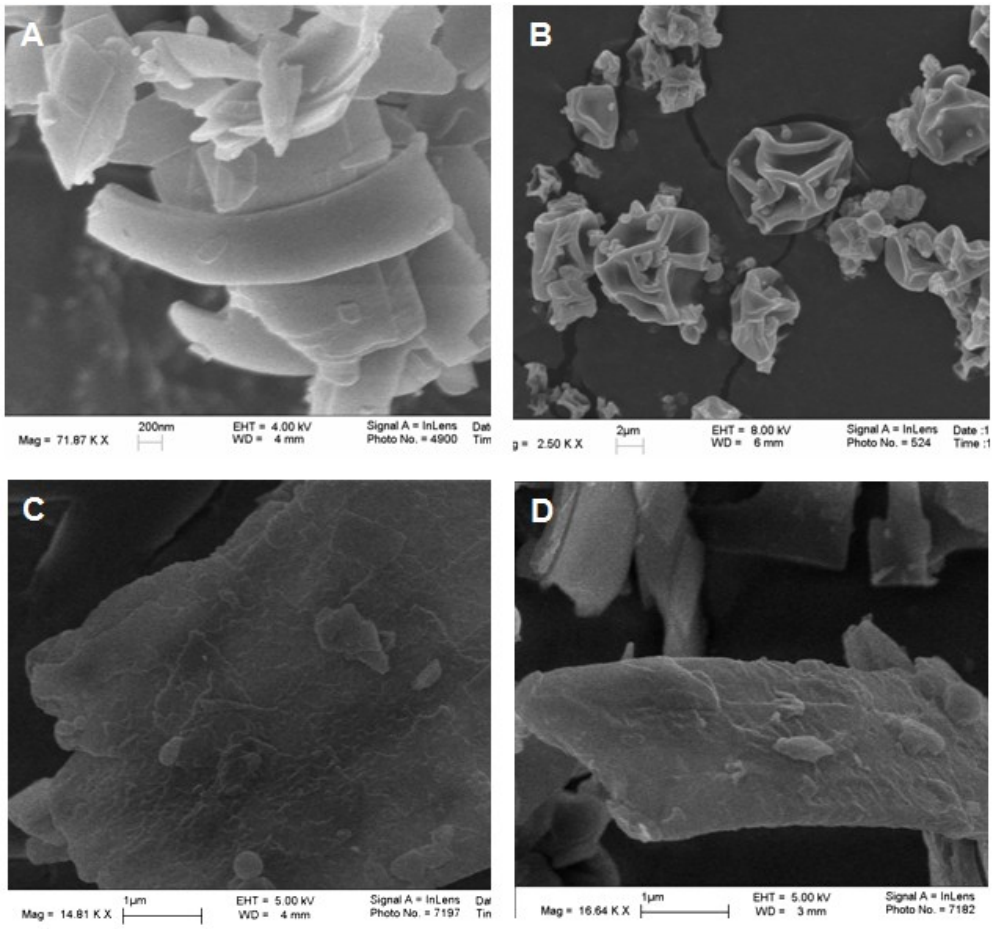

Figure 6.3 The intensity profiles obtained from the cross-section confocal laser scanning images of (A) the surface of uncoated RFDH and (B) the surface of coated RFDH particle with FITC embedded PLA (C50L-S).

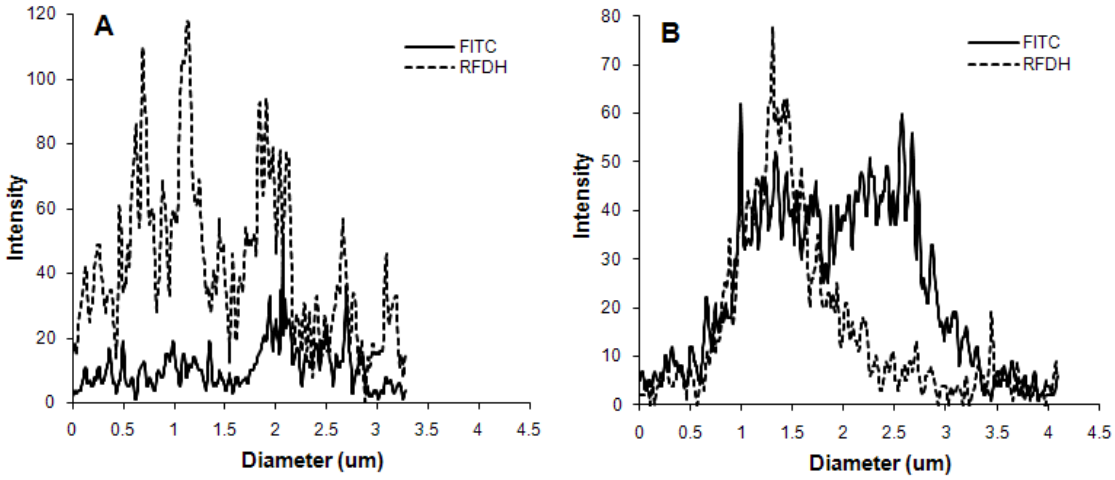

Figure 6.4 Powder X-ray diffractograms of (A) RFDH, (B) coated RFDH (C50L-M) and (C) MRF microsphere (M50L).

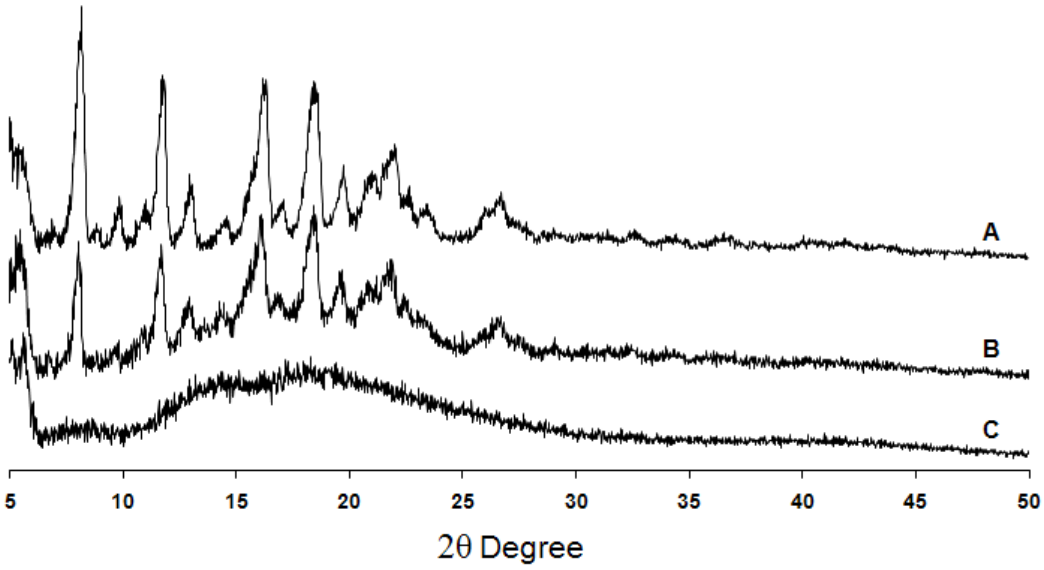

Figure 6.5 Average particle size distribution measured by Spraytec® at a flow rate of 60L/min for (A) RFDH, (B) coated RFDH (C50L-M) and (C) MRF microsphere (M50L).

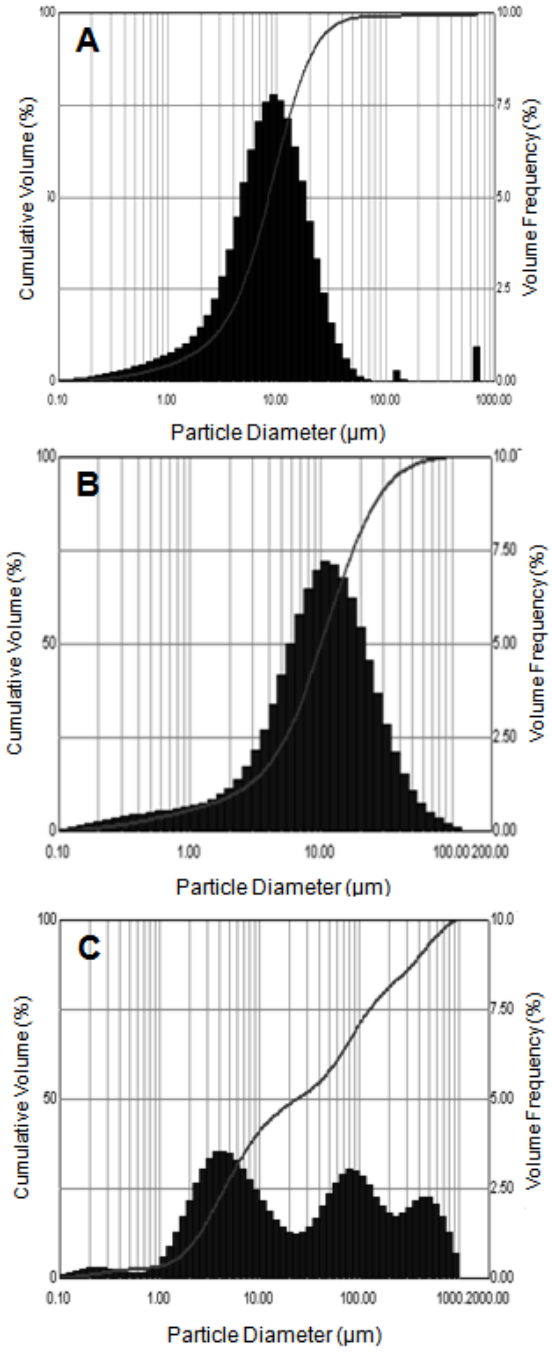

Figure 6.6 *In vitro* powder deposition profiles for RFDH, coated RFDH and MRF microspheres at a flow rate of 60 L/min with Aerolizer®, expressed as the percentage of total loaded dose. (Values are means± SD, n = 3).

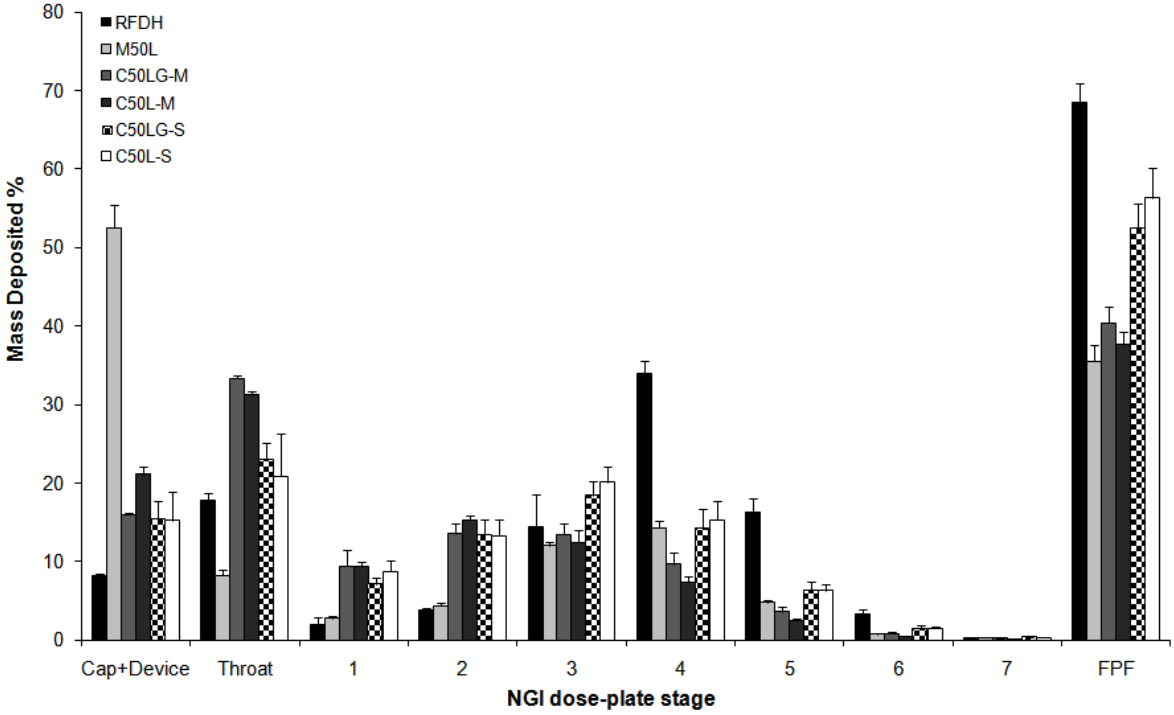

Figure 6.7 RF release profiles for the RFDH, coated RFDH, and MRF microsphere formulations in PBS containing 0.02% ascorbic acid (pH 7.4); (A) PLGA containing formulations and (B) PLA containing formulations (powders accumulated on the dose-collection plate 3 were selected for dissolution, the error bars indicate the standard deviation of three tests).

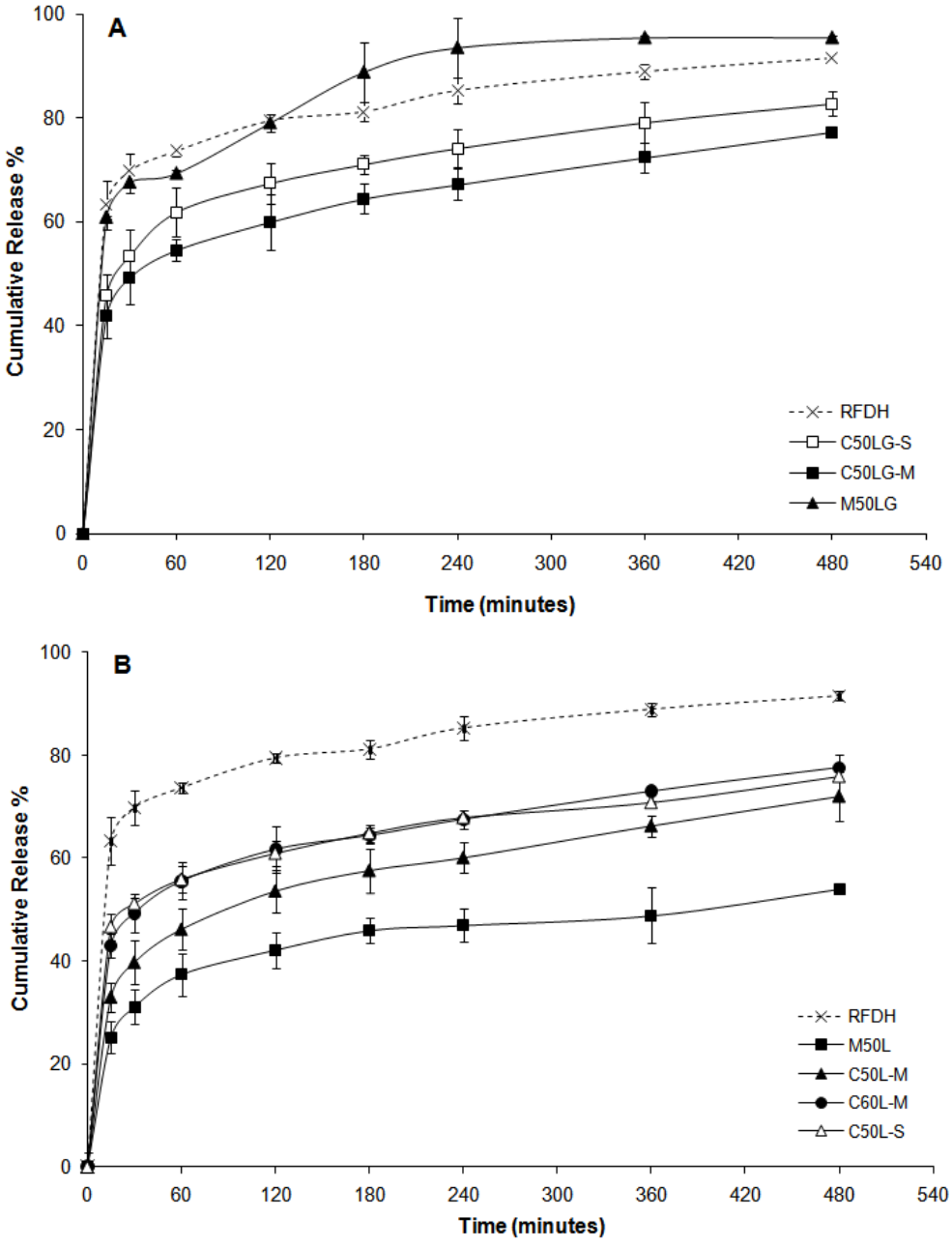

Figure 6.8 RF release profiles for the RFDH and coated RFDH (C50L-M) formulations in 0.2 M citrate buffer (pH 5.2) containing 0.02% ascorbic acid. Powders accumulated on the dose-collection plate 3 were selected for dissolution (Plotted data are average of three tests).

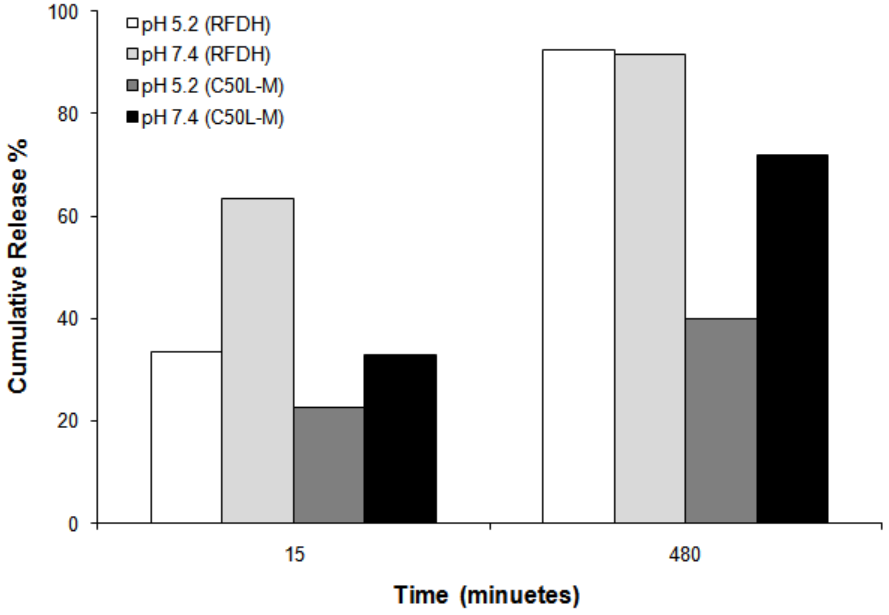

Figure 6.9 Dynamic vapor sorption (DVS) isotherm of (A) MRF microsphere (M50LG), and (B) coated RFDH (C50L-M). The absorption is shown as solid lines and desorption as dashed line.

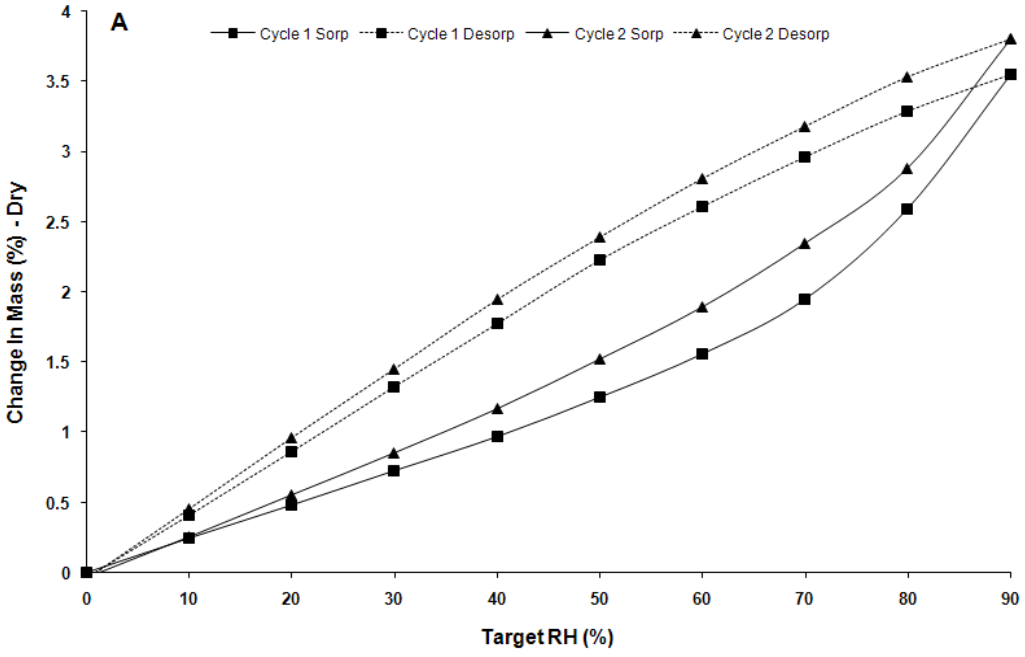

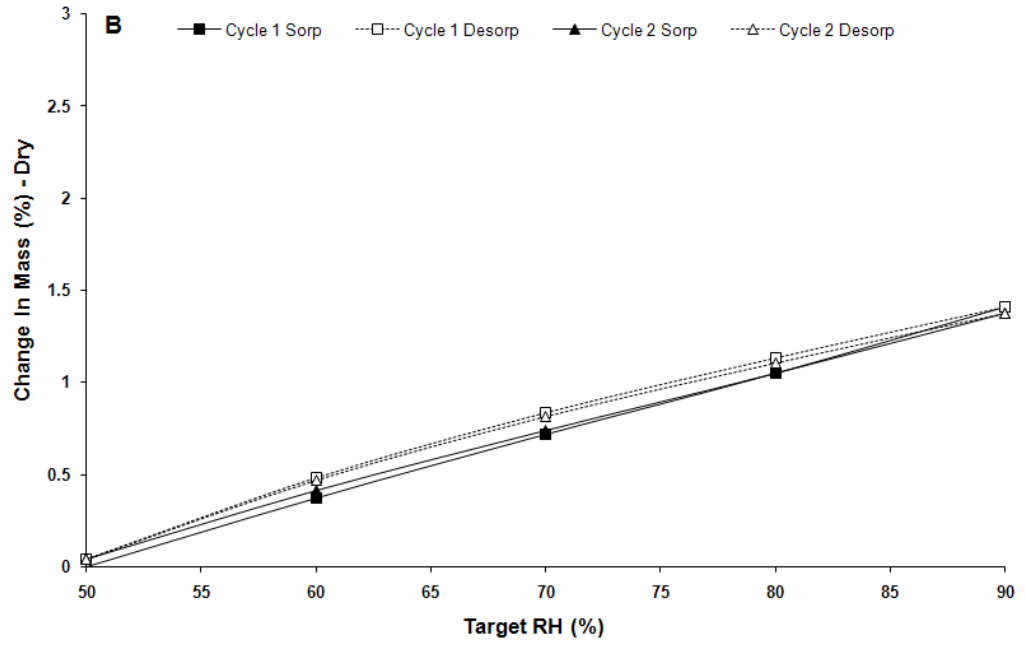

Figure 6.10 DSC thermograms of (a) RFDH and (b) coated RFDH (C50LG-S) and (c) MRF microsphere (M50LG) formulations over 6 months

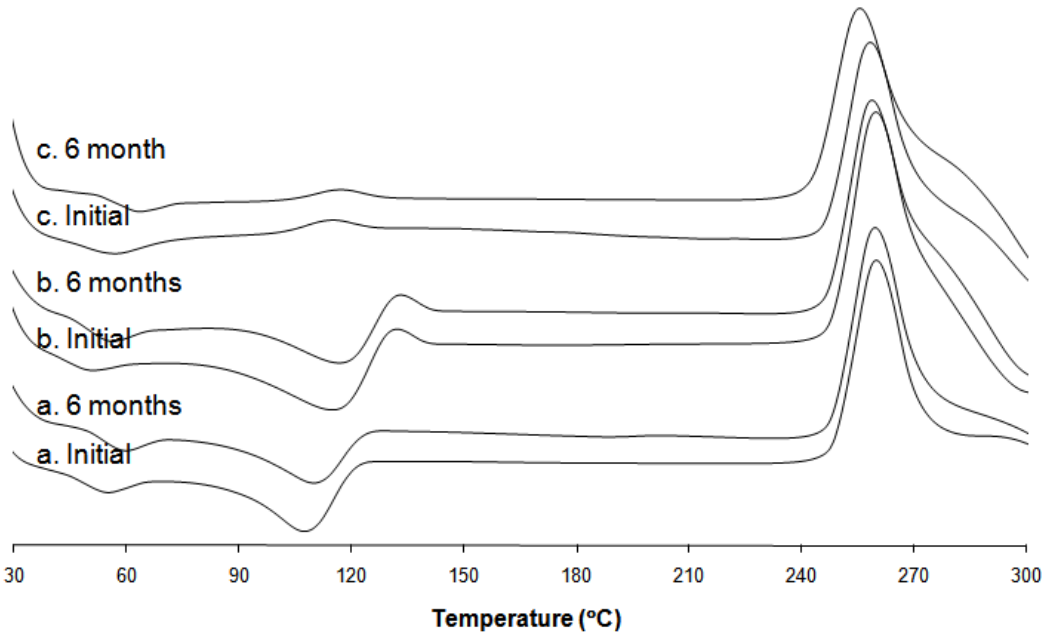

6.7. REFERENCES

[1] Rifampin. Tuberculosis 88(2) (2008) 151-154.

[2] J. Schreiber, G. Zissel, U. Greinert, M. Schlaak, J. Muller-Quernheim, Lymphocyte transformation test for the evaluation of adverse effects of antituberculous drugs. Eur J Med Res 4(2) (1999) 67-71.

[3] P. O'Hara, A.J. Hickey, Respirable PLGA microspheres containing rifampicin for the treatment of tuberculosis: Manufacture and characterization. Pharmaceutical Research 17(8) (2000) 955-961.

[4] J.C. Sung, D.J. Padilla, L. Garcia-Contreras, J.L. VerBerkmoes, D. Durbin, C.A. Peloquin, K.J. Elbert, A.J. Hickey, D.A. Edwards, Formulation and Pharmacokinetics of Self-Assembled Rifampicin Nanoparticle Systems for Pulmonary Delivery. Pharmaceutical Research 26(8) (2009) 1847-1855.

[5] S. Suarez, P. O'Hara, M. Kazantseva, C.E. Newcomer, R. Hopfer, D.N. McMurray, A.J. Hickey, Respirable PLGA microspheres containing rifampicin for the treatment of tuberculosis: Screening in an infectious disease model. Pharmaceutical Research 18(9) (2001) 1315-1319.

[6] S. Suarez, P. O'Hara, M. Kazantseva, C.E. Newcomer, R. Hopfer, D.N. McMurray, A.J. Hickey, Airways delivery of rifampicin microparticles for the treatment of tuberculosis. Journal of Antimicrobial Chemotherapy 48(3) (2001) 431-434.

[7] R. Sharma, D. Saxena, A.K. Dwivedi, A. Misra, Inhalable microparticles containing drug combinations to target alveolar macrophages for treatment of pulmonary tuberculosis. Pharmaceutical Research 18(10) (2001) 1405-1410.

[8] S.P. Vyas, M.E. Kannan, S. Jain, V. Mishra, P. Singh, Design of liposomal aerosols for improved delivery of rifampicin to alveolar macrophages. International Journal of Pharmaceutics 269(1) (2004) 37-49.

[9] F. Tewes, J. Brillault, W. Couet, J.C. Olivier, Formulation of rifampicin-cyclodextrin complexes for lung nebulization. Journal of Controlled Release 129(2) (2008) 93-99.

[10] F. Ito, K. Makino, Preparation and properties of monodispersed rifampicin-loaded poly(lactide-co-glycolide) microspheres. Colloids and Surfaces B-Biointerfaces 39(1-2) (2004) 17-21.

[11] C. Becker, J.B. Dressman, H.E. Junginger, S. Kopp, K.K. Midha, V.P. Shah, S. Stavchansky, D.M. Barends, Biowaiver Monographs for Immediate Release Solid Oral Dosage Forms: Rifampicin. J. Pharm. Sci. 98(7) (2009) 2252-2267.

[12] R. Sankar, N. Sharda, S. Singh, Behavior of decomposition of rifampicin in the presence of isoniazid in the pH range 1-3. Drug Development and Industrial Pharmacy 29(7) (2003) 733-738.

[13] C.J. Shishoo, S.A. Shah, I.S. Rathod, S.S. Savale, J.S. Kotecha, P.B. Shah, Stability of rifampicin in dissolution medium in presence of isoniazid. International Journal of Pharmaceutics 190(1) (1999) 109-123.

[14] S. Singh, T.T. Mariappan, R. Sankar, N. Sarda, B. Singh, A critical review of the probable reasons for the poor/variable bioavailability of rifampicin from anti-tubercular fixed-dose combination (FDC) products, and the likely solutions to the problem. International Journal of Pharmaceutics 228(1-2) (2001) 5-17.

[15] R.O. Cook, R.K. Pannu, I.W. Kellaway, Novel sustained release microspheres for pulmonary drug delivery. Journal of Controlled Release 104(1) (2005) 79-90.

[16] T.P. Learoyd, J.L. Burrows, E. French, P.C. Seville, Chitosan-based spray-dried respirable powders for sustained delivery of terbutaline sulfate. European Journal of Pharmaceutics and Biopharmaceutics 68(2) (2008) 224-234.

[17] R.O. Salama, D. Traini, H.K. Chan, P.M. Young, Preparation and characterisation of controlled release co-spray dried drug-polymer microparticles for inhalation 2: Evaluation of in vitro release profiling methodologies for controlled release respiratory aerosols. European Journal of Pharmaceutics and Biopharmaceutics 70(1) (2008) 145-152.

[18] J.G. Hardy, T.S. Chadwick, Sustained release drug delivery to the lungs - An option for the future. Clinical Pharmacokinetics 39(1) (2000) 1-4.

[19] K. Hirota, T. Hasegawa, H. Hinata, F. Ito, H. Inagawa, C. Kochi, G.I. Soma, K. Makino, H. Terada, Optimum conditions for efficient phagocytosis of rifampicin-loaded PLGA microspheres by alveolar macrophages. Journal of Controlled Release 119(1) (2007) 69-76.

[20] T. Onoshita, Y. Shimizu, N. Yamaya, M. Miyazaki, M. Yokoyama, N. Fujiwara, T. Nakajima, K. Makino, H. Terada, M. Haga, The behavior of PLGA microspheres containing rifampicin in alveolar macrophages. Colloids and Surfaces B-Biointerfaces 76(1) (2010) 151-157.

[21] T. Mizoe, T. Ozeki, H. Okada, Application of a Four-fluid Nozzle Spray Drier to Prepare Inhalable Rifampicin-containing Mannitol Microparticles. Aaps Pharmscitech 9(3) (2008) 755-761.

[22] P. Muttil, J. Kaur, K. Kumar, A.B. Yadav, R. Sharma, A. Misra, Inhalable microparticles containing large payload of anti-tuberculosis drugs. European Journal of Pharmaceutical Sciences 32(2) (2007) 140-150.

[23] T. Onoshita, Y. Shimizu, N. Yamaya, M. Miyazaki, M. Yokoyama, N. Fujiwara, T. Nakajima, K. Makino, H. Terada, M. Haga, The behavior of PLGA microspheres containing rifampicin in alveolar macrophages. Colloids and Surfaces B-Biointerfaces 76(1) 151-157.

[24] T. Gumbo, A. Louie, M.R. Deziel, W.G. Liu, L.M. Parsons, M. Salfinger, G.L. Drusano, Concentration-dependent Mycobacterium tuberculosis killing and prevention of resistance by rifampin. Antimicrobial Agents and Chemotherapy 51(11) (2007) 3781-3788.

[25] J.D. Talton, G. Hachhaus, R.K. Snigh, J.M. Fiz-Gerld, Method for preparing coated particle and phamraceutical formulations thereof. US. 6,984,404 (2006).

[26] M. Katsuma, H. Kawai, T. Mizumoto, Novel dry powder inhalation for lung-delivery and menufacturing method thereof. US 2004/0184995 (2004).

[27] M.K. Taylor, A.J. Hickey, M. VanOort, Manufacture, characterization, and pharmacodynamic evaluation of engineered ipratropium bromide particles. Pharm. Dev. Technol. 11(3) (2006) 321-336.

[28] Y.-J. Son, J.T. McConville, A new respirable form of Rifampicin. European Journal of Pharmaceutics and Biopharmaceutics(under reviewing) (2010).

[29] Y.-J. Son, J.T. McConville, Development of a standardized dissolution test method for inhaled pharmaceutical formulations. International Journal of Pharmaceutics 382(1-2) (2009) 15-22.

[30] Y.-J. Son, M. Horng, M. Copley, J.T. McConville, Optimization of an in vitro dissolution test method for inhalation formulations. Dissolution Technologies 17(2) (2010) 6-13.

[31] General chapter <616>: Bulk density and tapped density,USP32-NF27, Rockville, MD, 2009.

[32] D.A. Edwards, J. Hanes, G. Caponetti, J. Hrkach, A. BenJebria, M.L. Eskew, J. Mintzes, D. Deaver, N. Lotan, R. Langer, Large porous particles for pulmonary drug delivery. Science 276(5320) (1997) 1868-1871.

[33] K. Tomoda, K. Makino, Effects of lung surfactants on rifampicin release rate from monodisperse rifampicin-loaded PLGA microspheres. Colloids and Surfaces B-Biointerfaces 55(1) (2007) 115-124.

[34] A.H.L. Chow, H.H.Y. Tong, P. Chattopadhyay, B.Y. Shekunov, Particle engineering for pulmonary drug delivery. Pharmaceutical Research 24(3) (2007) 411-437.

[35] R. Vehring, Pharmaceutical particle engineering via spray drying. Pharmaceutical Research 25(5) (2008) 999-1022.

[36] T. Kristmundsdottir, O.S. Gudmundsson, K. Ingvarsdottir, Release of diltiazem from Eudragit microparticles prepared by spray-drying. International Journal of Pharmaceutics 137(2) (1996) 159-165.

[37] T.T. Hu, H. Zhao, L.C. Jiang, Y. Le, J.F. Chen, J. Yun, Engineering Pharmaceutical Fine Particles of Budesonide for Dry Powder Inhalation (DPI). Industrial & Engineering Chemistry Research 47(23) (2008) 9623-9627.

[38] H.K. Chan, What is the role of particle morphology in pharmaceutical powder aerosols? Expert Opinion on Drug Delivery 5(8) (2008) 909-914.

[39] H.K. Chan, I. Gonda, Physicochemical characterization of a new respirable form of nedocromil. J. Pharm. Sci. 84(6) (1995) 692-696.

[40] H.K. Chan, Dry powder aerosol drug delivery - Opportunities for colloid and surface scientists. Colloids and Surfaces a-Physicochemical and Engineering Aspects 284 (2006) 50-55.

[41] H. Murakami, M. Kobayashi, H. Takeuchi, Y. Kawashima, Preparation of poly(DL-lactide-co-glycolide) nanoparticles by modified spontaneous emulsification solvent diffusion method. International Journal of Pharmaceutics 187(2) (1999) 143-152.

[42] Y. Kawashima, H. Yamamoto, H. Takeuchi, T. Hino, T. Niwa, Properties of a peptide containing DL-lactide/glycolide copolymer nanospheres prepared by novel emulsion solvent diffusion methods. European Journal of Pharmaceutics and Biopharmaceutics 45(1) (1998) 41-48.

[43] M. Asada, H. Takahashi, H. Okamoto, H. Tanino, K. Danjo, Theophylline particle design using chitosan by the spray drying. International Journal of Pharmaceutics 270(1-2) (2004) 167-174.

[44] S. Jaspart, P. Bertholet, G. Piel, J.M. Dogne, L. Delattre, B. Evrard, Solid lipid microparticles as a sustained release system for pulmonary drug delivery. European Journal of Pharmaceutics and Biopharmaceutics 65(1) (2007) 47-56.

[45] R.S. Pillai, D.B. Yeates, I.F. Miller, A.J. Hickey, Controlled dissolution from wax-coated aerosol particles in canine lungs. Journal of Applied Physiology 84(2) (1998) 717-725.

[46] J.K. Hagerman, S.A. Knechtel, M.E. Klepser, Tobramycin solution for inhalation in cystic fibrosis patients: a review of the literature. Expert Opinion on Pharmacotherapy 8(4) (2007) 467-475.

[47] S.Q. Henwood, W. Liebenberg, L.R. Tiedt, A.P. Lotter, M.M. de Villiers, Characterization of the solubility and dissolution properties of several new rifampicin polymorphs, solvates, and hydrates. Drug Development and Industrial Pharmacy 27(10) (2001) 1017-1030.

[48] S. Agrawal, Y. Ashokraj, P.V. Bharatam, O. Pillai, R. Panchagnula, Solid-state characterization of rifampicin samples and its biopharmaceutic relevance. European Journal of Pharmaceutical Sciences 22(2-3) (2004) 127-144.

Chapter 7: Conclusions and Recommendations

7.1. CONCLUSION

7.1.1. Development of a standardized dissolution test method for inhaled pharmaceutical formulations

A new dissolution testing prototype apparatus for evaluating the *in vitro* dissolution behavior of inhalation formulations has been introduced. The Next Generation Pharmaceutical Impactor (NGI) was modified with polycarbonate (PC) membranes to collect air-classified primary particles prior to dissolution assessment. The dissolution rates of hydrocortisone (HC), a model active pharmaceutical ingredient (API), powders with different particle sizes (0.5-5 μm), were tested using the newly designed dissolution apparatus. From the dissolution study, it was discovered that aerodynamic particle separation had a significant influence on dissolution profiles; the air-classified particles demonstrated at least a three-fold increase in HC dissolution rate than that of non-separated particles over the test period. This result indicates that an inappropriate introduction of test compounds into the dissolution media may produce misleading dissolution results. The performance of inhalers, particularly dry powder inhalers (DPIs), and the aerodynamic properties of test compounds greatly affected the dissolution profiles; homogeneously dispersed HC particles in the lactose carrier showed more consistent dissolution behavior than that of carrier-free bulk HC. This is because that the variations in the amount of powder loaded in the membrane holder, which is generally due to poor aerodynamic properties of formulations, lead to differences in

dissolution/diffusion activity that required to release all of the drug out to the reservoir from the to the membrane holder. Thus, we can conclude that this dissolution method may be used as a quality control study for various dry powder inhalers (DPIs). Specifically, the *in vitro* dissolution profiles of drug may provide an estimate of its dispersion characteristics which directly related to the device or aerosol performances.

7.1.2. Study factors affecting the dissolution behaviors of aerosol products using experimental and mathematical analysis

A novel, easy to use dissolution membrane holder (NGI membrane holder), which was designed specifically to be incorporated into the NGI for better dose collection performance than a previously developed prototype membrane holder, has been introduced. The new NGI membrane holder was easier and more efficient in dose collection than the previous prototype holder since the NGI membrane holder has a larger impaction area for particle collection than the prototype one. Additionally, aerodynamically separated particles can be directly collected on the NGI membrane holder without the modification of NGI with PC membranes. Dissolution procedures, the apparatus, the dose collection, the medium, and test conditions were developed with reference to the USP General Chapter <1092>. Dissolution profiles of two commercially available products, Ventolin® HFA and Pulmicort Flexhaler™, were successfully tested using the optimized *in vitro* dissolution test method. It was found that the most critical factor in dissolution assessment using the NGI membrane holder was the amount of powder loading (thickness of powder bed), and the significance of this factor was shown

to be dependent on the hydrophobicity of the API tested. The dissolution kinetics of drug particles loaded in the NGI membrane holder was analyzed by mathematical simulation. From the mathematical analysis, it was further confirmed that the thick, dense, hydrophobic powder bed created by multiple device actuations, may retard the diffusion of dissolved drug molecule within a powder bed, resulting in retarded drug release from the membrane holder. Three different dissolution media with the same ionic strength and pH, phosphate buffered saline (PBS), phosphate buffer and simulated lung fluid (SLF), were screened to determine a suitable dissolution medium for evaluating a broad range of APIs. The SLF media is found to not be preferable for the routine quality control (QC) study for inhalation products due to its low buffering effect, whereas the PBS and phosphate buffer showed good pH stability whilst providing equivalent dissolution profiles to that of SLF. This dissolution method using the NGI membrane holder has several advantages over other existing methods. The advantages are as follows: i) commercially available USP dissolution apparatus can be incorporated with the membrane holder, thus further validation on the dissolution apparatus is not required, ii) the dissolution behaviors of primary particles that may be delivered to the various target sites of the lung can be evaluated by pre particle separation, iii) a particle separation prior to the dissolution study is easily achieved by aerodynamic separation of formulations using the NGI incorporated with the impaction insert of the NGI membrane holder, iv) several problems associated with poor powder wetting and particle aggregation in the dissolution study can be solved by enclosing the test compound in the NGI membrane

holder, and v) the thin liquid layer in the membrane holder allows the technique to more closely simulate conditions in the lung.

7.1.3. A new respirable form of rifampicin

Rifampicin dihydrate (RFDH) powders with MMAD of 2.2 μm were successfully prepared using a simple recrystallization process. The RFDH powders have a thin flaky structure that provides improved aerosolization properties at maximal API loading. The spray drying process used to prepare the dry powder form of RFDH crystal also contributed to the formation of fluffy powder structure. No excipients or carrier particles were added to improve powder flow or aerodynamic properties, which is ideal for delivering a maximum potency of antibiotics directly to the site of infection, the lung. Moreover, possible drug-excipient interaction can be prevented by removing excipients from the formulation. The maximum FPF_{TD} of the RFDH achieved with a low resistant dry powder inhaler, Aerolizer® device, was 68%. There were no considerable differences in FPF_{TD} and ED for the RFDH formulations between two devices with different device resistance, whereas the spray-dried RF (SP-RF) control formulation, showed significant differences in both FPF_{TD} and ED, indicating that the aerodynamic performances of RFDH is less device dependent than the SP-RF. This is attributed to the relatively low interparticulate forces of flaky RFDH particles, compared to the small spherical SP-RF powders. The RFDH powders are predicted to deposit predominately in the central and peripheral regions of the lung following inhalation, with minimal oropharyngeal deposition. RFDH powders delivered via the pulmonary route are anticipated to provide

higher local (lung) drug concentrations than that of orally delivered powders, since the RF dissolves immediately in low pH media (pH 1.2) (and is rapidly decomposed by hydrolysis in acidic media) but dissolves slowly in neutral conditions. In the dissolution study using the NGI membrane holder method, the RFDH and SP-RF showed 74% and 82% RF release in 1 hour. Additionally, RFDH powders show much better physical and chemical stability than the amorphous SP-RF formulation, which is attributed to the less hygroscopic nature of RFDH powders compared to the SP-RF. From the Dynamic Vapor Sorption (DVS) study, we found that water absorbed from the atmosphere is strongly bound to the SP-RF. The excipient free formulation of the RFDH offers the benefit of delivering a maximum potency formulation of the antibiotic directly to the site of infection, with minimum inspiratory efforts, through the use of a low resistant DPI device.

7.1.4. Preparation of sustained release rifampicin microparticles for inhalation

A novel surface coating method utilizing a multi-channel spray nozzle has been introduced. The three-fluid (3F) nozzle has two separate nozzles for spraying of aqueous solution, and the 3F nozzle was modified by adjusting a position of inner nozzle. The coating performance of two nozzles, a standard 3F nozzle (3F-S) and a modified nozzle (3F-M) were compared. The coated rifampicin dihydrate (RFDH) powders with hydrophobic polymers, PLGA and PLA, were prepared using two different types of 3F nozzles. The coated formulations contained at least 50% w/w of RF. The thin flaky morphology of RFDH powders was not changed by coating with PLA/PLGA polymers.

Overall, the aerodynamic properties of coated RFDH particles were somewhat worsened compared to the RFDH, due to an increased aerodynamic diameter by polymer coating; the MMAD values of coated formulations were in the range of 3.5 to 4.6 μm, whereas the RFDH has a MMAD of 2.2 μm . However, the coated formulations still provide more than 40% of FPF_{TD} without a carrier. The maximum FPF_{TD} was obtained from the powders coated by the 3F-S as 54%, which was higher than that of the powder coated by 3F-M, due to the thinner coating layer.

The coated formulations showed lowered initial RF release followed by a slower RF release after the initial release, compared to the uncoated RFDH crystals. The lowest initial RF release was observed from the coated powders with PLA polymer using the 3F-M nozzle as 32% among other coated formulations. Overall, the formulations coated by the 3F-M nozzle showed lower initial RF release with higher drug loading than the3F-S nozzle. The RF release from the coated RFDH formulation showed pH-dependency; the RF release slowed in an acidic dissolution medium (pH 5.2). The significance of pH-dependent RF dissolution was larger for the coated formulation than for the uncoated RFDH powders, due to the polymer barrier surrounding the core particle. The delivered coated RFDH powders via the pulmonary route is anticipated to provide higher local (lung) drug concentrations with a longer drug residence time in the lung, than that of an uncoated formulation. From the series of studies, we can conclude that the coated RFDH powders deposited in the alveolar region, deliver a first therapeutic dose of RF that is immediately followed by a sustained release from the coated particles. Additionally, parts of coated particles may be phagocytosed by alveoli macrophages (AMs), which is the

main site of *Mycobacterium tuberculosis* (MTB) proliferation, thus targeting AMs and building up high intracellular drug concentrations may be achieved. The coated RFDH powders are predicted to provide much better stability than the amorphous RF or uncoated RFDH crystals, due to their decreased hygroscopicity.

7.2. FUTURE STUDIES

7.2.1. *In vitro-in vivo* correlation (IVIVC) study

There have been several methods to replicate the dissolution behaviors of APIs in the fluids that line the respiratory tracts where drugs are deposited. However, there have been no standardized *in vitro* systems to simulate lung dissolution since the lung has very unique features which are difficult to replicate *in vitro*. The dissolution system we developed has several features that replicate the dissolution of particles in the lung, such as aerodynamic separation prior to dissolution, and the thin liquid layer in the membrane holder. However, our dissolution study has been more focusing on the process optimization and comparison of *in vitro* dissolution profiles between inhaled drug products than the *in vitro-in vivo* correlation (IVIVC). Actually, to date, no IVIVC studies have been completed for inhalation products. Therefore, it may be valuable to do an IVIVC study to explore the potential of the developed dissolution method as an alternative test method of *in vivo* drug absorption study. Specifically, the pharmacokinetic study for budesonide (BD) (PulmicortFlexhaler™) would provide information about the dissolution system that offers the most bio-relevant dissolution

profiles among the methods developed by this group [1], Davies et al. [2], and Arora et al. [3]. All three methods examined the *in vitro* dissolution profiles of air-classified BD powders (either Pulmicort Flexhaler™ or Pulmicort Turbuhaler™), and huge differences in the dissolution profiles were found between the methods; 80% BD dissolution was achieved in about 15 minutes, 1 hour and 6 hours from the study conducted by this group, Davies et al. and Arora et al., respectively. T_{max} of inhaled dry powder BD obtained from several clinical pharmacokinetic studies is in the range of 0.28 to 0.4 hours [4, 5]. From the results, our dissolution system can be predicted to be the most bio-relevant system. However, to verify the estimation, an IVIVC study needs to be conducted.

7.2.2. Development of a novel apparatus for pulmonary dry powder administration to animal lung

In this study, the *in vitro* dissolution behaviors of developed rifampicin (RF) formulations have been intensively studied using a novel dissolution method developed by this group. We believed that the *in vitro* dissolution method has a capability to differentiate formulation types, and perhaps give an estimate of a dissolution behavior *in vivo* since the RF is a class II drug of the Biopharmaceutic Classification System (BCS) where rate and extent of dissolution is critical for optimum bioavailability [6]. However, *in vivo* drug absorption study for the developed RF formulations with animal models hasn't been conducted since there were several technical difficulties in the intra-tracheal administration of dry powder formulations. There have been several devices utilized for delivery of powders into the lung, such as an insufflators and ventilators. These methods,

however, often necessitate surgery to introduce a tube into the trachea. Moreover, currently available powder dispersing devices cannot effectively classify the aerosol particles into the respirable particle size (1-5 μm) range, resulting in the administration of either carrier or API particles that may not be delivered to the lung by actual inspiration. Since the aerodynamic particle separation and particle size has a great influence on the dissolution properties of drugs, inappropriate drug dosing to an animal model would provide a wrong estimation of drug dissolution and absorption *in vivo*. Therefore, the development of new inhalation systems or powder dispersing devices which is able to deliver the respirable size of dry powder aerosols to the animal models, is necessary to achieve successful preclinical study with animal models.

7.2.3. Pharmacokinetic study with animal model of TB

In this study, two different types of RF formulations, immediate release RF (RFDH) and sustained release RFDH (coated RFDH), were developed. The microbial killing effect of the prepared formulations will be evaluated with animal model infected with *Mycobaterium tuberculosis* (MTB). As the microbial killing effect by RF is known to be dose-dependent [7], the appropriate dose range for the RFDH and coated RFDH to effectively kill the MTB or prevent the regrowth of MTB will be explored. Additionally, the combinations of RFDH and coated RFDH formulations will be dosed to the animal model to evaluate whether the administration of immediate release formulation (RFDH) and the sustained release formulation (coated RFDH) have a synergistic effect.

7.3. REFERENCES

[1] D. Arora, K.A. Shah, M.S. Halquist, M. Sakagami, In Vitro Aqueous Fluid-Capacity-Limited Dissolution Testing of Respirable Aerosol Drug Particles Generated from Inhaler Products. Pharmaceutical Research 27(5) (2010) 786-795.

[2] Y.-J. Son, M. Horng, M. Copley, J.T. McConville, Optimization of an in vitro dissolution test method for inhalation formulations. Dissolution Technologies 17(2) (2010) 6-13.

[3] N.M. Davies, M.I.R. Feddah, A novel method for assessing dissolution of aerosol inhaler products. International Journal of Pharmaceutics 255(1-2) (2003) 175-187.

[4] R. Donnelly, J.P. Seale, Clinical pharmacokinetics of inhaled budesonide. Clinical Pharmacokinetics 40(6) (2001) 427-440.

[5] H. Kaiser, D. Aaronson, R. Dockhorn, S. Edsbacker, P. Korenblat, A. Kallen, Dose-proportional pharmacokinetics of budesonide inhaled via Turbuhaler (R). British Journal of Clinical Pharmacology 48(3) (1999) 309-316.

[6] S. Agrawal, Y. Ashokraj, P.V. Bharatam, O. Pillai, R. Panchagnula, Solid-state characterization of rifampicin samples and its biopharmaceutic relevance. European Journal of Pharmaceutical Sciences 22(2-3) (2004) 127-144.

[7] T. Gumbo, A. Louie, M.R. Deziel, W.G. Liu, L.M. Parsons, M. Salfinger, G.L. Drusano, Concentration-dependent Mycobacterium tuberculosis killing and prevention of resistance by rifampin. Antimicrobial Agents and Chemotherapy 51(11) (2007) 3781-3788.

Appendix A: Modeling of Dissolution-Diffusion Controlled Drug Release Kinetics from the NGI Membrane Holder

A.1. DISSOLUTION MODEL

A.1.1. Primary model

Mathematical model for the drug release from planner polymeric matrix systems was applied to estimate the dissolution kinetics of pharmaceutical compounds loaded in the NGI membrane holder [1, 2]. The dissolution kinetics of drug particles loaded in the NGI membrane holder was explained by Noyes-Whitney equation. The diffusion of dissolved drug molecules in the membrane holder was described according to Fick's second law. A primary model for the system containing drug particles assembled on the cross-sectional area of the membrane holder at $x=x_1$ (Figure A.1) was derived. Concentration gradient of drug in two regions of membrane holder, C_I and C_{II}, can be described by the diffusion of dissolved drug in the $0 < x < x_1$ and $x_1 < x < L$ regions, which are coupled by a concentrated drug dissolution source at $x=x_1$. The mass balance equations for the drug release process from the NGI membrane holder are as follows:

$$\frac{\partial}{\partial t} C_{\mathrm{I}}(x,t) - D\frac{\partial^2}{\partial x^2} C_{\mathrm{I}}(x,t) = 0 \qquad \text{(A. 1)}$$

in $0 < x < x_1, t > 0$

$$\frac{\partial}{\partial t} C_{\mathrm{II}}(x,t) - D\frac{\partial^2}{\partial x^2} C_{\mathrm{II}}(x,t) = 0 \qquad \text{(A. 2)}$$

in $x_1 < x < L\ t > 0$

which are subjected to the following boundary and initial conditions:

$$\frac{\partial}{\partial x} C_{\mathrm{I}}(x,t) = 0, at\ x = 0, t > 0 \ \text{(no flux)} \qquad (A.3)$$

$$D\frac{\partial}{\partial x} C_{\mathrm{I}} - D\frac{\partial}{\partial x} C_{\mathrm{II}} = \emptyset_D\,(x,t), at\ x = x_1, t > 0 \qquad (A.4)$$

($\emptyset_{\mathrm{D}}$ is a surface mass source arising from drug dissolution process, which can be described as Noyes-Whitney equation.)

$$D\frac{\partial}{\partial x} C_{\mathrm{II}}(x,t) = J = -P[C_{\mathrm{II}}(x,t) - C_{\mathrm{B}}(t)], at\ x = L\ , t > 0 \qquad (A.5)$$

$$C_{\mathrm{I}}(x,t) = C_{\mathrm{I}}^0(x) \quad for\ t = 0, in\ 0 \le x\ < x_1 \qquad (A.6)$$

$$C_{\mathrm{II}}(x,t) = C_{\mathrm{II}}^0(x) \quad for\ t = 0, in\ x_1 < x\ \le L \qquad (A.7)$$

$$C_{\mathrm{I}}(x,t) = C_{\mathrm{II}}(x,t), at\ x = x_1\ , t > 0 \qquad (A.8)$$

where D is diffusion coefficient of drug, P is the permeability coefficient, J is a flux, C_{I}^0 and C_{II}^0 are initial concentrations of dissolved drug in the $0 < x < x_1$ and $x_1 < x <$ L regions, and C_{B} is the concentration of dissolved drug in the reservoir (dissolution vessel).

The partial differential equations (PDEs) above can be described by a single PDE as follows:

$$\frac{\partial}{\partial t} C(x,t) - D\frac{\partial^2}{\partial x^2} C(x,t) = \delta(x - x_1)\emptyset_{\mathrm{D}}\,(x,t) \qquad (A.9)$$

in $0 < x < L,\ t > 0$

which are subject to following boundary conditions (where δ is the Dirac delta function):

$$\frac{\partial}{\partial x}C(x,t) = 0, at\ x = 0, t > 0 \qquad (A.10)$$

$$D\frac{\partial}{\partial x}C(x,t) = -P[C(x,t) - C_{\mathrm{B}}(t)], at\ x = L\ , t > 0 \qquad (A.11)$$

According to diract delta function, the Eq. A.9 is a function of drug diffusion within the $0 \le x < L$, except $x=x_1$. At $x=x_1$, the A.9 equation can be expressed as a function of both drug dissolution rate and diffusion as follows:

$$\frac{\partial}{\partial t}C(x_1,t) - D\frac{\partial^2}{\partial x^2}C(x_1,t) = \emptyset_{\mathrm{D}}\,(x_1,t), t > 0 \qquad (A.12)$$

($\emptyset_{\mathrm{D}}$ represents the dissolution rate of particles. It can be described as following equation according to Noyes-Whitney equation.)

$$\emptyset_{\mathrm{D}}\,(x_1,t) = K_{\mathrm{D}}S_1a_1(t)[C_{\mathrm{s}} - C(x_1,t)] \qquad (A.13)$$

where K_{D} is the dissolution rate constant of drug, S_{n} is the number of particle at $x=x_{\mathrm{n}}$, a_{n} is the surface area of single drug particles located at the position of $x=x_{\mathrm{n}}$, C_{s} is the saturation solubility of drug in the matrix and $C\,(x_{\mathrm{n}}, \mathrm{t})$ is the concentration of drug at $x=x_{\mathrm{n}}$. It should be noted that $\emptyset_{\mathrm{D}}\,(x_{\mathrm{n}},\mathrm{t})$ exists in time as long as $a_{\mathrm{n}} > 0$, namely, while some drug particles remain undissolved at $x=x_{\mathrm{n}}$. The term of a_1 is a function of time and can be expressed in terms of the mass of said particle, m_1, since the particles are assumed to be spherical and also assumed that the particles maintain their spherical shape while dissolving.

$$\frac{a_1(t)}{a_1^0} = \left(\frac{r_1(t)}{r_1^0}\right)^2 = \left(\left(\frac{\frac{3m_1(t)}{4\pi}}{\frac{3m_1^0}{4\pi}}\right)^{\frac{1}{3}}\right)^2 = \left(\frac{m_1(t)}{m_1^0}\right)^{\frac{2}{3}} \qquad \text{(A. 14)}$$

(Density of particle was assumed to be 1)

where a_1^0 and m_1^0 are the initial values. According to Eq. A.13, the time-dependent m_1 is governed by following dissolution rate equation:

$$\frac{d}{dt}m_1(t) = -K_{\mathrm{D}}a_1(t)[C_{\mathrm{s}} - C(x_1,t)] \quad for\ t > 0 \qquad \text{(A. 15)}$$

From the Eq. A.14 and A.15, time-dependent a_1 equation can be expressed as a following deferential equation:

$$\frac{d}{dt}a_1(t) = -\frac{2K_{\mathrm{D}}\sqrt{(a_1^0)^3}}{3m_1^0}\sqrt{a_1(t)}[C_{\mathrm{S}} - C(x_1,t)] \text{ for } t > 0 \qquad \text{(A. 16)}$$

with following initial conditions:

$a_1(t) = a_1^0$ for $t = 0$

A.1.2. Expanded model for systems containing multiple layers of drug particles

The primary model can be expanded for the systems containing several drug dissolution sources arbitrarily distributed at $x_1, x_2, \ldots x_{\mathrm{n}}$ of membrane holder, as shown in Figure A.1 (B). The Eq. A.9 can be simply expended by summation of the functions for the primary model at x_{n} positions, as follows:

$$\frac{\partial}{\partial t}C(x,t) - D\frac{\partial^2}{\partial x^2}C(x,t) = \sum_1^N \delta(x - x_{\mathrm{n}})K_{\mathrm{D}}S_{\mathrm{n}}a_{\mathrm{n}}(t)\,[C_{\mathrm{s}} - C(x_{\mathrm{n}},t)] \qquad \text{(A. 17)}$$

in $0 < x < L$, $t > 0$, $\delta(x - x_{\mathrm{n}})$ is $+\infty$ at $x = x_{\mathrm{n}}$ and 0 at $x \neq x_{\mathrm{n}}$.

To solve the time-dependent surface area (a_n) function at $x_1, x_2, \ldots x_n$, following equation can be used:

$$\frac{d}{dt}a_{\mathrm{n}}(t) = -\frac{2K_{\mathrm{D}}\sqrt{(a_{\mathrm{n}}^0)^3}}{3m_{\mathrm{n}}^0} \cdot \sqrt{a_{\mathrm{n}}(t)} \cdot [C_{\mathrm{s}} - C(x_{\mathrm{n}}, t)] \qquad (A.18)$$

for n = 1, 2,…, N , t > 0, with $a_1^0, a_2^0, \ldots\ldots a_n^0$ as initial conditions.

A.1.3. Numeric calculation

To simulate the changes in concentration gradient and surface area of loaded drug particles in the progress of drug dissolution within the membrane holder, the Eq. A.17 and A.18 were combined in the form of partial differential equation (PDE) as follows:

$$\frac{\partial}{\partial t}\begin{bmatrix}C(x,t)\\a(x,t)\end{bmatrix} = \frac{\partial}{\partial x}\begin{bmatrix}D\dfrac{\partial}{\partial x}C(x,t)\\0\end{bmatrix} + \begin{bmatrix}K_{\mathrm{D}} \cdot S(x) \cdot a(x,t) \cdot [C_{\mathrm{S}} - C(x,t)]\\-\dfrac{2K_{\mathrm{D}}\sqrt{(a_{\mathrm{n}}^0)^3}}{3m_{\mathrm{n}}^o} \cdot \sqrt{a(x,t)} \cdot [C_{\mathrm{S}} - C(x,t)]\end{bmatrix} \qquad (A.19)$$

which are subjected to the following boundary conditions:

$$\frac{\partial}{\partial x}C(x,t) = O, at\ x = 0$$

$$D\frac{\partial}{\partial x}C(x,t) = -P[C(x,t) - C_{\mathrm{B}}(t)], at\ x = L$$

Since Dirac delta function, $\delta(x - x_{\mathrm{n}})$, is non-zero only at x=x_{n}, the Eq. A.17 can be expressed as following equation:

$$\frac{\partial}{\partial t}C(x,t) - D\frac{\partial^2}{\partial x^2}C(x,t) = K_{\mathrm{D}}S_{\mathrm{n}}a_{\mathrm{n}}(t)[C_{\mathrm{s}} - C(x,t)]\sum_{1}^{N}\delta(x - x_{\mathrm{n}}) \qquad (A.20)$$

In Eq. (A.20), $\sum_1^N \delta\,(x - x_{\mathrm{n}})$ is a "pulse train". As N increases, the density of Dirac delta function within the range ($0 < x < L$) increases, as a result, it approaches a constant value 1 in the range with N being infinity.

Accordingly, the Eq. A.17, when N is sufficiently large, can be approximately described as follows:

$$\frac{\partial}{\partial t}C(x,t) - D\frac{\partial^2}{\partial x^2}C(x,t) = K_{\mathrm{D}}S_{\mathrm{n}}a_{\mathrm{n}}(t)[C_{\mathrm{s}} - C(x,t)] \qquad (\mathrm{A.21})$$

Also, $a_{\mathrm{n}}(t)$ in Eq. A.18 can be substituted with $a(x_{\mathrm{n}}, t)$. As N goes towards infinity, the Eq. A.18 can be re-written with a continuous variable x instead of a discrete variable x_{n}, yielding a following Eq. A.22.

$$\frac{d}{dt}a(x,t) = -\frac{2K_D\sqrt{(a_{\mathrm{n}}^0)^3}}{3m_{\mathrm{n}}^0}\cdot\sqrt{a(x,t)}\cdot[C_{\mathrm{s}} - C(x,t)] \qquad (\mathrm{A.22})$$

Combining Eq. A.21 and Eq. A.22 yields Eq. A.19.

A.2. PARAMETERS AND VARIABLES

Parameter and variables used for mathematical analysis are listed in Table A.1

Diffusion coefficient, D, of drug can be calculated by Stokes-Einstein equation. The Stokes-Einstein equation is a classically theoretical model of the diffusion coefficient based on hydrodynamic theory [3].

$$D = \frac{kT}{6\pi\eta r} \qquad (\mathrm{A.20})$$

where k is Boltzman constant, T is the temperature of solution, r is the molecular radius of budesonide and η is the viscosity of dissolution medium at 37°C. Eq. A.20 is applied to the diffusion process of spherical molecules in non-viscose solution. The r value of drug can be calculated by following equation:

$$M_{\mathrm{w}} = N_{\mathrm{a}}\rho V = N_{\mathrm{a}}\rho \frac{3}{4}\pi r^3 \qquad (\mathrm{A}.21)$$

where M_{w} is a molecular weight of drug, N_{a} is Avogadro's number and ρ is density of drug (assumed as 1).

Permeability coefficient, P, is calculated by following equation [4]:

$$P = \frac{D \cdot K}{h_{\mathrm{M}}} \qquad (\mathrm{A}.22)$$

D is a diffusion coefficient of drug calculated by Stokes-Einstein equation above, K is partition coefficient of drug to polycarbonate (PC) membrane, and h_{M} is the thickness of membrane. K is assumed to be 1, since the PC membrane allows for dissolved drug molecule to free diffusion and no drug absorption on the membrane were observed by experimental analysis.

Surface area of single BD particles, a_{n}^{o}, deposited at x=x_{n} position of the NGI dose-collection plate for dissolution study was given by the formula for the surface area of a sphere, since the particles are assumed to be spherical and the shapes are maintained while dissolution. Particle size of BD varies with the particles deposited on each NGI dose-collection plate. Dose-collection plate cut-off particle sizes calibrated from the NGI are reported to be 4.46, 2.82, 1.66, 0.94, 0.55, 0.34 μm at an inlet flow rate 60 L/min for dose-collection plate stage 2-7, respectively [5, 6]. The geometric particle

size distribution (GSD) of BD particles is assumed to be same as the aerodynamic particle size distribution, since the micronized BD particles are dense spherical structure (density of micronized budesonide was assumed to be 1).

The thickness of matrix containing dispersed particles, L, is estimated based on the number of device actuation and the particle size deposited on the NGI dose-collection plate. It was assumed that every device actuation creates a one particle layer at $x=x_{n,}$ thus L can be calculated by multiplying the number of device actuation by the particle size of budesonide particles deposited on each NGI dose-collection plate.

Number of particles associated to the drug dissolution source at $x=x_{n,}$ $S_{n,}$ can be calculated by dividing the total number of particle loaded on the membrane holder by the number of particle layer, n. The total number of particle loaded on the membrane holder, S, can be calculated by following mass balance equation:

$$S = \frac{m_{total} \cdot \rho}{V_{single}} = \frac{V_{total}}{V_{single}} \qquad (A.23)$$

m_{total} is the total amount of drug loaded on the membrane holder and V_{total} is the total volume of the particle loaded, ρ is a density of drug particle (assumed as 1) and V_{single} is the volume of single drug particle.

Saturation solubility, C_s, of drug in the matrix can be obtained from a solubility study. The saturated solubility of drug in dissolution medium at 37 °C is considered as the C_s, since the sealed membrane holder with PC membrane has a liquid layer consisting of dissolution medium, thus the liquid layer is assumed as the matrix layer of the

membrane holder. Drug concentration in the reservoir ,C_B, can be obtained from the dissolution experiment.

Dissolution rate constant of drug, K_D, can be obtained by means of an iterative process based on solving the Eq. A.18. The K_D of drug particles loaded in the membrane holder is hard to be measured by dissolution assessment since only the amount of drug in the reservoir, which is released amount of drug from the membrane holder by diffusion, can be detected in the dissolution study using the membrane holder. To estimated the K_D value, randomly selected values are plugged into Eq. A.18 until the surface area values obtained by the dissolution assessment (a_{ex}^{f}) and the mathematical calculation using the Eq. A.18 (a_{cal}^{f}) for the surface area of undissolved drug particles in the holder at the last time point of experiment become similar. The parameters for the sample containing single layer of particles assembled at $x=x_n$ are used to estimate K_D value. Obtained K_D value is constant for the drug substance having same particle size distribution.

The surface area value obtained by experiment, a_{ex}^{f} , can be calculated by following equation:

$$a_{ex}^{f} = \frac{4\pi}{S}\left(\frac{3m_r}{4\pi}\right)^{\frac{2}{3}} \qquad (A.24)$$

m_r represents the amount of undissolved drug in the membrane holder after dissolution study.

A.3. TABLES

Table A.1 Parameters and variables used for modeling

Factors	Abbreviation	Unit	Value
Diffusion coefficient (when particles are aligned in monolayer, Figure 4.1(A))	D	cm^2/s	$6.3e^{-6}$
Thickness of membrane	h_M	cm	$6e^{-4}$
Partition coefficient (matrix/membrane)	K	-	1
Permeability coefficient	P	cm/s	$1.01e^{-2}$
Saturation solubility of drug in the matrix	C_s	g/cm^3	16.2
Drug concentration in the reservoir	C_B	g/cm^3	Experiment data
Surface area of single drug particle at $x = x_n$ (as an initial condition)	a_n^0	cm^2/s	Varies with the particle size deposited on each NGI dose-collection plate
Number of particles associated to the drug dissolution source at $x = x_n$	S_n	-	Varies with the amount of drug loaded on the NGI membrane holder
Dissolution rate constant	K_D	cm/s	$6e^{-4}$
Thickness of matrix	L	cm	Varies with both the number of device actuation and the particle size

A.4. FIGURES

Figure A.1 Schematic illustration of different structures of the NGI membrane holder containing aerodynamically classified drug particles to be mathematically described within a framework. Wide line represents impermeable boundary and dashed line represents permeable membrane barrier. (A) Primary system containing drug particle at x_1 position and (B) Matrix system containing drug particles assembled on N cross-sectional areas arbitrarily loaded at x_N positions.

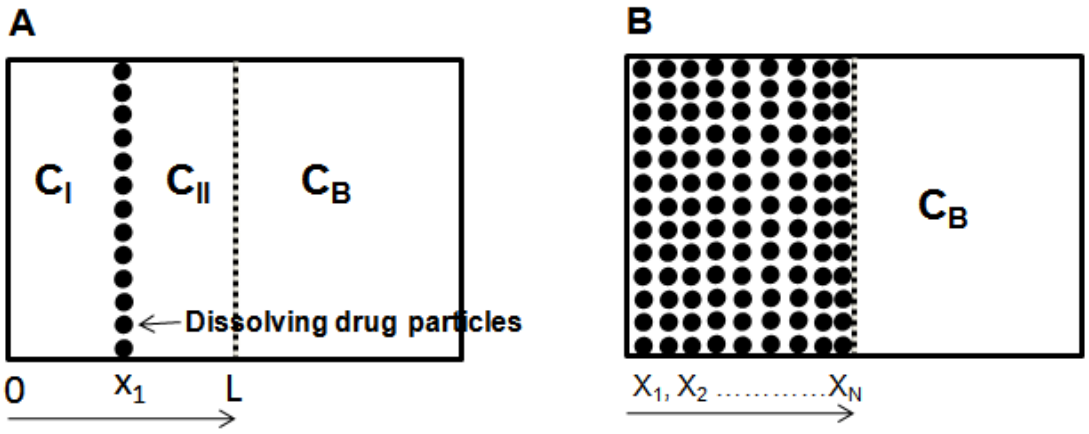

A.5. REFERENCES

[1] R.T. Kurnik, R.O. Potts, Modeling of diffusion and crystal dissolution in controlled release systems. Journal of Controlled Release 45(3) (1997) 257-264.

[2] M.I. Cabrera, J.A. Luna, R.J.A. Grau, Modeling of dissolution-diffusion controlled drug release from planar polymeric systems with finite dissolution rate and arbitrary drug loading. Journal of Membrane Science 280(1-2) (2006) 693-704.

[3] Y.G. Ma, C.Y. Zhu, P.S. Ma, K.T. Yu, Studies on the diffusion coefficients of amino acids in aqueous solutions. Journal of Chemical and Engineering Data 50(4) (2005) 1192-1196.

[4] P.J. Sinko, Martin's physical pharmacy and pharmaceutical sciences : physical chemical and biopharmaceutical principles in the pharmaceutical sciences, Lippincott Williams & Wilkins, Philadelphia 2005.

[5] V.A. Marple, D.L. Roberts, F.J. Romay, N.C. Miller, K.G. Truman, M.J. Holroyd, J.P. Mitchell, D. Hochrainer, Next generation pharmaceutical impactor (A new impactor for pharmaceutical inhaler testing). Part I: Design. Journal of Aerosol Medicine-Deposition Clearance and Effects in the Lung 16(3) (2003) 283-299.

[6] V.A. Marple, B.A. Olson, K. Santhanakrishnan, J.P. Mitchell, S.C. Murray, B.L. Hudson-Curtis, Next generation pharmaceutical impactor (A new impactor for pharmaceutical inhaler testing). Part II: Archival calibration. Journal of Aerosol Medicine-Deposition Clearance and Effects in the Lung 16(3) (2003) 301-324.

Appendix B: Impacts of Drying Conditions on the Physicochemical Properties of Resultant Rifampicin Dihydrate (RFDH) Crystal

B.1. INTRODUCTION

Generally, the drying of recrystallized particles involves heat or vacuum conditions to remove solvents used in the recrystallization process. However, those conditions may not be suitable if the prepared crystal is in the hydrate or solvate form, since desolvation may occur during the drying process [1, 2]. It has been known that desolvation of hydrate form of crystal usually results in the rearrangement of the crystal lattice, generally leading to loss of crystallinity or significant structural change [1, 2]. Beside, the particles for inhaled therapy have very fine particle size (1-5 μm), thus the aggregation of particles in the process of drying often leads to a decrease in aerodynamic performances. In this study, the impacts of various drying conditions on the physicochemical properties and aerodynamic properties of rifampicin dihydrate (RFDH) are studied to find suitable processing methods for the RFDH crystal.

B.2. METHODS

B.2.1. Preparation of rifampicin hydrate using two different drying methods

A dry powder form of rifampicin dihydrate was prepared by two different drying method, spray drying (RFDH-S) and filter drying (RFDH-F). To prepare the rifampicin dihydrate crystal, RF powder (900 mg) was added to the hot anhydrous ethanol solution

(60°C, 30 mL) and stirred until a saturated solution was obtained at room temperature. The suspension was placed into a Branson 5500 sonic bath (Branson ultrasonics, Danbury, CT) and sonicated at 25°C for 2 minutes to homogeneously disperse the particles. The resultant suspension was then spray dried with constant stirring using a Büchi Minispray dryer B-290 (Büchi Laboratory-Techniques, Flawil, Switzerland). The following conditions were used during spray drying: drying airflow, $40m^3/h$; spraying airflow, 500 L/h; suspension feed rate, 5 mL/min; nozzle size, 0.5 mm; the inlet temperature was established at 70 ºC and the outlet temperature was between 40 and 50 ºC. Another RFDH suspension was prepared as above. The prepared suspension was filtered to remove the ethanol and dried in the fume hood for 6 hours.

B.2.2. Desolvation study

The desolvation behavior of RFDH-S was studied. The prepared powder stored in the uncapped amber vial was vacuum dried (25°C/5% RH) in the desiccators for 1 week.

Dynamic vapor sorption (DVS) was also used to investigate the desolvation behavior of RFDH-S. Samples (20 mg) were pre-weighed and added to quartz sample pans which were placed in the sample chamber of a DVS-1 apparatus (Surface Measurement Systems Ltd., London, UK). During this measurement, the RFDH-S powders were exposed to a continuous flow of N_2. The sample was then dried at 0% RH until desolvated form of RFDH (dRFDH) is obtained. The dried samples were analyzed using thermal analysis to confirm the desolvation and the crystalline structure were examined using the XRD.

B.3. Results and Discussion

B.3.1. Impact of drying conditions on the resulting crystal forms

Significant differences in powder properties were observed between RFDH crystals dried by two different methods, spray drying and filtering. As shown in Figure B.1, the RFDH-S powders were very bulky, whereas the RFDH-F was dried in the form of a highly packed sheet. Although the properties of bulk powders were greatly affected by drying conditions, the shape of single RFDH-S and RFDH-F crystals were identical as flaky structures, the result of a polymorphic transformation of RF, (Figure B.2). The spray drying process allows the RFDH crystal to dry without caking or aggregation since the powders can be further deaggregated by atomization involving the break-up of liquid feed into very fine droplets. Conversely, general solvent removing processes, such as filtering, centrifuge and evaporation, involve high pressure or vacuum to remove solvents, leading to strong interparticular adhesion.

A process-induced transformation of RFDH crystal was studied using thermal analysis. The drying conditions have a great influence on the polymorphic forms of the resulting crystals. Particularly, upon heating, the desolvation of the hydrate form of crystal is often reported, resulting in an inevitable change in original crystalline structure [1, 2]. As shown in Figure B.3, the TGA weight losses corresponding to the dehydration of the water of crystallization were similar for the RFDH-S and RFDH-F as 4.24% and 4.25% (w/w), respectively. These TGA results imply that although the the spray drying

process accompanies heat, the RFDH crystals can be dried without desolvation by spray drying due to its' very rapid drying process [3].

Significant changes in the DSC thermogram were observed from the RFDH-F sample; the peak corresponding to the decomposition of RF at 257-260°C was broad and split into two peaks, whereas the RFDH-S samples showed a single peak at 257 °C (Figure B.3). Additionally, the RFDH-F crystal reflected endothermic processes associated with weight loss after desolvation (90-150ºC), which contradicts the results for RFDH-S showing an exothermic peak without weight loss after desolvation (Figure B.3 and B.4). The color change was also found for the RFDH-F sample after drying for 6 hours; the bright orange color of RFDH was changed into a dark orange color (Figure B.1 (B)). These results suggest that the RFDH-F may be the mixture of different polymorphic forms or degradation products, probably due to long exposure time of the filtered RFDH crystal to air with remaining solvents. Polymorphic transformation or chemical degradation may occur by uptake of atmospheric moisture, specifically, the RF is known to be prone to polymorphic transformation or chemical decomposition in the presence of moisture [4, 5].

B.3.2. Desolvation

The impact of desolvation on the physicochemical and aerodynamic properties of the RFDH crystal were studied, since the loss of crystallographically coordinated solvent molecules can induce the solubility, bioavailabiity, dissolution rate and stability of solid state materials [1, 2]. To prepare desolvated forms of RFDH crystal (dRFDH) without

chemical decomposition, the RFDH-S powders were dried under very low humidity conditions (0-5% RH) with either vacuum or continuous N_2 gas purging. The changes in DSC thermogram were observed for both RFDH-S samples dried under different conditions (Figure B.4); the peak corresponding to the desolvation at 90-150°C disappeared, and the peak corresponding to the evaporation of physically absorbed water (30-100°C) increased after desolvation. This result indicates that the dihydrate form of RF can be desolvated at very low humidity conditions, and the dRFDH is more hygroscopic than the RFDH-S, which can be attributed to an increase of the amorphous form of RF in the powder. The structural change was further confirmed by XRD. As shown in B.5, after desolvation, the XRD pattern shifted, with a small halo at the baseline, indicating that the original crystal lattice collapses upon desolvation. Additionally, the desolvation was accerelated by N_2 gas, which is in agreement with previous reports [1, 2]. From the desolvation study, we can deduce that pharmaceutical processing involving heat, vacuum or N_2 gas can cause the desolvation of RFDH crystal, leading to a rearrangement of the crystal lattice.

There was no significant difference in the solubility and dissolution profiles between two samples, the RFDH-S and dRFDH; the saturation solubility values for the RFDH-S and dRFDH sample were 1.24 and 1.28 mg/mL at 37 °C, and the dissolution profiles showed 72 and 74% of RF release in 1 hour for the RFDH-S and dRFDH, respectively (B.6 and B.7). This is because, although the RFDH-S has a crystalline structure, the packing density is low and the surface area of those two powders, RFDH-S and dRFDH, are very similar each other. Additionally, well separated particle status in

the membrane holder may contribute to the subsequent increase in the surface area of drug presented to the media.

As shown in Figure B.8, no significant differences were observed in ED and FPF_{TD} for both samples, since the morphology and particle size of RFDH-S were not changed by desolvation (B.2). In general, the morphology of particles can affect the aerodynamic performance of powders at various levels (molecular, particulate and aerosol) since the different particle shapes lead to a variation in surface energy and interparticulate forces [6-9]. Specifically, at the molecular level, different particle shapes of crystalline materials may have different chemical functional groups on specific faces of the particles, leading to variation in the hygroscopicity and electrostatic interactions. In RFDH-S crystals, the changes in the crystalline lattice structure and hygroscopicity upon desolvation were observed, whereas the shapes of crystal habit (flake-like) were maintained for both RFDH-S and dRFDH. Consequently, the improved aerosolization properties of RFDH-S are primarily attributed to the flaky morphology (crystal habit) of powders rather than the structure of crystal lattice.

B.4. CONCLUSION

Different drying conditions have great influences on the structure of resulting RFDH powders. Spray drying process offers the flaky rifampicin dihydrate (RFDH) crystal to dry without caking or aggregation, and this unique morphology coupled with drying process provides improved aerosolization properties. The desolvated form of

RFDH (dRFDH) was obtained by exposing the powders at very low humidity with either vacuum or N_2 gas. There are no significant differences in physicochemical properties and aerodynamic properties between the hydrated and desolvated forms. However, the dRFDH are predicted to be more easily prone to chemical decomposition associated with humidity than the RFDH-S since the dRFDH is more hygroscopic. Moreover, the degradation products in the bulk powder may lead to poor aerolization properties since the physicochemical properties of degradation products will be significantly different from original crystals. Therefore, the transformation of hydrated form of crystals to desolvated form should be prevented, which always require gentle and careful drying process.

B.5. FIGURES

Figure B.1 Appearances of dried RFDH crystals by (A) spray drying (RFDH-S) and (B) filtering (RFDH-F).

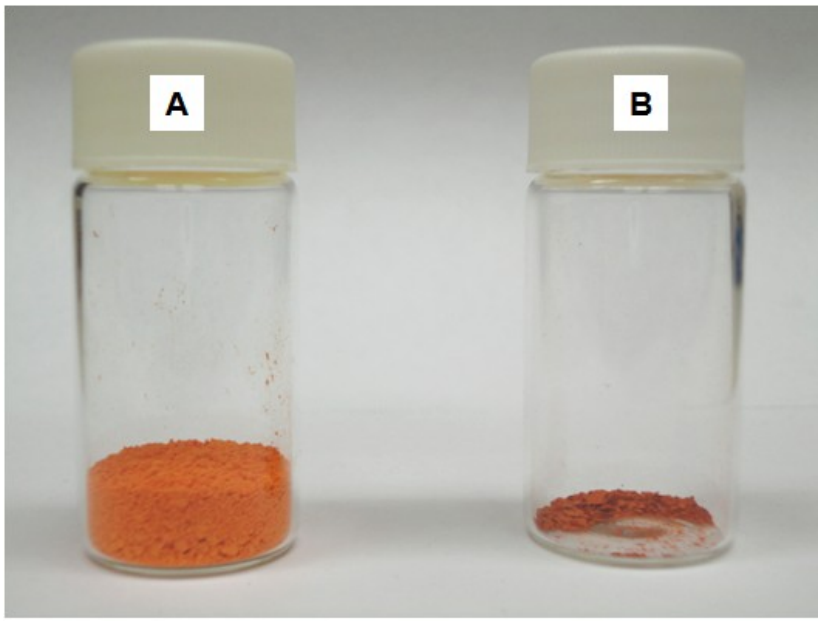

Figure B.2 Scanning electron microscopy images of (A) RFDH-S, (B) dRFDH, (C) RFDH-F and (D) RFDH-F (magnified).

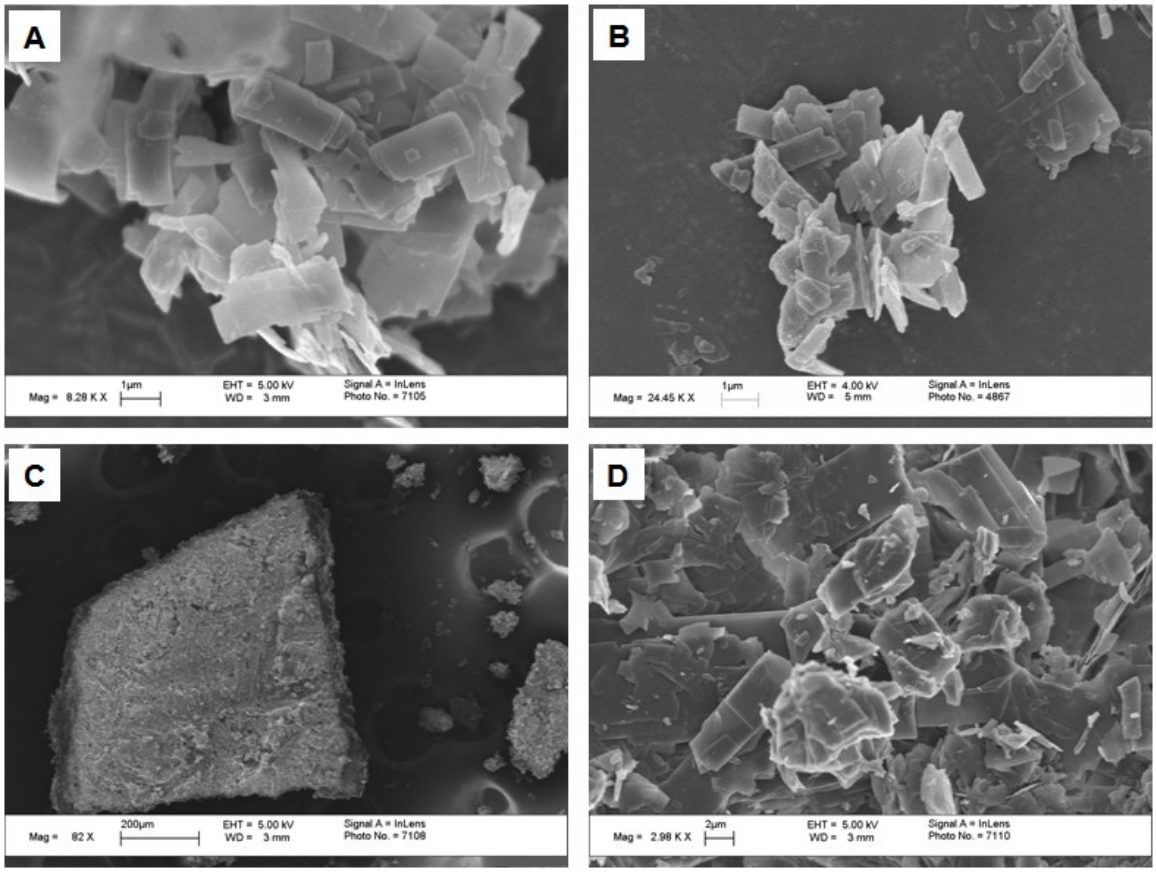

Figure B.3 (A) DSC thermograms of a) RFDH-S and b) RFDH-F, and (B) TGA results for a) RFDH-S, b) RFDH-F and c) dRFDH (DSC and TGA were operated at a heating rate of 10 °C /min from 30 to 350°C).

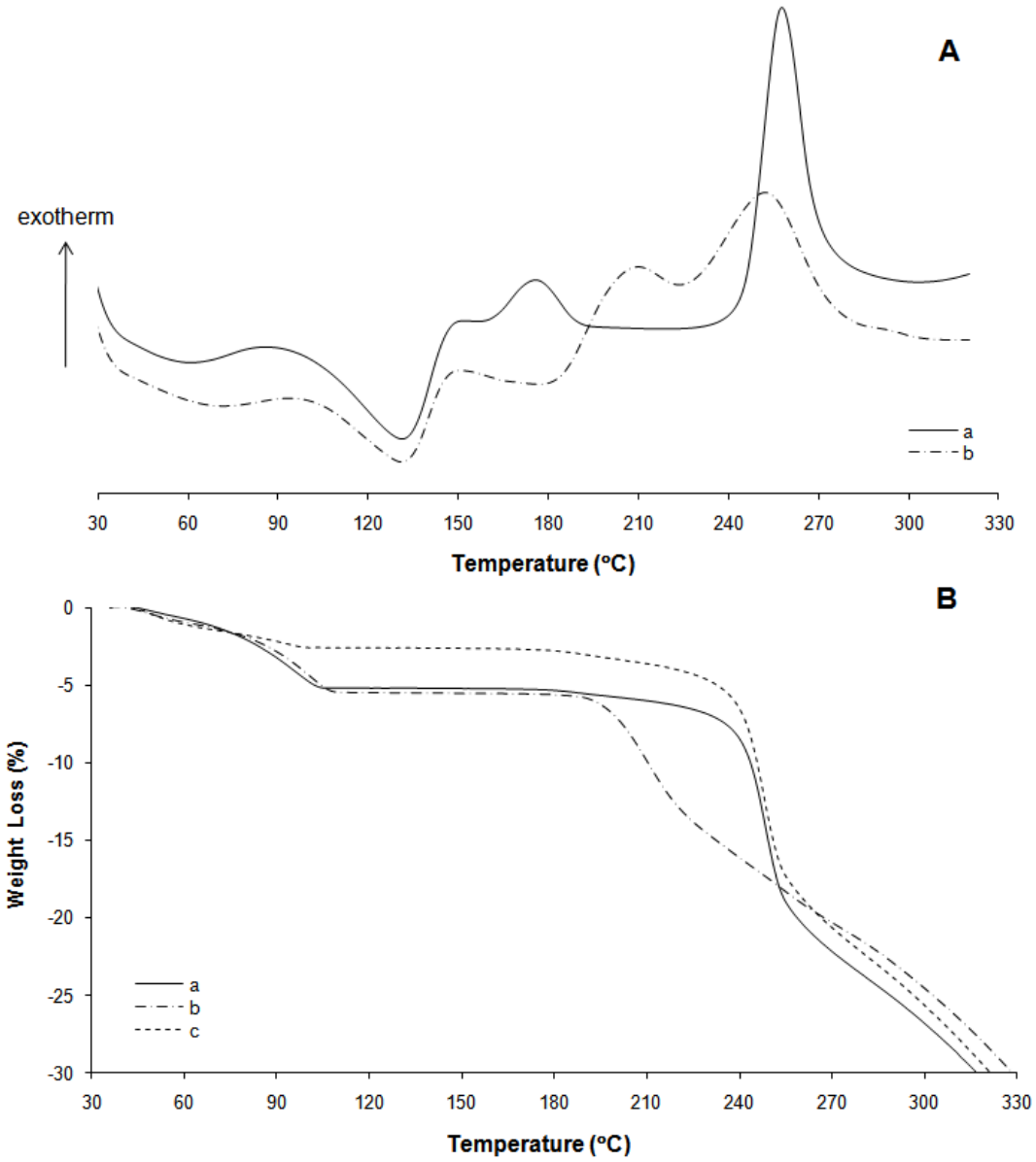

Figure B.4 DSC thermograms of (A) RFDH-S, (B) RFDH-S dried under vacuum for 2 days (RFDH-VC-2D), (C) RFDH-S dried under vacuum for 7 days (RFDH- VC-7D), and (D) desolvated RFDH-S (dRFDH) by drying at 0% RH with continuous N_2 purging for 4000 minuets.

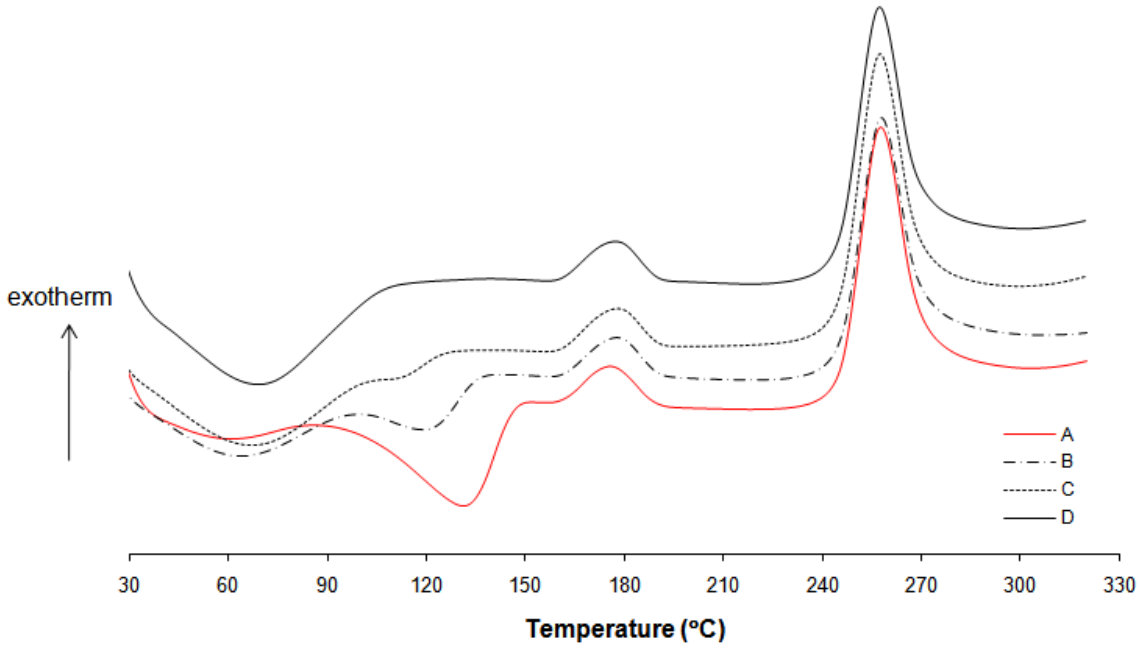

Figure B.5 Powder X-ray diffractograms of (a) RFDH-S and (b) dRFDH.

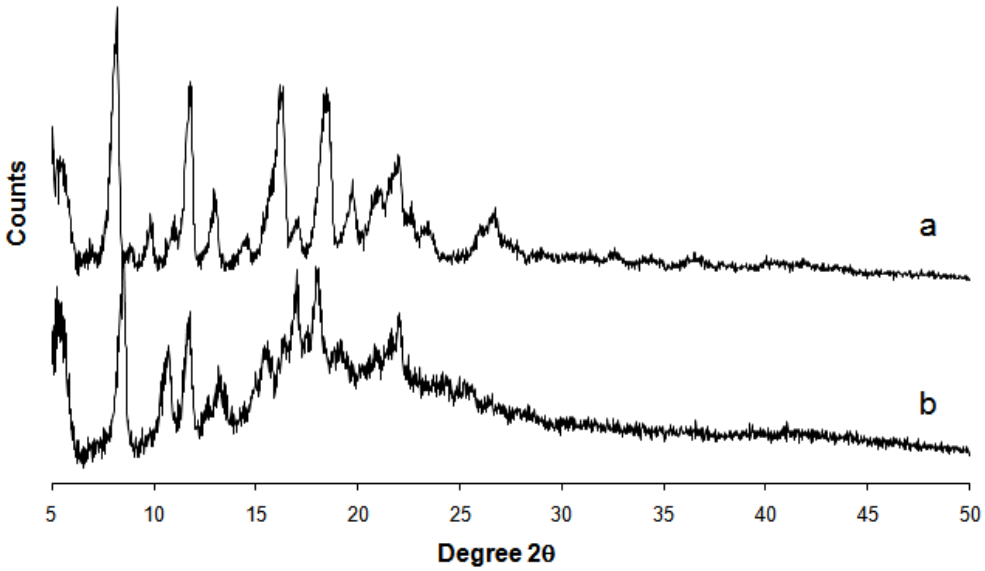

Figure B.6 Saturation solubility of RFDH-S, and dRFDH in PBS containing 0.02% ascorbic acid (pH 7.4) at 37°C for 24 hours.

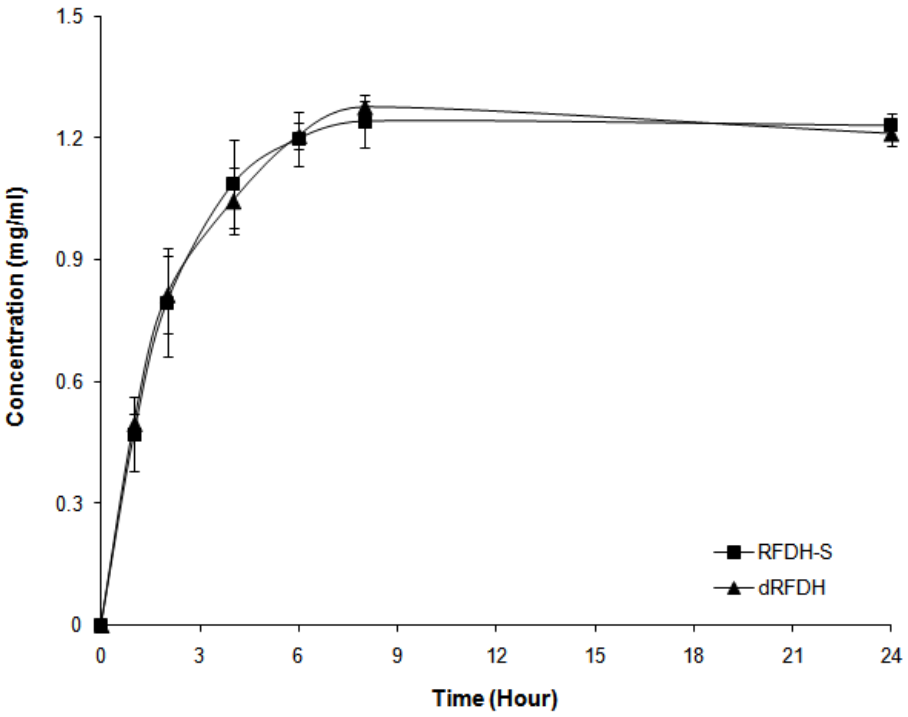

Figure B.7 Release profiles of RFDH-S and dRFDH in PBS containing 0.02% ascorbic acid (pH 7.4). Powders accumulated on the dose-collection plate 3 were selected for dissolution. The error bars indicate the standard deviation of three tests.

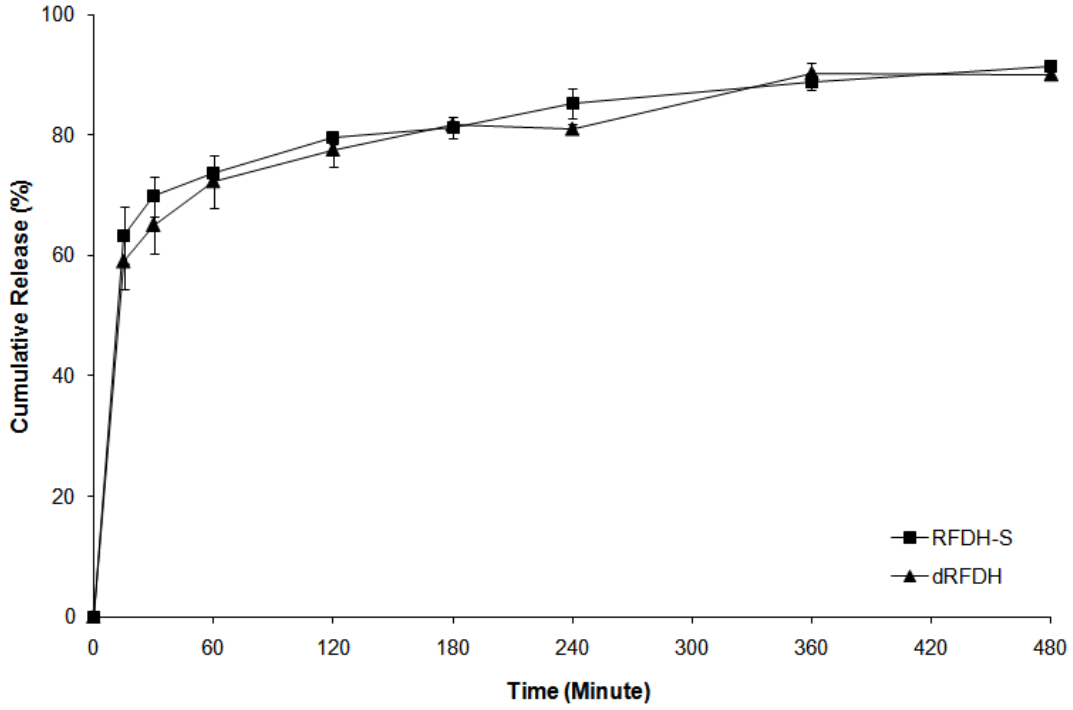

Figure B.8 Powder deposition profiles for the RFDH-S and dRFDH actuated from Aerolizer® inhaler at a flow rate of 60 L/min, expressed as the percentage of total loaded dose. (Values are means ± SD, n = 3)

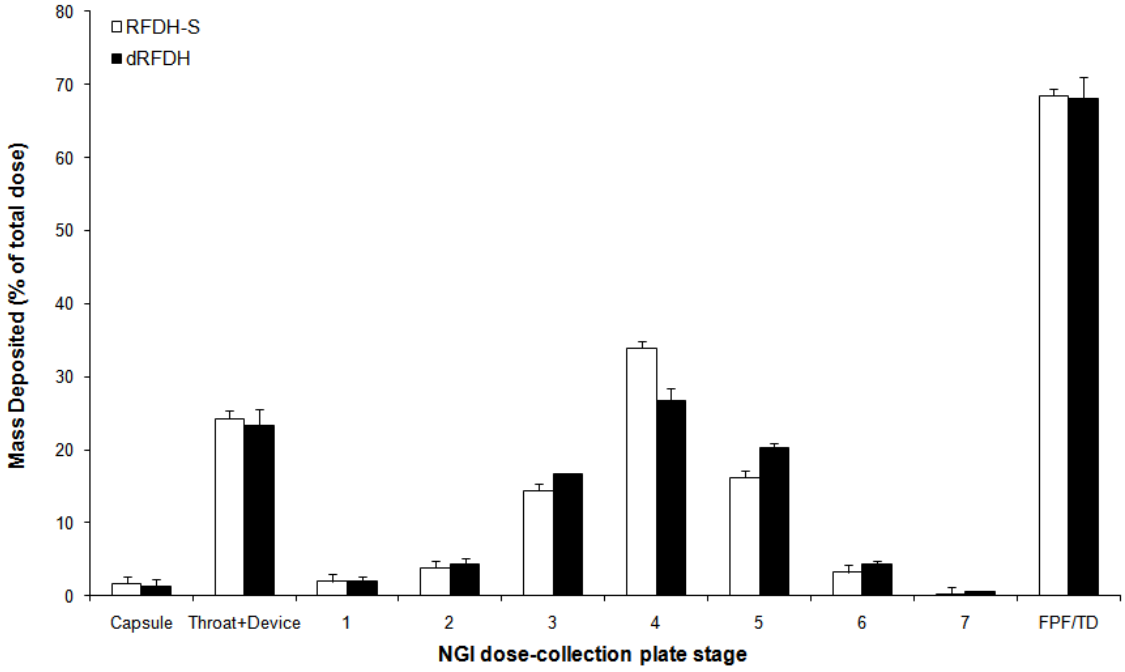

B.6. REFERENCES

[1] H.G. Brittain, Polymorphism in pharmaceutical solids, Informa healthcare, New York, 2009.

[2] R. Hilfiker, Polymorphism in the pharmaceutical industry, Wiley-VCH, Weinheim, 2006.

[3] K. Masters, Spray drying handbook, Longman Scientific & Technical, 1991.

[4] G. Pelizza, M. Nebuloni, P. Ferrari, G.G. Gallo, Polymorphism of rifampicin. Farmaco-Edizione Scientifica 32(7) (1977) 471-481.

[5] H. Bhutani, T.T. Mariappan, S. Singh, The physical and chemical stability of anti-tuberculosis fixed-dose combination products under accelerated climatic conditions. International Journal of Tuberculosis and Lung Disease 8(9) (2004) 1073-1080.

[6] H.K. Chan, Dry powder aerosol drug delivery - Opportunities for colloid and surface scientists. Colloids and Surfaces a-Physicochemical and Engineering Aspects 284 (2006) 50-55.

[7] H.K. Chan, What is the role of particle morphology in pharmaceutical powder aerosols? Expert Opinion on Drug Delivery 5(8) (2008) 909-914.

[8] M.D. Louey, M. Van Oort, A.J. Hickey, Aerosol dispersion of respirable particles in narrow size distributions produced by jet-milling and spray-drying techniques. Pharmaceutical Research 21(7) (2004) 1200-1206.

[9] M.D. Louey, M. Van Oort, A.J. Hickey, Aerosol dispersion of respirable particles in narrow size distributions using drug-alone and lactose-blend formulations. Pharmaceutical Research 21(7) (2004) 1207-1213.

Appendix C: Impacts of Amount of Drug Loading on the Dissolution Profiles of RFDH Crystals

C.1. METHODS

C.1.1. Dissolution study

An impact of amount of drug loading on the dissolution profiles of RFDH was studied by a membrane holder method. The prepared powders (7 mg and 15 mg) were filled into size 3 HPMC capsules, placed into the Aerolizer® device, and actuated into the NGI equipped with a gravimetric sampling cup (MSP Co. Shoreview, MN) including a dissolution impaction insert (Copley Scientific, Nottingham,UK) at a flow rate 60 L/min for 4 seconds. The dissolution impaction insert containing air classified particles was removed from the gravimetric sampling cup, and a pre-soaked polycarbonate membrane was placed onto the top and sealed in place with a push fitted sealing ring. The membrane covered dissolution impaction plate was placed into each dissolution vessel containing 300 mL of PBS containing 0.02% of ascorbic acid.

C.1.2. Scanning electron microscopy (SEM)

RFDH, polymer coated RFDH (C50L-M), and micronized budesonide (BD) (PulmicortFlexhaler®) following particle separation by impingement were observed using a LEO 1530 SEM (Zeiss/LEO, Oberkochen, Germany). The RFDH (7mg) and coated RFDH powders (15 mg) were filled into size 3 HPLC capsule. Each formulation was fired into the NGI fitted with a wax paper at the base of dose-collection plate 3,

which was the stage used for dissolution study. The RFDH and coated RFDH formulations were actuated one time and the PulmicortFlexhaler® device was actuated 10 times to obtain a thick powder bed for each formulation. The wax paper containing separated particles was removed from the NGI and cut into a small segment (suitable for mounting on a pin plate SEM stub). The cut membrane segments from each dose-collection plate were mounted separately onto the stubs using double-sided copper tape, before sputter coating with silver for 40 seconds under vacuum at 30 mTorr.

C.2. Results and Discussion

Overall, there was a no significant difference in the dissolution profiles between test samples loaded 1 and 2.2 mg of RFDH powder, except the values at 15 minute, but variability was greatly affected. As shown in Figure C.1, the test sample loaded 2.2 mg of RFDH shows more variable dissolution profiles than that of the 1mg sample, particularly, the values within 30 minutes, attributed to thicker powder bed leading to an incomplete wetting of powders. However, the release profiles of two different test samples become similar as the dissolution progresses. These results indicate that the diffusion of dissolved RF molecule and the dissolution media in the powder bed is not hindered, although the thicker RFDH powder bed takes more time until all the powders within the bed are completely wet, which is not in agreement with the results found from BD study showing a significant dose-dependency in the dissolution profiles. The difference in the dose-dependent dissolution rate between two APIs is due to the differences in solubility and

packing density of drug particles loaded in the membrane holder. As shown in Figure C.2, the powder bed consisting of air-classified RFDH and coated RFDH particles have much more spaces between particles than that of BD powders since the flake-like RFDH particles are not closely packed, implying that the powder bed consisting of flaky particles is less dense than that of spherical BD. Moreover, the RFDH is much more soluble than BD; the saturation solubility of RFDH and BD at 37°C is 1.28 and 0.016 mg/ml, respectively. Accordingly, more spaces between RFDH particles will be created by dissolving of particles, leading to a faster diffusion of dissolved drug molecule and dissolution media in the powder bed. In other word, the dissolution of flaky structure particles with higher solubility is expected to be less influenced by the amount of drug loading than spherical particles with lower aqueous solubility.

C.3. FIGURES

Figure C.1 Release profiles of RFDH crystals for the test samples loaded 1 mg and 2.2 mg of RFDH powders in PBS containing 0.02% ascorbic acid (pH 7.4). Powders accumulated on the dose-collection plate 3 were selected for dissolution. The error bars indicate the standard deviation of three tests.

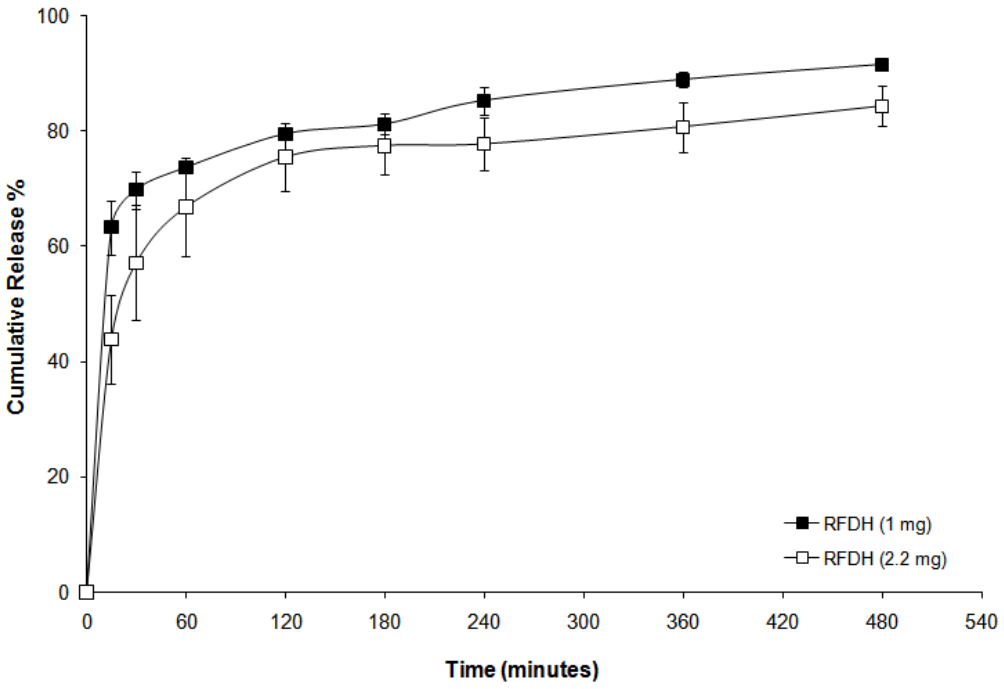

Figure C.2 Scanning electron microscope (SEM) images of aerodynamically separated (A) RFDH, (B) coated RFDH (C50L-M) and (C) BD particles on the NGI dose-collection plate stage 3.

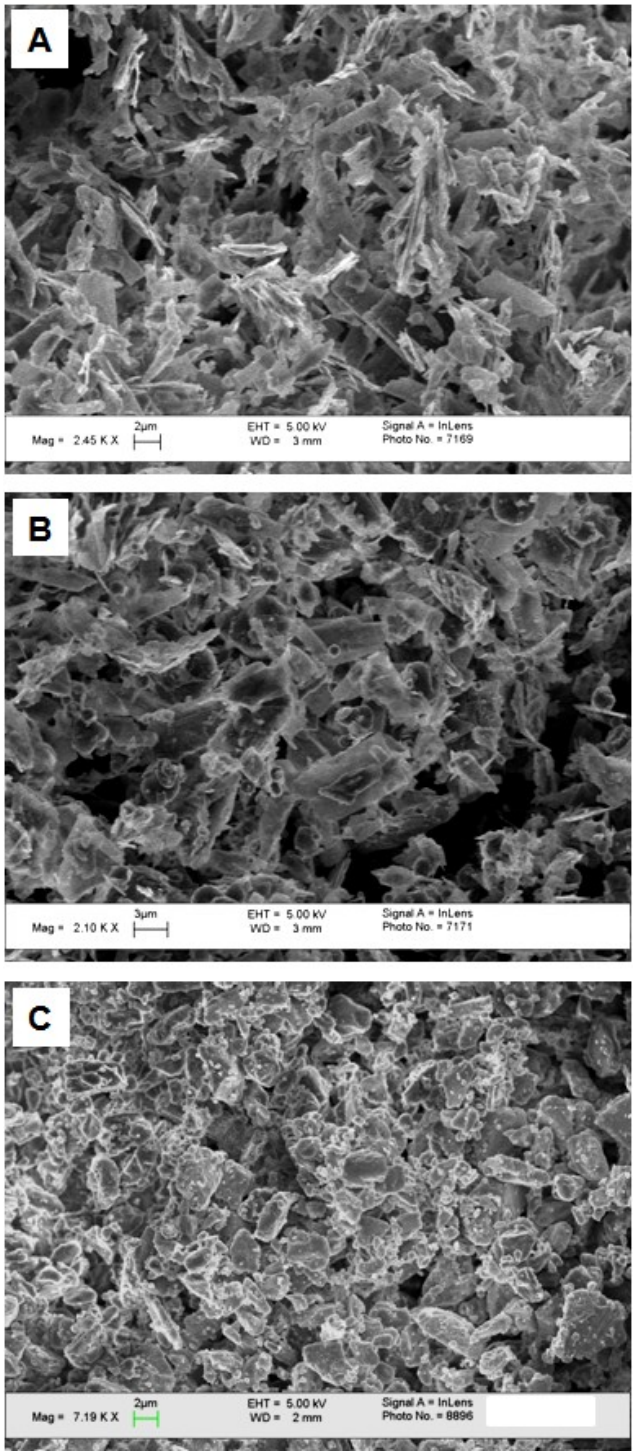

Appendix D: Properties of Lipid Coated RFDH Crystals

D.1. METHODS

D.1.1. Preparation of lipid coated RFDH using a spray dryer equipped with three-fluid (3F) spray nozzle

The RFDH suspension (4% w/v) was prepared by recrystallization of RF in anhydrous ethanol solution. The coating solutions of lipid mixture (0.3% w/v), consisting of cholesterol and distearyl phosphatidylcholine (DSPC) in a ratio of 75: 25, respectively, was prepared by dissolving them in anhydrous ethanol. Two prepared spraying solutions were sprayed separately through two different liquid channels of the three-fluid (3F-S) spray nozzle (Büchi Laboratory-Techniques, Flawil, Switzerland). The RFDH suspension was introduced through the inner nozzle with constant stirring at the feed speed of 1mL/min (40 mg/min). The coating solution was supplied through the outer spray nozzle disposed concentrically about a core nozzle at the feed speed of 8 mL/min, provided 62.5% RFDH loading. The 3F nozzles used in this study had two separate nozzles for aqueous solution and one for gas fluid. The spray drying was performed using a Büchi Minispray dryer B-290 (Büchi Laboratory-Techniques, Flawil, Switzerland) under following conditions for both nozzles: drying airflow, 40 m^3/h; spraying airflow, 600 L/h; the inlet temperature was established at 70°C and the outlet temperature was adjusted between 40 and 50°C.

D.2. RESULTS AND DISCUSSION

Unexpectedly, the dissolution of lipid coated RFDH powders was significantly increased compared to that of uncoated RFDH particles, although lipids, cholesterol and DSPC, used for coating are not aqueous soluble materials (Figure D.1). This is may be due to the water absorbing powder of DSPC surrounding the RFDH particles. This finding suggests that the surface modification with materials have hydrophilic moieties, although the portion of hydrophilic moiety is very small, will increase dissolution rate. The moisture sorption-desorption study further confirmed the hygroscopicity of coated RFDH. As shown in Figure D.2, the coated RFDH powders show higher moisture up-take at 90% RH than the RFDH, although the formulation contains 40% of lipid (30 and 10% of cholesterol and DSPC, respectively). However, overall, the lipid coated powders shows smaller hysteresis between sorption and desorption profiles than RFDH. From the DVS results, we can estimate that the dissolution rate of RFDH powders may be increased, but the chemical degradation of RFDH under ambient storage condition can be minimized by coating with the lipids since the chemical degradation of RF is accelerated by the moisture binding to the molecule. As we seen from the series of data, the DVS study is very useful in evaluating the hygroscopicity as well as the dissolution properties of materials.

D.3. FIGURES

Figure D.1 RF release profiles from RFDH and lipid coated RFDH (C60LP-S) in PBS containing 0.02% ascorbic acid (pH 7.4). Powders accumulated on the dose-collection plate 3 were selected for dissolution. (the error bars indicate the standard deviation of three tests).

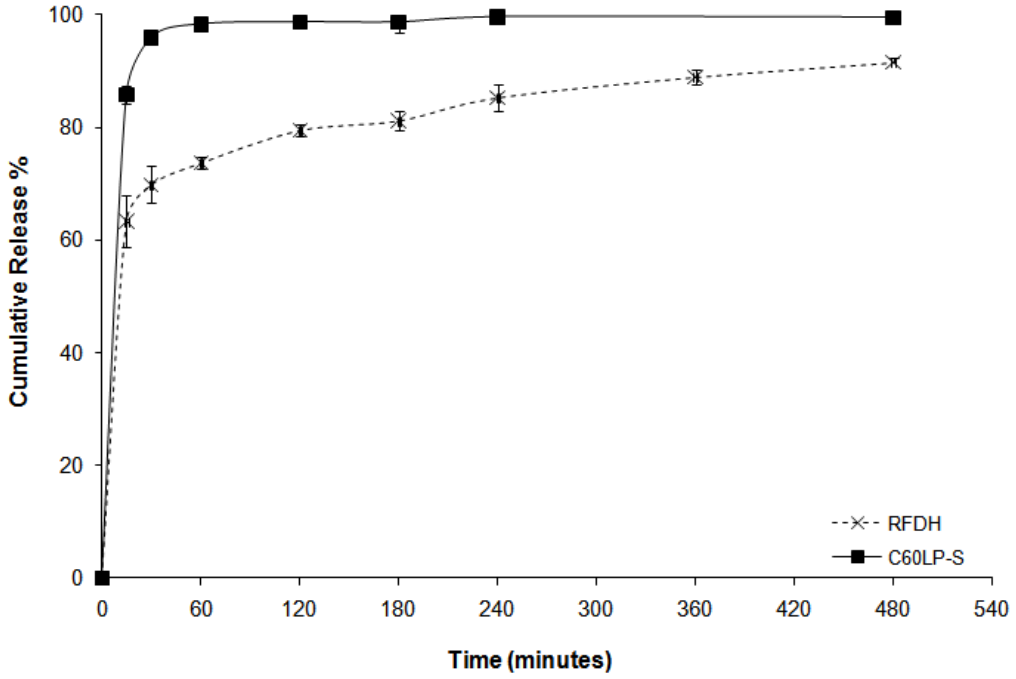

Figure D.2 Dynamic vapor sorption (DVS) isotherm of (A) RFDH, and (B) lipid coated RFDH (C60LP-S) formulation. The absorption is shown as solid lines and desorption as dashed line.

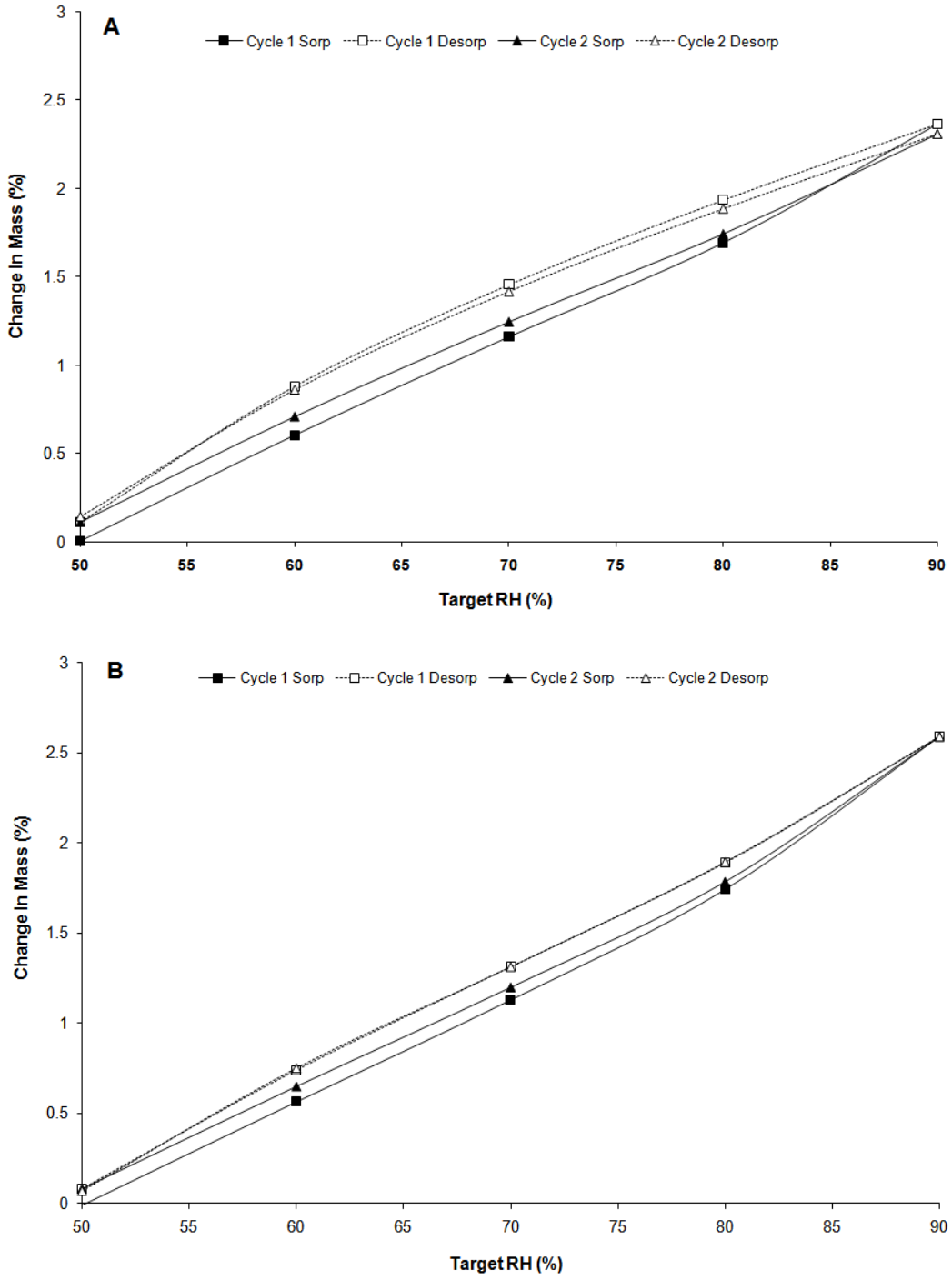

Bibliography

Acerbi, D., G. Brambilla and I. Kottakis, Advances in asthma and COPD management: Delivering CFC-free inhaled therapy using Modulite (R) technology, Pulmonary Pharmacology & Therapeutics 20 (3) (2007) 290-303.

Adi, H., D. Traini, H. K. Chan and P. M. Young, The influence of drug morphology on the aerosolisation efficiency of dry powder inhaler formulations, Journal of Pharmaceutical Sciences 97 (7) (2008) 2780-2788.

Adi, S., H. Adi, P. Tang, D. Traini, H. K. Chan and P. M. Young, Micro-particle corrugation, adhesion and inhalation aerosol efficiency, European Journal of Pharmaceutical Sciences 35 (1-2) (2008) 12-18.

Agrawal, S., Y. Ashokraj, P. V. Bharatam, O. Pillai and R. Panchagnula, Solid-state characterization of rifampicin samples and its biopharmaceutic relevance, European Journal of Pharmaceutical Sciences 22 (2-3) (2004) 127-144.

Ansoborlo, E., R. A. Guilmette, M. D. Hoover, V. Chazel, P. Houpert and M. H. Henge-Napoli, Application of in vitro dissolution tests to different uranium compounds and comparison with in vivo data, Radiation Protection Dosimetry 79 (1-4) (1998) 33-37.

Arora, D., K. A. Shah, M. S. Halquist and M. Sakagami, In Vitro Aqueous Fluid-Capacity-Limited Dissolution Testing of Respirable Aerosol Drug Particles Generated from Inhaler Products, Pharmaceutical Research 27 (5) (2010) 786-795.

Arthanareeswaran, G., P. Thanikaivelan, K. Srinivasn, D. Mohan and M. Rajendran, Synthesis, characterization and thermal studies on cellulose acetate membranes with additive, European Polymer Journal 40 (9) (2004) 2153-2159.

Asada, M., H. Takahashi, H. Okamoto, H. Tanino and K. Danjo, Theophylline particle design using chitosan by the spray drying, International Journal of Pharmaceutics 270 (1-2) (2004) 167-174.

Ashurst, I., Malton Ann, Prime David, Sumby Barry, Latest advances in the development of dry powder inhalers Pharmaceutical Science & Technology Today 3 (2000) 246-256.

Asking, L. and B. Olsson, Calibration at different flow rates of a multistage liquid impinger, Aerosol Science and Technology 27 (1) (1997) 39-49.

Barichello, J. M., H. Handa, M. Kisyuku, T. Shibata, T. Ishida and H. Kiwada, Inducing effect of liposomalization on the transdermal delivery of hydrocortisone: Creation of a drug supersaturated state, Journal of Controlled Release 115 (1) (2006) 94-102.

Barnes, P. J., Drugs for asthma, British Journal of Pharmacology 147 (2006) S297-S303.

Becker, C., J. B. Dressman, H. E. Junginger, S. Kopp, K. K. Midha, V. P. Shah, S. Stavchansky and D. M. Barends, Biowaiver Monographs for Immediate Release Solid Oral Dosage Forms: Rifampicin, Journal of Pharmaceutical Sciences 98 (7) (2009) 2252-2267.

Bhutani, H., T. T. Mariappan and S. Singh, The physical and chemical stability of anti-tuberculosis fixed-dose combination products under accelerated climatic conditions, International Journal of Tuberculosis and Lung Disease 8 (9) (2004) 1073-1080.

Borgstrom, L., E. Derom, E. Stahl, E. WahlinBoll and R. Pauwels, The inhalation device influences lung deposition and bronchodilating effect of terbutaline, American Journal of Respiratory and Critical Care Medicine 153 (5) (1996) 1636-1640.

Brambilla, G., D. Ganderton, R. Garzia, D. Lewis, B. Meakin and P. Ventura, Modulation of aerosol clouds produced by pressurised inhalation aerosols, International Journal of Pharmaceutics 186 (1) (1999) 53-61.

Brittain, H. G., Polymorphism in pharmaceutical solids, Informa healthcare, New York, (2009).

Cabrera, M. I., J. A. Luna and R. J. A. Grau, Modeling of dissolution-diffusion controlled drug release from planar polymeric systems with finite dissolution rate and arbitrary drug loading, Journal of Membrane Science 280 (1-2) (2006) 693-704.

Chan, H. K., Dry powder aerosol drug delivery - Opportunities for colloid and surface scientists, Colloids and Surfaces a-Physicochemical and Engineering Aspects 284 (2006) 50-55.

Chan, H. K., What is the role of particle morphology in pharmaceutical powder aerosols?, Expert Opinion on Drug Delivery 5 (8) (2008) 909-914.

Chan, H. K. and I. Gonda, RESPIRABLE FORM OF CRYSTALS OF CROMOGLYCIC ACID, Journal of Pharmaceutical Sciences 78 (2) (1989) 176-180.

Chan, H. K. and I. Gonda, Physicochemical characterization of a new respirable form of nedocromil., Journal of Pharmaceutical Sciences 84 (6) (1995) 692-696.

Chen, Y. H., J. Yang, A. Mujumdar and R. Dave, Fluidized bed film coating of cohesive Geldart group C powders, Powder Technology 189 (3) (2009) 466-480.

Chew, N. Y. K. and H. K. Chan, Use of solid corrugated particles to enhance powder aerosol performance, Pharmaceutical Research 18 (11) (2001) 1570-1577.

Chew, N. Y. K., H. K. Chan, D. F. Bagster and J. Mukhraiya, Characterization of pharmaceutical powder inhalers: estimation of energy input for powder dispersion and effect of capsule device configuration, Journal of Aerosol Science 33 (7) (2002) 999-1008.

Chew, N. Y. K., P. Tang, H. K. Chan and J. A. Raper, How much particle surface corrugation is sufficient to improve aerosol performance of powders?, Pharmaceutical Research 22 (1) (2005) 148-152.

Chow, A. H. L., H. H. Y. Tong, P. Chattopadhyay and B. Y. Shekunov, Particle engineering for pulmonary drug delivery, Pharmaceutical Research 24 (3) (2007) 411-437.

Christopher, D., P. Curry, B. Doub, K. Furnkranz, M. Lavery, K. Lin, S. Lyapustina, J. Mitchell, B. Rogers, H. Strickland, T. Tougas, Y. Tsong and B. Wyka, Considerations for the development and practice of cascade impaction testing, including a mass balance failure investigation tree, Journal of Aerosol Medicine-Deposition Clearance and Effects in the Lung 16 (3) (2003) 235-247.

Cochrane, M. G., M. V. Bala, K. E. Downs, J. Mauskopf and R. H. Ben-Joseph, Inhaled corticosteroids for asthma therapy - Patient compliance, devices, and inhalation technique, Chest 117 (2) (2000) 542-550.

Cohen-Atiya, M., P. Vadgama and D. Mandler, Preparation, characterization and applications of ultrathin cellulose acetate Langmuir-Blodgett films, Soft Matter 3 (8) (2007) 1053-1063.

Cook, R. O., R. K. Pannu and I. W. Kellaway, Novel sustained release microspheres for pulmonary drug delivery, Journal of Controlled Release 104 (1) (2005) 79-90.

Criee, C. P., T. Meyer, W. Petro, K. Sommerer and P. Zeising, In vitro comparison of two delivery devices for administering formoterol: Foradil (R) P and formoterol ratiopharm single-dose capsule inhaler, Journal of Aerosol Medicine-Deposition Clearance and Effects in the Lung 19 (4) (2006) 466-472.

Dalby, R., M. Spallek and T. Voshaar, A review of the development of Respimat((R)) Soft Mist (TM) Inhaler, International Journal of Pharmaceutics 283 (1-2) (2004) 1-9.

Darbandi, M. A., N. A. Rouholamini, K. Gilani and H. Tajerzadeh, The effect of vehicles on spray drying of rifampicin inhalable microparticles: In vitro and in vivo evaluation, Daru-Journal of Faculty of Pharmacy 16 (3) (2008) 128-135.

Davies, N. M. and M. I. R. Feddah, A novel method for assessing dissolution of aerosol inhaler products, International Journal of Pharmaceutics 255 (1-2) (2003) 175-187.

de Boer, A. H., P. Hagedoorn, D. Gjaltema, J. Goede and H. W. Frijlink, Air classifier technology (ACT) in dry powder inhalation - Part I. Introduction of a novel force distribution concept (FDC) explaining the performance of a basic air classifier on adhesive mixtures, International Journal of Pharmaceutics 260 (2) (2003) 187-200.

Dellamary, L. A., T. E. Tarara, D. J. Smith, C. H. Woelk, A. Adractas, M. L. Costello, H. Gill and J. G. Weers, Hollow porous particles in metered dose inhalers, Pharmaceutical Research 17 (2) (2000) 168-174.

Dolovich, M., New propellant-free technologies under investigation, Journal of Aerosol Medicine-Deposition Clearance and Effects in the Lung 12 (1999) S9-S17.

Donnelly, R. and J. P. Seale, Clinical pharmacokinetics of inhaled budesonide, Clinical Pharmacokinetics 40 (6) (2001) 427-440.

Duddu, S. P., S. A. Sisk, Y. H. Walter, T. E. Tarara, K. R. Trimble, A. R. Clark, M. A. Eldon, R. C. Elton, M. Pickford, P. H. Hirst, S. P. Newman and J. G. Weers, Improved lung delivery from a passive dry powder inhaler using an engineered PulmoSphere (R) powder, Pharmaceutical Research 19 (5) (2002) 689-695.

Edwards, D. A., J. Hanes, G. Caponetti, J. Hrkach, A. BenJebria, M. L. Eskew, J. Mintzes, D. Deaver, N. Lotan and R. Langer, Large porous particles for pulmonary drug delivery, Science 276 (5320) (1997) 1868-1871.

Feddah, M. R., K. F. Brown, E. M. Gipps and N. M. Davies, In-vitro characterisation of metered dose inhaler versus dry powder inhaler glucocorticoid products: Influence of inspiratory flow rates, Journal of Pharmacy and Pharmaceutical Sciences 3 (3) (2000) 317-324.

Ganderton, D., General factors influencing drug delivery to the lung, Respiratory Medicine 91 (1997) 13-16.

General chapter <616>: Bulk density and tapped density, USP32-NF27, Rockville, MD, (2009).

General chapter <1092>: The Dissolution Procedure Development and Validation, USP32-NF27, Rockville, MD, (2009).

Global Tuberculosis Control, 2007, World Health Organization (WHO) Report (2009)

Gondaa, I. and A. F. A. E. Khalikb, On the calculation of aerodynamic diameter of fibers, Aerosol Science and Technology 4 (2) (1985) 233-238.

Grey, V. A., A. J. Hickey, P. Balmer, N. M. Davies, C. Dunbar, T. S. Foster, B. L. Olsson, M. Sakagami, V. P. Shah, M. J. Smurthwaite, J. M. Veranth and K. Zaidi, The Inhalation Ad Hoc Advisory Panel for the USP Performance Tests of Inhalation Dosage Forms, Pharmacopeial Forum 34 (4) (2008) 1068-1074.

Guenette, E., A. Barrett, D. Kraus, R. Brody, L. Harding and G. Magee, Understanding the effect of lactose particle size on the properties of DPI formulations using experimental design, International Journal of Pharmaceutics 380 (1-2) (2009) 80-88.

Guidance for Industry: Dissolution Testing of Immediate Release Solid Oral Dosage Forms, U.S. Department of Health and Human Services, Food and Drug Administration (FDA) (1997)

Gumbo, T., A. Louie, M. R. Deziel, W. G. Liu, L. M. Parsons, M. Salfinger and G. L. Drusano, Concentration-dependent Mycobacterium tuberculosis killing and prevention of resistance by rifampin, Antimicrobial Agents and Chemotherapy 51 (11) (2007) 3781-3788.

Hada, N., T. Hasegawa, H. Takahashi, T. Ishibashi and K. Sugibayashi, Cultured skin loaded with tetracycline HCl and chloramphenicol as dermal delivery system: Mathematical evaluation of the cultured skin containing antibiotics, Journal of Controlled Release 108 (2-3) (2005) 341-350.

Hagerman, J. K., S. A. Knechtel and M. E. Klepser, Tobramycin solution for inhalation in cystic fibrosis patients: a review of the literature, Expert Opinion on Pharmacotherapy 8 (4) (2007) 467-475.

Hardy, J. G. and T. S. Chadwick, Sustained release drug delivery to the lungs - An option for the future, Clinical Pharmacokinetics 39 (1) (2000) 1-4.

Harris, J. A., S. W. Stein and P. B. Myrdal, Evaluation of the TSI aerosol impactor 3306/3321 system using a redesigned impactor stage with solution and suspension metered-dose inhalers, Aaps Pharmscitech 7 (1) (2006) E1-E8.

Hayashi, T., T. Yamazaki, Y. Yamaguchi, K. Sugibayashi and Y. Morimoto, Release kinetics of indomethacin from pressure sensitive adhesive matrices, Journal of Controlled Release 43 (2-3) (1997) 213-221.

Hendeles, L., G. L. Colice and R. J. Meyer, Current concepts - Withdrawal of albuterol inhalers containing chlorofluorocarbon propellants, New England Journal of Medicine 356 (13) (2007) 1344-1351.

Henwood, S. Q., M. M. de Villiers, W. Liebenberg and A. P. Lotter, Solubility and dissolution properties of generic rifampicin raw materials, Drug Development and Industrial Pharmacy 26 (4) (2000) 403-408.

Henwood, S. Q., W. Liebenberg, L. R. Tiedt, A. P. Lotter and M. M. de Villiers, Characterization of the solubility and dissolution properties of several new rifampicin polymorphs, solvates, and hydrates, Drug Development and Industrial Pharmacy 27 (10) (2001) 1017-1030.

Hickey, A. J., H. M. Mansour, M. J. Telko, Z. Xu, H. D. C. Smyth, T. Mulder, R. McLean, J. Langridge and D. Papadopoulos, Physical characterization of component particles included in dry powder inhalers. I. Strategy review and static characteristics, Journal of Pharmaceutical Sciences 96 (5) (2007) 1282-1301.

Higuchi, W. I., Analysis of data on the medicament release from ointments, J. Pharm. Sci. 51 (1962) 802-804.

Hilfiker, R., Polymorphism in the pharmaceutical industry, Wiley-VCH, Weinheim, (2006).

Hirota, K., T. Hasegawa, H. Hinata, F. Ito, H. Inagawa, C. Kochi, G. I. Soma, K. Makino and H. Terada, Optimum conditions for efficient phagocytosis of rifampicin-loaded PLGA microspheres by alveolar macrophages, Journal of Controlled Release 119 (1) (2007) 69-76.

Hu, T. T., H. Zhao, L. C. Jiang, Y. Le, J. F. Chen and J. Yun, Engineering Pharmaceutical Fine Particles of Budesonide for Dry Powder Inhalation (DPI), Industrial & Engineering Chemistry Research 47 (23) (2008) 9623-9627.

Ikegami, K., Y. Kawashima, H. Takeuchi, H. Yamamoto, N. Isshiki, D. Momose and K. Ouchi, Improved inhalation behavior of steroid KSR-592 in vitro with Jethaler (R)

by polymorphic transformation to needle-like crystals (beta-form), Pharmaceutical Research 19 (10) (2002) 1439-1445.

Islam, N., P. Stewart, I. Larson and P. Hartley, Surface roughness contribution to the adhesion force distribution of salmeterol xinafoate on lactose carriers by atomic force microscopy, Journal of Pharmaceutical Sciences 94 (7) (2005) 1500-1511.

Ito, F. and K. Makino, Preparation and properties of monodispersed rifampicin-loaded poly(lactide-co-glycolide) microspheres, Colloids and Surfaces B-Biointerfaces 39 (1-2) (2004) 17-21.

Jaspart, S., P. Bertholet, G. Piel, J. M. Dogne, L. Delattre and B. Evrard, Solid lipid microparticles as a sustained release system for pulmonary drug delivery, European Journal of Pharmaceutics and Biopharmaceutics 65 (1) (2007) 47-56.

Jones, M. D. and R. Price, The influence of fine excipient particles on the performance of carrier-based dry powder inhalation formulations, Pharmaceutical Research 23 (8) (2006) 1665-1674.

Kaiser, H., D. Aaronson, R. Dockhorn, S. Edsbacker, P. Korenblat and A. Kallen, Dose-proportional pharmacokinetics of budesonide inhaled via Turbuhaler (R), British Journal of Clinical Pharmacology 48 (3) (1999) 309-316.

Katsuma, M., H. Kawai and T. Mizumoto, Novel dry powder inhalation for lung-delivery and menufacturing method thereof, US 2004/0184995 (2004)

Kawashima, Y., H. Yamamoto, H. Takeuchi, T. Hino and T. Niwa, Properties of a peptide containing DL-lactide/glycolide copolymer nanospheres prepared by novel emulsion solvent diffusion methods, European Journal of Pharmaceutics and Biopharmaceutics 45 (1) (1998) 41-48.

Kesting, R. E., Synthetic polymeric membranes - A structural perspective, Wiley-Interscience, New York (1985)

Kristmundsdottir, T., O. S. Gudmundsson and K. Ingvarsdottir, Release of diltiazem from Eudragit microparticles prepared by spray-drying, International Journal of Pharmaceutics 137 (2) (1996) 159-165.

Kurnik, R. T. and R. O. Potts, Modeling of diffusion and crystal dissolution in controlled release systems, Journal of Controlled Release 45 (3) (1997) 257-264.

Kwon, M. J., J. H. Bae, J. J. Kim, K. Na and E. S. Lee, Long acting porous microparticle for pulmonary protein delivery, International Journal of Pharmaceutics 333 (1-2) (2007) 5-9.

Kwona, M. J., J. H. Baea, J. J. Kima, K. Nab and E. S. Lee, Long acting porous microparticle for pulmonary protein delivery, International Journal of Pharmaceutics 333 (1-2) (2007) 5-9.

Labiris, N. R. and M. B. Dolovich, Pulmonary drug delivery. Part I: Physiological factors affecting therapeutic effectiveness of aerosolized medications, British Journal of Clinical Pharmacology 56 (6) (2003) 588-599.

Labiris, N. R. and M. B. Dolovich, Pulmonary drug delivery. Part II: The role of inhalant delivery devices and drug formulations in therapeutic effectiveness of aerosolized medications, British Journal of Clinical Pharmacology 56 (6) (2003) 600-612.

Lasic, D. D., Liposomes in gene delivery, CRC Press, Boca Raton, FL, (1997).

Leach, C. L., P. J. Davidson and R. J. Boudreau, Improved airway targeting with the CFC-free HFA-beclomethasone metered-dose inhaler compared with CFC-beclomethasone, European Respiratory Journal 12 (6) (1998) 1346-1353.

Learoyd, T. P., J. L. Burrows, E. French and P. C. Seville, Chitosan-based spray-dried respirable powders for sustained delivery of terbutaline sulfate, European Journal of Pharmaceutics and Biopharmaceutics 68 (2) (2008) 224-234.

Lewis, D., Metered-dose inhalers: actuators old and new, Expert Opinion on Drug Delivery 4 (3) (2007) 235-245.

Louey, M. D., M. Van Oort and A. J. Hickey, Aerosol dispersion of respirable particles in narrow size distributions produced by jet-milling and spray-drying techniques, Pharmaceutical Research 21 (7) (2004) 1200-1206.

Louey, M. D., M. Van Oort and A. J. Hickey, Aerosol dispersion of respirable particles in narrow size distributions using drug-alone and lactose-blend formulations, Pharmaceutical Research 21 (7) (2004) 1207-1213.

Ma, Y. G., C. Y. Zhu, P. S. Ma and K. T. Yu, Studies on the diffusion coefficients of amino acids in aqueous solutions, Journal of Chemical and Engineering Data 50 (4) (2005) 1192-1196.

Marple, V. A. and B. Y. H. Liu, Characteristics of laminar jet impactors, Environmental Science & Technology 8 (7) (1974) 648-654.

Marple, V. A., B. A. Olson and N. C. Miller, A low-loss cascade impactor with stage collection cups- calibration and pharmaceutical inhaler applications, Aerosol Science and Technology 22 (1) (1995) 124-134.

Marple, V. A., B. A. Olson, K. Santhanakrishnan, J. P. Mitchell, S. C. Murray and B. L. Hudson-Curtis, Next generation pharmaceutical impactor (A new impactor for pharmaceutical inhaler testing). Part II: Archival calibration, Journal of Aerosol Medicine-Deposition Clearance and Effects in the Lung 16 (3) (2003) 301-324.

Marple, V. A., D. L. Roberts, F. J. Romay, N. C. Miller, K. G. Truman, M. J. Holroyd, J. P. Mitchell and D. Hochrainer, Next generation pharmaceutical impactor (A new impactor for pharmaceutical inhaler testing). Part I: Design, Journal of Aerosol Medicine-Deposition Clearance and Effects in the Lung 16 (3) (2003) 283-299.

Marre, S. and J. Palmeri, Theoretical study of aerosol filtration by nucleopore filters: The intermediate crossover regime of Brownian diffusion and direct interception, Journal of Colloid and Interface Science 237 (2) (2001) 230-238.

Masters, K., Spray drying handbook, Longman Scientific & Technical, (1991).

McConville, J. T., N. Patel, N. Ditchburn, M. J. Tobyn, J. N. Staniforth and P. Woodcock, Use of a novel modified TSI for the evaluation of controlled-release aerosol formulations. I, Drug Development and Industrial Pharmacy 26 (11) (2000) 1191-1198.

McDonald, K. J. and G. P. Martin, Transition to CFC-free metered dose inhalers - into the new millennium, International Journal of Pharmaceutics 201 (1) (2000) 89-107.

Mitchell, J. P. and R. N. Dalby, Characterization of Aerosol Performance. Chapter 5 in Pulmonary Drug Delivery – Basics, Applications and Opportunities for Small Molecules and Bio-Pharmaceuticals, Editio Cantor Verlag, Lüssen, K. B.-P. a. H., Aulendorf, Germany, , (2006).

Mizoe, T., T. Ozeki and H. Okada, Application of a Four-fluid Nozzle Spray Drier to Prepare Inhalable Rifampicin-containing Mannitol Microparticles, Aaps Pharmscitech 9 (3) (2008) 755-761.

Molina, M. J., Rowland, F.S., Stratospheric risk for chlorofluoromethanes: chlorine atom-catalysed destruction of ozone, Nature 249 (1974) 810-812.

Moss, O. R., Simulants of lung interstitial fluid, Health Phys. 36 (1979) 447-448.

Muchmore, D. B., B. Silverman, A. de la Pena and J. Tobian, The AIR (R) Inhaled Insulin System: System components and pharmacokinetic/glucodynamic data, Diabetes Technology & Therapeutics 9 (2007) S41-S47.

Murakami, H., M. Kobayashi, H. Takeuchi and Y. Kawashima, Preparation of poly(DL-lactide-co-glycolide) nanoparticles by modified spontaneous emulsification solvent diffusion method, International Journal of Pharmaceutics 187 (2) (1999) 143-152.

Muttil, P., J. Kaur, K. Kumar, A. B. Yadav, R. Sharma and A. Misra, Inhalable microparticles containing large payload of anti-tuberculosis drugs, European Journal of Pharmaceutical Sciences 32 (2007) 140-150.

Muttil, P., J. Kaur, K. Kumar, A. B. Yadav, R. Sharma and A. Misra, Inhalable microparticles containing large payload of anti-tuberculosis drugs, European Journal of Pharmaceutical Sciences 32 (2) (2007) 140-150.

Nancy A. Dennis, H. Mark Blauser and J. E. Kent, Dissolution fractions and half-times of single sorce yellowcake in simulated lung fluids, Health Phys. 42 (4) (1982) 469-477.

Newhouse, M. T., P. H. Hirst, S. P. Duddu, Y. H. Walter, T. E. Tarara, A. R. Clark and J. G. Weers, Inhalation of a dry powder tobramycin PulmoSphere formulation in healthy volunteers, Chest 124 (1) (2003) 360-366.

Newman, S. P. and S. W. Clarke, BRONCHODILATOR DELIVERY FROM GENTLEHALER, A NEW LOW-VELOCITY PRESSURIZED AEROSOL INHALER, Chest 103 (5) (1993) 1442-1446.

Nichols, S. C., D. R. Brown and M. Smurthwaite, New concept for the variable flow rate Andersen cascade impactor and calibration data, Journal of Aerosol Medicine-Deposition Clearance and Effects in the Lung 11 (1998) S133-S138.

O'Hara, P. and A. J. Hickey, Respirable PLGA microspheres containing rifampicin for the treatment of tuberculosis: Manufacture and characterization, Pharmaceutical Research 17 (8) (2000) 955-961.

Oenbrink, R. J., Unexpected adverse effects of Freon 11 and Freon 12 as medication propellants in: (Ed.)^(Eds.), Journal of the American Osteopathic Association, Vol. 93, 1993, p.^pp. 714-718.

Olson, B. A., V. A. Marple, J. P. Mitchell and M. W. Nagel, Development and calibration of a low-flow version of the Marple-Miller impactor (MMI (TM)), Aerosol Science and Technology 29 (4) (1998) 307-314.

Onoshita, T., Y. Shimizu, N. Yamaya, M. Miyazaki, M. Yokoyama, N. Fujiwara, T. Nakajima, K. Makino, H. Terada and M. Haga, The behavior of PLGA microspheres containing rifampicin in alveolar macrophages, Colloids and Surfaces B-Biointerfaces 76 (1) 151-157.

Onoshita, T., Y. Shimizu, N. Yamaya, M. Miyazaki, M. Yokoyama, N. Fujiwara, T. Nakajima, K. Makino, H. Terada and M. Haga, The behavior of PLGA microspheres containing rifampicin in alveolar macrophages, Colloids and Surfaces B-Biointerfaces 76 (1) (2010) 151-157.

Panchagnula, R., S. Agrawal, Y. Ashokraj, M. Varma, K. Sateesh, V. Bhardwaj, S. Bedi, L. Gulati, J. Parmar, C. L. Kaul, B. Blomberg, B. Fourie, G. Roscigno, R. Wire, R. Laing, P. Evans and T. Moore, Fixed dose combinations for tuberculosis: Lessons learned from clinical, formulation and regulatory perspective, Methods and Findings in Experimental and Clinical Pharmacology 26 (9) (2004) 703-721.

Panchagnula, R. and V. Bhardwaj, Effect of amorphous content on dissolution characteristics of rifampicin, Drug Development and Industrial Pharmacy 34 (6) (2008) 642-649.

Pandey, R. and G. K. Khuller, Antitubercular inhaled therapy: opportunities, progress and challenges, Journal of Antimicrobial Chemotherapy 55 (4) (2005) 430-435.

Patton, J. S., Mechanisms of macromolecule absorption by the lungs, Advanced Drug Delivery Reviews 19 (1) (1996) 3-36.

Patton, J. S., Deep-lung delivery of therapeutic proteins, Chemtech 27 (12) (1997) 34-38.

Patton, J. S., J. Bukar and S. Nagarajan, Inhaled insulin, Advanced Drug Delivery Reviews 35 (2-3) (1999) 235-247.

Peart, J., Magyar, C., Byron, P.R. , Aerosol electrostatics—metered dose inhalers (MDIs): Reformulation and device design issues, Proceedings of Respiratory Drug Delivery VI, South Carolina (1998) 227-233.

Pelizza, G., M. Nebuloni, P. Ferrari and G. G. Gallo, Polymorphism of rifampicin, Farmaco-Edizione Scientifica 32 (7) (1977) 471-481.

Pethe, K., D. L. Swenson, S. Alonso, J. Anderson, C. Wang and D. G. Russell, Isolation of Mycobacterium tuberculosis mutants defective in the arrest of phagosome maturation, Proceedings of the National Academy of Sciences of the United States of America 101 (37) (2004) 13642-13647.

Pham, S. and T. S. Wiedmann, Dissolution of aerosol particles of budesonide in Survanta (TM), a model lung surfactant, Journal of Pharmaceutical Sciences 90 (1) (2001) 98-104.

Pillai, G., P. B. Fourie, N. Padayatchi, P. C. Onyebujoh, H. McIlleron, P. J. Smith and G. Gabriels, Recent bioequivalence studies on fixed-dose combination anti-tuberculosis drug formulations available on the global market, International Journal of Tuberculosis and Lung Disease 3 (11) (1999) S309-S316.

Pillai, R. S., D. B. Yeates, I. F. Miller and A. J. Hickey, Controlled dissolution from wax-coated aerosol particles in canine lungs, Journal of Applied Physiology 84 (2) (1998) 717-725.

Prime, D., P. J. Atkins, A. Slater and B. Sumby, Review of dry powder inhalers, Advanced Drug Delivery Reviews 26 (1) (1997) 51-58.

Raula, J., A. Laehde and E. I. Kauppinen, A novel gas phase method for the combined synthesis and coating of pharmaceutical particles, Pharmaceutical Research 25 (1) (2008) 242-245.

Raula, J., F. Thielmann, J. Kansikas, S. Hietala, M. Annala, J. Seppala, A. Lahde and E. I. Kauppinen, Investigations on the humidity-induced transformations of salbutamol sulphate particles coated with L-leucine, Pharmaceutical Research 25 (10) (2008) 2250-2261.

Rifampin, Tuberculosis 88 (2) (2008) 151-154.

Rzepka, S. and B. Neidhart, Transport processes through track-etch membrane filters in a reagent delivery cell, Fresenius Journal of Analytical Chemistry 366 (4) (2000) 336-340.

Saint-Lorant, G., P. Leterme, A. Gayot and M. P. Flament, Influence of carrier on the performance of dry powder inhalers, International Journal of Pharmaceutics 334 (1-2) (2007) 85-91.

Salama, R., S. Hoe, H. K. Chan, D. Traini and P. M. Young, Preparation and characterisation of controlled release co-spray dried drug-polymer microparticles for inhalation 1: Influence of polymer concentration on physical and in vitro

characteristics, European Journal of Pharmaceutics and Biopharmaceutics 69 (2) (2008) 486-495.

Salama, R., D. Traini, H.-K. Chan and P. M. Young, Recent advances in controlled release pulmonary therapy, Current Drug Delivery 6 (2009) 404-414.

Salama, R. O., D. Traini, H. K. Chan and P. M. Young, Preparation and characterisation of controlled release co-spray dried drug-polymer microparticles for inhalation 2: Evaluation of in vitro release profiling methodologies for controlled release respiratory aerosols, European Journal of Pharmaceutics and Biopharmaceutics 70 (1) (2008) 145-152.

Sankar, R., N. Sharda and S. Singh, Behavior of decomposition of rifampicin in the presence of isoniazid in the pH range 1-3, Drug Development and Industrial Pharmacy 29 (7) (2003) 733-738.

Sarinas, P. S. A., T. E. Robinson, A. R. Clark, J. Canfield, R. K. Chitkara and R. B. Fick, Inspiratory flow rate and dynamic lung function in cystic fibrosis and chronic obstructive lung diseases, Chest 114 (4) (1998) 988-992.

Schreiber, J., G. Zissel, U. Greinert, M. Schlaak and J. Muller-Quernheim, Lymphocyte transformation test for the evaluation of adverse effects of antituberculous drugs, Eur J Med Res 4 (2) (1999) 67-71.

Sdraulig, S., R. Franich, R. A. Tinker, S. Solomon, R. O'Brien and P. N. Johnston, In vitro dissolution studies of uranium bearing material in simulated lung fluid, Journal of Environmental Radioactivity 99 (3) (2008) 527-538.

Sharma, R., D. Saxena, A. K. Dwivedi and A. Misra, Inhalable microparticles containing drug combinations to target alveolar macrophages for treatment of pulmonary tuberculosis, Pharmaceutical Research 18 (10) (2001) 1405-1410.

Shishoo, C. J., S. A. Shah, I. S. Rathod, S. S. Savale, J. S. Kotecha and P. B. Shah, Stability of rifampicin in dissolution medium in presence of isoniazid, International Journal of Pharmaceutics 190 (1) (1999) 109-123.

Shishoo, C. J., S. A. Shah, I. S. Rathod, S. S. Savale and M. J. Vora, Impaired bioavailability of rifampicin in presence of isoniazid from fixed dose combination (FDC) formulation, International Journal of Pharmaceutics 228 (1-2) (2001) 53-67.

Singh, S., T. T. Mariappan, R. Sankar, N. Sarda and B. Singh, A critical review of the probable reasons for the poor/variable bioavailability of rifampicin from anti-

tubercular fixed-dose combination (FDC) products, and the likely solutions to the problem, International Journal of Pharmaceutics 228 (1-2) (2001) 5-17.

Smith, I. J. and M. Parry-Billings, The inhalers of the future? A review of dry powder devices on the market today, Pulmonary Pharmacology & Therapeutics 16 (2) (2003) 79-95.

Smyth, H. D. C., Hickey, A.J., Carriers in Drug Powder Delivery: Implications for Inhalation System Design, American Journal of Drug Delivery 3 (2005) 117-132.

Son, Y.-J., M. Horng, M. Copley and J. T. McConville, Optimization of an in vitro dissolution test method for inhalation formulations, Dissolution Technologies 17 (2) (2010) 6-13.

Son, Y.-J. and J. T. McConville, Development of a standardized dissolution test method for inhaled pharmaceutical formulations, International Journal of Pharmaceutics 382 (1-2) (2009) 15-22.

Son, Y.-J. and J. T. McConville, A new respirable form of Rifampicin, European Journal of Pharmaceutics and Biopharmaceutics (under reviewing) (2010)

Son, Y. J. and J. T. McConville, Advancements in dry powder delivery to the lung, Drug Development and Industrial Pharmacy 34 (9) (2008) 948-959.

Srichana, T., G. P. Martin and C. Marriott, Dry powder inhalers: The influence of device resistance and powder formulation on drug and lactose deposition in vitro, European Journal of Pharmaceutical Sciences 7 (1) (1998) 73-80.

Stanescu, D., C. Veriter and K. P. Van de Woestijne, Maximal inspiratory flow rates in patients with COPD, Chest 118 (4) (2000) 976-980.

Steckel, H. and N. Bolzen, Alternative sugars as potential carriers for dry powder inhalations, International Journal of Pharmaceutics 270 (1-2) (2004) 297-306.

Steckel, H., P. Markefka, H. teWierik and R. Kammelar, Functionality testing of inhalation grade lactose, European Journal of Pharmaceutics and Biopharmaceutics 57 (3) (2004) 495-505.

Suarez, S., P. O'Hara, M. Kazantseva, C. E. Newcomer, R. Hopfer, D. N. McMurray and A. J. Hickey, Airways delivery of rifampicin microparticles for the treatment of tuberculosis, Journal of Antimicrobial Chemotherapy 48 (3) (2001) 431-434.

Suarez, S., P. O'Hara, M. Kazantseva, C. E. Newcomer, R. Hopfer, D. N. McMurray and A. J. Hickey, Respirable PLGA microspheres containing rifampicin for the treatment of tuberculosis: Screening in an infectious disease model, Pharmaceutical Research 18 (9) (2001) 1315-1319.

Sung, J. C., D. J. Padilla, L. Garcia-Contreras, J. L. VerBerkmoes, D. Durbin, C. A. Peloquin, K. J. Elbert, A. J. Hickey and D. A. Edwards, Formulation and Pharmacokinetics of Self-Assembled Rifampicin Nanoparticle Systems for Pulmonary Delivery, Pharmaceutical Research 26 (8) (2009) 1847-1855.

Talton, J. D., G. Hachhaus, R. K. Snigh and J. M. Fiz-Gerld, Method for preparing coated particle and phamraceutical formulations thereof, US. 6,984,404 (2006)

Taylor, M. K., A. J. Hickey and M. VanOort, Manufacture, characterization, and pharmacodynamic evaluation of engineered ipratropium bromide particles, Pharmaceutical Development and Technology 11 (3) (2006) 321-336.

Telko, M. J. and A. J. Hickey, Dry Powder Inhaler Formulation, Respiratory Care 50 (2005) 1209-1227.

Tewes, F., J. Brillault, W. Couet and J. C. Olivier, Formulation of rifampicin-cyclodextrin complexes for lung nebulization, Journal of Controlled Release 129 (2) (2008) 93-99.

Timsina, M. P., G. P. Martin, C. Marriott, D. Ganderton and M. Yianneskis, Drug-Delivery To The Respiratory-Tract Using Dry Powder Inhalers, International Journal of Pharmaceutics 101 (1-2) (1994) 1-13.

Tobyn, M., J. N. Staniforth, D. Morton, Q. Harmer and M. E. Newton, Active and intelligent inhaler device development, International Journal of Pharmaceutics 277 (1-2) (2004) 31-37.

Tomoda, K. and K. Makino, Effects of lung surfactants on rifampicin release rate from monodisperse rifampicin-loaded PLGA microspheres, Colloids and Surfaces B-Biointerfaces 55 (1) (2007) 115-124.

Traini, D. and P. M. Young, Delivery of antibiotics to the respiratory tract: an update, Expert Opinion on Drug Delivery 6 (9) (2009) 897-905.

Traini, D., P. M. Young, F. Thielmann and M. Acharya, The influence of lactose pseudopolymorphic form on salbutamol sulfate-lactose interactions in DPI formulations, Drug Development and Industrial Pharmacy 34 (9) (2008) 992-1001.

Treatment of tuberculosis; guidelines, World Health Organization (WHO) 4th. edition (2010)

Tsukada, M., R. Irie, Y. Yonemochi, R. Noda, H. Kamiya, W. Watanabe and E. I. Kauppinen, Adhesion force measurement of a DPI size pharmaceutical particle by colloid probe atomic force microscopy, Powder Technology 141 (3) (2004) 262-269.

Ungaro, F., G. De Rosa, A. Miro, F. Quaglia and M. I. La Rotonda, Cyclodextrins in the production of large porous particles: Development of dry powders for the sustained release of insulin to the lungs, European Journal of Pharmaceutical Sciences 28 (5) (2006) 423-432.

USP 32- NF27, R., MD, US Pharmacopeial Convention, Inc., (2009)

Vaswani, S. K. and P. S. Creticos, Metered dose inhaler: past, present, and future, Annals of Allergy Asthma & Immunology 80 (1) (1998) 11-19.

Vehring, R., Pharmaceutical particle engineering via spray drying, Pharmaceutical Research 25 (5) (2008) 999-1022.

Veldhuizen, R., K. Nag, S. Orgeig and F. Possmayer, The role of lipids in pulmonary surfactant, Biochimica Et Biophysica Acta-Molecular Basis of Disease 1408 (2-3) (1998) 90-108.

Voss, A. and W. H. Finlay, Deagglomeration of dry powder pharmaceutical aerosols, International Journal of Pharmaceutics 248 (1-2) (2002) 39-50.

Vyas, S. P., M. E. Kannan, S. Jain, V. Mishra and P. Singh, Design of liposomal aerosols for improved delivery of rifampicin to alveolar macrophages, International Journal of Pharmaceutics 269 (1) (2004) 37-49.

Watano, S., H. Nakamura, K. Hamada, Y. Wakamatsu, Y. Tanabe, R. N. Dave and R. Pfeffer, Fine particle coating by a novel rotating fluidized bed coater, Powder Technology 141 (3) (2004) 172-176.

Wiedmann, T. S., R. Bhatia and L. W. Wattenberg, Drug solubilization in lung surfactant, Journal of Controlled Release 65 (1-2) (2000) 43-47.

Yang, Y., N. Bajaj, P. Xu, K. Ohn, M. D. Tsifansky and Y. Yeo, Development of highly porous large PLGA microparticles for pulmonary drug delivery, Biomaterials 30 (10) (2009) 1947-1953.

Young, P. M., R. Price, M. J. Tobyn, M. Buttrum and F. Dey, Investigation into the effect of humidity on drug-drug interactions using the atomic force microscope, Journal of Pharmaceutical Sciences 92 (4) (2003) 815-822.

Zeidler, M., Corren, J., Hydrofluoroalkane formulations of inhaled corticosteroids for the treatment of asthma, Treatments in Respiratory Medicine 3 (2004) 35-44.

Zeng, X. M., G. P. Martin, C. Marriott and J. Pritchard, The effects of carrier size and morphology on the dispersion of salbutamol sulphate after aerosolization at different flow rates, Journal of Pharmacy and Pharmacology 52 (10) (2000) 1211-1221.

Zeng, X. M., G. P. Martin, S. K. Tee, A. Abu Ghoush and C. Marriott, Effects of particle size and adding sequence of fine lactose on the deposition of salbutamol sulphate from a dry powder formulation, International Journal of Pharmaceutics 182 (2) (1999) 133-144.

Vita

Yoen Ju Son was born in Seoul, South Korea on October 8, 1977 to Mr. Jung-Gon Son and Mrs. Woon-Seon Jung. After she graduated from high school in February 1996, she enrolled in the Engineering program at the Sung Kyun Kwon University in Seoul. In February 2000, she graduated with a Bachelor of Science degree in Material Science and Engineering. She then enrolled in the Material Science and Engineering department at the Seoul National University (Seoul, Korea) in March, 2000, to pursue a Master degree. She obtained her Master of Science degree in February 2002, and worked as a research scientist at the Korea Institute of Science and Technology (KIST) in Seoul until August, 2003. She then joined the pharmaceutical development department at the Yuhan Corporation (Seoul, Korea) in August, 2003, and worked as a senior research scientist until March, 2006. In September 2006, Yoen Ju was admitted into the graduate school in the College of Pharmacy at The University of Texas at Austin to pursue her Ph.D. under the supervision of Dr.McConville. Her research focused on the development of novel dry powder formulations for pulmonary drug delivery. During this time, she worked as a teaching and research assistant, served as a reviewer for pharmaceutical journals and attended various international conferences to present her work.

Permanent address (or email): yeonju.sohn@gmail.com

This dissertation was typed by Yoen Ju Son.